Immunocytochemical localisation of proteins implicated in Ca^{2+} and free radical homeostasis in normal and axotomised cat spinal motoneurones: a segmental comparison with reference to amyotrophic lateral sclerosis.

Alisa Shira Pearlstone

Institute of Neurology
University College, London

Submitted for PhD
February 2000

Supervisors: Dr. A. H. Pullen
Prof. R.N. Lemon

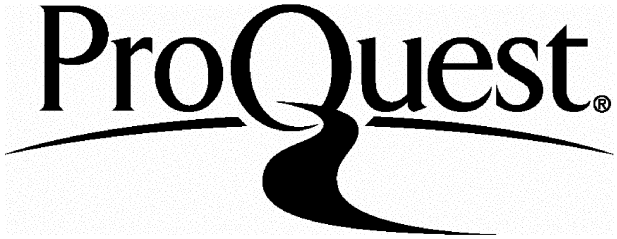

ACKNOWLEDGEMENTS

With many thanks to Dr. A. H. Pullen, for the skills which I have acquired through his patient training, for his helpful guidance, his boundless contributions of time, and innumerable engaging discussions. Thanks also to Professor, R.N. Lemon, for his helpful contributions as second supervisor.

With eternal gratitude to Dr. C.P. Seers, for his endless patience, his infinite wisdom, and for always keeping the door open.

With love and thanks to my husband, Patrick, who has supported me and encouraged me throughout..

With indebtedness to my good friends, Julie Smith, Moona Taslim-Saif, Louise Seheult, Rachel Spinks, and Shani Taylor, for keeping me going.

Also with gratitude to my wonderful parents for showing me the joys of learning and giving me a hunger to understand the world around me, and who have helped me practically in so many ways.

Finally, many thanks to the Brain Research Trust for financial support.

Abstract

Motoneurones of Onuf's nucleus (ON) in the sacral spinal cord enjoy relative resistance to degenerative motor conditions. It has been suggested that, in the case of amyotrophic lateral sclerosis (ALS), this resistance may relate to the differences between these motoneurones and other somatic motoneurones in the levels of Ca^{2+} buffering proteins ordinarily present. Ca^{2+} regulation and free radical homeostasis are central to the current understanding of the causes of neuronal death in ALS and therefore six proteins relevant to both of these activities were selected for further investigation in the spinal cord of the adult cat. To determine their localisation and investigate the possibility of segmental differences, immunocytochemical analyses were carried out in cervical, thoracic, lumbar, and sacral segments in the normal cat. In a second set of experiments aimed at characterising the regulation of these proteins after injury in a group of ALS-vulnerable neurones, motoneurones innervating the sartorius muscle were axotomised. Finally, post-axotomy alterations of immunoreactivity levels in sartorius motoneurones were compared with the alterations seen after axotomy of the pudendal nerve, arising from ON.

The proteins examined were calbindin (CaBP-D28k), parvalbumin (PV), calmodulin (CM), calcineurin (CaN), neuronal nitric oxide synthase (nNOS), and superoxide dismutase (SOD). Immunocytochemical labelling of perfusion fixed cat spinal cord revealed high levels of nNOS, SOD, and CaBP-D28k in ON. Full quantitative analysis showed that nNOS immunoreactivity (IR) and CaBP-D28k-IR were significantly higher in sacral motoneurones than motoneurones from cervical, thoracic, or lumbar spinal cord. Axotomised sartorius motoneurones showed significant bilateral decreases in CaBP-D28k-IR, CM-IR, and CaN-IR, and a bilateral increase in nNOS-IR. By contrast, post-axotomy alterations in ON were found to be unilateral. Furthermore, nNOS-IR in

axotomised ON was found to be decreased on the side of the lesion. The higher levels of CaBP-D28k in ON are discussed in the context of the current understanding of the functional importance of CaBP activity. It is suggested that higher levels of nNOS may relate to the possibility that pudendal motoneurones synthesise and release NO as a transmitter substance. Differential post-axotomy regulation of nNOS is hypothesised to reflect post-axotomy transmitter regulation in ON compared to a pure injury response in the sartorius motoneurones, which do not utilise NO as a transmitter. Segmental differences in the laterality of injury responses are considered in the context of segmental variations in bilateral connectivity. These findings are also discussed alongside the concept of differential vulnerability in ALS.

CONTENTS

TABLES

FIGURES

The outcomes of both experimental injuries and neuropathologies affecting motoneurones indicate that different motoneuronal populations in spinal cord and brainstem have differential vulnerabilities to these insults. Onuf's nucleus (ON), for example, which contains the motoneurones innervating the anal and urethral sphincters (Sato et al, 1978; Thor et al, 1989), is unique amongst spinal motoneurone groups in being vulnerable to the disease process in Shy Drager syndrome, which targets autonomic motoneurones. Meanwhile alongside the oculomotor nucleus of the brainstem, ON is relatively resistant to the disease process in amyotrophic lateral sclerosis (ALS) whilst other groups of somatic motoneurones in the spinal cord and brainstem bear the brunt of the ALS pathology.

There are a number of factors which might influence the likelihood of a neurone surviving pathological, toxic, or mechanical damage. One such factor has been selected as a focus for the research in this project. Specifically this is the role of certain proteins which are believed to play a critical part in mediating either neuronal cytotoxicity or cytoprotection through the control of intracellular Ca^{2+} and reactive oxygen species.

It is of value to establish the relationship between pre and post injury levels of such proteins in a cell group and the response of that cell group to the insult. The assumption here is that the neurone's pre- and post-injury protein regulation is an important determinant of its susceptibility or resistance to certain types of pathological state. A further extension of this idea leads to the possibility that differences in protein content between cell groups may relate to differences in their injury response. This principle is illustrated by work showing a prolonged expression of neuronal nitric oxide synthase (nNOS) in neuron groups destined to die after axotomy, which is not observed in other more resistant neuronal populations (e.g. Kristensson et al, 1994; Yu, 1997).

Three kinds of differences are of interest in this project, namely:

1. differences in the pre- and post-injury profile of motoneurones in terms of proteins involved in cytotoxic or protective pathways (i.e. the cytotoxic/cytoprotective capacity of the motoneurone)
2. segmental differences in baseline features between motoneuronal groups, and whether such differences are predictive of a difference in response to injury
3. segmental differences in post-injury alterations of certain features, examination of which prior to injury revealed no distinctive differences from one motoneuronal group to the next

The motoneurone should not be considered in isolation however, but as part of an integrative system involving a number of interdependent components, an appreciation of the mutual relationships of which will be vital for a correct interpretation of the nature of the injury response. Therefore the story of this thesis begins with the normal motoneurone in its anatomical and physiological context within the ventral horn of the spinal cord, particularly in the cat (Section 1.1). In sections 1.2 and 1.3 the focus will shift to a consideration of those situations in which the motoneurone's viability is challenged. The possible consequences for motoneurones of excessive Ca^{2+} influx will be considered with reference to a number of theories explaining cell death, particularly in ALS.

1.1. The normal spinal motoneurone

1.1.i The spinal cord

The spinal cord runs from the brainstem to the cauda equina. It is composed of clusters of interneurones, autonomic neurones, and somatic motoneurones, which are interspersed with glia and blood vessels. Together these conspire to form the characteristic butterfly shape of the grey matter. The grey matter is surrounded by the ascending and descending fibre tracts of myelinated nerve fibres which form the spinal white matter.

The grey matter has a high degree of internal organisation. At a gross level it is divided into four regions: these are the dorsal horns, bilateral protuberances at the base of the dorsal horn, known as the lateral horns, the ventral horns and an intermediate region between these areas.

In his 1811 pamphlet, Bell observed that disturbance of the dorsal roots had no effect upon the muscles, whilst similar disturbance of the ventral roots caused a dramatic contraction of the muscles (Bell, 1987 - modern reprint). This finding led to the now accepted view that the dorsal half of the spinal cord comprises the spinal component of the body's sensory system, with sensory information arriving in the dorsal roots, while the ventral part of the grey matter belongs to the body's motor system, with efferent motor information leaving the cord through the axons of the ventral roots. This division is hence known as the law of separation of function of the spinal roots, or the law of Bell and Magendie (Bell, 1987, also see Sherrington, 1906 , and Coggeshall, 1980).

Secondly, at a cellular level, the spinal grey is composed largely of groups of functionally related cells. In toluidine blue-stained transverse section the organisation of the grey gives rise to the histological appearance of a laminar structure, and on the basis of this

appearance a nomenclature was devised by Rexed in 1952 (see Figure 1.1-1). This nomenclature has become the major system for conveying information about anatomical locations in transverse sections of spinal cord and hence is now part of the language of modern neuroscience. Rexed's terminology will be used throughout this thesis.

1.1.ii The ventral horn

As stated earlier the ventral horn is largely motor in function. The motoneurones are in receipt of a massive convergence of supraspinal, propriospinal, and afferent (peripheral) information which arrives at the ventral horn, with the motoneurone representing the "final common pathway" to the muscle (Sherrington, 1906). The peripheral accessibility of the motoneurone, along with its large soma size, has also made it - until relatively recently - one of the most studied cell types in the ventral horn (Romanes, 1951).

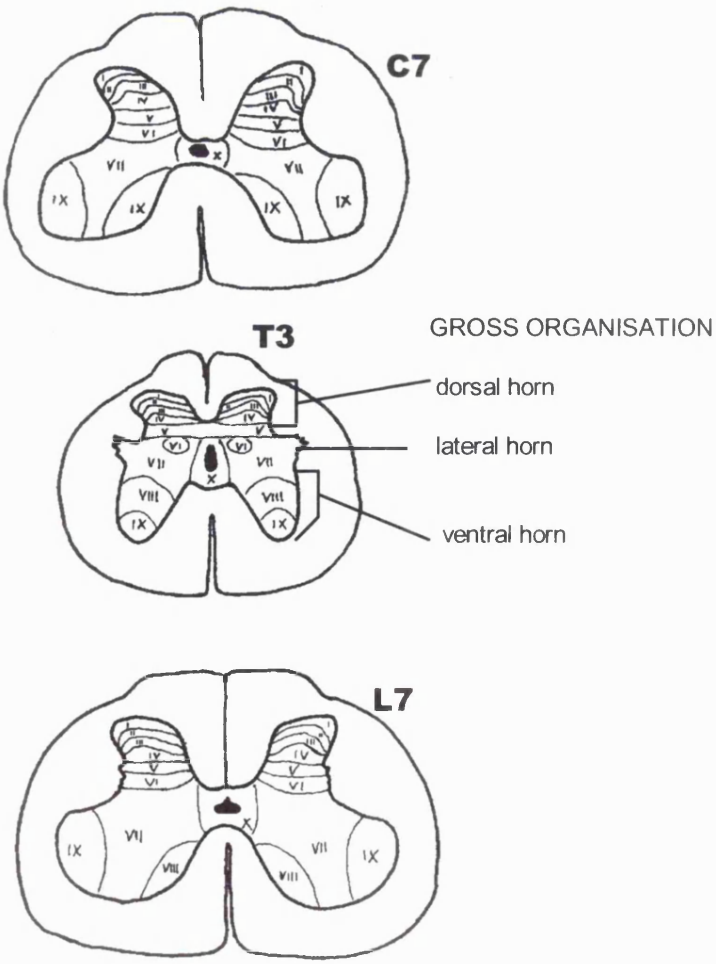

Figure 1.1-1.: The gross organisation of the grey matter and Rexed's laminar classification system.

Under Rexed's system, the ventral horn is divided into laminae VIII and IX, although at the levels of the intumescences (e.g. C7 and L7 as shown above), lamina VII continues to the ventrolateral border of the grey matter, interrupted by the motor nuclei (lamina IX). Adapted from Rexed, 1954.

Clearly severe nerve injury or neuropathology at this culminatory level can have devastating effects, and yet the motoneurone itself may, by its very nature, be more vulnerable to infection and damage. The features of motoneurone injury and neuropathology can only be fully appreciated in the light of an understanding of the motoneurone's normal function and its relationship with other cells of the spinal motor system. Therefore, before focusing more closely on the central issue of the disease and injury response of motoneurones, an overview of the spinal motor system and its cell groups will be given below. In the experimental work of this study, the identification of different ventral horn cell types will rely on morphological and anatomical criteria, so the following overview will also outline the major findings with regard to the location, size, shape, and number of primary dendrites associated with each of the cell types discussed. The information is summarised in Table 1.1-1.

1.1.iii The composition of the ventral horn - an overview of the cell types

In essence the motor system is an efferent, descending system, sending a stream of motor commands all the way from brain to muscle. The motor commands for voluntary movement are initiated largely in the primary motor cortex, but also in supplementary and other secondary motor cortex areas, whose large lamina Vb Betz cells send their axons into the brainstem where they decussate to descend in the contralateral spinal cord. There is a great deal of species variation in terms of how much of this large descending input actually provides direct monosynaptic excitation to the motoneurone (Armand, 1982). Physiological and anatomical evidence suggests that in the cat there are no monosynaptic cortico-motoneuronal (C-M) connections. After cortical lesion the degenerating axons and terminals of the descending tracts are seen in the dorsal and intermediate zones of the grey matter, at some distance from the motoneuronal cell bodies (Nyberg-Hansen and Brodal, 1963), and the duration of the shortest central delay after pyramidal stimulation indicates that the minimal C-M linkage is disynaptic (Illert et

al, 1976a and b). Meanwhile in the primate, the presence of C-M projections has been well documented (see Armand, 1982 for a review).

Within Rexed's laminae, the motoneuronal cell bodies are concentrated in the motor pools that constitute lamina IX. Although still technically known as a layer of the spinal grey, the organisation of these nuclei is more aptly described by the term "columnar" (Romanes, 1951). From here the axons travel to the muscle, exiting the cord in the ventral roots and thereafter joining the appropriate nerve.

On the basis of histological analyses of motor nerve endings and muscle fibres, and physiological recording experiments, two major classes of motoneurone have long been known to exist (Granit, 1970). These are the α-motoneurone, which innervates and causes the contraction of the skeletal muscle fibres, with one motor axon contacting many fibres (a motor unit), and the γ motoneurone which innervates and causes the contraction of the intrafusal fibres of the muscle spindles (evidence reviewed in Matthews, 1964 and in Granit, 1970).

The ability of neurones to take up horseradish peroxidase (HRP) after it has been injected into muscle and to then retrogradely transport it to the cell body where it can be readily visualised (Kristensson and Olsson, 1971) has been and continues to be exploited in the identification of cell bodies associated with particular muscle groups, but did little to distinguish the different neuronal subtypes within these groups. Morphological analysis of the various cell types present in the ventral horn, both motoneuronal and interneuronal, was greatly facilitated by the development of techniques for the intracellular staining and visualisation of physiologically identified cells, where the recording electrode tip is a micropipette which can be used to introduce dyes or HRP into

Motoneuronal Heterogeneity

As described earlier, alpha motoneurones form functional motor units with the pool of muscle fibres (or the muscle unit) that they innervate. Denny-Brown and Pennybacker's (1938)[1] early observations of the anatomical features of motoneurones suggested that lower input resistance and, hence, faster recruitment is a feature of the smaller motoneurones. Subsequent developments revealed that, far from existing as a homogeneous population, motor units can be typed according to five mutually interdependent characteristics. These are: a/ histochemical muscle unit reactivity profiles, reflecting the predominance of oxidative or glycolytic metabolism; b/ motoneuronal firing frequencies; c/ motoneuronal membrane resistance; d/ fatiguability and e/ neuronal size. Because of subtle species differences in histochemically typed muscle fibre appearance, and the current work involves cat motoneurones, the table below summarises information for the cat.

Table - adapted from Burke 1982 in *Human Motor Neuron Diseases* (LP Rowland, ed.), Raven Press, New York: pp31–44.

Type	Muscle unit histomchemical profile	Relative twitch speed	Relative tetanic force output	Relative fatigue resistance
FF	HB	Fast	Large	Low
FR	HA	Fast	Medium	High
S	I	Slow	Small	Very high

Further speculation has raised the question of whether differences in motor unit types might predispose differential vulnerabilities to degenerative changes, particularly in degenerative motoneurone diseases. Indeed, the selective preservation of Type I muscle fibres that has been observed in spinal muscular atrophy would lend some support to this concept (Engel, cited in Burke 1982). It is possible, that the physiological profiles of the different motor unit types also relate to differences in the relative contribution of excitatory and inhibitory presynaptic inputs. As discussed later, the relative frequency of excitatory inputs on a given neurone, and in particular the relative distribution of calcium permeable receptor subtypes, may be an important factor determining vulnerability to motor degenerative conditions where excitotoxicity is involved in the development of the pathology. However, to date, there is no evidence to suggest that the pathology of ALS preferentially involves any one type of motor unit (Burke, 1982; Swash and Schwartz, 1995[2]).

[1] Denny-Brown D and Pennybacker JB. *Brain* 1938; **61**: 311–333.
[2] In *Motor Neuron Disease - Biology and Management* (PN Leigh and M Swash, Eds.): Chapter 14 pp 331–344.

Table 1.1-1 To show the basic morphological features of a range of cell types from the ventral horn.

Data from [1] Ulfhake and Kellerth, 1981; Ulfhake and Kellerth, 1983; Russell-Mergenthal et al, 1986; Lipski and Martin-Body, 1987; Ritz et al, 1992. [2] Ulfhake and Cullheim, 1981. [3] Jankowska and Lindstrom, 1972 [4] Jankowska and Lindstrom, 1971; Lagerback and Kellerth, 1985; Lagerback and Ronnevi, 1982; Fyffe, 1990; Fyffe, 1991. [5] Cooper and Sherrington, 1940; Grant et al, 1982; Bras et al, 1988. Except where otherwise indicated these studies were carried out using cat tissue.

CELL TYPE	MEAN DIAMETER RANGE	NO. 1° DENDRITES	SHAPE	LAMINAR LOCATION
α-motoneurone [1]	27-82μm	6-18	ovoid, quadratic, triangular, ellipsoid	IX
γ-motoneurone [2]	22-37μm	5-9		IX
Ia interneurone[3]	21.3 - 28.3μm	4-5	?	VII(I)
Renshaw cell[4]	21-36μm	3-8	multipolar, ovoid/irregular or bipolar, fusiform	VII(I)
VSCT[5]	58μm in cat 30μm+ in kittens-70μm in monkey	10-14	multipolar, indistinguishable from motoneurones	VII(I), IX

a cell (Stretton and Kravitz, 1968). Using such techniques it has been shown that α-motoneurones are larger than most ventral horn cell types including the γ-motoneurones.

Intramuscular injection of retrogradely transported label, however, results in the staining of a large group of cells, including cells much smaller than the α-motoneurones visualised after intracellular HRP injection (Ulfhake and Kellerth, 1983, Ritz et al, 1992). Although it is likely that the majority of these smaller cells are γ-motoneurones, it should be borne in mind that the intracellular staining technique is likely to be biased towards the selection of larger cells because these will have larger diameter fibres, increasing the relative probability of their being encountered by the micropipette. It is thus likely that there will be some degree of overlap of the cell body sizes of the α and γ motoneurone. A further level of complexity is added by the fact that these cell measurements are usually done in transverse sections when the long axis of the cell may be oriented in the sagittal plane, as has been shown to be the case for intercostal α-motoneurones (Lipski and Martin-Body, 1987).

In the sacrocaudal regions of the spinal cord a third type of motoneurone has more recently been documented, whose axons innervate both intrafusal and extrafusal muscle fibres (Bessou et al, 1965). It has been suggested that these skeletofusimotor or β-motoneurones may be of an intermediate size to α and γ motoneurones and thus account for the unimodal distributions of cell sizes found in these nuclei (Ritz et al, 1992; Hoover and Durkovic, 1991), where the presence of only α and γ motoneurones would be expected to give rise to a bimodal size distribution (eg. Johnson, 1986).

1.1.iv. Ventral horn cell types involved in feedback and reflexes

A motor system which consisted of only an efferent flow of information would of course be a nonsense. For effective and precise motor control, not to mention for the effective prevention of body damage, it is essential that information regarding the extent of muscle contraction, the limb angle and position, etc., is quickly fed back into the system and integrated into motor unit activity. A number of afferent pathways exist to serve this purpose. Some of these influence motor activity via monosynaptic connections with the motoneurones, some have di- and polysynaptic connections to motoneurones via propriospinal interneurones (Jankowska, 1975), and some provide sensory cues to higher, supraspinal centres (eg. Cooper and Sherrington, 1940).

Afferent fibres from the muscle belong to four main categories, namely group Ia, group Ib, group II, and group III (the smallest diameter muscle afferent fibres). Group Ia and II fibres carry information from different types of intrafusal fibre regarding the degree and rate of muscle stretch. Group Ib fibres, meanwhile, are receptive to the stretch arising in the Golgi tendon organ during both stretching and contraction of the muscle (Granit,

1970). Other afferent information originates at the motor axon itself, which gives recurrent collaterals within the spinal cord. These then contact inhibitory Renshaw cells, which in turn inhibit other motoneurones, giving rise to a phenomenon known as recurrent inhibition (Renshaw, 1941; Renshaw, 1946). Finally, cutaneous afferents are also involved in the feedback/reflex pathways to the motor system. Groups II-III, cutaneous afferents, and high threshold joint afferents from flexor muscles are all involved in the flexor reflex, and are grouped together by the collective term 'flexor reflex afferents' or FRAs.

Although these systems are often described in terms of segregated pathways having discrete effects on the motoneurones, the true picture, revealed mainly by physiological experiments, is far more complex. The Ia inhibitory interneurone, for example, can monosynaptically inhibit α-motoneurones but has also been shown to inhibit other Ia inhibitory interneurones, as well as receiving monosynaptic inhibition from Renshaw cells (Jankowska, 1975). Polysynaptic excitation arrives at the Ia interneuron from FRAs and supraspinal tracts (Jankowska, 1975). The convergence is so great, in fact, that Jankowska suggests that the interneurone be thought of as the "final common pathway" to the motoneurone (see also Figure 1.1-2).

Located in the ventromedial portion of the ventral horn, in Rexed's lamina VII, are the somas of the Renshaw cells (Jankowska and Lindstrom, 1971; Lagerback and Kellerth, 1985; Fyffe, 1990; Fyffe, 1991), which are involved in recurrent inhibition of the α-motoneurones. Renshaw cells have elongated somas which may be ovoid or irregularly shaped, with a multipolar arrangement of their 3-8 primary dendrites (Lagerback and Kellerth, 1985; Fyffe, 1990) or less frequently may be bipolar, with fusiform cell bodies (Fyffe, 1990; Fyffe, 1991). These cells are smaller than most α-motoneurones and far

more elongated, although there is a degree of overlap in mean diameter for the smallest α-motoneuronal groups (27-49μm; Russell-Mergenthal et al, 1986; Lipski and Martin-Body, 1987) and Renshaw cells (22-36μm; Fyffe, 1990).

Dorsal to the Renshaw cells and dorsomedial to the motor nuclei are another class of inhibitory interneurone, which receives input from the Ia afferent fibres arising in the muscle spindles. These are cells of 20 by 30 μm in size with 3-5 primary dendrites (Jankowska and Lindstrom, 1972).

The cells of the ventral spinocerebellar tract (VSCT), with long axons coursing up to the cerebellum, are the only projection cells which have been described in the ventral horn other than the motoneurones themselves. According to the results of HRP tracing and degeneration studies, these cells are as large as the α-motoneurones, and are located by the ventrolateral edge of the grey matter, with a few cells occasionally found at the medial edge (Cooper and Sherrington, 1940; Grant et al, 1982).

Cells of the VSCT can be excited monosynaptically by group I afferents only, inhibited disynaptically by group I afferents, FRAs and cutaneous afferents, and can be further inhibited polysynaptically by afferents belonging to groups I - III, and cutaneous and joint afferents (Bras et al, 1988). In his review of the physiology of the VSCT, Oscarsson (1965) concluded that VSCT cells are responsible for the transmission of information regarding whole limb positions and limb movement to be integrated in the cerebellum.

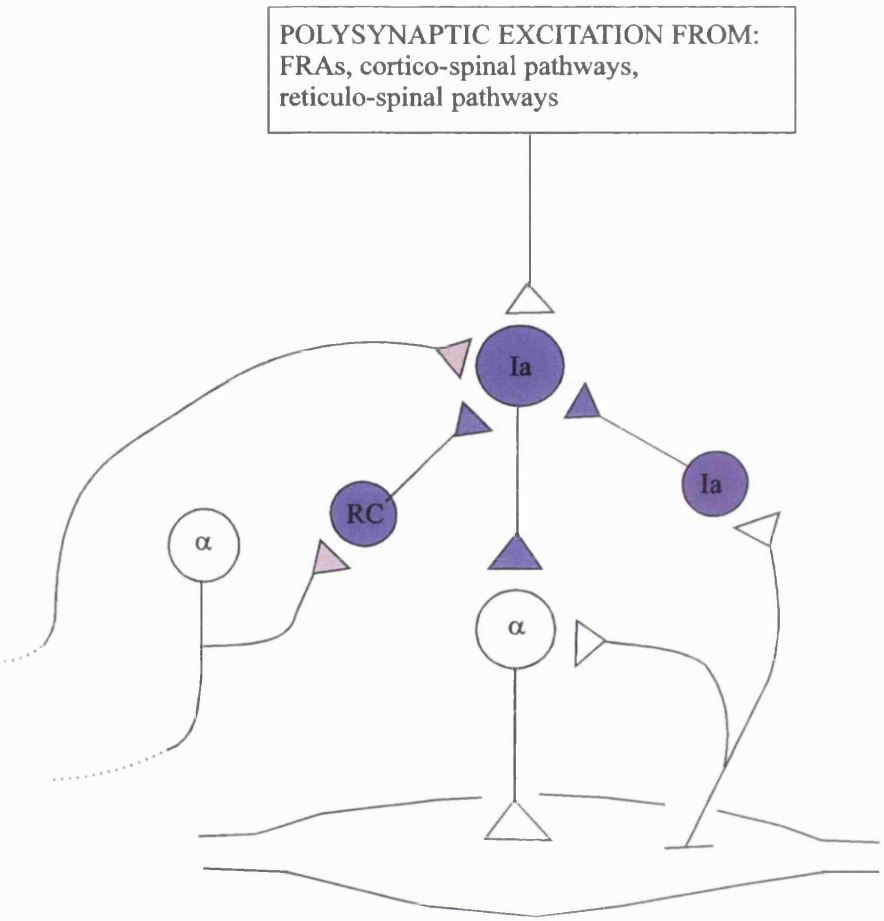

Figure 1.1-2. Connectivity of an alpha motoneurone - inhibitory contacts are shown in blue. For details see text. Abbr. RC - Renshaw cell; Ia - inhibitory Ia interneurone.

1.1.v. The vulnerability of the motoneurone

In its role as the 'final common path' the spinal motoneurone extends its axon into the periphery towards its muscular target. It has often been speculated that this long axonal trajectory may create for the motoneurone an exceptional state of vulnerability for a number of reasons. Firstly maintaining the length of the axon itself, and its internal structures, may place the cell body and nucleus under added "strain" by necessitating high rates of protein metabolism and hence increased bioenergetic requirement. In addition, the barrier between the vascular system and nervous system, which affords such high protection to the bulk of the nervous system from circulating toxins and

pathogens (see Olsson, 1975), is absent at the neuromuscular junction (Kristensson, 1977). Thus the motoneurone may be more likely to be exposed to circulating toxins, antibodies, or viruses than many other neuronal cell types, rendering the motoneurone an interesting class of cell because of its relatively unique environment.

However these are intuitive speculations at best. In relation to the first suggestion that the axon length necessitates increased protein and bioenergetic metabolism, it is worth noting that a relatively early study investigating enzyme activity in the electron transport chain using histochemistry revealed a far higher rate of mitochondrial activity in the comparatively short-axoned interneurones of the spinal cord (Campa and Engel, 1970). With regard to the latter argument concerning unusually high exposure to circulating sources of neurotoxicity, Olsson (1975) documents increased vascular permeability at a variety of peripheral nervous loci, particularly pinpointing sensory and autonomic ganglia as regions of vulnerability, suggesting no particular differential motoneuronal vulnerability to toxins of vascular origin.

In spite of such vagaries, it is nevertheless true that due to their peripheral accessibility motoneurones are clearly vulnerable to accidental damage to their axons, which may disrupt the mutually dependent relationship between the motoneurone and its target. In addition motoneurones bear the brunt of the pathology in a number of motor degenerative diseases including ALS. Interestingly however, for reasons as yet unknown, the response to these abnormal states is not homogeneous across motoneurone groups. Such motor nucleus-related heterogeneity in neuronal cell death will be considered further in section 1.3.

A common factor unifying many theories of neuronal cell death is Ca^{2+} entry. It has even been suggested that the motoneurone's ability to chelate Ca^{2+} may relate to its degree of resistance or susceptibility to the ALS disease process (Alexianu et al, 1994) and that the motoneurones themselves are more likely to experience higher levels of Ca^{2+} influx in normality than other neuronal cell types rendering them more vulnerable to further Ca^{2+}-related damage (Plaitakis, 1991). In what follows, the involvement of Ca^{2+} in neuronal cell death will be discussed, leading to an analysis of the significance of this toxicity to motoneurones.

1.2. Ca^{2+} and mechanisms of cell death

Neuronal Ca^{2+} entry is a normal event which, along with the transmembrane flow of other charged ions, creates the alterations in membrane potential which form the basis of the electrochemical signalling for which neurones are specialised. Once within the cell Ca^{2+} has a fundamental role in activating a large range of pathways, by binding to a variety of proteins. Intracellular Ca^{2+} ($[Ca^{2+}]_i$) is maintained within physiologically safe levels by a number of mechanisms, almost all of which are ATP-dependent. For instance, Ca^{2+} ions may be sequestered by calcium binding proteins (CaBPs), extruded via the Na^+/Ca^{2+} exchanger, or stored in the endoplasmic reticulum (ER).

Under certain conditions $[Ca^{2+}]_i$ levels may be dangerously elevated. One such circumstance which has been very well-defined is that of excitotoxicity.

1.2.i. Excitotoxicity

Excitatory amino acids (EAAs), in the form of both endogenous neurotransmitters (esp. glutamate (Glu)) and their exogenous analogues, have long been known to have the potential to cause injury and death to neurones (Lipton and Rosenberg, 1994; Albin and Greenamyre, 1992). Glu is known to act on four receptors, three of which are ionotropic

and are named according to their preferred agonists (AMPA, kainate, and NMDA receptors). A range of substances acting at these sites are capable of destroying neurones when present at sufficient concentrations and such excitotoxic effects can be blocked by competitive antagonists for the appropriate receptor (Meldrum, 1994). All three ionotropic receptors are associated with a degree of Ca^{2+} permeability although none so much as the NMDA receptor.

In essence, once a cell has been 'terminally excited' a number of intracellular cascades are turned on (Rothman and Olney, 1995). $[Ca^{2+}]_i$ levels increase after exposure to NMDA and AMPA, with the actual $[Ca^{2+}]_i$ concentrations being predictive of the likelihood of cell death (Hyrc et al, 1997). Recent evidence suggests that the mitochondrion is a primary target of the NMDA-related Ca^{2+} increase. NMDA receptor activation *in vitro* causes a large increase in the levels of mitochondrial Ca^{2+} ($[Ca^{2+}]_m$) which becomes irreversible after repeated exposures (Peng et al, 1998). Furthermore, inhibition of mitochondrial Ca^{2+} uptake is sufficient to prevent neuronal death in culture (Kruman and Mattson, 1999).

The recognition of the importance of excitotoxicity in explaining neuronal injury and loss in epileptic conditions, after trauma, and following cerebral ischaemic attacks, has helped excitotoxicity to become more of a paradigm than a concept, being implicated in a huge range of diseases involving the impairment of neuronal systems (around 30 according to Lipton, 1994). We will return to a consideration of excitotoxicity when we focus on the particular case of ALS in section 1.3. First, though, it remains to be shown how elevations in $[Ca^{2+}]_i$ might lead to cell death.

1.2.ii. Downstream events mediating the toxicity of Ca^{2+}

When $[Ca^{2+}]_i$ becomes dangerously high, nerve cells become vulnerable to damage through proteolysis, the effects of mitochondrial Ca^{2+} accumulation - ATP depletion and oxidative stress - and NO-related damage.

Of the many pathways which Ca^{2+} activates, a number are proteolytic. In particular, Ca^{2+} -related cell death has been linked to the activation of the Ca^{2+} -activated neutral proteases - the calpains - and the caspases. Calpains are known to proteolyse a large range of important cytoskeletal proteins, such as fodrin, spectrin, tubulin, microtubule associated proteins and neurofilament proteins (NFs) (see Croall and Demartino, 1991, for a review). Elevated levels of calpain-I cleaved spectrin breakdown products have been found in the hippocampus after *in vivo* intracerebroventricular infusion of NMDA. The prevention of these elevations by antiglutamatergic therapy suggested a specific role for calpain-I in mediating cell death (Siman et al, 1989).

As mentioned earlier, high levels of $[Ca^{2+}]_i$ lead to a build up of Ca^{2+} in mitochondria ($[Ca^{2+}]_m$) (Peng et al, 1998) where it may directly damage the respiratory chain itself. This will have two major consequences for the neuron. Firstly, the generation of ATP will *decrease*, and, secondly, the production of reactive oxygen species (ROS) will *increase*.

A decrease in ATP levels renders the neurone prone to excitotoxic damage, even in the absence of an initial excitotoxic event. ATP levels have been shown to fall after exposure to glutamate agonists, such as NMDA or kainate, or to compounds causing direct damage to the respiratory chain, such as MPP+, rotenone, or 3-NP (Leist et al, 1998). Concomitant cell death can be blocked not only by anti-glutamatergic treatment with AP-5, CNQX, DNQX, MK801, but also by inhibitors of the voltage gated Ca^{2+} channels (VGCCs), and yet none of these treatments prevent the fall in ATP production (Leist et al,

1998). This suggests that the chief effect of ATP depletion is not on cell viability per se, but on neuronal glutamate and Ca^{2+} sensitivity thus creating *indirect* or *secondary excitotoxicity.*

Indirect excitotoxicity through ATP depletion may be mediated by a number of outcomes, including a drop in normal resting potential, the failure of cellular mechanisms for maintaining $[Ca^{2+}]_i$ homeostasis, and the reversal of the glutamate transporter. ATP contributes to the maintenance of the normal voltage gradient across the neuronal membrane through the activity of Ca^{2+} and Na^+/K^+ ATP-ases. ATP depletion can therefore cause an initial drop in membrane potential because of the failure of these pumps. This would cause the opening of VGCCs as well as allowing the lifting of the voltage dependent NMDA receptor Mg^{2+} block permitting Ca^{2+} to enter the cell (Dykens, 1994; Lipton and Rosenberg, 1994; Choi, 1995). Once a cell's ATP levels are diminished its vulnerability to Ca^{2+} overload also increases because its mechanisms for reducing $[Ca^{2+}]_i$ are largely ATP dependent. Finally, Leist et al (1998) have shown that toxins inhibiting exocytosis have an anti-excitotoxic effect after acute and mild but not prolonged and severe conditions of bioenergetic challenge with mitochondrial respiratory inhibitors. From this it is concluded that the reversal of the glutamate transporter also contributes to secondary excitotoxicity during extreme energy depletion. Hence once damaged by Ca^{2+} overload, a neuron may enter a vicious circle of increasing Ca^{2+} entry and decreasing resistance (see Figure 1.2-1).

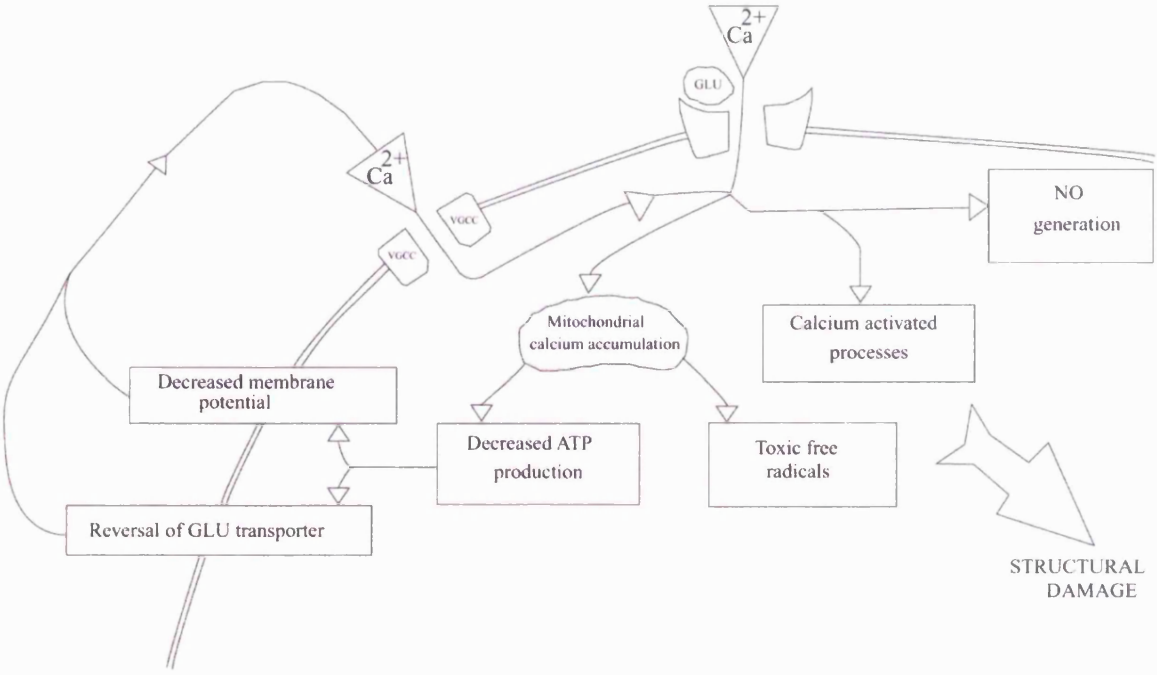

Figure 2.2-1 The circular influence of calcium accumulation on calcium entry - see text for details. Refs. A. Peng et al, 1998; B. Siman et al, 1989; C. Dykens, 1994; D. Leist et al, 1998. Abbr. VGCC - voltage gated calcium channel; Glu - glutamate

Besides bioenergetic crisis and related alterations in Ca^{2+} handling, the second major consequence of high levels of $[Ca^{2+}]_m$ and damage to the respiratory chain is the incomplete electron transfer which may subsequently occur. This may give rise to an increased production of ROS (Dykens, 1994). These are compounds possessing unpaired electrons; a fact which renders them highly reactive and therefore capable of causing damage to cells in a number of ways. Consequences of free radical damage include lipid peroxidation, damage to DNA, essential enzymes, and structural proteins, and a variety of other uncontrolled chain reactions.

There is some evidence to indicate that the effects of excitotoxicity can be mediated by the secondary generation of reactive free radicals. For example, NMDA toxicity may be

blocked by a number of antioxidant substances (Li et al, 1992; Supko and Johnston, 1992). Furthermore, kainate induced death of cerebellar granule cells in culture has been related to lipid peroxidation (Puttfarcken et al, 1992).

It has already been noted that Ca^{2+} may cause elevations of free radicals by its effects on mitochondria, but elevations in oxidative stress can be traced back to Ca^{2+} via other mechanisms such as the Ca^{2+}-dependent generation of nitric oxide (NO).

Evidence that NO has a role in neuronal damage comes from a large body of work which testifies to the elevation in levels of nNOS/NADPH-d that occurs after motoneuronal injury induced by axotomy or ventral root avulsion (e.g. Yu, 1994; Kristensson et al, 1994, Wu et al, 1994a, Wu et al, 1994b, Wu et al, 1995, Wu, 1996, Hu et al, 1996). There is also a great deal of evidence that the degree and duration of this elevation is directly related to the likelihood of ensuing cell death (e.g. Kristensson et al, 1994, Wu et al, 1994a, Wu et al, 1996, Yu, 1997), whilst suppression of nNOS activity coincides with survival promotion in these same models (Wu and Li, 1993; Wu et al, 1994a; Novikov et al, 1995). Excitotoxic lesions induced by the striatal injection of quinolinic acid are also accompanied by large increases in NADPH-d activity (thought to be synonymous with nNOS) (Schmidt et al, 1995) and neuroprotection against NMDA-mediated cell death can be attained by the use of nNOS inhibitors (Dawson et al, 1991; Dawson et al, 1993). Furthermore, cortical cultures from nNOS-deficient mice are resistant to NMDA-mediated neurotoxicity (Dawson et al, 1996).

The ways in which increases in levels of nNOS might contribute to cytotoxicity are considered below. These include the generation of peroxynitrite (ONOO) with its own

toxic effects, the interaction of ONOO with superoxide dismutase (SOD- the enzyme which catalyses the dismutation of $O_2^{\cdot -}$), and the production of $O_2^{\cdot -}$ per se.

In the first instance, nNOS activity may lead to an increase in cellular damage from raised levels of ONOO. nNOS is responsible for a short burst of NO production from arginine in response to neuronal Ca^{2+} influx, such as occurs after excitatory amino acid (EAA) receptor stimulation (Garthwaite, 1991). NO may act as a signalling molecule, stimulating cGMP production, but can also react with superoxide ($O_2^{\cdot -}$) to produce ONOO which, according to Beckman et al (1994) is capable of damaging all major components of the cell. Indeed at supraphysiological concentrations, NO outcompetes SOD for superoxide. It is hardly surprising then that decreases of SOD activity, which would allow an elevation of $O_2^{\cdot -}$ and increases of NO levels *in vitro* both precipitate cell death (Troy et al, 1996), presumably via ONOO generation. This cell death can be prevented either by inhibition of NOS or the addition of other free radical scavengers to the medium.

Apart from the direct toxic effects of ONOO on cellular components, ONOO may also challenge cellular viability through its interactions with SOD. When ONOO is bound to SOD, it forms a highly stable compound which nitrates protein tyrosine residues (Crow et al, 1997a). Tyrosine nitration may subsequently interfere with the target protein's normal activity.

In addition, there is some indication that nNOS might be capable of generating $O_2^{\cdot -}$ itself. In conditions where arginine is depleted, superoxide is generated in response to EAA receptor activation. This production follows a similar timecourse to NO production, is

blocked by NOS inhibitors, and is associated with cell death (Culcasi et al, 1994). It is likely, therefore, that NOS is responsible for the production of the $O_2^{\cdot -}$ itself and related toxic effects under such circumstances.

It should be noted that $O_2^{\cdot -}$ can also trigger cell death through other reductive interactions. The Haber-Weiss reaction, for instance, which involves $O_2^{\cdot -}$ results in the conversion of H_2O_2 to the highly reactive hydroxyl radical. $O_2^{\cdot -}$ can thus directly cause oxidative degradation of DNA, lipids, and proteins.

A final twist to the nNOS story is that some evidence indicates a neuroprotective role for nNOS. NO donors rescue cultured neurones deprived of trophic support (Farinelli et al, 1996) and prevent H_2O_2 mediated neurotoxicity in cultured mesencephalic dopaminergic neurones (Wink et al, 1993). Furthermore cells in the striatum, which are both somatostatin (SOM)-IR and NADPH-d positive and hence believed to be nNOS-containing cells, are selectively resistant to the pathology of Huntington's Chorea (in Kowall, 1987) and to certain types of excitotoxic (Ferrante et al, 1993) and bioenergetic lesions (Beal et al, 1993a and b; Brouillet et al, 1993) although the selectivity of the excitotoxic lesion is questionable (Davies and Roberts, 1988; Susel, et al, 1991; Forloni et al, 1992). On the other hand, in nNOS- mice this resistance persists, indicating that some other property of these cells may be responsible for conferring such neuroprotection (Dawson et al, 1996).

NOS/NO - a role in regeneration?

Furthermore, a potential role for NOS/NO in the acute stages of neural regeneration in the CNS is suggested by the studies of hypophysectomised rats reported by Wu & Scot (1993)[1]. Combined immunocytochemical and EM examinations revealed increased numbers of NOS positive neurites and neurones in the supraoptic and paraventricular nuclei 2w after lesioning in association with the appearance of regenerating axons. By 4w, NOS staining of neurites and neurones had returned to normal levels despite the continuance of immature axons. A role in regeneration is also suggested for cranial motoneurones. Nerve avulsion normally induces neuronal death in both spinal and cranial nuclei , and the neurones destined to die express elevated NOS reactivity (Wu et al., 1995). However, axotomy-induced apoptosis of neonatal rat facial motoneurones, whilst associated with elevation of NADPH-diaphorase (NOS) activity, contrasts with the situation in spinal motoneurones in that elevation of diaphorase activity occurs in motoneurones *surviving* apoptosis and *after* the onset of DNA fragmentation (a mark of apoptosis; Rossiter, Riopelle & Bisby, 1996[2]). On this basis, NOS does not initiate neuronal death in facial motoneurones, but is more associated with neuronal survival. A similar conclusion was drawn by Yu (1994), who identified a differential response by NOS to axotomy in the hypoglossal, dorsal vagal, and facial motor nuclei. Up-regulation of NOS occurred in all three nuclei, but neuronal death (represented as the loss of NOS-immunostained neurones) occurred solely in the dorsal vagal nucleus and up-regulation of NOS in the facial nucleus was associated with cell survival. In the hypoglossal nucleus, the response by NOS was found variable and muscle target-dependent (Yu, 1997). The initial elevation of NOS on denervation was found to be sustained after nerve transection, but returned to normal levels after a nerve crush when contact between neurone and muscle was re-established. Finally, neurotomy of the rat cavernosus nerve (Carrier, et al, 1995[3]) induced axonal regeneration with expression of NOS seen in the regenerating axons.

More recent research has indicated an additional involvement for nNOS in synaptogenesis after nerve injury to the facial nucleus. A protein critically involved in the regulation of synaptic plasticity – post-synaptic density-95 (PSD-95) – has been shown to bind to nNOS (Jaffrey et al, 1998[4]) and both nNOS and PSD-95 have been shown to be up-regulated during periods of synaptogenesis (Ogilvie et al, 1995[5]; Che et al, 2000[6]). After facial nerve axotomy, the correlation between the timing of axonal mRNA and protein expression of nNOS, the expression of PSD-95, and the re-innervation of the target muscle has been seen to provide further support to the notion that nNOS may also have a central role in the regenerative process (Che et al, 2000).

---

[1] Wu W, Scott DE (1993) Increased expression of NOS in hypothalamic neuronal regenration. Exp Neurol, 121: 279-283.

[2] Rossiter JP, Riopelle RJ Bisby MA (1996) Axotomy-induced apoptostic cell death of neonatal rat facial motoneurons: Time-course analysis and relation to NADPH-diaphorase activity. Exp Neurol, 138: 33-44.

[3] Carrier S, Zvara P, Nunes L., et al (1995) Regeneration of nitric oxide synthase containing nerves after cavernosus nerve neurotomy in the rat. J Urol, 153: 1722-1727.

[4] Jaffrey SR, Snowman AM, Eliasson MJL et al (1998) CAPON: a protein associated with neuronal nitric oxide synthase that regulates its interactions with PSD-95. *Neuron* 20: 115–124.

[5] Ogilvie P, Schilling K, Billingsley ML et al (1995) Induction and variants of neuronal nitric oxide synthase type I during synaptogenesis. *FASEB J* 9: 799–806.

[6] Che YH, Tamatani M, Yohyama M (2000) Changes in mRNA for post-synaptic density-95 (PSD-95) and carboxy-terminal PDZ ligand of neuronal nitric oxide synthase following facial nerve transection. *Mol Br Res* 76: 325–335.

1.3. Motoneurones and Ca^{2+} related toxicity

In the previous section it was shown that excessive levels of $[Ca^{2+}]_i$ can be cytotoxic for a number of reasons. In what follows the possible relevance of $[Ca^{2+}]_i$ to the pathological cell death of motoneurones in ALS and after axotomy will be discussed.

1.3.1 ALS - a clinical and scientific introduction

Motor neurone disease (MND) is a collective term which encompasses three major clinical syndromes, namely these are: *amyotrophic lateral sclerosis (ALS)* involving the loss of both upper and lower motoneurones of the spinal cord; *primary lateral sclerosis* whose progressive pathology is restricted to upper motoneurones; and lastly *progressive bulbar palsy* involving mostly brainstem motor systems (Swash and Schwartz, 1992). There is a degree of confusion in the literature over the correct usage of these terms so in this thesis ALS will be used to describe a disease of the motoneurones which always affects lower motoneurones and may affect upper motoneurones.

The hallmarks of the ALS pathology include the presence of two main types of inclusion bodies: Bunina bodies and Hirano bodies. In addition there is a breakdown of the axonal infrastructure with the presence of neurofilamentous tangles associated with ubiquitinous accumulations.

Among those cells known to be lost in the disease, Hirano (1991) reports that there is a preferential loss of large diameter motoneurones, although it is acknowledged that there may be an even distribution of cell death across the spectrum of cell sizes in the motor system most affected by the disease. There is believed to be a relative degree of resistance of motoneurones in Onuf's nucleus (ON), a beaded column of cells giving rise to the innervation of anal and urethral sphincters (Sato et al, 1978; Thor et al, 1989), and also

of motoneurones in the oculomotor nuclei. This is reflected clinically in preservation of oculomotor and sphincteric function until relatively late in the disease process.

The resistance of ON, along with its vulnerability to a disease of the autonomic nervous system (ANS), Shy Drager Syndrome, has led to the suggestion that ON in fact should be considered to be autonomic in nature, however its innervation of striated muscle and the presence of C-type synapses (found only in apposition to α-motoneurones (Conradi., 1969; McLaughlin, 1973a, 1973b, & 1973c)) on the somas of large diameter neurones therein suggest that such an explanation is inappropriate (Pullen, 1988; Pullen, 1995). Furthermore, the establishment of ALS-typical inclusion bodies and other ultrastructural abnormalities within ON suggest that these cells are not entirely protected against the effects of the disease (Pullen and Martin, 1995).

1.3.ii. ALS and Ca^{2+}

1.3.ii.a Excitotoxicity

Evidence for an excitotoxic involvement in ALS comes from several lines of work. The key findings in this regard are: a/increased levels of glutamate in the fasting plasma and CSF of ALS patients, with decreased CNS tissue levels of glutamate (Rothstein et al, 1990; Plaitakis, 1990); b/reports of a disease-specific impairment of high-affinity, Na^{+}-dependent glutamate uptake in ALS, selective to affected tissues (Rothstein et al, 1992) the *in vitro* modelling of which, using selective inhibitors of this transport system, causes a slow and selective neurotoxicity to ventral horn motoneurones (Rothstein et al, 1993); c/delayed motoneuronal degenerative changes, reminiscent of those seen in ALS, and cell death following intrathecal injections of the glutamate agonist, kainic acid (Hugon et al, 1989); d/the toxicity of CSF from ALS patients to cultured neurones which is blocked by CNQX, the AMPA antagonist (Couratier et al, 1993); and finally e/the possible

association of the western Pacific ALS-PD (parkinsonism-dementia) complex with the dietary intake and medicinal use of substances containing the glutamate analogue BMAA (Spencer et al, 1987).

On the basis of these findings Plaitakis formally proposed an hypothesis of glutamate dysfunction in 1990. The theory centres on the idea that decreased tissue levels and increased plasma/CSF levels of glutamate in ALS patients indicate a shift of intracellular glutamate pools to extracellular locations. Hence cells are undergoing prolonged exposure to potential toxins, whilst the unusually high spinal cord levels of glycine from interneurones are invoked to explain selectivity of cell loss (Plaitakis, 1991). Glycine enhances the activity of the NMDA receptor by acting at a strychnine-insensitive site to accelerate recovery from receptor desensitisation, and Plaitakis proposes that, in this manner, glycine diffusing from local interneurones in the spinal cord increases the toxicity of abnormally high levels of extracellular glutamate.

Further support for this hypothesis comes from autoradiographic work examining the regional distribution of the Ca^{2+}-permeable NMDA receptor and that of the relatively Ca^{2+}-impermeable non-NMDA receptors. Results from this work suggests that numbers of NMDA receptors are decreased in ALS ventral horn but increased in motor cortex (Shaw et al, 1991; Shaw et al, 1994a). This group has also established that non-NMDA receptor expression is of a low density in the normal ventral horn and brainstem, with the highest levels found in the oculomotor nucleus (Chinnery et al, 1993; Shaw and Ince, 1994), which is spared in ALS. Non-NMDA receptor binding was, however increased in the intermediate grey matter and substantia gelatinosa of ALS spinal cord and in ALS motor cortex (Shaw et al, 1994b).

Findings of increased glutamate levels in CSF and fasting plasma, however, have been inconsistent. Perry and associates (1990) failed to establish significant changes in levels of glutamate, with the exception of a small increase in plasma glutamate levels in some patients, which they felt could be explained by the age difference between the patients and controls. Trials of antiglutamatergic drugs yielded a positive therapeutic effect only for patients with the bulbar onset variant of the disease, hinting at aetiological heterogeneity.

The direct contradiction between the data of Rothstein's and Perry's groups, the former of which established significant increases in CSF glutamate levels in ALS patients, warrants further examination. In spite of their similar results for all other substances measured in both studies, there was a 15-fold difference in the concentration of glutamate (2.9 μmol/L vs. 0.2 μmol/L). The main difference between the two procedures was the use of sulfasylic acid by the Perry group to deproteinise the CSF and avoid artefactual elevation of glutamate and aspartate by CSF enzyme activity. Young (1990) suggests that this procedure may precipitate the glutamate and aspartate along with the protein.

In addition the selection criteria employed by the two groups differed somewhat. The Perry group included patients with progressive motor atrophy, a pure lower motor neurone disorder, whilst the Rothstein group did not. There is no *a priori* reason to assume that the different forms of ALS share a single initial pathogenic pathway, and in this case the inclusion of these non-ALS patients may well have contaminated the data.

There has also been disagreement about the contribution of EAAs to the western Pacific ALS-PD complex. This disease has been observed in three western Pacific foci: the Kii peninsula of Japan, the Auyu and Jakai populated villages of West New Guinea, and the

islands of Guam and Rota, where initial records indicated a prevalence 50 to 100 times greater than that of control populations (Lavine et al, 1991). This disorder is believed to be related to some element of the environment and suspect factors include the use of cycad seeds for both dietary and medicinal purposes by the indigenous populations of these regions. BMAA, a glutamate analog capable of exerting NMDA- and non-NMDA-receptor-mediated excitotoxic damage (Ross et al, 1987, Weiss and Choi, 1991), is one of the toxic substances found in cycad seeds. When administered orally to cynomolgus monkeys, a clinical syndrome and pathology similar to the ALS-PD complex emerges (Spencer et al, 1987).

The prevalence of the ALS-PD complex had been observed to be decreasing (Garruto et al, 1985), such that in 1985 the Guam neurological centre was closed down due to the apparent disappearance of the problem for which it had been set up (Lavine et al, 1991). This was seen to support the implication of cycad use in the pathogenesis of this disorder (Weiss and Choi, 1991), as increasing Westernisation meant that the use of traditional foods and medicines were declining seemingly in parallel with the prevalence of the disease (Spencer et al, 1991). The apparent disappearance of Guam's ALS-PD complex now appears to have been an artefact of the increasing use of private medicine, where private doctors have been reluctant to diagnose this disorder in the knowledge that free medical care was available for patients with such a diagnosis (Lavine et al, 1991). These authors show that the prevalence of ALS in the most rural village in the south of Guam is still 100 times that in control, with other slightly less rural areas being intermediate between the two. They also, however, suggest that incomplete detoxification is still occurring in cycad preparation in the more rural regions of Guam.

A further anomaly in the BMAA/ALS-PD connection is raised by the question of toxic dosages. BMAA concentrations in untreated cycad seeds are extremely low (Spencer et al,

1991; Duncan, 1991). In spite of findings of *in vitro* toxic effects after application of purified BMAA by some workers (Ross et al, 1987), Duncan and associates found that the limited toxicity of cycad extracts did not correlate with their BMAA content. It should be noted that Duncan did not report whether he had used a bicarbonate-buffered solution which is vital to the excitotoxic actions of BMAA (Weiss and Choi, 1991). In practice, samples of cycad flour made by the Chamorro Indians were found to have a BMAA concentration of between 0 and 146μg/g with the most BMAA-rich flours being produced by the areas with the highest incidence of the disease (Duncan, 1991).

1.3.ii.b Oxidative stress

The discovery of a mutation of a free radical scavenging enzyme in patients with the familial form of ALS (FALS) has focused attention on the possibility that oxidative damage may underlie motoneurone pathology in all forms of ALS. Findings pertaining to alterations in the antioxidant activity of this and other relevant enzymes underlie the more recent shift of research effort to investigating possible gains of function of the mutant gene product.

The primary finding linking ALS to oxidative stress is the linkage of approximately 20% of FALS cases to a mutation in the gene coding for the cytosolic (Cu-Zn-binding) form of superoxide dismutase (SOD-1) (Rosen et al, 1993). SOD-1 acts as an antioxidant force in the cytosol, converting $O_2^{\cdot-}$ to H_2O_2 and O_2. H_2O_2 can then be removed by catalase and glutathione peroxidase. Since H_2O_2 is involved in reactions which give rise to the potently toxic hydroxyl radical ($HO^{\cdot}$), both overactivity and underactivity of SOD-1 might potentially be harmful to the cell. Of course, it is not necessarily the case that a mutation of SOD-1 will result in increases of oxidative stress.

Is oxidative stress a significant factor in ALS-related cell death?

Attempts have been made to answer the question of whether oxidative damage has occurred in ALS by looking at markers of free radical damage in affected tissues. In particular, this work has focused on the levels of: a/ malondialdehyde - a marker of lipid peroxidation which leads to membrane breakdown; b/ protein carbonyl groups - seen in proteins modified by oxidative stress, and c/ 8'-hydroxy-2'-deoxyguanosine (OH8dG) - a marker of oxidative DNA damage. Malondialdehyde is found to be significantly increased in the motor cortex of SALS patients and of FALS patients with no known SOD mutation (FALS (unknown linkage)), and immunoreactivity for malondialdehyde modified proteins is also increased in the spinal cord of SALS and FALS patients (Ferrante et al, 1997a). Similarly, protein carbonyls have been found to be increased in SALS and FALS (unknown linkage) motor cortex (Bowling et al, 1993; Ferrante et al, 1997a) and in SALS spinal cord (Shaw et al, 1995). Finally, levels of OH8dG are increased in motor cortex of SALS and FALS (unknown) patients, and OH8dG immunoreactivity is increased in SALS and FALS spinal cord (Ferrante et al, 1997a). These data strongly support the hypothesis that oxidative stress is heightened in neurones affected by ALS, and it is tempting to conclude that the SOD mutations may therefore be critical in reducing the cell's protection against free radicals. A summary of these findings is presented in Table 1.3-1.

Table 1.3-1 Alterations in levels or immunoreactivity of markers of oxidative damage in the spinal cord and motor cortex of SALS patients

	MARKER FOR	Motor Cortex	Spinal Cord
Malondialdehyde	Lipid peroxidation	↑[1]	
Malondialdehyde-modified protein-IR	"		↑[1]
Protein carbonyls	Protein damage	↑[1,2]	↑[3]
OH8Dg	DNA damage	↑[1]	
OH8dG-IR	"		↑[1]

[1]Ferrante et al, 1997a, [2]Bowling et al, 1993, [3]Shaw et al, 1995.

It might be expected that if free radicals are elevated as a result of the mutant SOD activity in SOD-linked FALS, and by an unknown mechanism in other ALS variants, then the levels of other neuronal antioxidants may be altered by way of a compensatory response. Catalase and glutathione are of interest in this respect, as they are involved in clearing cellular H_2O_2, preventing the formation of the hydroxyl radical. In the tissue of ALS patients, catalase activity is unaltered in the cerebellum and motor cortex (Przedborski et al, 1996), but immunoreactivity is increased in the spinal cord (Shaw et al, 1997). Glutathione activity is also unchanged in the ALS cerebellum, but decreased in the motor cortex (Przedborski et al, 1996) and either unchanged (Fitzmaurice et al, 1995) or increased in the spinal cord (Shaw et al, 1995). Within the motor cortex the lowest levels of glutathione activity were seen in patients with the fastest disease progression suggesting a relationship between the level of glutathione mediated neuroprotection and the rate of disease progression (Przedborski et al, 1996). Finally, immunoreactivity for hemeoxygenase-1, an antioxidant whose expression is induced by oxidative stress, is increased in the spinal cord of ALS patients (Ferrante et al, 1997a). These findings are summarised in Table 1.3-2.

Investigations of mice bearing the mutant SOD1 gene are also supportive of a role for oxidative damage in ALS. Gurney and co-workers (1994) have raised a line of transgenic mice expressing the human FALS SOD mutation, G93A. These mice develop a profound upper and lower motor neuronopathy in adulthood with ALS typical neurofilamentous accumulations and swellings. Onset of the neuronopathy can be delayed significantly by premorbid treatment with antioxidant Vitamin E, but not the putative anti-glutamatergic compound riluzole (Gurney et al, 1996). In these mice, both malondialdehyde and hemeoxygenase-1 immunoreactivity were found to be elevated in the spinal cord (Ferrante et al, 1997b) although neither malondialdehyde levels nor hydroxyl levels were found to be elevated in transgenic mice expressing the G37R mutation (Brujin et al, 1997).

Table 1.3-2: A summary of reported changes in the activity or immunoreactivity of antioxidants in the tissues of ALS patients.

	Cerebellum/Area 6 (unaffected tissues)	Motor cortex	Spinal Cord
Glutathione activity	▶[ref]1	▼[ref]1	▶[ref]5 ▲[ref]3
Catalase activity	▶[ref]1	▶[ref]1	
Catalase IR			▲[ref]2
Hemeoxygenase-1IR			▲[ref]4

▶[ref] - unchanged, ▲[ref] - increased, ▼[ref] decreased. [1] Przedborski et al, 1996 [2] Shaw et al, 1997 [3]Ince et al, 1994 [4]Ferrante et al, 1997a [5]Fitzmaurice et al, 1995.

Does the SOD mutation decrease antioxidant activity?

Whilst the above evidence generally seems to give credence to the notion that ALS-affected neurones are under increased attack by free radicals, it is not necessarily the case that this is directly caused by an alteration in SOD antioxidant activity.

Studies of SOD-immunoreactivity and expression in ALS patient tissues suggest that levels of SOD may be higher in ALS neurones. Although qualitative decreases in SOD immunoreacitivity in the ALS spinal cord have been reported (Uchino et al, 1994), statistically significant quantitative increases in SOD immunoreactivity in spinal cord (Shaw et al, 1997) and motor cortex (Blaauwgeers et al, 1996) have also been demonstrated. Moreover, increases have been detected in the expression of SOD-1 mRNA in SALS patient motoneurones (Bergeron et al, 1994).

Evidence regarding SOD enzyme activity, however, suggests that the mutation may not affect activity per se. Contrary to expectations that the mutations would engender a near complete loss of function, primate COS-1 cells transfected with 5 of the known SOD-1 mutations showed near normal enzyme activity (Borchelt et al, 1994). On this basis, it is predicted that individuals heterozygous for the various SOD-1 mutations studied would have between 50% and 80% of normal activity levels (Borchelt et al, 1994). Indeed the activity of SOD-1 and SOD-2 (the mitochondrial isoenzyme) has been found to show no significant alterations in patient motor cortex, cerebellum (Predzborski et al, 1996), Area 6 (Bowling et al, 1993) and spinal cord (Uchino et al, 1994) although in a limited sample (N=7) a decrease of SOD-1 activity in ALS spinal cord was observed with a concomitant, possibly compensatory, small increase in SOD-2 activity (Fitzmaurice et al, 1995).

Table 1.3-3 summarises the above findings with regard to SOD levels and activities, along with the N for each finding. From this it can be seen that the total sample of ALS patients with elevated SOD-1 is only slightly larger than the sample of ALS patients with decreased SOD-1 (16:12). A closer examination of the study showing no change in spinal cord SOD-1 activity (Uchino et al, 1994), suggests that the results did show a clear trend towards an increase in spinal cord activity of SOD-1. This was particularly

apparent in the cervical cord, where the greatest increases were observed in SOD-immunoreactivity by Shaw's group (Shaw et al, 1997). The statistical significance or otherwise of Uchino's data is difficult to interpret, given that the paper does not cite which rejection level was employed. Ultimately, on the basis of the available data and notwithstanding the above speculations, it is not possible to conclude that SOD-1 activity is altered in either direction.

Table 1.3-3: A summary of reported changes in the activity or immunoreactivity of SOD-1 and SOD-2 in the tissues of ALS patients.

	Cerebellum/Area 6 (unaffected tissues)	Motor cortex	Spinal Cord
SOD-1 activity	◗1 *(9)*, 6(15)	◗1 *(9)*	◗3 *(5)* ↓7 *(7)*
SOD-2 activity	◗1 *(9)*	◗1 *(9)*	◗3 *(5)* ↑7 *(7)*
SOD-1 IR		↑4(22)	↑2 *(10)* ↓3 *(5)*
SOD-2 IR			↑2 *(10)* ↓3 *(5)*
SOD-1 mRNA			↑5(6)
Total N for each direction of alteration SOD-1	◗ *(24)*	◗ *(9)* ↑ *(22)*	◗ *(5)* ↑ *(16)* ↓ *(12)*
SOD-2	◗ *(9)*	◗ *(9)*	◗ *(5)* ↑ *(17)* ↓ *(5)*

◗ref (N=) - unchanged, ↑ ref (N=) - increased, ↓ ref (N=) - decreased. [1] Przedborski et al, 1996 [2] Shaw et al, 1997 [3]Uchino et al, 1994 [4]Blaauwgeers et al, 1996 [5]Bergeron et al, 1994 [6]Bowling et al, 1993 [7]Fitzmaurice et al, 1995.

Has mutant SOD gained a novel toxic action?

Given the near normal levels of activity of SOD, there is general agreement that the contribution of the SOD-1 mutation to ALS is likely to be by way of a gain of function. There is less agreement over what that gain of function might be. One idea, for instance, is that the mutated gene product might be capable of generating the hydroxyl radical,

using H_2O_2 as a substrate, although, as we have seen, hydroxyl levels were not found to be elevated in the G37R transgenic mice (Brujin et al, 1997). Another suggestion is that conformational changes may give rise to protein accumulation which in turn interferes with neuronal function. In the disease, as well as in a number of transgenic mice expressing different mutations, Cu/Zn SOD-IR is seen in the neuronal inclusions by some researchers (e.g. Chou et al, 1996; Shibata et al, 1996; see Brujin et al, 1998 for a review).

A third theory suggests that the ability of SOD to interact with ONOO may be enhanced by the mutations, through alterations of the structure of the protein's metal core, causing increases in protein nitration at tyrosine residues (Beckman and Koppenol, 1996). Crow et al (1997a) have shown that normal SOD binds zinc with an affinity of up to 30 times that of a number of ALS SOD mutations, suggesting that ALS-SOD might be zinc-deficient. The addition of ONOO and zinc-deficient SOD to a tyrosine-containing tripeptide leads to a 2.5-fold increase in nitrotyrosine yield, which is blocked by the addition of zinc, copper or cobalt (Crow et al, 1997a). Thus, the mutant protein is likely to be zinc-deficient and, therefore, capable of nitrating protein tyrosines.

The idea that the formation of a nitrating intermediate, formed by mutant SOD and ONOO, may be a pathogenetic factor in ALS is lent weight by findings linking nitrotyrosylation specifically to the breakdown of neurofilaments. It has been shown that a principle target of protein tyrosine nitration is the light subunit of the neurofilament protein (NF-L) (Crow et al, 1997b). Once nitrated, NF-L subunits lose their ability to form stable filaments with medium and heavy subunits, as it appears that the tyrosine residues are instrumental in maintaining both the relationships between the subunits and the coiled structure of the rod domain (Crow et al, 1997b). Since NF-L binds zinc atoms with 12 times the affinity of wt-SOD (Crow et al, 1997a), neurofilament

fragments created by the nitrotyrosylation of NF-L may further exacerbate the formation of nitrotyrosines by removing zinc and thus increasing the levels of zinc-deficient SOD. Given the recognised breakdown of neurofilaments in ALS, the ability of this hypothesis to predict neurofilament-specific damage resulting from the gain of function of the mutated gene product, makes the hypothesis a particularly powerful one.

In vivo evidence from transgenic mice and human patients is far from clear cut. Levels of free nitrotyrosine are significantly elevated in the spinal cord of the G37R mouse, up to 10 weeks prior to the onset of clinical symptoms (Brujin et al, 1997) and cultured motoneurones from G93A mice have significantly elevated nitrotyrosine levels in comparison to wild types (Kruman et al, 1999).. Also, there have been findings of increased 3-nitrotyrosine-IR in the spinal cord of G93A mice (Ferrante et al, 1997b), of SALS and FALS human patients (Beal et al, 1997), and 3-nitrotyrosine-IR has been shown to co-localise with SOD-IR and nNOS-IR in the neurofilamentous accumulations of ALS motoneurones (Chou et al, 1996). These immunopositive reactions were completely blocked by preadsorption with 3-nitrotyrosine. However, in contrast to these findings, 3-nitrotyrosine-IR was not detected in the spinal cords of mice over-expressing the G37R mutation (Brujin et al, 1997). Furthermore, immunoblotting of whole spinal cord extract or of purified intermediate filaments, from both G37R mice and human patients, revealed two nitrated bands corresponding to NF-L and glial fibrillary acidic protein (GFAP). These bands did not differ from controls in the level of staining (Brujin et al, 1997; Strong et al, 1998). These results suggest that 3-nitrotyrosine elevations detected in transgenic mice and ALS patients are related to elevations of free nitrotyrosine, rather than protein bound levels, casting doubt on the protein nitration hypothesis of ALS.

In assessing the relevance of these hypothesis falsifying results, a number of caveats should be borne in mind. Firstly, Chou et al (1996) reported that the 3-nitrotyrosine

antibody is highly capricious and only worked within very exact dilution and incubation parameters. Brujin does not report either the dilution or the incubation protocols, and this may account for some of the discrepancy in the immunocytochemical results. A similar problem comes from the failure of the author to elaborate the details of the double labelling protocol used. Given that the 3-nitrotyrosine antibody is known to be difficult to use to begin with, immunobinding may well have been reduced by further processing for the second label (ChAT). Moreover, the 3-nitrotyrosine positive staining of the NF-L band, which did not differ between immunoblots from ALS and control spinal cord, failed to disappear after preadsorption with 3-nitrotyrosine in Brujin's study (1997). One cannot rule out the possibility, therefore, that a more specific antibody may well reveal differences in protein nitration between the experimental groups. Finally, Crow et al (1997b) demonstrated that nitration of less than 1% of NF-L tyrosines is sufficient to inhibit neurofilament assembly, whilst Brujin calculates that the antibody is only capable of detecting nitrated tyrosines representing > 3% of total tyrosines at a concentration of 0.16% of NF-L protein, suggesting that the technique employed may be too insensitive to detect significant differences at low levels of nitration. Ultimately, the question of whether NF-L nitration is increased in ALS can only be answered using a more specific technique such as mass spectroscopy.

In Section 1.2(ii) evidence was presented that excitotoxicity may be mediated by the secondary generation of reactive oxygen species (Li et al, 1992; Supko and Johnson, 1992; Puttfarcken et al, 1992). In light of such evidence, McNamara and Friedovich (1993) have argued that ALS may well result from the specific combination of motoneurone vulnerability to glutamate toxicity (Plaitakis, 1990 - see Section 1.3(ii.a)) and the dysfunction of cellular antioxidant forces such as SOD-1. Recent evidence indeed suggests that the ALS-linked SOD-1 mutation increases the vulnerability of motoneurones to excitotoxic injury (Kruman et al, 1999).

1.3.ii.c Autoimmunity, Ca^{2+}, and ALS

The presence of paraproteinemias, malignant neoplasms, and lymphomas in a sub-population of ALS patients (see Rowland, 1995 for a review) combined with the discovery of a cytotoxic element in ALS sera and CSF (e.g. Wolfgram and Myers, 1973; Couratier et al, 1993; Smith et al, 1994), and the generation of autoimmune animal models (Engelhardt et al, 1989) has stimulated interest in the possibility of an autoimmune factor in ALS disease pathogenesis. Although interest has been shown in a number of possible autoimmune mechanisms, in the following text the focus is on theories of autoimmunity to Ca^{2+} channels.

Research into the toxicity of ALS CSF, sera, and IgG, was initiated by the discovery that the serum of ALS patients selectively causes the degeneration of neuronal cell types in anterior horn cultures (Wolfgram and Myers, 1973). No toxicity was observed with the serum from patients with other motoneuronal degenerative diseases, such as Werdnig-Hoffman's disease, suggesting that the toxicity was not secondary to the degeneration of motor neurones per se. Couratier and colleagues (1993) found similar toxicity to rat cortical neurones in ALS CSF, which was shown to be dependent on the activation of AMPA receptors, linking the toxic element to Ca^{2+} entry and excitotoxicity. Purified IgG from ALS patient sera achieved maximal levels of cell death in a hybrid motoneurone cell line - VSC 4.1 - after applications lasting as little as 30 minutes (Smith et al, 1994). Degeneration caused by purified patient IgG continued over a 48 hour period, and could be prevented by a variety of treatments: EGTA (a Ca^{2+} chelator); voltage gated Ca^{2+} channel (VGCC) antagonists ω-conotoxin and AGA IV toxin (antagonists to the N and P type channels found on neurones); pre-incubation with purified L-type VGCCs (from skeletal muscle); pre-incubation with the VGCC α subunit (Smith et al, 1994); and retroviral transfection of VSC 4.1 neurones with the calcium buffering protein, calbindin

(CaBP-D28K) (Ho et al, 1998). Antagonists to the L-type channel, however, were ineffective (Smith et al, 1994). Together these data suggest that ALS IgG are capable of killing neurones by an effect on the alpha subunit of N and P-type VGCCs which causes an elevation of intracellular Ca^{2+} .

Nevertheless, other laboratories have failed to find support for a toxic component. For example, no neuronal degeneration was observed in cultured mouse anterior horn cells in the 5 days following exposure to the sera of 21 ALS patients (Horwich et al, 1974). In addition, no loss of ChAT activity was found in the dissociated spinal cords of human embryos (Touzeau and Kato, 1986) and transverse slices of rat spinal cord (Drachman et al, 1995) following application of ALS sera or purified ALS IgG respectively. The relevance of ChAT activity, however, is not clear. For example, it is known that quantal release is increased in the early alterations of motoneuronal end-plate activity in autoimmune animal models (Uchitel et al, 1992: see later). It follows that the loss of ChAT activity from neuronal death may be balanced by increased ChAT activity in surviving neurones, in order to support these quantal increases. Furthermore, Touzeau and Kato used heat inactivation in serum preparation, which may have affected the binding properties of the IgG.

The idea that the toxic component might immunologically target nerve cells and their Ca^{2+} channels has been further supported by binding studies. In 1986, Dhib-Jalbut and Liwnicz found that serum IgG from a patient with oat cell tumour and paraneoplastic motoneurone disease bound strongly to nervous tissues, but not to other body tissues. They also found that this binding was prevented by preadsorption with neural, but not liver, tissue homogenates. Engelhardt and Appel (1974) also found IgG localised in the motoneurones of ALS patient spinal cords. Subsequent evidence from Appel's laboratory indicated that the binding of ALS sera and IgG was specific to the alpha subunit of

VGCCs (Uchitel et al, 1988; Smith et al, 1992). Other groups have been unable to support this finding using immunoprecipitation of radiolabelled VGCCs (Drachman et al, 1995; Seagar et al, 1995). This same technique was successfully used to prove VGCC binding of auto-antibodies in a disorder now known to be caused by VGCC autoimmunity - Lambert Eaton myasthenic syndrome (LEMS) (in Drachman et al, 1995).

If these antibodies do achieve toxicity by binding to VGCCs, then it would be expected that they would alter the physiological activity of neurones. Indeed, *in vitro* evidence shows that ALS IgG increases spontaneous transmitter release from motor nerve terminals (Uchitel et al, 1988). Furthermore, whilst decreasing the peak amplitude of the voltage gated Ca^{2+} current through L-type channels in skeletal myotubules (Delbono et al, 1991) purified ALS IgG also increases current flow through P-type VGCCs in Purkinje cells and in lipid bilayers (Llinas et al, 1993).

The most compelling evidence for the autoimmune hypothesis comes from the successful generation of animal models by Appel's laboratory. Inoculating guinea pigs with bovine motoneurones causes the development of a degenerative motor neurone disease known as experimental autoimmune motoneurone disease (EAMND), involving muscle denervation and neuronal cell death, accompanied by clinical signs of motor deficits and reduced muscle tone (Engelhardt et al, 1989). In these animals, strong IgG staining was found within motoneurones and yet not in other cell types. In addition, IgG reactive to bovine and guinea pig motoneurones was purified from their sera, suggesting a selective immune response.

A series of passive transfer experiments followed, where antibodies from ALS patients and EAMND guinea pigs were injected into mice, either intraperitoneally (Appel et al, 1991; Engelhardt et al, 1995) or subcutaneously over superficial muscles (Uchitel et al,

1992). Although these experiments failed to produce a measurable motor deficit, substantial physiological and ultrastructural alterations were observed. Physiologically, passive transfer has been shown to produce an increased frequency of miniature end plate potentials (MEPPs) (Appel et al, 1991; Uchitel et al, 1992) and increases in quantal release and spontaneous transmitter release (Uchitel et al, 1992). Ultrastructurally, these changes are reflected in significantly increased vesicle density at motor nerve terminals and in presynaptic terminal boutons synapsing on motoneurones (Engelhardt et al, 1995). Other ultrastructural alterations included increased mitochondrial density and Golgi dilation; increases in Ca^{2+} precipitates in mitochondria, vesicles, Golgi, and rough endoplasmic reticulum (RER); increased phosphorylation of neurofilaments; and IgG localised to all structures found to contain elevated Ca^{2+} precipitates (Engelhardt et al, 1995). These changes were not seen in cerebellar Purkinje neurones or local glial cells. Current research in our laboratory supports these observations, with ultrastructural signs of neuronal degeneration in the spinal cords of mice injected with ALS IgG coupled with atypical Ca^{2+} deposition in the Golgi and in presynaptic terminals (Pullen, 1999).

In spite of the strong support for an autoimmune aetiology in ALS, a number of factors need to be resolved. Firstly, a number of laboratories have failed to find supporting evidence for the binding of ALS IgG to VGCCs. Given that the hypothesis of VGCC binding antibodies in ALS sera is central to the theory, the reasons for the problems in replicating these findings need attention and elucidation. Besides issues of antibody binding, it is not clear how circulating antibodies might gain access to spinal motoneurones - another area requiring more probing investigation. Furthermore, clinical trials of immunosuppression have not produced any significant effect on disease progression or mortality (e.g. Drachman et al, 1994). Nevertheless, this remains an exciting area of ALS research and adds support to the notion that abnormal Ca^{2+} regulation is an important component of the pathogenesis in ALS.

1.3.iii. Axotomy and Ca^{2+}

In the work carried out in this thesis, axotomy will be used as an experimental nerve injury to investigate the possibility of differences in the responses of ALS-vulnerable and ALS-resistant motoneurones. Axotomy involves the transection of nerve axons and is associated with a host of alterations, extending beyond the axotomised neurone itself. Of particular interest to this thesis are the changes noted in $[Ca^{2+}]_i$ in axotomised neurones.

The first clue to the involvement of Ca^{2+} influx in the neuronal alterations after axotomy came from work on Wallerian degeneration. Wallerian degeneration descibes the "dying back" of the nerve axon which occurs after transection, first observed by Waller in 1850 (in George et al, 1995). In the early 1970s it was shown that post-axotomy degeneration was delayed by the Ca^{2+} chelator, EGTA, whilst added Ca^{2+} sped up the process (Schaepfler et al, 1973; Schaepfler et al, 1974). More recent evidence using Ca^{2+} imaging has shown that within the first three minutes after axotomy, local concentrations of $[Ca^{2+}]_i$ dramatically increase to levels of over 1 millimolar, in comparison to several 100s of micromolar distal to the lesion (Ziv and Spira, 1995) and concomitant activation of Ca^{2+}-dependent proteolysis (Gitler and Spira, 1998). Indeed levels of 200 micromolar have been found to be sufficient to initiate degeneration (George et al, 1995). Furthermore, the degeneration of axotomised DRGs in the mouse pup has been shown to be prevented by addition of EGTA, VGCC inhibitors, and calpain inhibitors (George et al, 1995). Nevertheless, recent findings show that, in aplysia, the Ca^{2+} dependent activation of calpains is required for the formation of a growth cone *in vitro* (Gitler and Spira, 1998) suggesting a paradoxical contribution of Ca^{2+}-dependent proteolysis to degenerative and regenerative alterations after axotomy.

Recent speculations focus on excitotoxicity as a mediator of axotomy-induced neuronal changes and death. Rossi and colleagues (1994) noted the similarity of the ultrastructural effects of axotomy and kainic acid exposure in rat cerebellar Purkinje cells, proposing common mechanisms of Ca^{2+} overload. Similarly, neurones resistant to MPTP induced degeneration in the SNc are immunoreactive for the calcium buffering protein, calbindin (Ng et al, 1996), and have recently been shown to be less sensitive than non-calbindinergic nigral neurones to medial forebrain bundle transection (Alexi and Hefti, 1996). Thus the expression of a Ca^{2+} buffering protein in this cell type may be protective against axotomy-induced Ca^{2+} damage. Furthermore, the expression of the Ca^{2+} impermeable AMPA receptor subunits, GluR2/3, has been shown to decrease after axotomy (Kennis and Holstege, 1997; Tang and Sim, 1997), causing an increase in the proportion of Ca^{2+} permeable AMPA receptors (i.e receptors lacking GluR2: Geiger et al, 1995) on the neuronal membrane and presumably, therefore, increasing the Ca^{2+} entry produced by presynaptic glutamate release.

More direct support comes from the ability of treatments aimed at reducing $[Ca^{2+}]_i$ to protect axotomised neurones. For example, the Ca^{2+} channel antagonist, cinnarizine has been found to prevent the degeneration and death of axotomised rat dorsal root ganglia (Eichler et al, 1994) and in the neonatal rat, where axotomies lead to cell death for the majority of affected neurones (Lowrie et al, 1982; Lowrie et al, 1987), both antiglutamatergic treatments and Na^+ channel inhibition were effective at preventing neuronal death of axotomised facial neurones (Casanovas et al, 1996).

Physiological studies suggest that ionic currents are altered in axotomised neurones. Surprisingly, evidence has been found for decreased Ca^{2+} conductances in axotomised neurones of the bullfrog sympathetic ganglion (Jassar et al, 1993), the guinea pig dorsal motor nucleus of the vagus (DMV) (Laiwand et al, 1988), and the rat sciatic dorsal root

ganglion (Eichler et al, 1994). Nevertheless, resting Ca^{2+} has been found to be unaltered in axotomised rat sympathetic ganglion cells and the kinetics of the Ca^{2+} current significantly slowed, leading to a prolonged exposure of the neurone to peak Ca^{2+} levels (Sanchez-Vives et al, 1994). Na^{+} conductance and channel density, by contrast, has been found to be increased in axotomised goldfish Mauthner cells (Titmus and Faber, 1986) and bullfrog sympathetic ganglia (Jassar et al, 1993). In a review of the area, LoPachin and Lehning (1997) concluded that the observed importance of $[Ca^{2+}]_I$ in mediating axotomy induced degeneration of neurones probably derived, not from increased conductances, but the reversal of the Na^{+} /Ca^{2+} exchanger, triggered by excessive levels of Na^{+} .

1.4 Summary and Hypotheses

At the outset of the introduction, three hypotheses were outlined, postulating the existence of:

1. segmental differences in baseline levels of relevant proteins between motoneuronal groups, which might be predictive of a difference in response to injury
2. differences in the pre- and post-injury profile of motoneurones in terms of proteins involved in cytotoxic or protective pathways (i.e. the cytotoxic/cytoprotective capacity of the motoneurone)
3. segmental differences in post-injury alterations of antigenicity, examination of which prior to injury revealed no distinctive differences from one motoneuronal group to the next

The proteins of interest have been selected on the basis of the arguments presented above concerning the involvement of calcium in excitotoxicity, ALS, and axotomy. The first two proteins are calcium binding proteins, calbindin (CaBP-D28k) and parvalbumin (PV), which are believed to buffer the neurone against high Ca^{2+} levels (see Baimbridge et al,

1992). Acting downstream of Ca^{2+} influx are calmodulin (CM) and the serine-threonine phosphatase, calcineurin (CaN). These are ubiquitous in the nervous system and have been implicated in a variety of pathways, including apoptosis (Wang et al, 1999) and modulation of calcium channels (Zhu and Yakel, 1997). Both of these proteins are also required for the activation of neuronal nitric oxide synthase (nNOS), implicated in free radical generation and excitotoxicity (Dawson et al, 1991; Dawson et al, 1993), and this is the fifth protein selected for study. Cu-Zn-superoxide dismutase (SOD-1), the free radical scavenging protein implicated in the pathogenesis of FALS (e.g. Rosen et al, 1993; see Section 1.3.2.ii), is the final antigen to complete the battery.

In an examination of segmental variability in immunostaining for these proteins, particular attention will be paid to the motoneurones of the sacral cord in Onuf's nucleus (ON). As was discussed in section 1.3.1, ON is a group of neurones arguably defined as alpha motoneurones by virtue of their innervation of striated musculature and ultrastructural features such as the formation of C-type synapses on their somas (Pullen, 1988). Nevertheless, this nucleus occupies an unusual position due to its prolonged resistance to ALS (and indeed other motoneuronal pathologies such as Werdnig Hoffman's disease (Sung and Mastri, 1980) and poliomyelitis (Sung, 1982)). For this reason, differences between ON and other motoneurones will be closely examined.

It has already been asserted that ON is different from other motoneurone groups in its relative levels of calcium binding protein (Alexianu et al, 1994) and nNOS (Pullen et al, 1997). It is the intention that in this study the immunoreactivity of motoneurones for these proteins will be quantified, in order to more stringently test this hypothesis. Furthermore, a full comparison with other segments will be made for all of the proteins listed above.

Finally, in carrying the notion of differential segmental responses one stage further, this thesis will compare the post-axotomy changes in immunoreactivity for these proteins with those of ALS-vulnerable motoneurones, such as those controlling limb muscles. To represent this group, the sartorius nerve branch of the femoral nerve has been selected for practical reasons, since it is easily accessible in surgery and the site of transection is approximately 10 cm from the spinal cord, as is also the case with transection of the pudendal nerve. Axotomy has been selected as it is an injury type that can be produced in a predefined population of motoneurones, and is associated with increases in $[Ca^{2+}]_i$ (see Section 1.3.3 above).

Studies will be performed in cat, since the topography of ON is closer to the human than in the rodent, and this preserves continuity with the previous work done in this laboratory. Since the localisation of the proteins examined in this study has been largely undocumented in the cat, the first part of the work, aimed at establishing normal localisation of these proteins in cat ventral horn, also provides important comparative data that is currently absent from the literature.

CHAPTER 2

METHODS AND MATERIALS

2.1: PHASE 1: MOTONEURONAL AND INTERNEURONAL ANTIGENIC PROFILE OF ADULT CAT

2.1.i Animals: (See Table 2.1-1) Six out of eight adult animals had previously undergone surgery to injure the axons or cell bodies of either sacral or thoracic motoneurones, however tissue from the injured segments was not included for analysis. The results from the uninjured segments of these animals did not differ from the findings in normal unoperated controls and hence these animals have been included in the results section as controls. The average age was 18 months, and there were 3 males and 5 females.

Table 2.1.-1. Animals used for Phase 1.

Expt Code	Sex	Weight	Date Of Sacrifice
cont 1	f	2.6kg	11/03/97
cont 2	f	2.15kg	03/02/97
cont 3	f	2.54kg	26/02/97
cont 4	m	2.2kg	14/04/97
cont 5	m	2.5kg	30/04/97
cont 6	f	2.46kg	27/05/97
norm 1	m	2.01kg	21/05/97
norm2	f	2.1 kg	23/06/97

Note: experiment codes beginning with 'cont' indicate control tissue used from experimental animals. Experiment codes beginning 'norm' indicate the use of animals which have not been subjected to experimental neuronal injury. These animals had, however, received intramuscular injections of retrograde tracers.

2.1.ii Perfusion: Young adult cats were anaesthetised with Domitor (medetomidine: 1mg/ml: 0.1mg/kg) and Ketaset (ketamine: 100mg/ml: 0.6 mg/kg). Terminal perfusion was initiated only once pupillary and extensor reflexes were absent. Animals were perfused transcardially, initially using a saline rinse (300-400ml 0.9% NaCl) to exsanguinate the blood vessels. Colouration of the liver was used as an indicator of blood clearance before the introduction of the fixative (4% paraformaldehyde, 0.5%

glutaraldehyde, in .02M PBS: pH = 7.3). Both saline rinse and fixative were warmed to around 30°C in order to decrease total peripheral resistance (TPR).

2.1.iii Tissue: The spinal cord was exposed by dorsal laminectomy. The intercostal nerve of the 13th rib was used to identify the dorsal roots of T13, and this segment was removed. Segments C7, L4-6, and S1-3 were identified by the location of their dorsal roots in relation to T13, and were also removed. Depending on the quality of fixation assessed by tissue hardness segments were cut into 3mm slices and post-fixed in the same fixative used for the perfusion for a period of 1-2 hours. 30-40μm thick sections were cut on a vibratome and placed in phosphate buffered saline containing 20mM glycine (PBS-gly). The glycine was added to unmask antigenic sites bound by fixative aldehyde carboxyl groups.

2.1.iv Immunocytochemistry: To reduce the possibility of artefactual differences in immunoreactivity (IR) between sections from different segmental levels arising, sections from all four segments were processed together for each antibody. Within each set of sections, care was taken to ensure that no two sections came from points in the spinal cord separated by less than 240μm longitudinally. This distance is greater than the major cell body diameter of any cell type described in the spinal grey matter and ensured that no individual cell could be analysed more than once after immunocytochemical processing.

To reduce non-specific antigen binding, tissue was incubated for 60 minutes at RT in 20mM PBS-glycine containing 5% foetal calf serum (FCS) and 5% normal goat serum (NGS), plus 1% bovine serum albumin (BSA). .02% saponin was added as tissue solubilizer in order to assist access of the antibody to the antigen.

Sections were washed 5 times, at 5 minutes per wash, in 20mM PBS-glycine before incubating in 1° antibody, diluted in 20mM PBS containing 20mM glycine, .02% saponin, 1% BSA, 1% FCS and 1% NGS. Incubations were at 4°C - dilutions and incubation times are given in Table 2.1-2. After a further 5 washes (as before) the tissue was incubated in diluted link antibody at 37°C for 3-4 hours (dilutions in Table 2.1.-2). The same buffer as had been used to dilute the 1° antibody was used for dilution of the link antibody (see above), which consisted of a biotinylated IgG raised against the species from which the primary antisera had been derived.

Following five 5 minute washes in 20mM PBS only, the tissue was placed in streptavidin-biotin-HRP at a dilution of 1:200 in buffer (20mM PBS containing 0.1% BSA, 1% FCS and 1% NGS), overnight at 4°C. Finally, and after a final five washes in 20mM PBS, label was visualised using 3-3 diaminobenzidine (DAB) with 0.18ml of 6% H_2O_2 as an activator. Sections were mounted in aquamount on glass slides and then coverslipped.

2.1.v Dilutions: To identify the optimal dilution, a range of dilutions were used in preliminary experiments bracketing the manufacturer's recommended dilutions.

Table 2.1-2 Dilution and incubation details for all primary and link antibodies used

1° Antibody	Manufacturer	Host species	Dilution	Incubation Time	Temp.
nNOS	Affiniti	rabbit	1:800	2 nights	4°C
CaN-β	Sigma	mouse	1:2000	overnight	4°C
CaBP-D28k	Sigma	mouse	1:200	overnight	4°C
CM (clone 6D4)	Sigma	mouse	1:2000	overnight	4°C
PB	Sigma	mouse	1:2000	overnight	4°C
SOD	Calbiochem	sheep	1:50	2 nights	4°C
Link Antibody	Manufacturer	Host species	Dilution	Incubation Time	Temp.
mouse	Amersham	sheep	1:200	3-4 hrs	37°C
rabbit	Amersham	donkey	1:200	3-4 hrs	37°C
sheep	Vector	goat	1:300	3-4 hrs	37°C

Optimal dilutions were evaluated visually on the basis of the resulting signal:background ratio. These dilutions are shown in Table 2.1-2.

2.1.vi Analysis:

Data were obtained from photographs of selected sections taken at a variety of magnifications, which were scanned into a PC. The resulting images were converted into grayscale format whereupon measurements were taken for individual neurones. Measurements were made in SigmaScan Version 2.0, which was used to calculate the average optical density, maximum diameters, and minimum diameters of the areas selected.

Average density of the grey matter background and white matter background were generated in the same manner, with care taken to avoid measuring other obvious structures when sampling the background. The density of each neurone was subsequently expressed as a percentage of the grey matter and white matter backgrounds.

Since size was one of the criteria used for distinguishing motoneurones from interneurones, neurones were measured from each experiment to verify that the presumed interneurones and motoneurones were within appropriate size ranges. Cell measurements were made from photographs taken at magnifications of 200x-400x. The minimum and maximum diameters were recorded and geometric means were calculated using the equation: $X = \sqrt{(D \times d)}$, where 'D' is the major diameter of the cell and 'd', the minor, and both diameters bisect one another.

2.2 PHASE 2: MOTONEURONAL AND INTERNEURONAL ANTIGENIC PROFILES AFTER INJURY

2.2.i Animals: see Table 2.2-1.

Table 2.2-1. Details of animals axotomised in Phase 2.

Expt Code	Sex	Weight	Days of Recovery
adsax1	f	2.6kg	13
adsax2	m	3.3kg	7
adsax3	m	4.2kg	7
adsax4	m	4kg	7
adsax5	f	3.2kg	14
adlax1	m	2.7kg	14
adlax2	m	2.7kg	14
adlax3	m	2.9kg	14

2.2.ii Sacral Axotomy: Under aseptic conditions, five adult cats underwent surgery to axotomise the pudendal nerve.

Animals were anaesthetised with medetomidine (1mg/ml; 0.1 mg/kg) and ketamine (100mg/ml; 0.6mg/kg). An incision was made on the right flank starting just lateral to the base of the tail, proceeding rostrally in continuance with the line of the tail for approximately 4cm. The pudendal nerve was exposed approximately 3 cm from its entry into the external anal sphincter and immediately proximal to the emergence of the branch to the urethral sphincter. The entire pudendal nerve was tightly ligated, sectioned immediately distal to the ligature, and a 5mm portion of the distal nerve stump was removed to prevent the rejoining of the two ends of the sectioned nerve.

Three animals were perfused one week after the surgery and three animals were perfused two weeks after surgery. One animal (adsax 6) also underwent surgery to axotomise the sartorius-innervating nerve branch of the femoral nerve (see 2.2.iii).

Figure 2.2-1

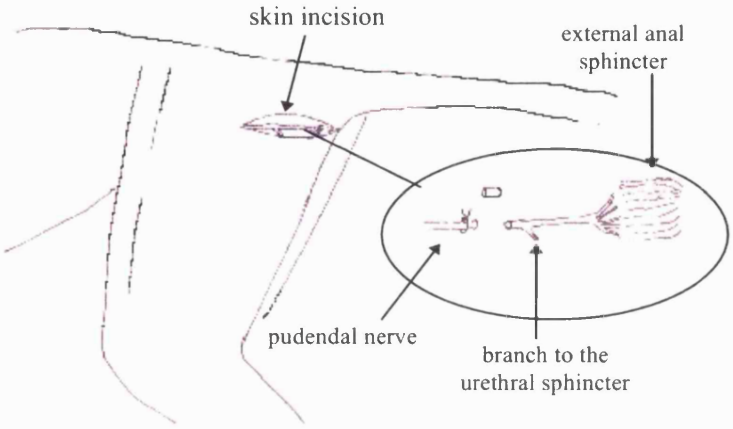

The pudendal nerve is found through a skin incision running rostrally from the base of the tail. The enlargement shows the ligature and removal of a piece of nerve prior to the emergence of the urethral branch of the pudendal nerve. The identity of the nerve can be verified in situ by locating the fan formed as the nerve separates to penetrate the external anal sphincter muscle, also shown in the enlargement.

2.2iii Lumbar Axotomy: Under aseptic conditions, three adult cats underwent surgery to axotomise the branch of the right femoral nerve innervating the sartorius muscle. Animals were anaesthetised with medetomidine (1mg/ml; 0.1mg/kg) and ketamine (100mg/ml; 0.6mg/kg). An incision was made on the lateral flank, following the line of the sartorius muscle (see figure 2.2-2). Using blunt dissection between the sartorius and tensor fasciae latae muscles, the nerve branch innervating the sartorius was located and followed into the muscle to verify its identity (see figure 2.2-3). The nerve was ligated and a short section of 3-5mm was removed (see figure 2.2-4).

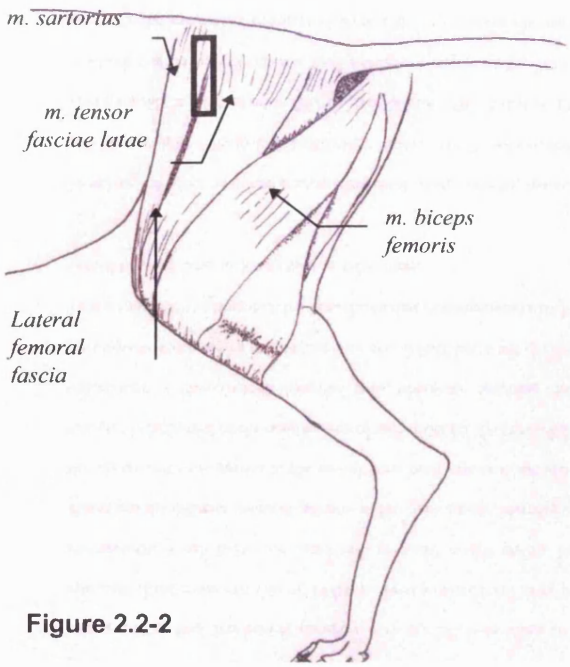

Figure 2.2-2

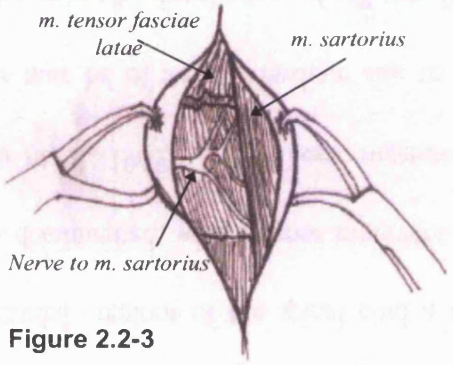

Figure 2.2-3

Figure 2.2-2. The superficial musculature of the cat hindlimb. The box indicates the location of the skin incision for the axotomy.

Figure 2.2-3. Dissection to show the location of the nerve branch innervating *m. sartorius* under *m. tensor fasciae latae,* a portion of which has been removed.

Figure 2.2-4. Axotomy of the nerve branch to *m. sartorius.* Two ligatures are made before the removal of a small piece of nerve.

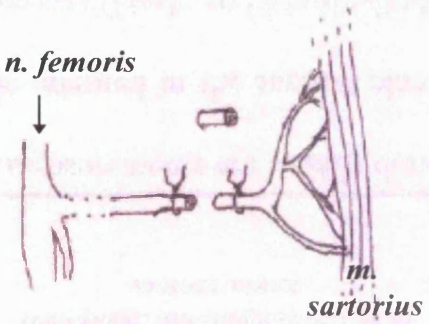

Figure 2.2-4

2.2.iv. Perfusion, Tissue, Immunocytochemistry, Dilutions: Perfusion technique, tissue removal and subsequent immunocytochemical processing methods were identical to those used for examination of normal adult tissue (see 2.1). To aid identification of the injured motoneuronal cell group, a small nick was made in the dorsal horn contralateral to the operated side after the dorsal laminectomy and before removal of the segments. Sartorius motoneurones were identified with reference to the retrograde labelling experiments of Vanderhorst and Holstege (1996) and Gordon et al (1991).

2.2.v. Analysis: At the beginning of this phase of work, I was fortunate enough to acquire a CCD video camera (Sony CC-IRIS), allowing the development of a new technique for translating the optical information into digital images. Advantages of this system were that it avoided extra interference with the image resulting from the photographic technique, which formerly interposed three steps into image acquisition in the form of developing, printing, and scanning.

Preliminary testing of the video camera showed it to be linear in its representation of a printed grayscale, making it highly likely that the optical density relationships between foreground and background components would be preserved from tissue to screen. In setting up the camera automatic gain control was turned off and in order to maximise linearity it was found that the framegrabber card (IntegralTech Flashbus MV-Lite) needed to have its contrast level set to the maximum, and brightness set to zero. With these settings in place the computer image appeared on visual inspection identical to the simultaneous output of the camera directly into a normal TV monitor. Thereafter only the light levels of the microscope lamp were modulated, keeping the background where possible within a range of 180 - 200 grayscale, where the camera was found to be the most linear. Under these conditions, the correlation between grayscale measurements made from a scanned photographic image of a grayscale and the same grayscale acquired through the CCD was 0.998. The calibration curves for the scanned photograph (fig. 2.2-5) and the digitally acquired image (fig 2.2-6) are shown below.

Figure 2.2-5

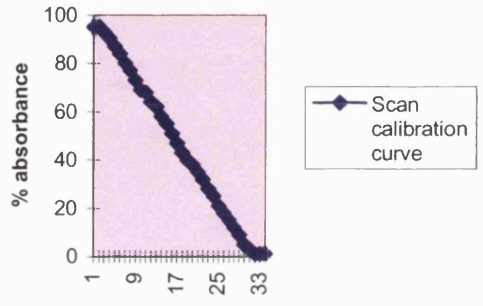

Figure 2.2-6

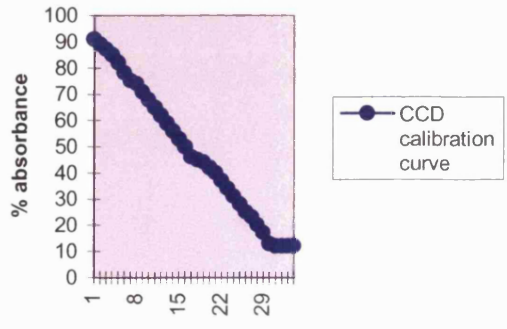

Measurement of a range of neurones

In order to derive a broad range for staining values, most of the ventral and intermediate neurones encountered were measured and grouped. The non-motoneuronal groups defined were: ventral horn interneurones, neurones of the VSCT (identified by size and position), autonomic neurones, neurones of Clarke's column, and neurones close to the central canal with commissurally oriented processes, which were defined as commissural neurones. The later comparisons that refer to ventral horn interneurones were made only with the group of small, multipolar or bipolar neurones in the ventral horn that lay dorsal to the motoneuronal groups identified. These neurones frequently possessed large numbers of processes and differed from the cells defined as motoneurones in a number of ways - please see Chapter 3 for a full discussion.

Comparisons between axotomised sartorius motoneurones and controls

At the time that initial lumbar motoneurones were measured, it was intended that the comparative injury would be done in the intercostal nerves. Hence, sartorius motoneurones were not specifically measured in the controls. Due to a poor sample of clearly identifiable motoneurones in the control thoracic cord, it was anticipated that injury results may prove difficult to ascertain statistically. This was because the motoneurone groups analysed in other segments were more discretely segregated within the ventral horn: there was less confidence associated with the identification of thoracic motoneurones and many ventral horn neurones were thus excluded from analysis at this segmental level. By the time the decision had been taken to injure the sartorius nerve in place of the intercostal, control tissue was nearly 2 years old and staining levels had significantly deteriorated such that it was no longer possible to generate control baseline values for sartorius. Because of this, it was necessary to compare the values of injured sartorius motoneurones with those of control lumbar motoneurones as a general group. Nevertheless, these were derived from the same segmental levels as sartorius motoneurones. Within-subject comparisons were also made between axotomised sartorius motoneurones and lumbar motoneurones either in the same sections but belonging to a different motor column (iliacus) or from L6-L7 - the results of these are discussed fully in Chapter 4.

Measurements were made using SigmaScan Version 2.0 as detailed in 2.1.vi above.

2.3. DEVELOPMENT OF A QUANTITATIVE APPROACH

Given the inherent variability in the immunocytochemical technique, a form of quantification was required that allowed a comparison of relative values instead of absolute values. In order to overcome problems arising from the subjectivity of the experimenter's perception, these relative values nevertheless had to be derived from absolute values. The data were therefore normalised as follows.

For each experiment the entire range of staining was calculated from the individual stain levels taken from each measured neurone of all measured cell types. It was important to measure a variety of neuronal types other than the neurones of interest to generate the broadest possible range of stain intensities within which the neuronal type of interest could be placed. That range was then broken down into 9 equal data bins, which were numbered from 1-9.[1] The actual grayscale measurement expressed as a % of background for a single neurone could then be replaced by the corresponding number of the data bin into which it fell. For each neuronal sub-type two useful forms of expression of the resulting data could then be used: 1. the mean bin location (MBL) and 2. the frequency distribution of a population of measured neurones across all nine bin locations.

It was found that data normalised in this way provided results that were much more comparable between experiments than absolute values. Two animals might have motoneurones with statistically different mean absolute staining intensities but, when normalised with reference to the staining range for the experiment, very similar MBLs.

[1] In comparison to the normal practice of selecting 3-4 data bins in qualitative work, it was found that a larger number of bins increased the sensitivity of the technique. An odd number was preferable since it improved the visual impact of graphical presentations by providing a central focal point. Finally, it was felt that any more than ten bins would become unwieldy to manage, leading to the choice of 9 data bins as

Furthermore, this technique provided a means of measuring relative shifts in staining intensities, so that after axotomy changes in distributions of data across bin locations could be tested.

2.4. ANTIBODY CONTROLS

2.4.1 Ca^{2+}

To control for the effects of Ca^{2+} on the immunoreactivity of Ca^{2+} -binding proteins, in one experiment either Ca^{2+} or the Ca^{2+} chelator, ETHYLENE GLYCOL-bis(β-AMINOETHYL ETHER) N,N,N',N'-TETRAACETIC ACID (EGTA), was added to the primary antibody prior to incubation. Only CM showed a clear effect, and hence all subsequent incubations with anti-CM took place in the presence of 18mM Ca^{2+} .

2.4.2 Calcineurin

Antibodies against the two subunits of calcineurin, designated by the manufacturers α and β and corresponding to the A and B subunits described by Strack et al (1996), did not stain coincident populations of neurones. CaN-A only gave rise to immunostaining in the dorsal horns or occasionally in some ventral horn interneurones. The antibody against the B subunit stained a large group of cells described as CaN-IR elsewhere in the literature (Strack et al, 1996; Goto et al, 1990). Given that the A subunit is the catalytic site of the protein it would be expected that it should be found in the same or at least in a largely overlapping population of cells. Since the A subunit is found in two isoforms, designated α and β, of which α is the common form, it was thought possible that the Sigma antibody may have been picking up the minor β isoform. The first priority was then to find out which isoform of the A subunit was picked up by the antibody to CaN-A. Purified rat brain CaN-Aα, the major isoform which was kindly donated by Professor B.

---

a suitable representation of the data.

Perrino, was used in an immunodot procedure to test the specificity of the antibody.

2.4.2i Immunodot assay

CaN-Aα was diluted in TRIS buffered saline (TBS: 20mM TRIS-base with .9%NaCl, pH 7.4) containing .05%BSA, giving final concentrations of CaN-Aα of .2μg, .02μg, and .004μg. 1μl drops of each concentration of CaN-Aα and 1μl drops of cat serum, normal goat serum, and TBS, were placed on a pair of .45μm nitrocellulose membranes (6cm x 1cm), with each drop separated from the last by approximately 5mm.

Membranes were air-dried for 30 minutes and then non-specific antigenicity was blocked by incubating membranes in 20mM TBS (pH 7.4) containing 5% BSA and 5% FCS at RT for 1 hour. The membranes then went through three 5 minute washes in 20mM TBS containing .1% BSA.

Primary antibodies to CaN-α and CaN-β were diluted in 20mM TBS (pH 7.4) containing 1% BSA and 1% FCS, at dilutions given in Table 2.1-2. The membranes were incubated in diluted primary antibody overnight at 4°C and then washed twice, for 10 minutes each wash, in 20mM TBS (pH 7.4) containing 0.1% BSA.

The resulting immunodots showed that purified CaN-Aα was only detected by the antibody raised against CaN-β (fig 2.4.2-1). Since it remained unclear what the antibody to CaN-α was detecting, and it did not stain any ventral horn neuronal populations, this antibody was omitted from subsequent experiments. Neurones stained by the antibody to "CaN-β" will hereafter be described as CaN-A-IR.

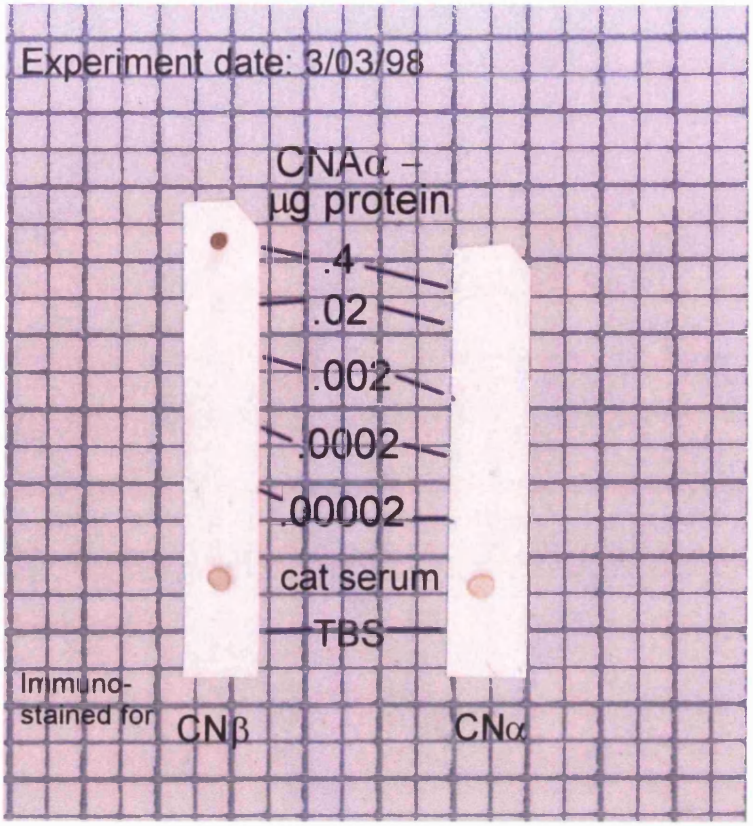

Figure 2.4.2-1. The detection of purified CaN-Aα by antibodies to different CaN subunits.

CHAPTER 3.

THE NORMAL ADULT CAT

3.1.1 Cell types and sizes

A number of parameters were used to help identify and differentiate between motoneurones and interneurones: numbers of visible processes, cell position in conjunction with size, cell size and shape. Qualitative evaluation of these features during measurement enabled the neurone to be categorised as either a motoneurone or interneurone. Post-hoc, the validity of the qualitative observations was confirmed by the measurement and analysis of both size and shape index.

In addition to the use of morphological cues, some stains aided the process of differentiation by the distinctive labelling pattern produced for different cell types. For example, with the Ca^{2+} binding protein PV small interneurone-like cells in medial and dorsal areas were intensely labelled. These often gave rise to many darkly stained fine processes traceable some distance from the soma. In contrast, cells designated to be motoneurones were ventrally located, in regions consistent with anatomically described motor nuclei. These were quite distinct from the interneurones described above in that they were usually devoid of stain, and were frequently paler than the neuropil, giving rise to the appearance of "holes" in the tissue. Processes from these larger cells were rarely visible and were never IR. In addition, the large pale cells were rounded in shape, compared to the elongated appearance of the darkly stained presumed interneurones.

In order to verify the qualitative impression of size and shape differences, geometric mean diameters were calculated according to the equation $X = \sqrt{D \times d}$, where 'D' represents the length of the major axis and 'd' the length of the minor axis, and differences between geometric means for presumed

motoneurones and presumed interneurones were found to be highly significant (t-test: $p < .00001$). Motoneurones of ON were considered separately as they are widely reported to be smaller in size than average motoneurones (e.g. Sato et al, 1978) and, indeed, their mean diameter was found to be intermediate to that of other motoneurones and interneurones (Fig. 3.1.1-1B). A scatterplot of minimum versus maximum diameters can be seen in Figure 3.1.1-1A. and a summary of the mean cell diameters for presumed motoneurones and interneurones in Figure 3.1.1-1B.

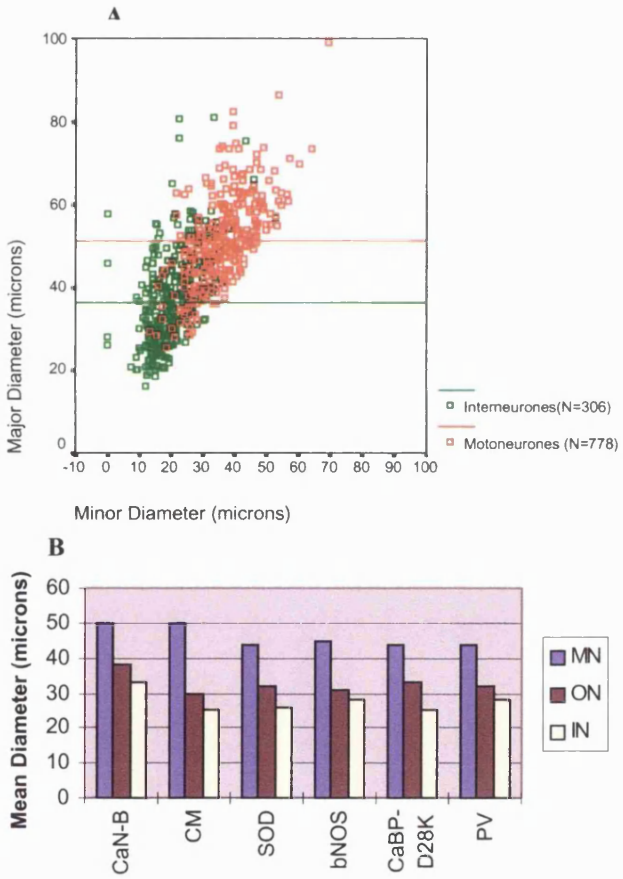

Figure 3.1.1-1. **A. To show the relationship between the minimum and maximum diameters of presumed motoneurones and interneurones. The mean maximum diameter for each neurone type is indicated by the horizontal line. The area between these two lines, where the overlap in cell size lies, shows clearly the differences in D:d ratio between motoneurones and interneurones. Interneurones with the same maximum diameter as motoneurones in this area are found shifted to the left of the motoneurones, because of their shorter minor axes. B. The mean diameter of motoneurones of ON (N=478), other motoneurones grouped from all spinal levels (N = 1940) and interneurones (N = 1074).**

As can be seen from figure 3.1.1-1B, estimates of mean diameter of all cell types were elevated in sections stained for CaN-B. This elevation was shown to be significant using a one-way ANOVA ($p < .002$), which also showed the three

cell types to be significantly different from one another in mean diameter ($p < .0001$). Other than this, the results from the remaining five antigens were not statistically distinguishable from one another. Furthermore, frequency distributions for the mean diameter of all cell types fitted the normal curve well and with minimal skewness.

In addition to the observed overall size difference between cells designated as interneurones and those designated as motoneurones, it was also apparent that where the interneuronal maximum diameter is similar to motoneuronal maximum diameter, the minimum diameter of the interneurone tends to be far smaller than that of the motoneurones (see Figure 3.1.1-1A).

Shape index (SI) was calculated using the formula;

$$\frac{4\Pi.A}{p^2}$$

where 'A' = area calculated by the formula;

$$\Pi Dd$$

and where 'p' is the perimeter, calculated by the formula;

$$\Pi \sqrt{2(D^2 + d^2)}.$$

The resulting figure lies somewhere between 0 and 1, where 1 is circular. Shape index analyses were carried out on a sample of 3592 neurones, and a highly significant difference (T-test: $p < .0001$) was found between the shape of presumed motoneurones (mean = .92) and interneurones (mean = .84). The

Further notes on the identification of motoneurones

A number of unsuccessful attempts were made to utilise double-labelling techniques in order to verify the identity of the motoneurones in conjunction with immunocytochemical labelling. Retrograde labelling of the motoneurones of ON and SART was carried out by the injection of fast blue (n=1), fluorogold (n=1) and CTB-HRP (n=1) into the anal sphincter muscle and the sartorius muscle. In each case, tissue was subsequently processed using the immunocytochemical protocols outlined in the methods section, but in the animal labelled using CTB-HRP, a fluorescent secondary antibody was used (Texas Red). In all three animals, subsequent immunocytochemistry led to the dilution of the fluorescent or HRP signal such that motoneurones were no longer clearly identifiable. Due to animal availability and time constraints, the decision was taken to rely on the parameters discussed in section 3.1.2 for the identification of relevant motoneurone groups. The maps included below demonstrate the location of motoneurones innervating sartorius and anal and urethral sphincter muscles as revealed by retrograde HRP labelling in our laboratory (ON) and in that of Gordon, Loeb and Richmond (1991) (sartorius).

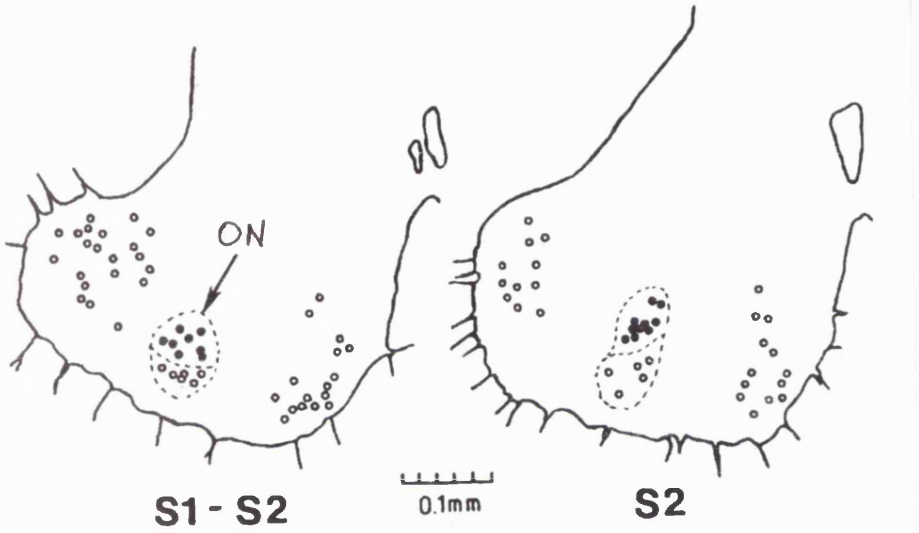

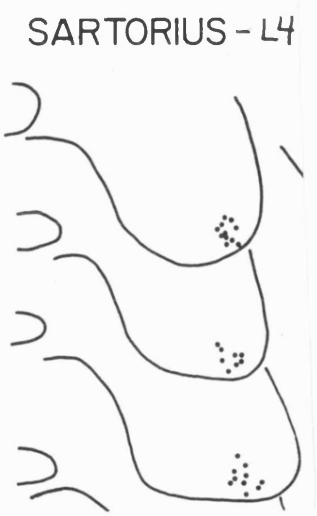

magnitude of the difference between the SI for motoneurones and interneurones appeared to be related to the antigen's localisation (see Table 3.1.1-1 below), such that, for antigens localised within the cell body only (nNOS, CaN-B, and SOD), the mean SI difference of motoneurones and interneurones was .048, representing 5% of the mean SI, whilst for antigens localised within the cell body and processes (CaBP-D28k, PV, and CM) the mean difference was .094, or 10% of the mean SI. This effect was non-significant ($F = 0.8$, $p = 0.6$).

Table 3.1.1-1 The difference between motoneuronal and interneuronal shape indices by antigen.

	Motoneurones	Interneurones	Difference
nNOS	0.91	0.88	0.03
CaN-B	0.917	0.871	0.046
SOD	0.901	0.832	0.069
PV	0.899	0.82	0.079
CaBP-D28K	0.921	0.84	0.081
CM	0.939	0.817	0.122

3.1.2 Discussion

3.1.2i Identification of motoneurones and other neuronal subtypes

For the purposes of this study it has not been possible to use labelling methods ideally suited to distinguishing motoneurones from other ventral horn cell types. To be certain of restricting such label to α-motoneurones only, lengthy physiological recording procedures followed by the labelling of a single cell are necessitated; procedures which are here precluded firstly by the number of segmental levels to be characterised and secondly the focus of this study on groups of cells of differing types. Previous work in the laboratory has utilised the injection of retrogradely transported label into the pudendal nerve to label ON (Pullen, 1988), and the labelled tissue resulting from this procedure was used as a reference template in the present study.

To a certain extent, therefore, in these experiments the identification of α-motoneurones has depended on criteria arising from the results of other studies. These morphological criteria are pattern of IR for certain antigens, cell shape, soma size, and number of primary dendrites. The number of dendrites was not analysed statistically in the present study, but was used in the decision making process at the point of assignment (as motoneurone or interneurone). The remaining three criteria - IR, size, and shape - were measured and will be discussed below.

3.1.2ii Distinguishing cells by immunostaining

As mentioned earlier, the task of identifying neuronal subtypes was made somewhat easier when the tissue was PV-IR or CaBP-D28k-IR. Typically, motoneurones were devoid of IR in contrast to intensely stained interneurones.

Of course there is something inherently tautological about identifying cells on the basis of different staining profiles, when the aim of the research is to see whether the staining profiles of neuronal subtypes are different. However, three arguments support this strategy. Firstly, PV and CaBP-D28K have both previously been exploited as neuronal labels (in Baimbridge et al, 1992) because of their tendency to selectively and intensely label discrete neuronal subtypes. Secondly, certain motor nuclei - particularly the three motor groups of S1 - are clearly distinguishable from other cell groups in transverse section and are further marked out by distinctive changes in the neuropil around them. Where the patterns of staining described above are seen to show clear differences between these easily identifiable motor groups and interneurones, it is likely that this "rule" may be extrapolated to segments where the anatomical

differentiation is not so straightforward. Finally, a total of 3592 neurones were sampled. The possible bias that may be introduced by the mis-identification of a small number of neurones is unlikely to significantly affect the outcome of such a large sample.

3.1.2iii Soma size and shape

Before taking actual and reasonably objective measurements, it is first necessary to define the boundary of the soma. This requires the experimenter to make a somewhat subjective leap in first delineating the contour of the cell body itself and hence defining the area to be included in these measurements. Deciding what belongs and what does not belong to the soma, or determining where begins the primary dendrite itself, is not a straightforward matter. Given the biological unity of the whole structure of the cell it is also, to a certain extent, an exercise in semantics.

Various methods have been employed in order to impose some objectivity on this decision. Such tactics include the superimposition of the closest fitting geometric shapes (Russell-Mergenthal et al, 1986) or largest fitting ellipses (Ulfhake and Kellerth, 1981; Ulfhake and Kellerth, 1983) onto the soma and measuring these. Meanwhile Lipski and Martin-Body (1987) followed the smooth contour of the soma itself and extended this across the base of dendrites.

The results of these techniques have shown some variability, which may be as much to do with motoneuronal size variations between segments as the technique itself. Neurones measured using largest fitting ellipses have larger mean diameters (58 - 60μm) than the neurones measured using the completed contour method or the closest fitting geometric shape method (38 - 44μm) (see Table 3.1.2-1). One factor in this difference is likely to be the differences

between motoneurones innervating limb muscles and those innervating intercostal and neck muscles. Clearly, though, the completed contour or closest fitting shape technique may provide measurements closer to the actual cell size, with the other method inflating diameter estimations.

Table 3.1.2-1. To show motoneuronal measurements derived from different techniques of cell body delineation.

MUSCLE GROUPS	*SEGMENTAL LEVEL*	*1° DENDRITES*	*MEAN d (μm) range (average)*	*SOMA DEFINITION*
Neck	*brainstem*	*Russell-Mergenthal et al, 1986*		
Lateral rectus		not given	27.5-50.9 (40.69)	best fit geometric shape
Intercostals	*T2-5, T9-11*	*Lipski and Martin-Body, 1987*		
Internal inspiratory		6-10	27.4 -49.1 (38.2)	soma contour extended across process origins
Internal expiratory		6-10	41.8-47.8 (44.8)	
External inspiratory		6-10	30.6- 51.5 (41)	
Hindlimb	*lumbosacral*	*Ulfhake & Kellerth, '81 & '83*		
grouped data		8-15	47.5-75.5 (58.3)	largest fitting ellipsoid
Soleus		9-15	49.5 - 57 (53.4)	
Plantaris brevis		6-14	53 - 71.5 (61.5)	
Quadriceps		7-18	51 - 67 (58.1)	
Posterior biceps		8-12	49.5- 65 (57.2)	
Gastrocnemius		8-15	47.5 - 75 (60.3)	
Tail	*S3-Ca7*	*Ritz et al, 1992*		
"sacrocaudal"		5-8	38-82 (60)	not described

In the present study the smooth contour technique was used, giving rise to a mean diameter for motoneurones intermediate to those summarised above (46μm). Since these measurements include motoneurones from the enlargements as well as from the thoracic cord, it is not surprising that the resulting cell sizes are larger than those measured from thoracic cord only in the Lipski and Martin-Body study. That the estimates are still substantially lower than those acquired using the largest fitting ellipse method suggests that

differences in technique are also likely to have contributed to the size difference. Ultimately however, the data for mean diameter for each cell type, and each antigen, showed a normal distribution around a mean which was well within the range found by other groups.

There were no antigen-dependent differences in the mean diameter of the neurones measured, except in the case of CaN-B. The reason for this difference is not clear. However, the number of CaN-B-IR neurones sampled for size mesurements was the lowest (N=276, compared with an average N of 709 for the other 5 antigens). In addition, the CaN-B-IR neurones measured were derived exclusively from the sacral cord, from only two animals, in comparison to the data for other antigens which were derived from all four spinal segments and at least five animals. Thus, the measurement of a restricted sample of neurones, from only two animals and one spinal segment may have contributed to the anomalous finding. The measurements were, nevertheless, still well within the expected ranges defined by numerous other experiments, as discussed above.

The other feature used to help distinguish the cell types was shape index (SI). Cells defined as interneurones had SIs consistently and significantly lower than cells defined as motoneurones or as belonging to the VSCT. This suggests that cells defined as motoneurones are more circular in shape and those defined as interneurones are more elongated. This is consistent with observations in the literature summarised in Table 3.1.2-2 below.

The extent to which interneurones are seen as elongated was somewhat (although not significantly) dependent on which antigen the tissue had been immunostained for, with a lower SI for interneurones IR for CaBP, PV, or CB. This is almost certainly related to the employment of the completed contour

method of delineating the cell body. When bipolar neurones are stained into the processes - as is often the case with CaBP, PV, and CM, - the proximal portion of the dendrites are less distinguishable from the soma until they begin to taper. It is therefore likely that the major diameter of the soma may be overestimated when using the completed contour method of delineating the cell body.

Table 3.1.2-2. The shape, size, and location of different spinal cord neuronal types. Data from [1] Ulfhake and Kellerth, 1981; Ulfhake and Kellerth, 1982; Russell-Mergenthal et al, 1986; Lipski and Martin-Body, 1987; Ritz et al, 1992. [2] Ulfhake and Cullheim, 1981. [3] Jankowska and Lindstrom, 1972 [4] Jankowska and Lindstrom, 1971; Lagerback & Ronnevi, 1982; Lagerback and Kellerth, 1985; Fyffe, 1990; Fyffe, 1991. [5] Cooper and Sherrington, 1940; Grant et al, 1982; Bras et al, 1988. Except where otherwise indicated these studies were carried out using cat tissue.

CELL TYPE	MEAN DIAMETER RANGE	SHAPE	LAMINAR LOCATION
α-motoneurone [1]	27-82μm	ovoid, quadratic, triangular, ellipsoid	IX
γ-motoneurone [2]	22-37μm		IX
Ia interneurone[3]	21.3 - 28.3μm	?	VII(I)
Renshaw cell[4]	21-36μm	multipolar, ovoid/irregular or bipolar, fusiform	VII(I)
VSCT[5]	58μm in cat 30μm+ in kittens-70μm in monkey	multipolar, indistinguishable from motoneurones	VII(I), IX

Overall, it has been shown that cells deemed to be interneurones were both smaller and more elongated than those categorised as motoneurones. This is consistent with descriptions of motoneurones and interneurones in the literature. These measurements were also normally distributed around the mean. Thus, these analyses supported the notion that distinct populations of cells had been selected.

3.2 Background levels

Throughout this project the intensity of staining of individual cells will be referred to as a percentage of the local background staining. It is important,

therefore, to be clear about what background measurements represent. Background measurements were taken from grey matter and white matter regions, providing two background measurements per image analysed. Grey matter background (GMBG) measurements were made by averaging the fluctuation of grayscale data over as large an area as possible of grey matter tissue *where no stained structures were discernible.* Regions of raised background due to an increased density of stained fibres etc. were avoided, as were regions containing obvious neuronal structures. Typically, the area measured to give GMBG was the palest region of grey matter present. White matter background (WMBG) was similarly measured by averaging the fluctuation of grayscale data over as large an area as possible of white matter. Grayscale values were converted to % Absorbance values by expressing the difference between the observed grey and 255 as a percentage of 255.

Since neuronal data was subsequently expressed as a percentage of this background, it was crucial that background levels were restricted to values that lie within the linear portion of the photographic/video sensitivity. With the analogue camera, light transmission levels were restricted by the requirement to maintain 8V of output from the light source, along with the use of a blue filter, to ensure the correct colour temperature for the daylight film that was used. Exposures were then varied to maintain the production of prints whose background measurements were restricted to below 60%.

Where background was > 60%, images were excluded from analysis for three reasons. Firstly, this was because of the possibility that the intensity of the photographic representation of the background may reflect insufficient light transmission/exposure to move into the linear portion of the film's sensitivity.

Also, if background is higher than 60% at measurement because of intrinsically high tissue levels of staining (rather than photographic technique), this could represent non-specific signal due to poor specificity of antigen binding. Finally, high levels of actual tissue staining could also be due to overexposure to the chromogen, such that heavily labelled structures may saturate before the background, which has continued to take on non-specific label, decreasing the relative intensity of the foreground structures.

When the changeover from analogue to digital photography took place, background levels were decreased to around 25% because it was found that this kept more darkly stained structures within the linear portion of the camera's sensitivity, as measured using a printed grayscale. Because imaging was live using the digital system, it was also possible to modify lighting during image acquisition to maintain a narrow range of background levels. To check the parity between the two methods, a random group of sections were analysed using both techniques. The resulting relationship of neurone to background was almost identical ($r = .98$).

Although measurements of GMBG and WMBG were taken for all tissue where possible, it is only necessary to present results in relation to both backgrounds if they do not vary together. The correlation of GMBG and WMBG measurements or each antigen was highly significant ($p < .0001$) and linear (see Figure 3.2-1).

The relationship was weakened by the introduction of the digital equipment because the overall range of background levels measured was greatly reduced through the increased control provided by the technique. Non-significant

correlations were observed in experiments where the range of background levels was particularly narrow (typically ranges restricted to below 15%). Given the predominance of a high and significant correlation between GMBG and WMBG levels throughout the majority of experiments whose ranges were above 15%[1], and given that all images have a GMBG associated with them, but for some images it was not possible to measure WMBG, results will be presented as a percentage of GMBG only.

[1] The significance of correlations for individual experiments was evaluated by the significance of the t-statistic which was calculated from the correlation co-efficient r using the equation:

$$t = r \frac{\sqrt{N-2}}{\sqrt{1-r^2}} .$$

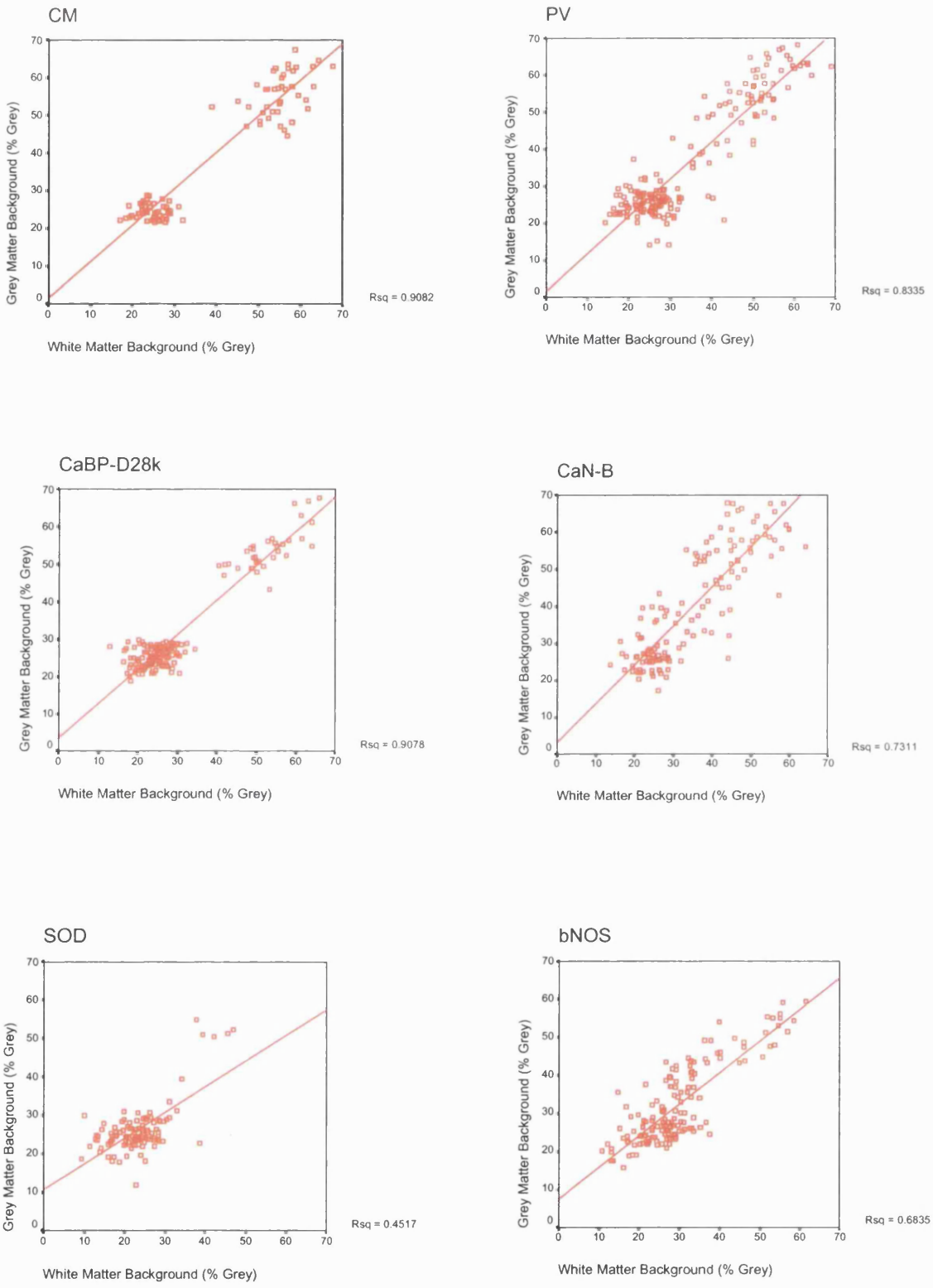

Figure 3.2-1: To show the relationship between GMBG and WMBG for each antigen. Outliers which were subsequently excluded from analyses are included here to avoid an over-restriction of the range which would reduce the visible relationship between the two measures.

3.3.1 Antigenicity: Observations and Analyses

It has been reported that the distributions of CaBPs are often complementary and that they demarcate discrete subpopulations of cells (Celio, 1990). CaBP-D28k-IR and PV-IR in the present study supported this proposition (see Table 3.3.1-1 and Figure 3.3.1-1).

	REGIONS OF MOST INTENSE STAINING		REGIONS OF LEAST INTENSE STAINING	
	CaBP-D28k	**PV**	**CaBP-D28k**	**PV**
Neurones	Superficial DH	Deep DH	Deep DH through VH	Superficial DH
	Autonomic neurones	Clarke's Column	MNs	MNs
	VH interneurones (occasional)	VH Interneurones		
Neuropil	Superficial DH	Clarke's Column	Deep DH through VH	Superficial DH
		Neuropil surrounding motor nuclei	White Matter	
		White Matter		

Table 3.3.1-1: Summary of complementary staining patterns of CaBP-IR and PV-iR.

Apart from the most superficial portion of the DH, PV-IR dominated grey and white matter because of high levels of immunoreactivity in fibres (Figure 3.3.1-1a), particularly around Clarke's column and surrounding the VH somatic motoneurones. In contrast, CaBP-D28k-IR was almost absent from most sections, except for a thick band of heavy staining in the neuropil and in small cells of the superficial DH (Figure 3.3.1-1b), in occasional VH interneurones (particularly medially), and in a discrete population of cells at the base of the dorsal horn corresponding in position and appearance to autonomic neurones (Figure 3.3.1-1c).

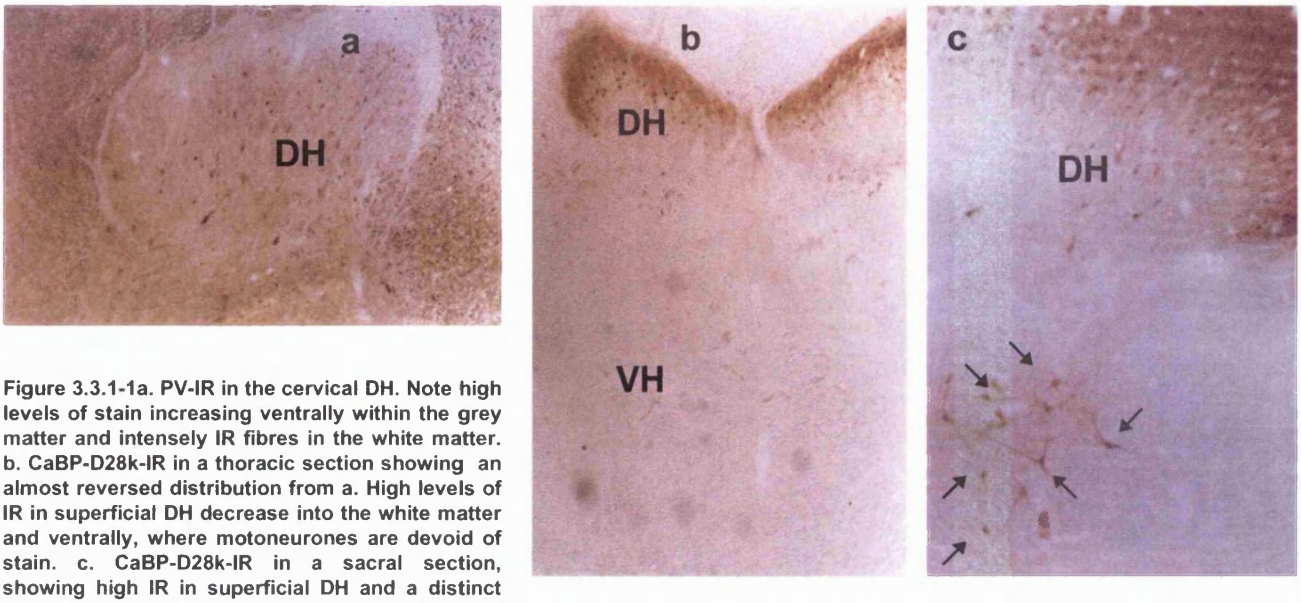

Figure 3.3.1-1a. PV-IR in the cervical DH. Note high levels of stain increasing ventrally within the grey matter and intensely IR fibres in the white matter. b. CaBP-D28k-IR in a thoracic section showing an almost reversed distribution from a. High levels of IR in superficial DH decrease into the white matter and ventrally, where motoneurones are devoid of stain. c. CaBP-D28k-IR in a sacral section, showing high IR in superficial DH and a distinct population of cells corresponding in location and size to autonomic neurones (arrows).

However, although the overall distributions of IR were quite different, four common features were observed for these Ca^{2+} binding proteins. Firstly, IR neurones were labelled in their entirety. In contrast to some of the other proteins examined in this study, cellular processes were equally as immunoreactive as the cell bodies and could therefore often be followed for some distance (figure 3.3.1-2b and e). Secondly, large immunopositive cells were often seen in dorsal areas of the ventral horn close to the lateral edge of the grey matter, particularly in lumbar segments (Figure 3.3.1-2b). These corresponded in location, size, and appearance to cells of the ventral spinocerebellar tract (VSCT)(Cooper and Sherrington, 1940). The third common feature of CaBP-D28K and PV staining is that, mostly, both of these are notably absent in motoneuronal cell bodies. With CaBP-D28K, motoneurones are indistinguishable from the background which is also negative (Figure 3.3.1-2b). In contrast, unstained motoneurones in PV-IR sections often stand out against the immunopositive neuropil (Figure 3.3.1-2a, c, d, e, and g). The fourth commonality was the variability of results. Between different segments within experiments, and between experiments, some

surprising differences were noted. Particularly, although motoneurones were usually unstained, in some segments and some animals, immunopositive motoneurones were observed (Figure 3.3.1-2f, g, and h). Since the tissue from all four segments was processed in one tube, these anomalies are not due to methodological artefacts.

The third Ca^{2+} binding protein examined, CM, showed much less variability in localisation between either cell types or segments (Figs 3.3.1-3a-c). Nevertheless, motoneuronal IR was variable, ranging from an absence of staining (Fig 3.3.1-4a) to more intense staining (Fig 3.3.1-4b), whilst interneurones were more consistently immunostained at a high level (Figs 3.3.1-4a-d). Neuronal immunostaining was generally fairly pale, although the addition of 18mM Ca^{2+} to the diluted primary antibody increased the levels of IR. Large numbers of cells were stained throughout the grey matter, including medium multipolar neurones at the base of the dorsal horn (Laminae IV-VI) (Fig 3.3.1-5a) and those oriented towards the central canal (Fig 3.3.1-5b). As with the other two Ca^{2+} binding proteins, IR fibres were often seen and immunostaining filled the processes of labelled cells. In addition, heavily labelled neuronal nuclei were frequently observed, whilst nucleoli were invariably unstained (Figs 3.3.1-4c and d).

Spinal cord CaN-IR had a very characteristic appearance which distinguished it from all other antigens examined. Motoneurones were frequently very heavily stained, with pale nuclei (Fig. 3.3.1-6) and segmental differences were not visibly apparent. In and around motor nuclei intense punctate IR was very common. At higher magnification these punctae resembled sections through dendritic processes.

Figure 3.3.1-2a. PV-IR section from the 4th lumbar segment. Note: intense staining of Clarke's column, strongly IR interneurones (small arrows) and one unstained motoneurone (arrowhead). b. CaBP-D28K-IR section from the 5th lumbar segment. The labelled process of an Intensely stained presumed autonomic neurone can be traced for some distance (arrowheads). Also, labelled cells of th VSCT can be seen (open arrows). Circle indicates region containing unstained motoneurones. c. PV-IR thoracic section with intensely stained interneurones (small arrows) and unstained motoneurones (arrowheads).

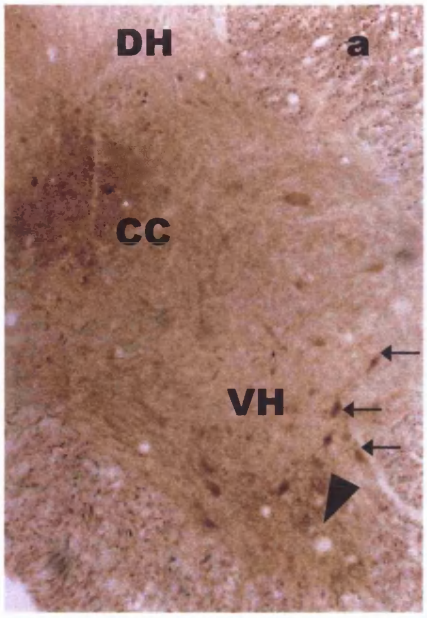

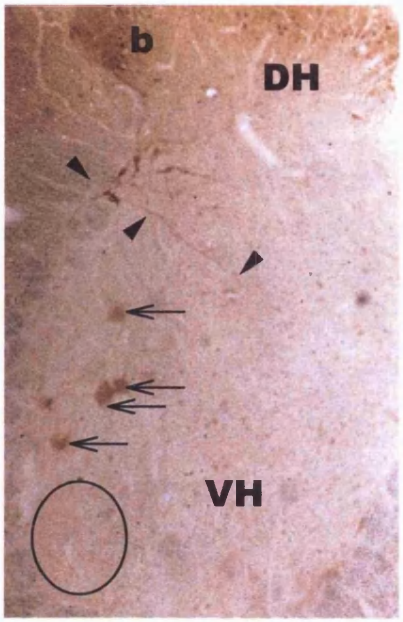

d. The same section taken with oblique illumination to show nucleoli of motoneurones to verify neuronal identity. e. PV-IR section from 7th cervical segment. Pale motoneurones (arrowheads) and PV-IR interneurones (small arrows) can be seen. The fibres which are traceable to a stained cell body are also indicated (open arrows). f & g Taken from one animal, the two images show PV +ve motoneurones (f- arrowheads) in a cervical section and PV -ve motoneurones (g- white arrows) in a lumbar section. h. CaBP-D28K-IR sacral section showing motoneurones of ON and VL (arrowheads).
Abbr. CC - Clarke's Column, DH - dorsal horn, ON- Onuf's nucleus, VH - ventral horn, VL - sacral ventrolateral nucleus

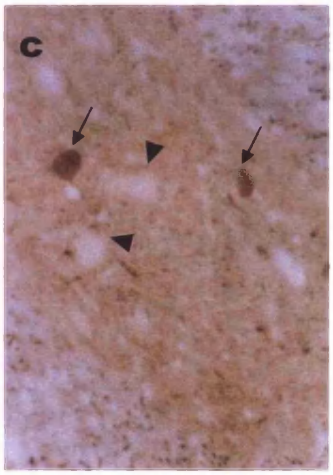

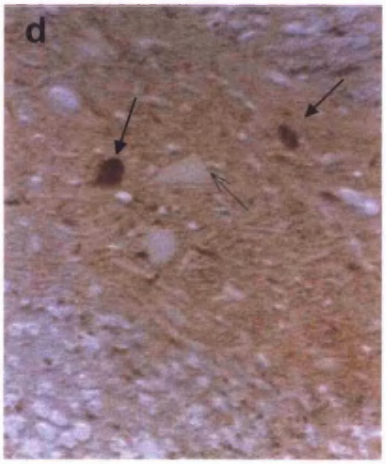

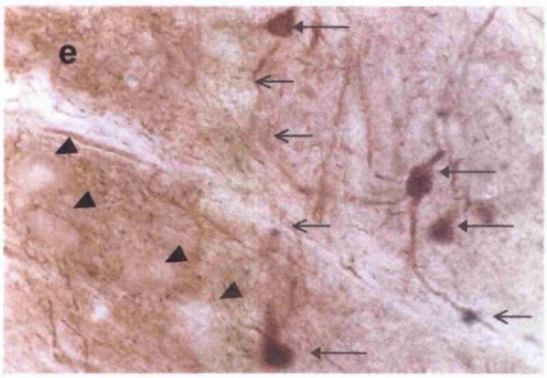

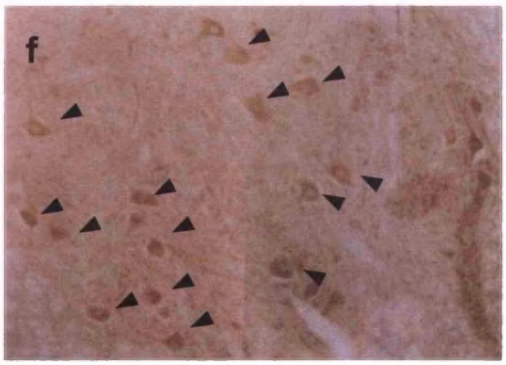

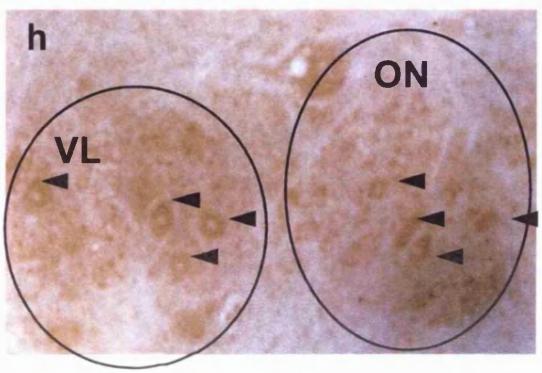

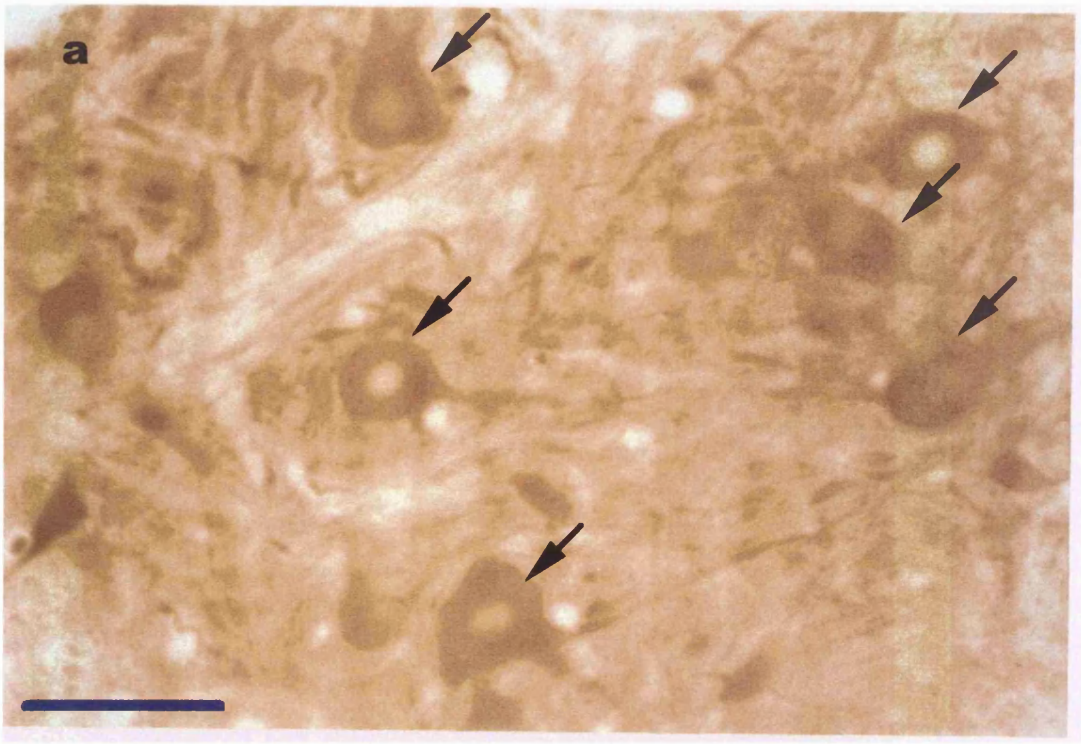

Figure 3.3.1-3. Showing CM-IR motoneurones (arrows) from cervical (a), sacral (b), and lumbar segments (c). In ON (b) the transverse dendritic bundle (dotted black line) shows high levels of CM-IR. Bar = 100μm.

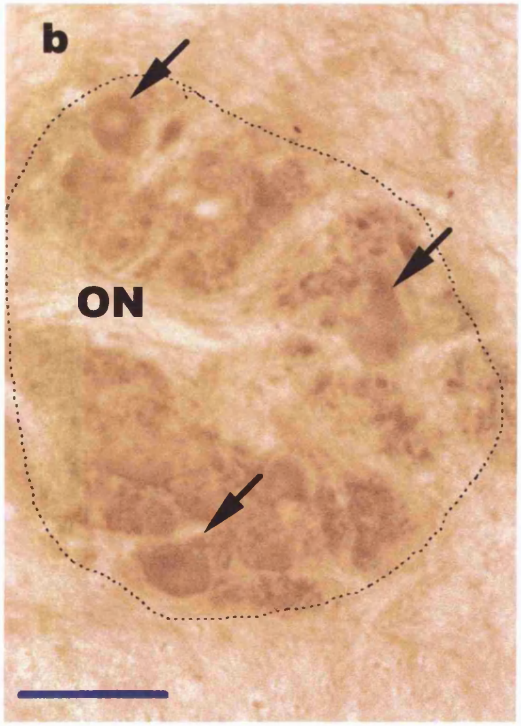

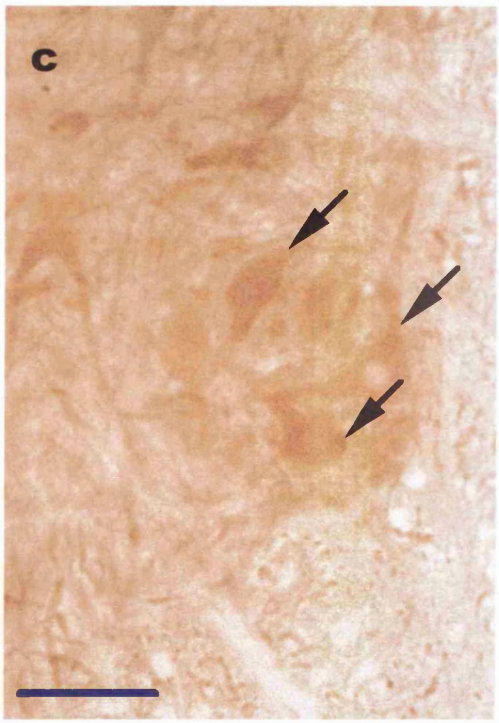

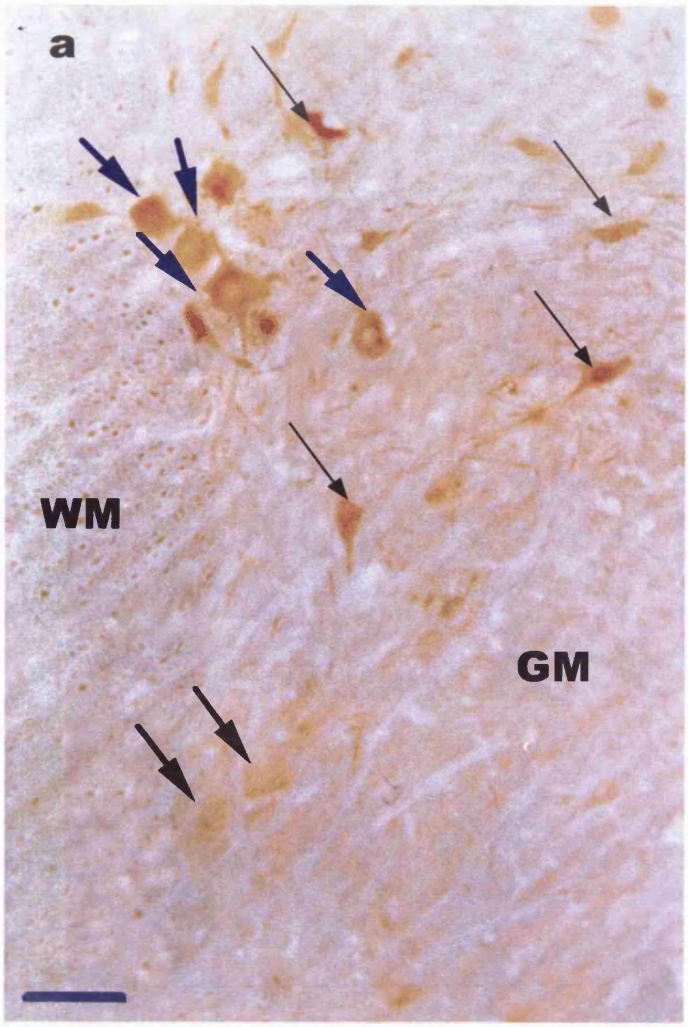

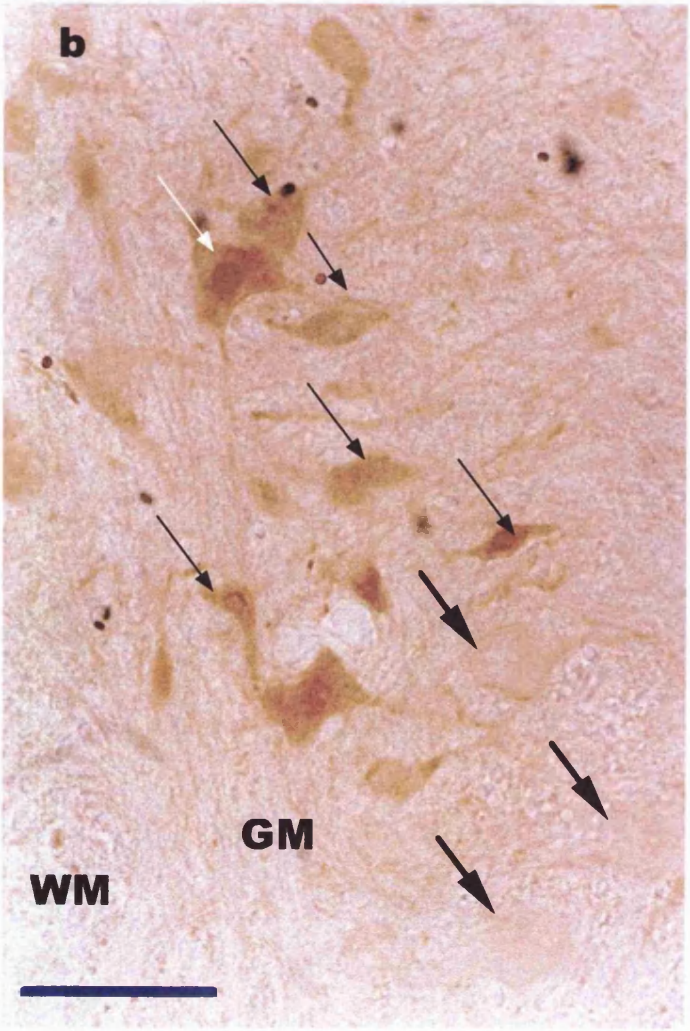

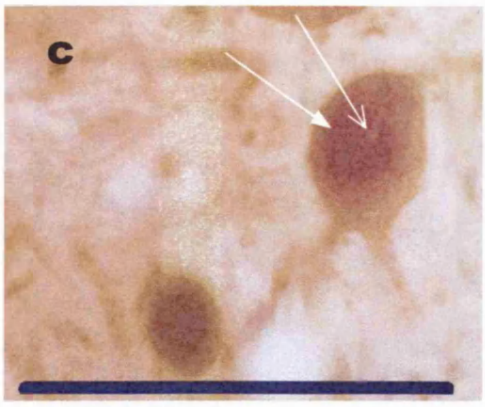

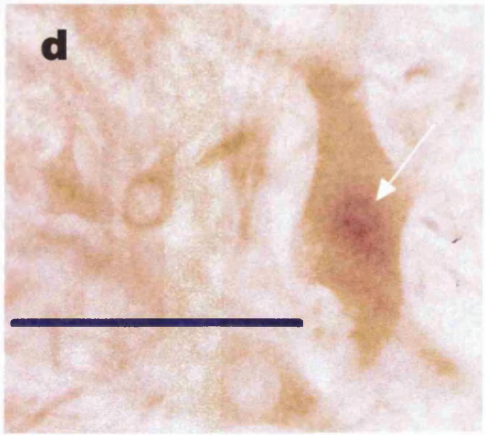

Figure 3.3.1-4. Two L4 sections showing pale (a) or negative (b) CM immunostaining of motoneurones (heavy arrows), in contrast with smaller, more dorsally located, intensely CM-IR neurones (light arrows) presumed to be interneurones. In (a) intense CM-IR is also seen in a cluster of cells corresponding in size and location to the VSCT (blue arrows). An example of nuclear IR is also seen in (b) (closed white arrow) with a pale nucleolus (open white arrow) in a presumed interneurone. Immunopositive interneuronal nuclei can be seen at higher magnification in plates (c) and (d). Plate (b) has been photographed using diffraction to sharpen the contours and increase the visibility of unstained neurones. GM - grey matter; WM - white matter; bars = 100μm.

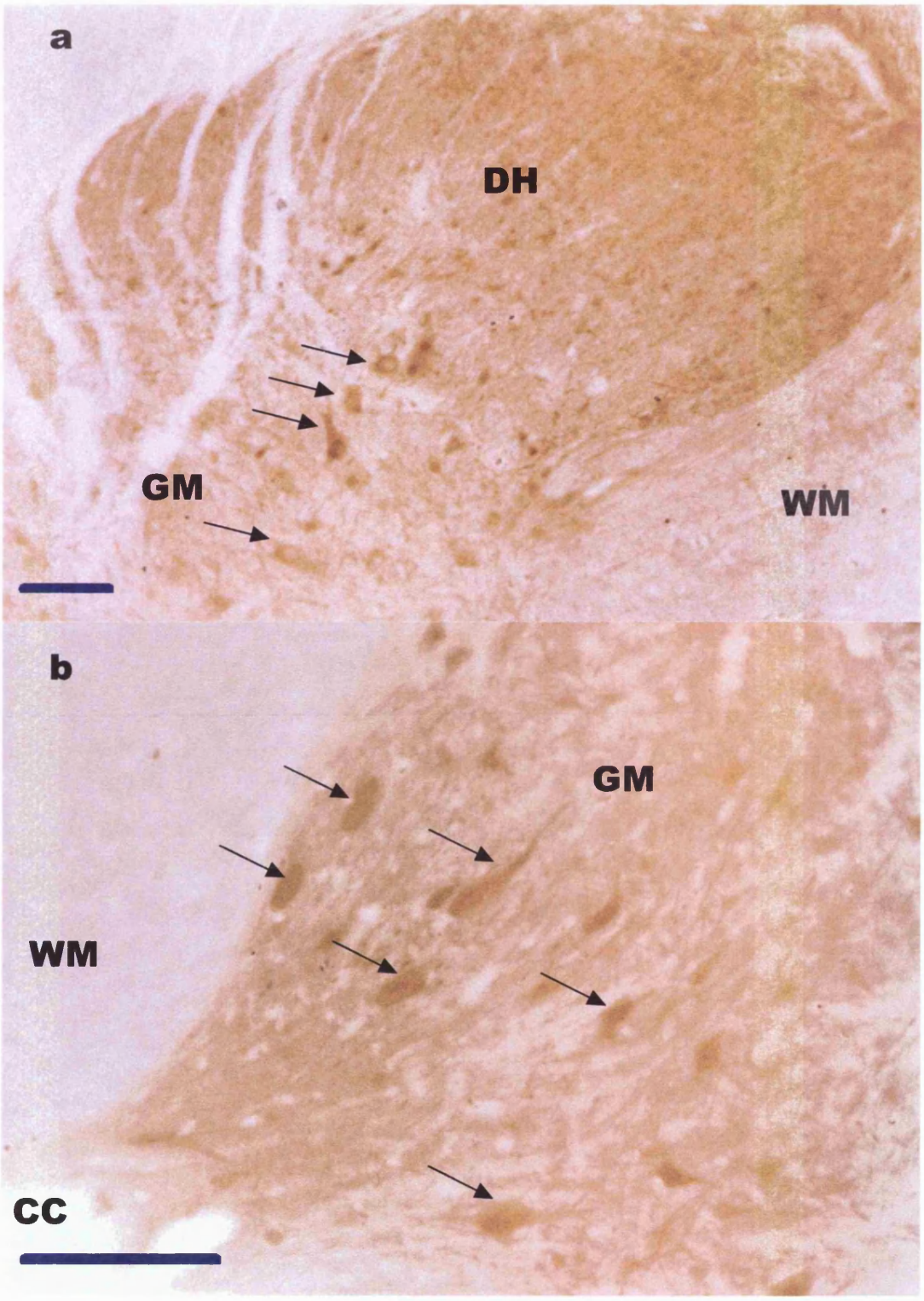

Figure 3.3.1-5. CM-IR in the dorsal horn (a) is seen in superficial fibres, and in the medium sized multipolar cells of laminae IV-VI (arrows). Ventromedially (b) bipolar CM-IR cells can be seen oriented with their long axis running in the mediolateral plane, towards the central canal (arrows). GM - grey matter; WM - white matter; DH - dorsal horn; CC - central canal; bars = 100μm.

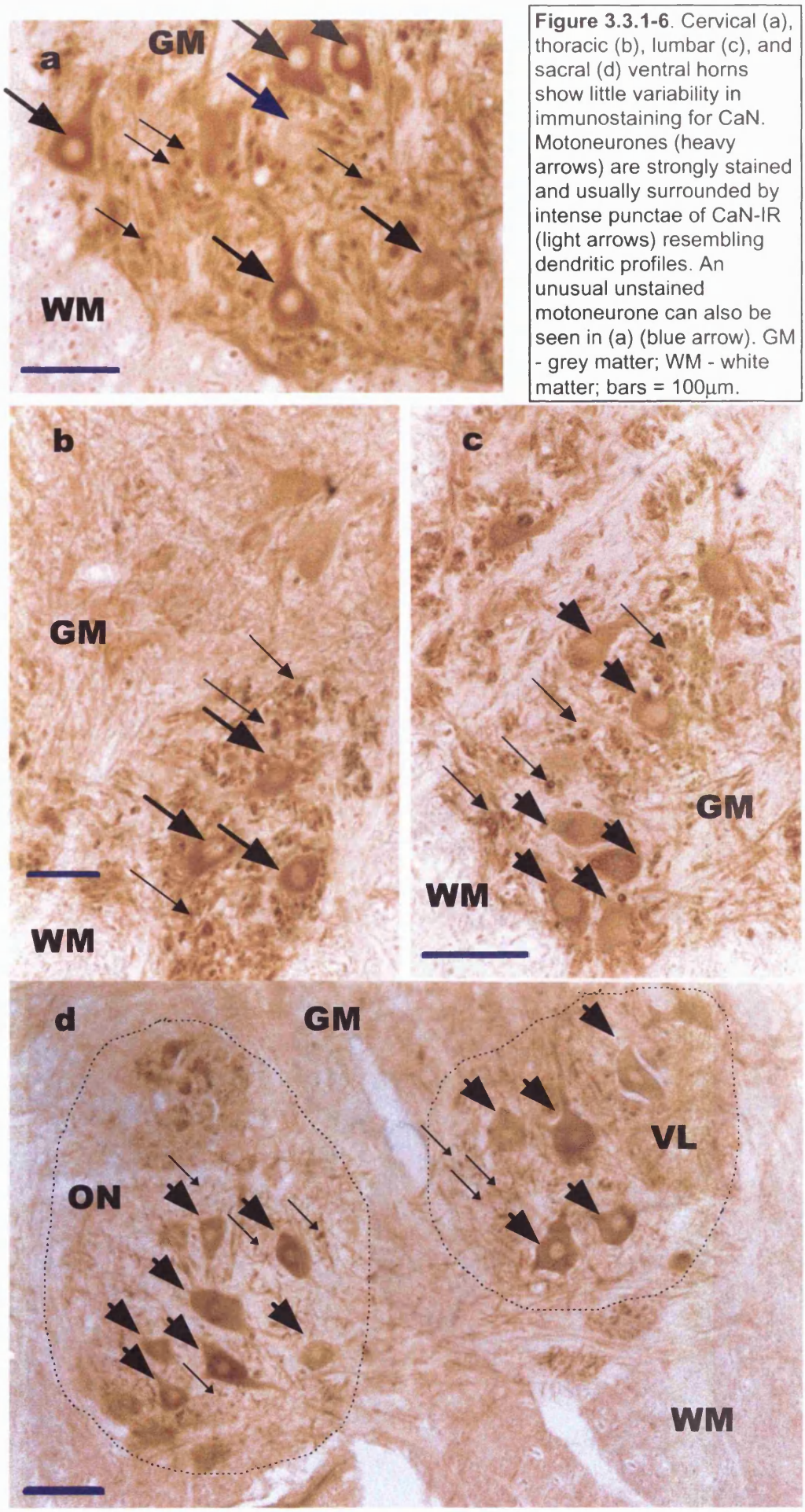

Figure 3.3.1-6. Cervical (a), thoracic (b), lumbar (c), and sacral (d) ventral horns show little variability in immunostaining for CaN. Motoneurones (heavy arrows) are strongly stained and usually surrounded by intense punctae of CaN-IR (light arrows) resembling dendritic profiles. An unusual unstained motoneurone can also be seen in (a) (blue arrow). GM - grey matter; WM - white matter; bars = 100μm.

Outside of these motor groups, very large numbers of interneurones were IR, although the staining intensity was much lower than that of the motoneurones (Fig. 3.3.1-7b). The grey matter had a low level of IR which increased into the superficial dorsal horn (Fig. 3.3.1-7a).

nNOS was somewhat similar to CaN in terms of its relative levels in motoneurones and interneurones, with highly IR motoneurones and paler interneurones (Figs. 3.3.1-8 and 3.3.1-9a). In addition, high levels of IR were often seen in the cells of Clarke's column. Grey matter background levels were paler than those observed with CaN. At higher magnification levels, somal staining could be seen to be patchy and "globular" in appearance (Fig. 3.3.1-9b), possibly suggesting association of the antigen with internal structural elements of the cell such as the ER.

SOD-IR was generally weaker than that of the other antigens, with the exception of CM. Motoneuronal staining (Fig. 3.3.1-10) was intermediate to the Ca^{2+} binding proteins PV and CB at the one extreme, and nNOS and CaN at the other, and did not appear to differ between segmental levels. The neuronal immunostaining had a granular appearance and was dispersed throughout the cytoplasm. Levels of background stain were generally low even into the deeper dorsal horn laminae, with IR increasing into the superficial layers (Fig. 3.3.1-11a). Punctate IR was observed around motor nuclei, as with CaN (Fig. 3.3.1-11b). In some lumbar sections, higher levels of SOD-IR were noted in the cells corresponding in size and location to the VSCT.

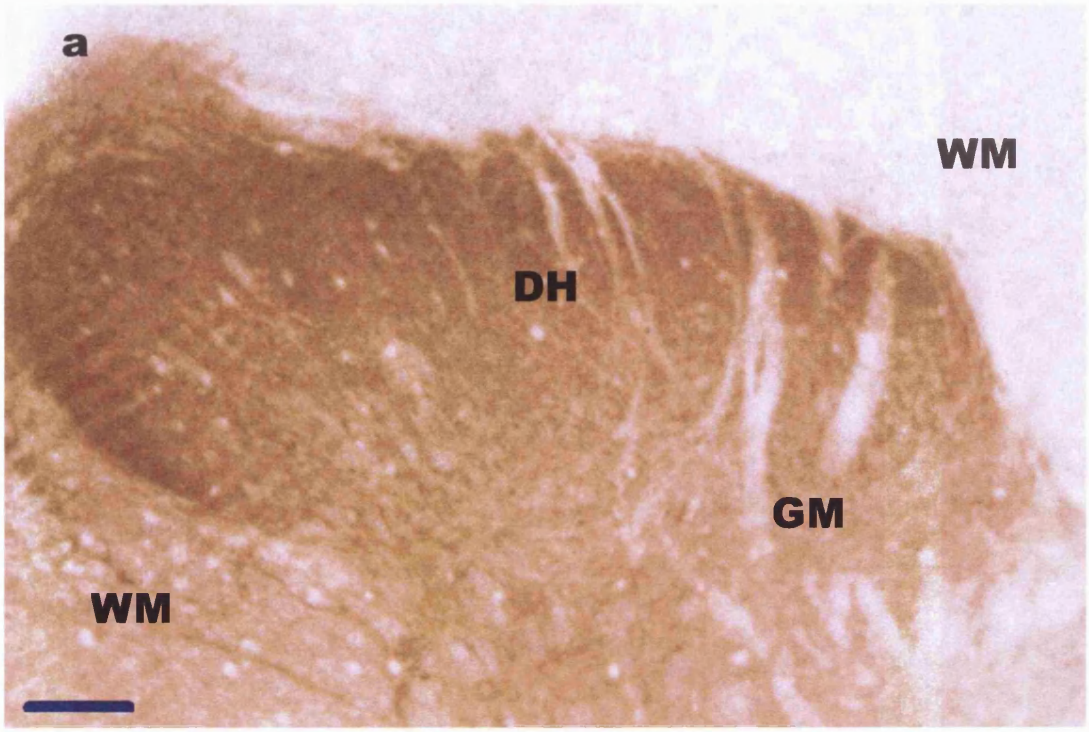

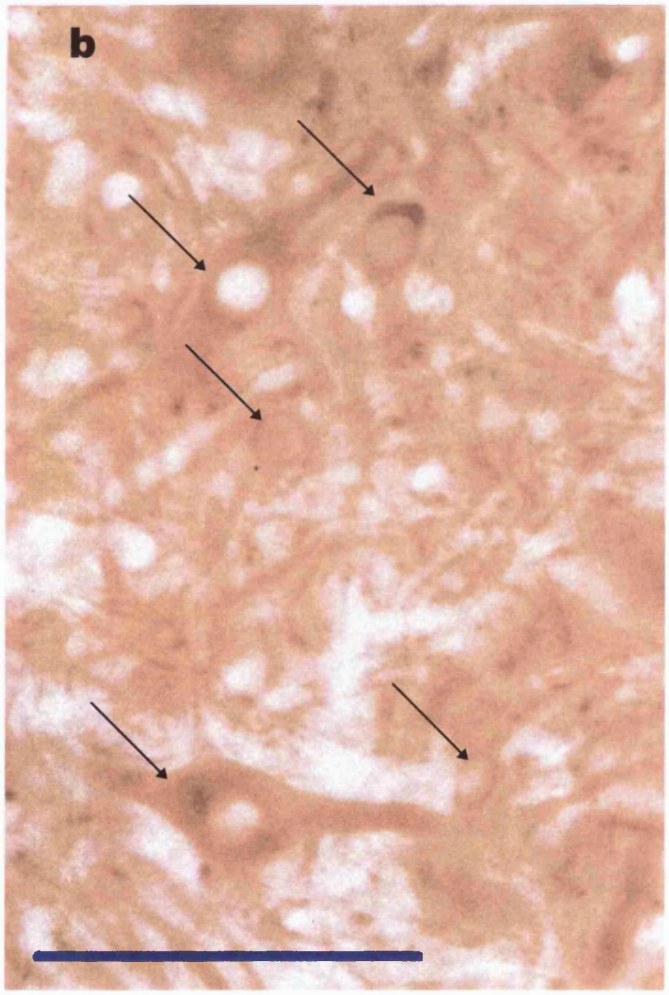

Figure 3.3.1-7. (a) CaN-IR in the dorsal horn. (b) Interneurones (light arrows) are not as intensely stained as motoneurones.

DH - dorsal horn; GM - grey matter; WM - white matter; bars = 100µm.

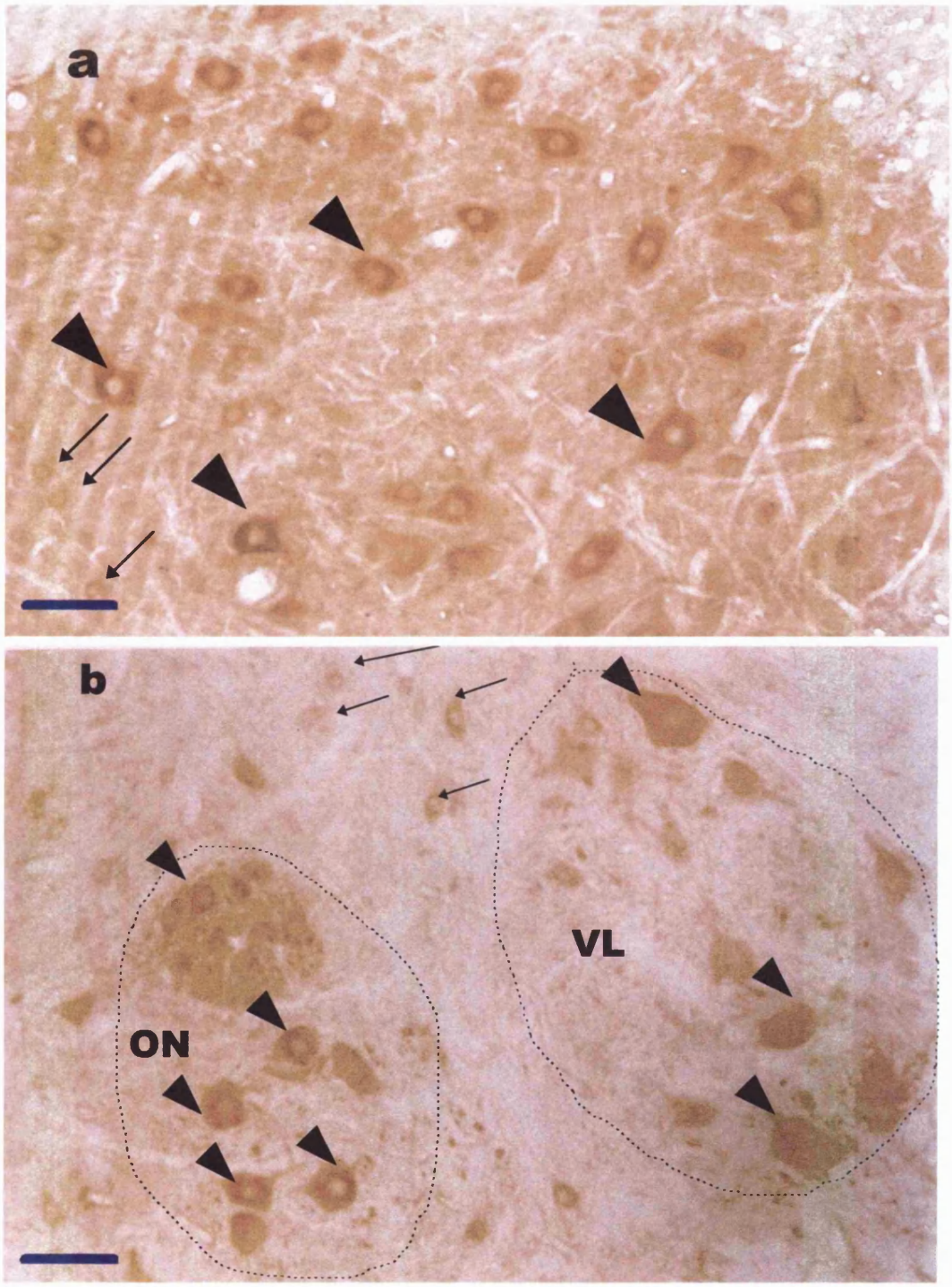

Figure 3.3.1-8. nNOS immunoreactivity in the cervical (a) and sacral (b) ventral horns. Heavy arrowheads - motoneurones; small arrows - interneurones.

Bars = 100μm.

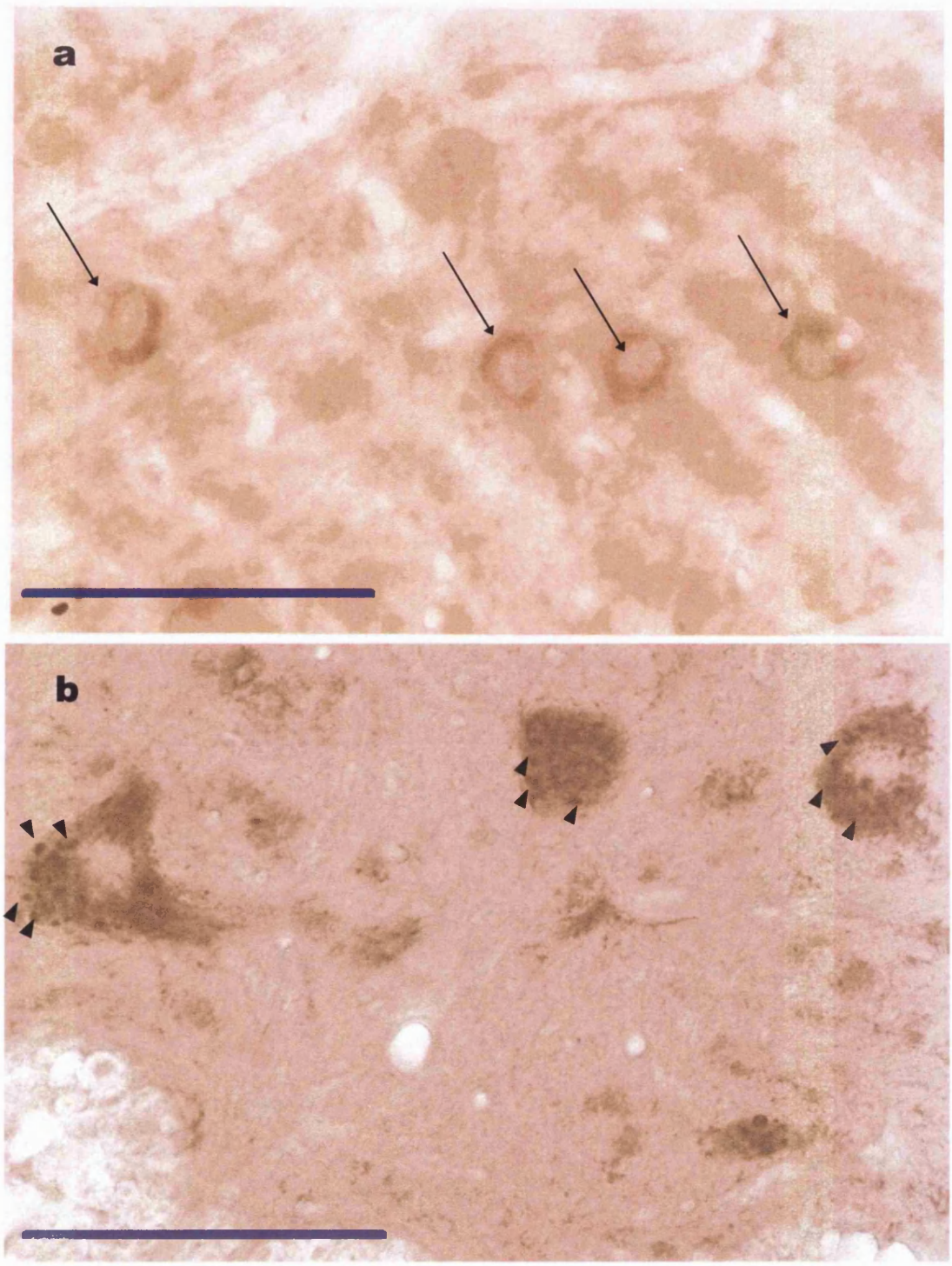

Figure 3.3.1-9. (a) nNOS-IR in interneurones of the cervical cord (small arrows). (b) nNOS-IR in thoracic motoneurones: note punctate accumulations of the chromogen (arrow heads) possibly indicating association of the protein with the ER system.

Bars = 100μm.

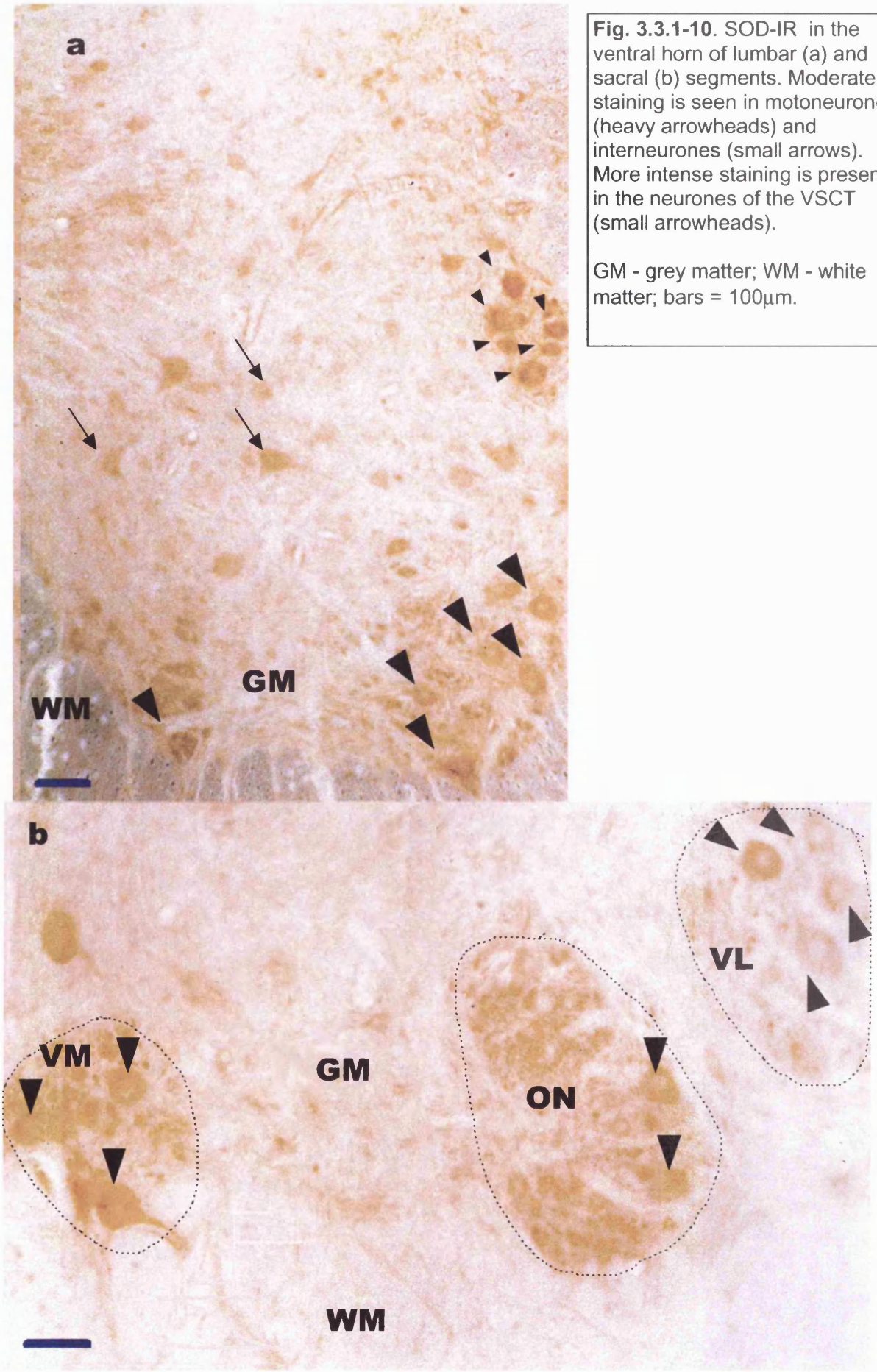

Fig. 3.3.1-10. SOD-IR in the ventral horn of lumbar (a) and sacral (b) segments. Moderate staining is seen in motoneurones (heavy arrowheads) and interneurones (small arrows). More intense staining is present in the neurones of the VSCT (small arrowheads).

GM - grey matter; WM - white matter; bars = 100μm.

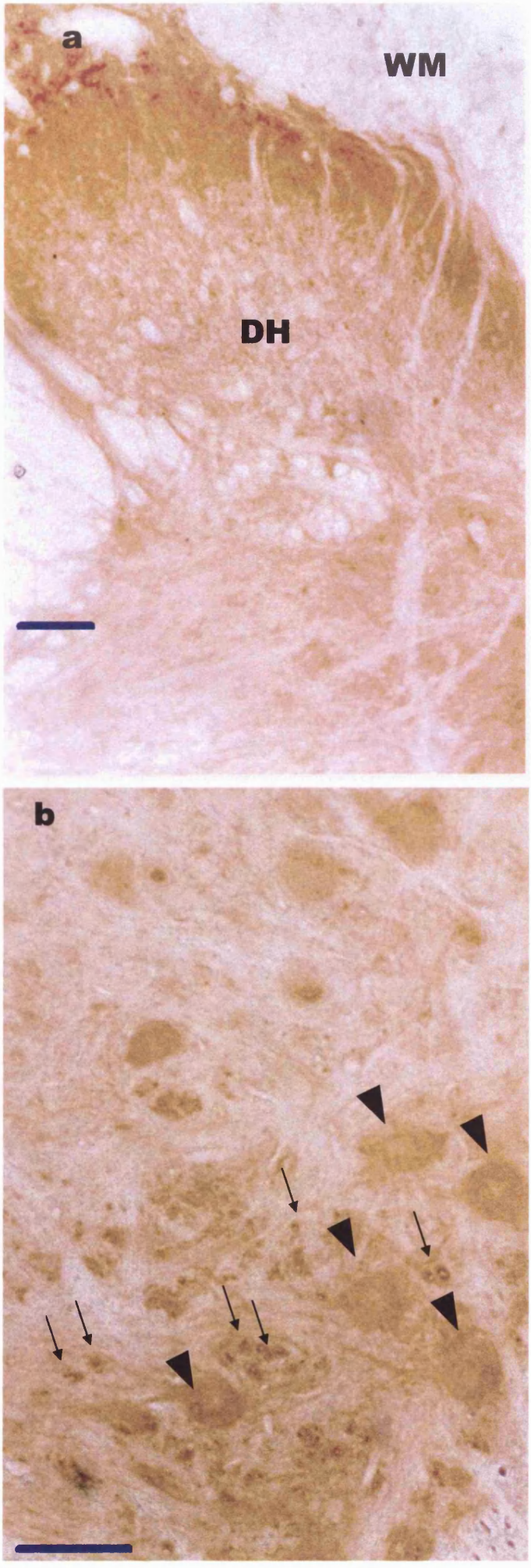

Figure 3.3.1-11. (a) SOD-IR in the dorsal horn. There are no immunoreactive neurones, but an increase in immunostaining levels can be seen into the superficial layers of the dorsal horn. (b) At higher magnification the motoneurones (heavy arrowheads) can be seen to be surrounded by punctate SOD-IR profiles (small arrows).

DH - dorsal horn; WM - white matter; bars = 100μm.

3.3.2 Distributions of Grayscale Values

Due to experimental variability, it was necessary to normalise measured grayscale values in order to examine the stain intensities quantitatively, as described in Chapter 2. Briefly, this was achieved by calculating grayscale ranges for each experiment (i.e. (darkest cell/GMBG x100)-(palest cell/GMBG x 100)) and then dividing each range into nine data bins of equal width. For the purposes of statistical analysis, the grayscale value for each cell was substituted by the number of the bin into which it fell. Mean scores for each cell type therefore represent the mean bin location (MBL) of that cell type.

3.3.2i Motoneurones vs Interneurones

Using this method, an initial ANOVA of cell type by bin location followed by post-hoc Dunnett's T3 and Tamhane's T2 tests (see below) and Kolmogorov-Smirnov two sample tests, showed interneurones to be significantly more intensely stained than motoneurones for both CB (Kolmogorov-Smirnov $Z = 3.61$, $p<.001$) and PV (K-S $Z = 7.5$, $p<.001$) and significantly less intensely stained for SOD (K-S $Z=8.29$, $p<.001$), CaN (K-S $Z=4.56$, $p<.001$), and nNOS (K-S $Z=9.34$, $p<.001$)(see Figure 3.3.2-1). Post-hoc Dunnett's T3 and Tamhane's T2 tests (neither of which assume equal variance), performed after an ANOVA in which cell types were broken down by segment, showed that this was true for all segments as well as between segments (e.g. interneurones in the lumbar cord were significantly more intensely stained than motoneurones in the cervical cord etc)($p <.05$).

No differences were observed between motoneurones and interneurones for CM, in an ANOVA of cell types by bin location. To explore this finding further, cell types were broken down by segment and post-hoc tests showed that the motoneurones of the cervical cord had a significantly lower MBL (3.41) than

Figure 3.3.2-1 The distribution of all motoneurones (yellow) and interneurones (blue) immunoreactive for calbindin, parvalbumin, and calmodulin. In each case, motoneurones are significantly more positively skewed than interneurones ($p < .001$). Ordinate scales have been adjusted for sample size to facilitate the visual comparison of the distributions.

Calbindin

Motoneurones

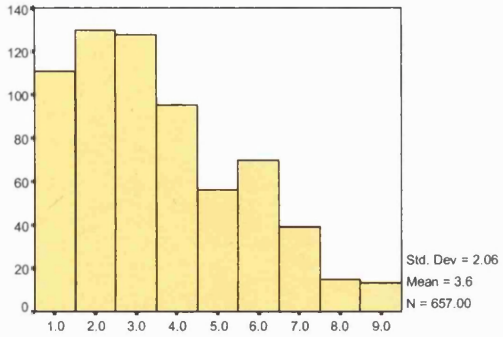

Interneurones

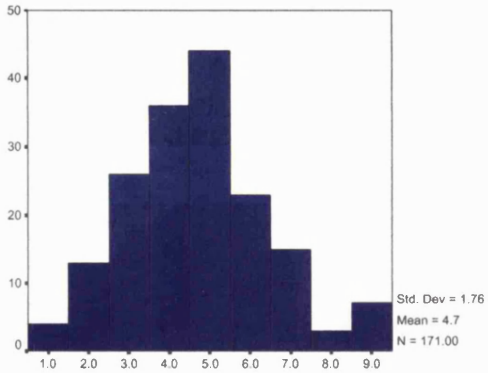

Parvalbumin

Motoneurones

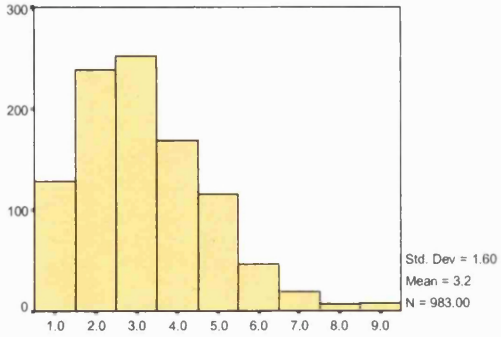

Interneurones

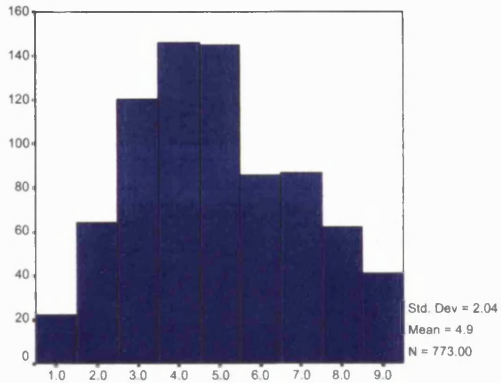

Calmodulin

Motoneurones

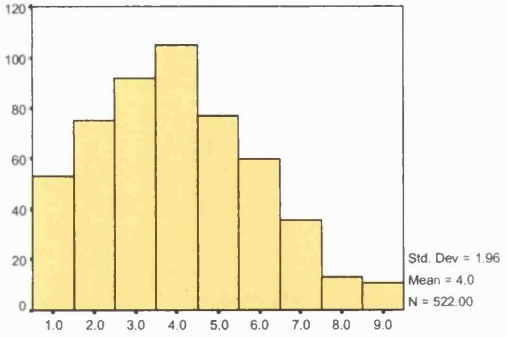

Interneurones

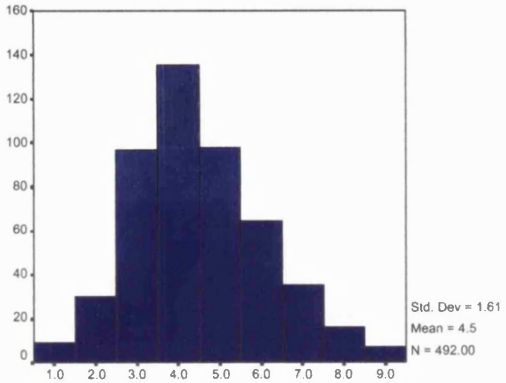

Figure 3.3.2-2 The distribution of all motoneurones (yellow) and interneurones (blue) immunoreactive for nNOS, CaN-B, and SOD. In each case, interneurones are significantly more positively skewed than motoneurones ($p < .001$). Ordinate scales have been adjusted for sample size to facilitate the visual comparison of the distributions.

nNOS

Motoneurones

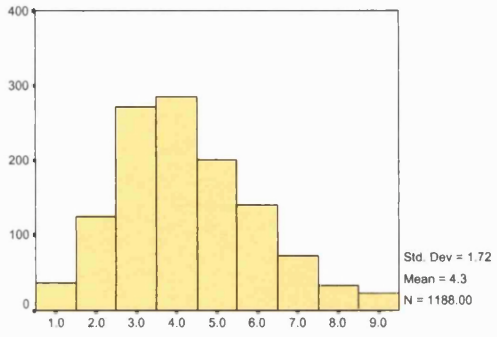

Interneurones

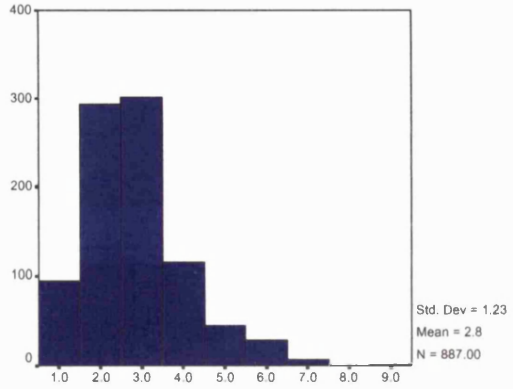

CaN

Motoneurones

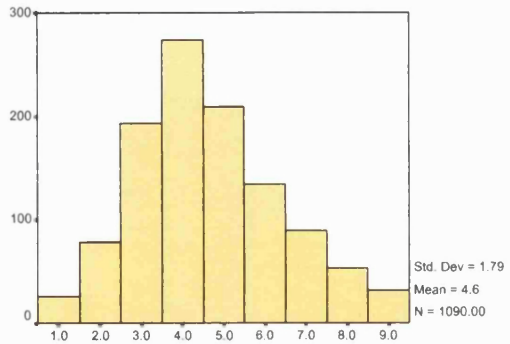

Interneurones

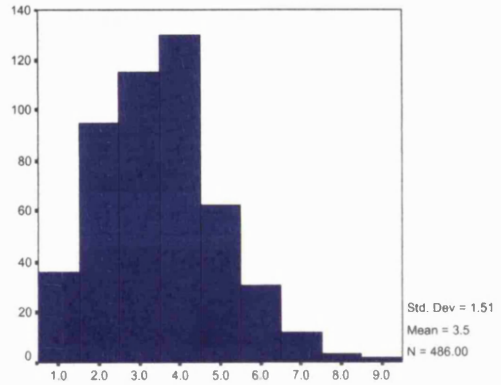

SOD

Motoneurones

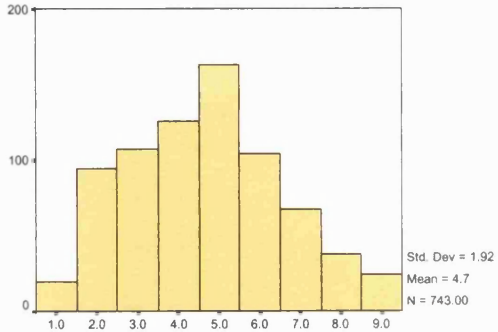

Interneurones

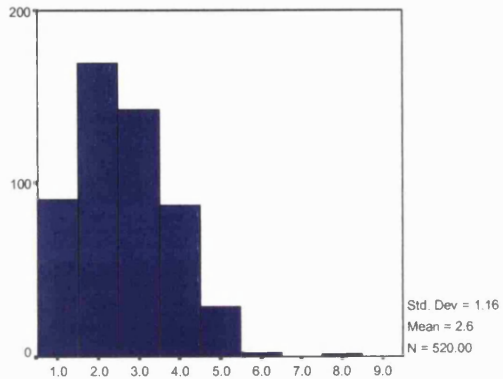

interneurones of all segments except the sacral cord, and interneurones of the cervical cord were significantly higher in terms of MBL (5.65) than all motoneurones (see Table 3.3.2-1) (all differences significant at $p < .05$). In addition, the overall distributions of all interneurones and motoneurones immunostained for CM were found to be significantly different (K-S $Z=2.64$, $p<.001$)(see Figure 3.3.2-2).

Table 3.3.2-1. To show the mean bin locations of motoneurones and interneurones immunostained for CM.

Segment	Motoneurones	Interneurones
Cervical	3.411	5.65
Thoracic	3.71	4.33
Lumbar	4.16	4.46
Sacral	3.4 - 4.7	4.16

The post-hoc tests also showed the significance of a number of other cell type differences which have not been explored in any more depth. The sympathetic cells located in the lateral horn region of L4, for example, were significantly more intensely stained than all motoneuronal groups other than those of the sacral cord.

3.3.2ii. Segmental Comparisons

Immunoreactivity for all antigens - with the exception of CaN - showed significant segmental differences in motoneuronal staining levels according to the results of post-hoc tests (as above) of highly significant ANOVAs of cell type broken down by bin location. The lumbar motoneurones had a significantly higher bin location than thoracic motoneurones when immunostained for nNOS, and a significantly lower bin location than thoracic motoneurones when immunostained for PV. Other than these two lumbar/thoracic differences the remaining differences were between all spinal motoneurones and the

motoneurones of the sacral cord. In fact, sacral motoneurones were significantly higher than the motoneurones of each of the other segments for all five antigens.

In order to investigate the origin of the result in more depth, ANOVAs and post-hoc tests were carried out entering VL, ON, and VM separately where formerly they were grouped as sacral motoneurones. MBLs for each cell type were averaged over the five antigens to give a summary bin location for each of the cell groups. The summary bin locations of the three sacral nuclei (ON: 4.34, VL: 4.63, VM: 4.9) were higher than all other segmental levels (Cervical:3.29, Thoracic:3.3, Lumbar:3.67) and these are presented in figure 3.3.2-3

Figure 3.3.2-3 Mean MBL averaged across antigens (excluding CaN)

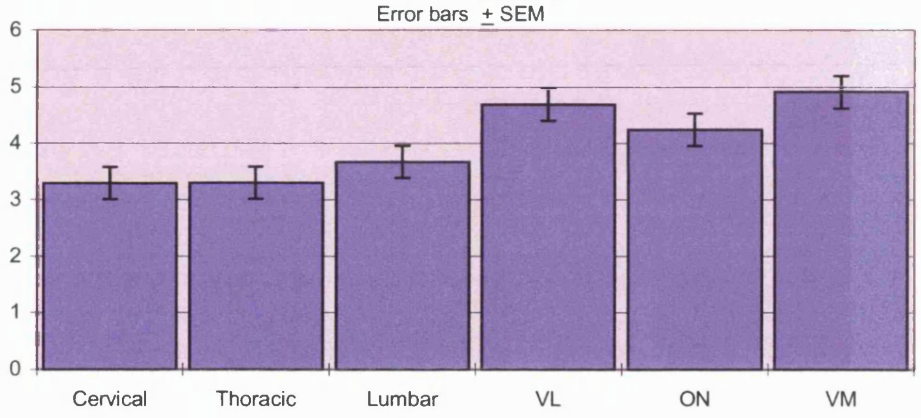

The actual MBLs for each antigen and cell group are presented in table 3.3.2-2 in ascending order. As can be seen, all three sacral nuclei tend towards the highest relative staining levels, particularly when immunostained for SOD, nNOS, and CB. Only ON deviates into the mid ranges of relative intensity when immunostained for the remaining antigens, PV and CM. The statistically significant differences (Dunnett's T3 and Tamhane's T2) are shown in Table 3.3.2-3.

Table 3.2.2-2: Table to show the MBLs of each cell group in ascending order. The highest three columns are clearly dominated by the cells of the sacral cord.

Antigen	Lowest MBL →	→	→	→	→	→	→ Highest MBL
PV	Lumbar 2.6	Cervical 3	ON 3.2	Thoracic 3.5	VL 3.6	VM 5.11	
SOD	Cervical 4.22	Thoracic 4.24	Lumbar 4.83	VL 5.17	ON 5.28	VM 5.45	
nNOS	Thoracic 2.33	Cervical 3.28	Lumbar 3.89	VM 4.89	ON 5.04	VL 5.2	
CB	Cervical 2.56	Thoracic 2.74	Lumbar 2.89	ON 4.22	VM 4.84	VL 5.01	
CM	Cervical 3.411	ON 3.48	Thoracic 3.71	Lumbar 4.16	VM 4.26	VL 4.48	

Table 3.2.2-3. Table to show significant differences between motoneuronal groups. Of each significant pair, the cell type with the significantly higher bin value is represented by the column, with the row representing the cell type with the lower value.

	Cell group of higher MBL				
	Thoracic	**Lumbar**	**VL**	**ON**	**VM**
Cervical			nNOS(p<.001) SOD(p<.001) CB(p<.001) PV(p<.001) CM(p=.015)	nNOS(p<.001) SOD(p<.001) CB(p<.001)	nNOS(p<.001) SOD(p<=.018) CB(p<.001) PV(p<.001)
Thoracic		nNOS (p<.001)	nNOS(p<.001) SOD(p<.001) CB(p<.001)	nNOS(p<.001) SOD(p=.002) CB(p<.001)	nNOS(p<.001) SOD(p=.026) CB(p<.001) PV(p<.001)
Lumbar	PV(p<.001)		nNOS(p<.001) CB(p<.001) PV(p<.001)	nNOS(p=.042) CB(p<.001)	CB(p<.001) PV(p<.001)

Further to this, the distributions of each cell type across the range of staining levels for each antigen were analysed and compared using the Kolmogorov-Smirnov Z-test for two samples. The test confirmed that the significant differences found with the Dunnett's T3 and Tamhane's T2 summarised above

were indeed representative of different distributions of the data. In addition, the test revealed significant differences in the distributions of other motoneuronal groups whose means do not differ significantly. These are summarised in Table 3.3.2-4 below. The distributions of motoneurones within the staining range for each antigen are shown graphically in Figures 3.3.2-4 to 3.3.2-9.

	Thoracic	**Lumbar**	**VL**	**ON**	**VM**
Cervical	nNOS PV	nNOS SOD PV	nNOS SOD CB PV CM CaN	nNOS SOD CB	nNOS SOD CB PV CM
Thoracic		nNOS PV	nNOS SOD CB CM	nNOS SOD CB CM	SOD CB PV CM
Lumbar			nNOS CB PV CM CaN	nNOS CB CM PV	CB PV
VL				CM CaN	PV CaN
ON					PV

Table 3.3.2-4. Matrix of cell group pairings showing significantly different distributions (Kolmogorov-Smirnov Z test: $p < .05$). Novel findings are shown in red

Given that there was a significant interaction between experiment code and cell type for all antigens ($p<.001$), plots were constructed to evaluate the impact of these experimental variations on the findings of significant differences between segmental distributions and means. These plots are presented in Figure 3.3.2-10.

Figure 3.3.2-4 Distributions of SOD IR by motoneurone type. Ordinate scales have been adjusted for sample size to facilitate the visual comparison of the distributions.

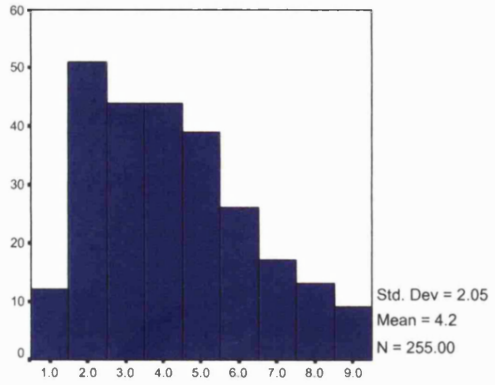

Cervical Motoneurones

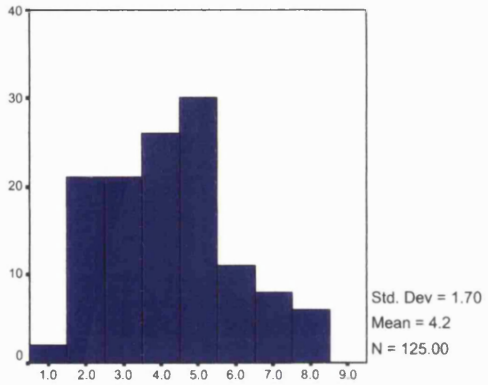

Thoracic Motoneurones

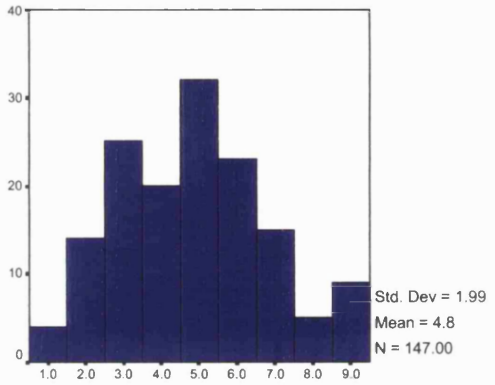

Lumbar Motoneurones

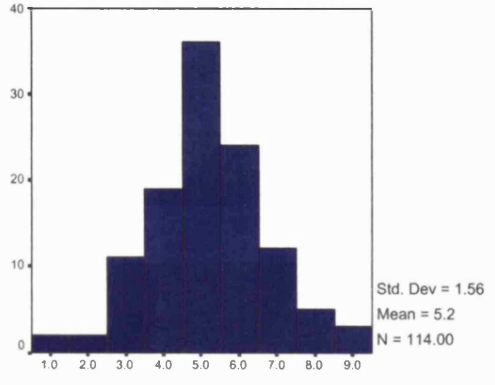

VL

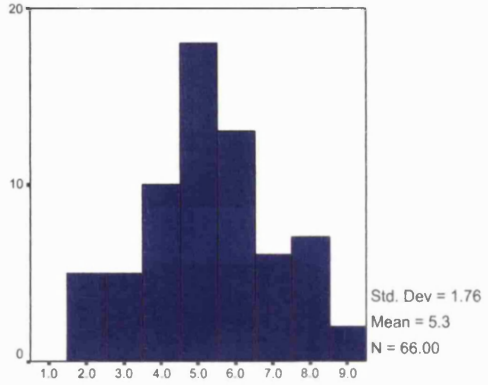

ON

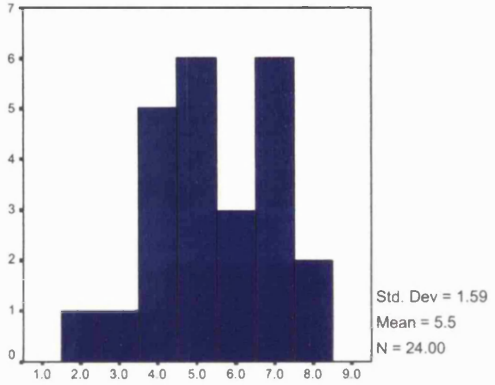

VM

Figure 3.3.2-5 Distributions of nNOS IR by motoneurone type. Ordinate scales have been adjusted for sample size to facilitate the visual comparison of the distributions.

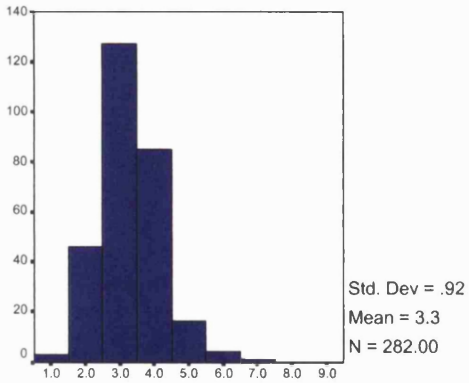

Cervical Motoneurones

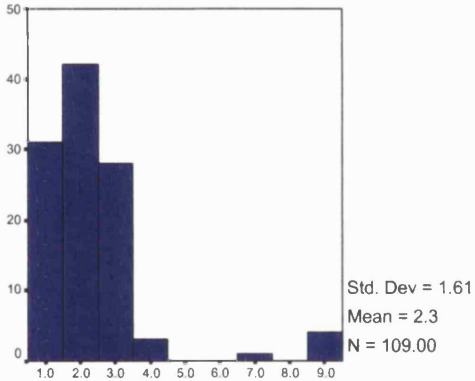

Thoracic Motoneurones

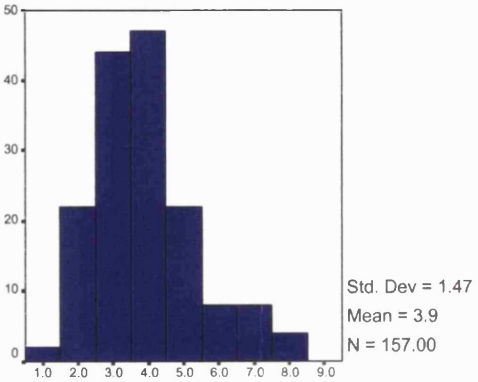

Lumbar Motoneurones

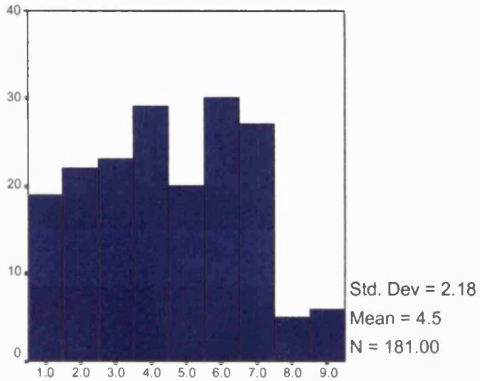

VL

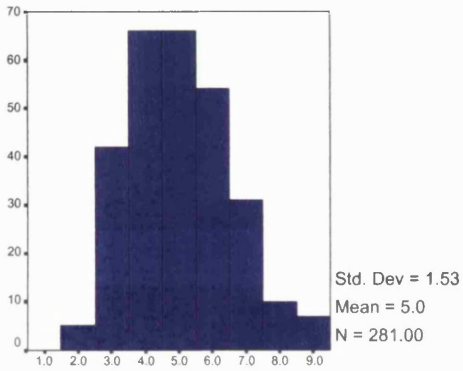

ON

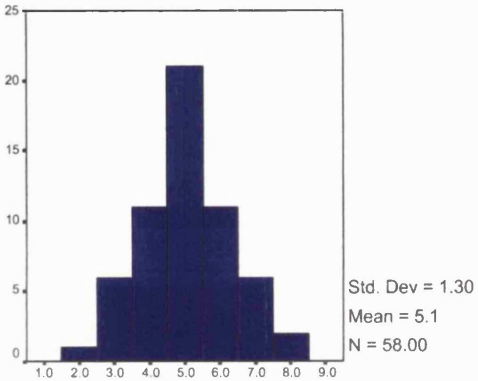

VM

Figure 3.3.2-6 Distributions of CB by motoneurone type. Ordinate scales have been adjusted for sample size to facilitate the visual comparison of the distributions.

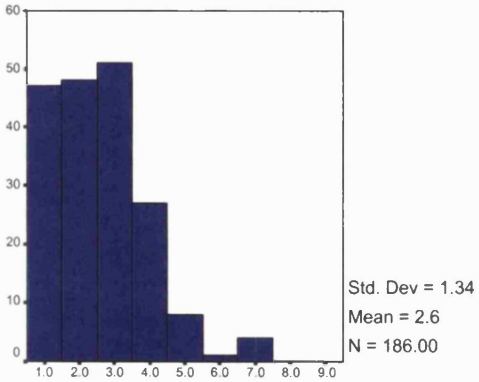

Cervical Motoneurones

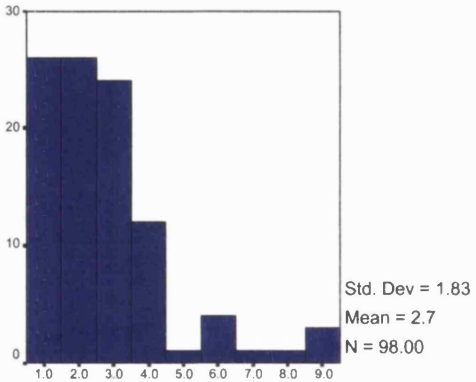

Thoracic Motoneurones

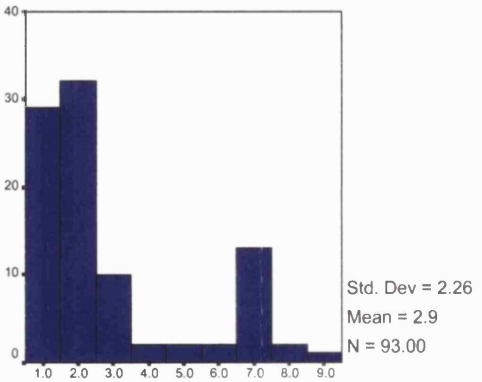

Lumbar Motoneurones

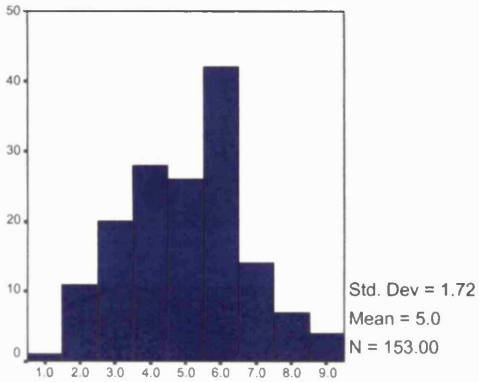

VL

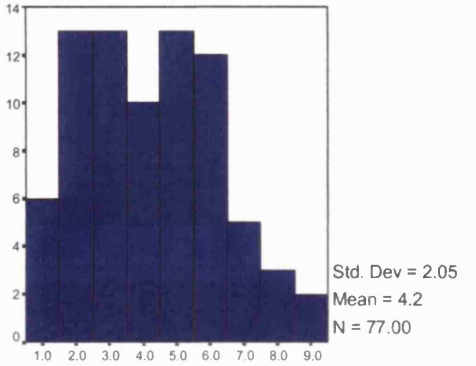

ON

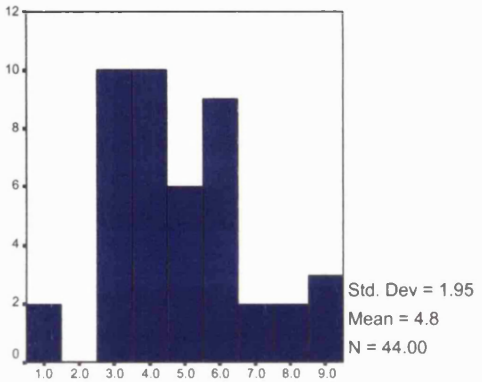

VM

Figure 3.3.2-7 Distributions of CM IR by motoneurone type. Ordinate scales have been adjusted for sample size to facilitate the visual comparison of the distributions.

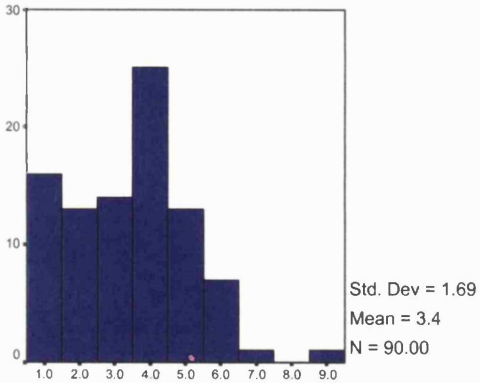

Cervical Motoneurones

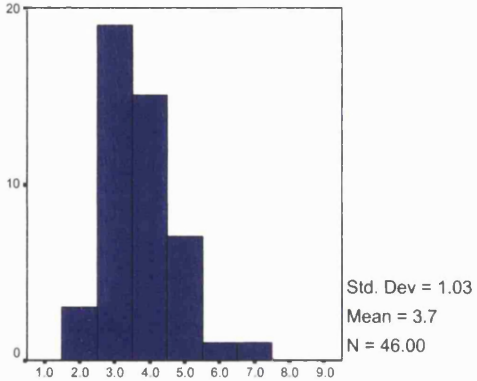

Thoracic Motoneurones

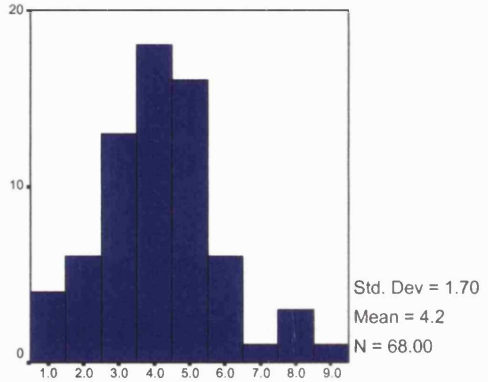

Lumbar Motoneurones

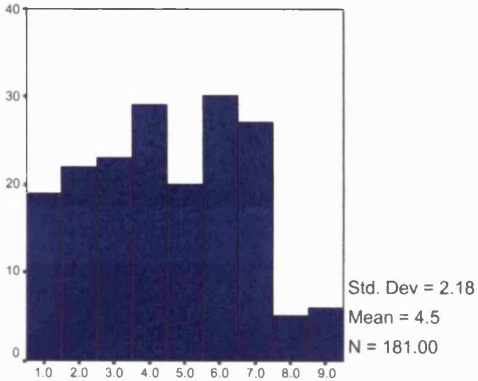

VL

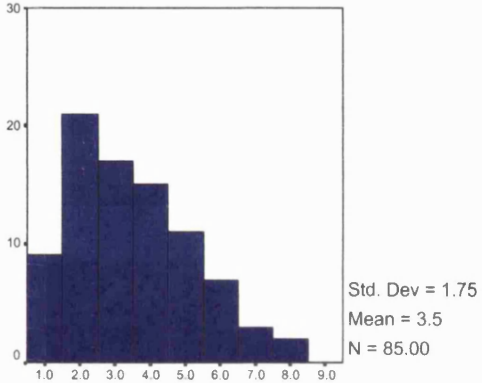

ON

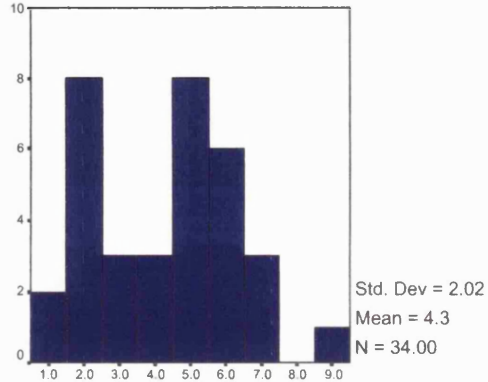

VM

Figure 3.3.2-8 Distributions of PV IR by motoneurone type. Ordinate scales have been adjusted for sample size to facilitate the visual comparison of the distributions.

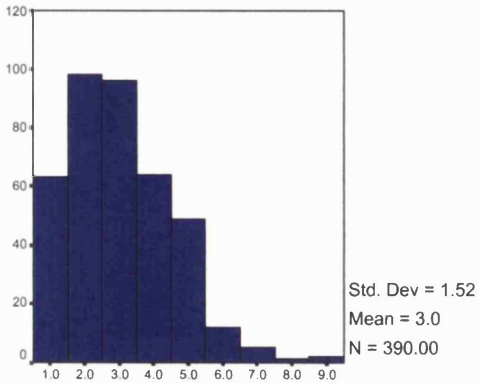

Cervical Motoneurones

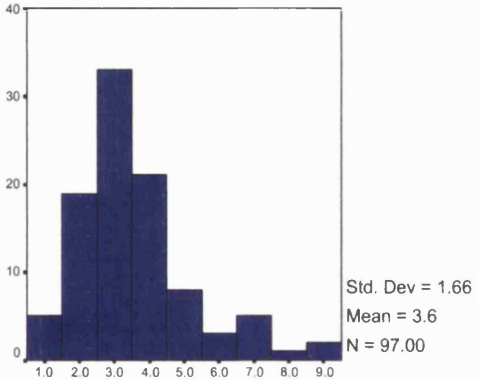

Thoracic Motoneurones

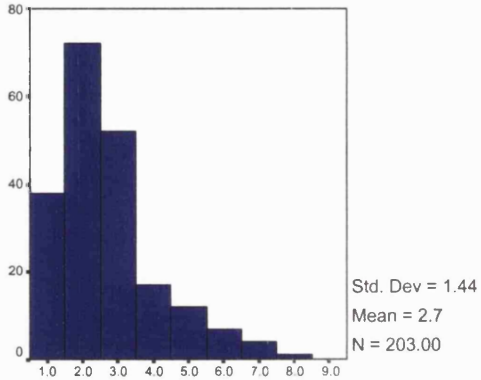

Lumbar Motoneurones

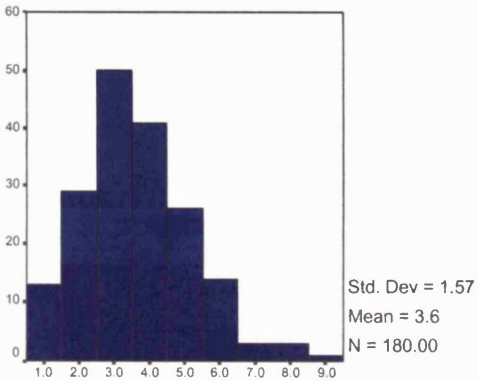

VL

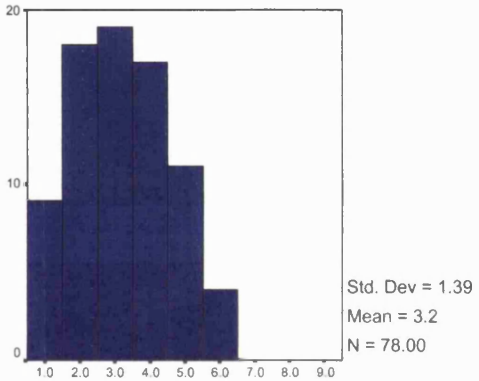

ON

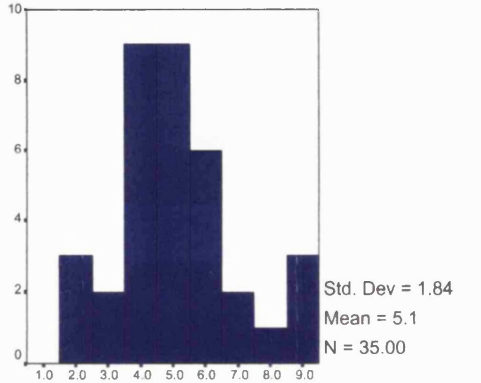

VM

Figure 3.3.2-9 Distributions of CaN IR by motoneurone type. Ordinate scales have been adjusted for sample size to facilitate the visual comparison of the distributions.

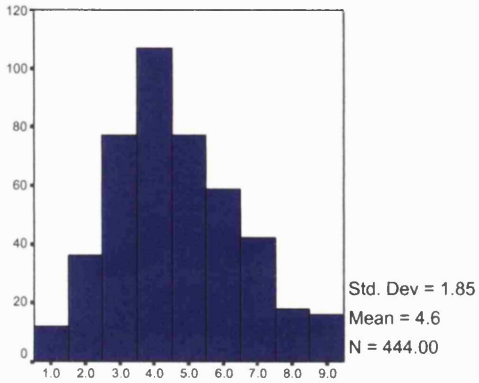

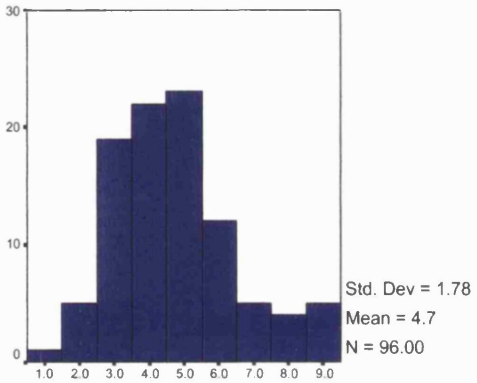

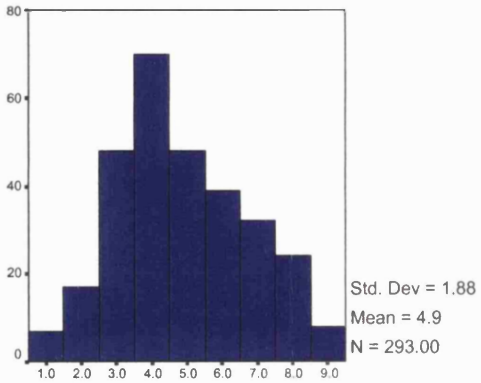

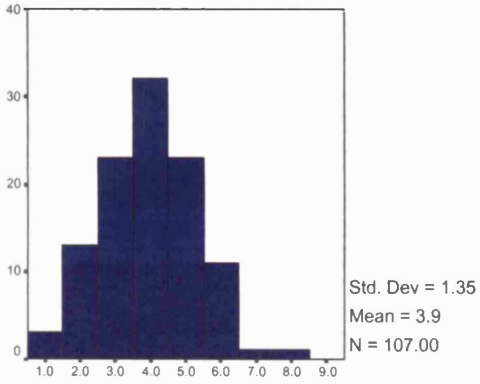

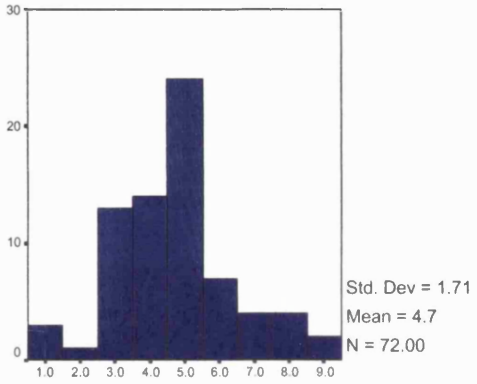

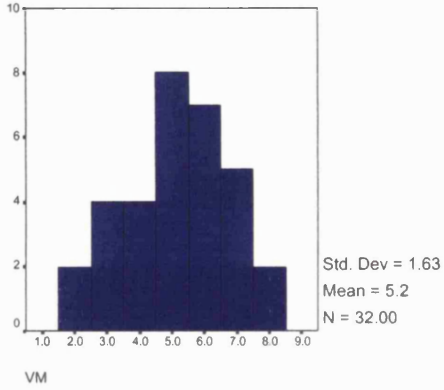

Figure 3.3.2-10 A series of plots showing the contribution of individual experiments on cell group variations in mean bin location. Each coloured line represents the results from a single animal. The main outliers are as follows: SOD: control segments from one 1 week sacral axotomy (---), CaN: control segments from all three one week sacral axotomies (---, ---, ---), CaBP-D28k: control segments from both 2 week sacral axotomies (---,---) and Unoperated Control No.2 (---), CM: Unoperated Control No. 2 (---), nNOS: Unoperated Control No. 2 (---).

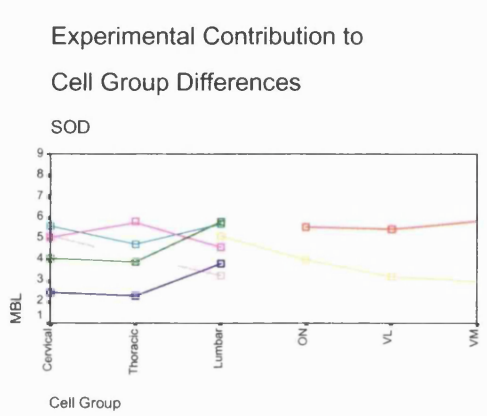

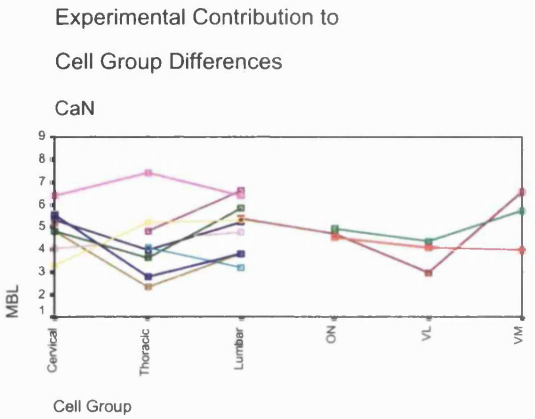

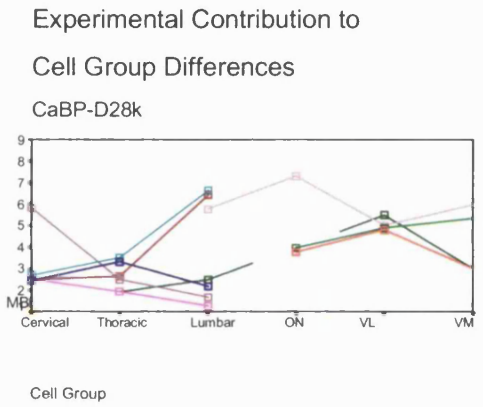

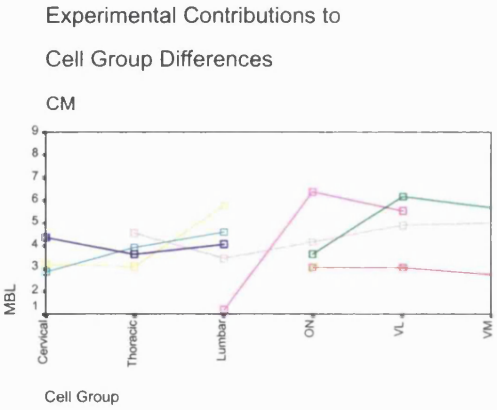

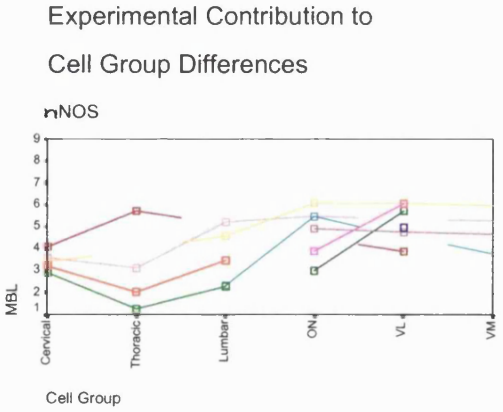

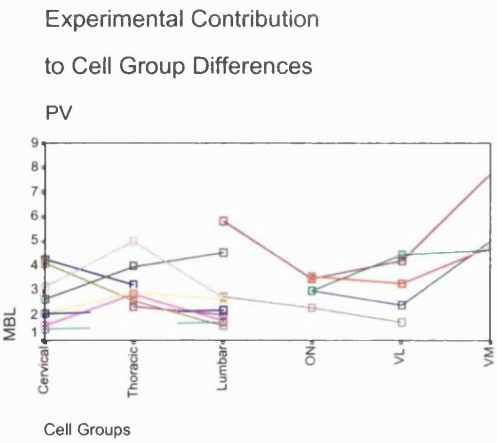

For most antigens and most experiments, the results show reasonable homogeneity, following similar trends in the direction of changes from one cell group to the next.

Nevertheless, the plot for SOD reveals a higher degree of variability between experiments than was seen with other antigens. Sacral motoneuronal data were derived from only two animals, which were clearly very different from one another in terms of staining distribution, rendering the finding of high sacral levels of SOD somewhat less reliable. For the rest of the spinal segments, all animals had similar peaks of high MBL for lumbar segments, with decreased MBL for cervical and thoracic segments. One experiment (pink line) deviates from this trend, with an outlying peak in thoracic MBL levels. This tissue was derived from the control segments of a 1 week sacral axotomy, and cervical and lumbar levels were found to be within the normal ranges. This possibly accounts for the non-significance of the mean or distributional difference between lumbar and thoracic segments. Meanwhile, the distributions of cervical and lumbar cord were significantly different (see Table 3.3.2-4).

The plot for nNOS shows a good deal of inter-experiment consistency, with the exception of one experiment which has a thoracic peak and dips back down to the sacral cord (brown line).This animal was a normal control and was found also to have very different patterns of staining for CM and CB (see below).

Since mean CM-IR was not found to differ significantly between segments, it is not surprising that the plot for this antigen shows fairly consistent results with little variation between segments, marked by one outlying experiment (pink line), being the same normal control lying outside the range of normal nNOS results. This may account for the significance of the distribution comparisons

found with the Kolmogorov-Smirnov, in the absence of significantly different means.

Conversely, the CaN plot reveals a fairly consistent thoracic "dip" and cervical/lumbar peak in values across 5 experiments. This pattern was reversed in the three sacral axotomy experiments that had had one week post-surgical recovery periods (pink, yellow, and cyan lines). Therefore, ANOVA and post-hoc Dunnett's T3 and Tamhane's T2 tests were performed on two week axotomies and unoperated controls, excluding the outlying control tissue from one week sacral axotomy experiments. Under these conditions, significant segmental differences were found. Unoperated animals or animals with two week old lesions have thoracic levels that are significantly lower than the levels of cervical motoneurones by a mean difference of -1.033 ($p<.001$), lower than lumbar motoneurones by a mean difference of -1.042 ($p<.001$), lower than ON motoneurones by a mean difference of -.9514 ($p = .014$), and lower than VM motoneurones by a mean difference of -1.3854 ($p=.005$). Cervical, lumbar, and VM levels are also significantly higher than those of the sacral ventrolateral nucleus by mean differences of .8601 ($p<.001$), .8689 ($p<.001$), and 1.2123 ($p=.017$) respectively.

Similarly, the variablilty in CaBP-D28k results was also affected by the inclusion of control segments of sacral axotomised animals. In this case, values higher than the normal range were observed selectively in the two axotomies which had had two weeks post-surgical recovery periods (brown and cyan lines), and in the same normal control experiment that had unusually high nNOS-IR and CM-IR (light grey line). The exclusion of these experiments increased the differences between the sacral motoneurone groups and each of the other segments. Since the probability associated with these differences was already

beyond the sensitivity of the software used for the analysis, it is not possible to estimate the effect of these exclusions on the significance of the differences which are all $p<.001$. Clearly, even before the exclusion of outliers, this is a robust finding.

The variability of PV immunostaining was mentioned earlier, and is represented in these plots by two peaks of unusually high staining in the lumbar cord. In spite of this variability, thoracic motoneurones were still found to be significantly higher in MBL than lumbar motoneurones, suggesting that this is a particularly robust finding.

It is therefore apparent that although there does seem to be some effect of sacral axotomy on the antigenicity of the unaxotomised segments, none of these outlying experiments have contributed to the significant differences observed, with their exclusion either not altering or increasing the significance of the findings. The exception to this was SOD-IR, where the results from the small sample of sacral tissue renders it difficult to draw clear conclusions.

3.3.3 Discussion

3.3.3i Ca^{2+} -binding "buffer" proteins: CaBP-D28k and PV

Qualitatively, many features of CaBP-D28k-IR and PV-IR reported previously in rat, monkey, and human were confirmed to exist in the cat. The distribution of these buffer proteins throughout the cytoplasm and nucleus of immunopositive cells, extending into the dendrites, leads to a distinctive appearance of neurones stained for these antigens (Celio, 1990, Baimbridge et al, 1992). In agreement with findings in mouse (Morrison et al, 1996), rat (Zhang et al, 1990; Celio, 1990; Ren and Ruda, 1994; Dassesse et al, 1998), primate (Reiner et al, 1995), and human (Satoh et al, 1991; Alexianu et al, 1994; Ince et al, 1993), CaBP-D28k-IR and PV-IR demarcate discrete sub-populations of cells in the cat spinal cord, where ventral horn motoneurones but not interneurones are void of immunostaining for either protein. Indeed, Morrison et al (1996) found that in mouse spinal cord, ChAT-IR was found in only 0.3% of CaBP-D28k-IR cells. Meanwhile, very low levels of mRNA* have been observed in hypoglossal motoneurones using *in situ* hybridisation (Dassesse et al, 1998).

CaBP-D28k and PV belong to a larger family of proteins known as the EF-hand family. Proteins in this family are characterised by the presence of a helix loop helix portion, known as the EF-hand, whose hydrophilic side chains bind Ca^{2+}. Two other members of this family, calretinin and neurocalcin, are also thought to function as "buffer proteins" (see Baimbridge et al, 1992). Although not examined in the present study, others have found a similar paucity of calretinin (Ren and Ruda, 1994) and neurocalcin (Junttila et al, 1995) in somatic spinal motoneurones. It would, therefore, seem that motoneurones are lacking in a notable endogenous Ca^{2+} buffering protein system. A number of more recent findings also suggest that motoneuronal AMPA receptors may be Ca^{2+} permeable (Roy et al, 1998) to a greater extent than other spinal cord cells (Williams et al,

*CaBP-D28k

1997) or cortical neurones (Regan, 1996). In combination with the lack of endogenous Ca^{2+} buffering, this fact may well render this population of neurones selectively vulnerable to a disease process whose deleterious effects are mediated by $[Ca^{2+}]_i$.

The critical test of such a theory is the comparative status of "protected" cells within that population. In the case of ALS, the oculomotor, trochlear, and abducens motor groups of the brainstem are more resistant than other motoneurones, and have been found to have higher PV-IR in comparison to other motoneurones of the brainstem and spinal cord (Celio, 1990; Reiner et al, 1995). Similarly, ON has also been observed to have higher levels of CaBP-IR and PV-IR in the human spinal cord by Appel's group (Alexianu et al, 1994), although the only other group to examine this nucleus (Ince et al, 1993), report levels of CaBP-IR in ON to be as low as in other motoneurones, with high neuropil staining around the nucleus.

In the present study, weak immunostaining for CaBP-D28k but not PV was noted in the motoneurones of ON as well as neighbouring VL and VM in some animals. It was not possible qualitatively to conclude that these cells were more highly stained than motoneurones of other segments, where weak staining could also be occasionally seen. In this sense, the current results are in agreement with the findings of Ince's group, whilst Alexianu and colleagues observed a clear qualitative difference with levels of immunoreactivity scoring "++" for both CaBP-D28k and PV in the cells of ON .

The lack of support for Appel's findings of high PV-IR in the sacral motor nuclei may reflect species differences. A feature of PV staining noted in the present study might also account for some of this discrepancy. Very high levels of

immunoreactivity were occasionally seen restricted to the motoneurones of a single segment, when tissue from all segments had been processed in a single tube. Thus, it is possible that PV may be expressed transiently within motoneuronal groups in response to an unknown stimulus, and this may have caused unusual transient PV-IR within ON in the tissue examined by Appel's group. In addition, these authors neither presented photographic evidence, nor described or quantified the immunoreactivity and it is therefore not at all clear how consistent this finding was throughout their sample (N=9), nor what is meant by the "++" score which was allocated to ON for PV-IR.

Morrison and colleagues (1996) caution against bold interpretations from the studies listed above since in all cases the observations were qualitative and require further quantitative investigation. Whilst the qualitative observations in this study were in agreement with Ince's group, with very low levels in the motoneurones of ON, quantification revealed that although weak, the motoneuronal immunostaining for CaBP-D28k within ON and VL was consistently significantly higher than that of motoneurones in cervical, thoracic, and lumbar segments.

Findings of these sort are commonly treated as evidence for a Ca^{2+} -mediated mechanism underlying the neuropathology of ALS, however, there is no clear evidence that either of these proteins do confer neuroprotection against Ca^{2+} -related injury. The primary argument is that by buffering Ca^{2+} levels, $[Ca^{2+}]_i$ must be reduced in neurones expressing Ca^{2+} binding proteins when compared with neurones lacking these endogenous buffers. In fact the effects of these proteins on $[Ca^{2+}]_i$ are far more complex, and the validity of the primary argument is examined below.

Ca^{2+} binding proteins and their effects on Ca^{2+} homeostasis

The precise effects of CaBP-D28k and PV on $[Ca^{2+}]_i$ are not clearly understood. The most obvious outcome of CaBP-D28k activity is a decrease in some part of the Ca^{2+} signal and indeed in the absence of CaBP-D28k, the amplitude of the fast component of Ca^{2+} transients is quadrupled as indicated by Ca^{2+} fluorescence imaging (Airaksinen et al, 1997a). Patch clamp recordings from a pituitary tumour cell line expressing CaBP-D28k demonstrate a decrease in the amplitude of inward Ca^{2+} currents through L and T type channels and the loss of the fast decay component of the Ca^{2+} transient (Lledo et al, 1992). Both of these studies support a role for CaBP-D28k as a fast, high-affinity buffer operating within the first 100msec of Ca^{2+} influx.

In contrast, the loss of long term potentiation (LTP) in hippocampal neurones from mice with reduced CaBP-D28k expression suggests that CaBP-D28k may serve to increase Ca^{2+} entry (Molinari et al, 1996). Inward Ca^{2+} currents may be inactivated in a voltage-dependent fashion, but channels are also sensitive to free $[Ca^{2+}]_i$ levels and are inactivated at certain concentrations of free $[Ca^{2+}]_i$ (Plant et al, 1983). Ca^{2+}-dependent Ca^{2+} channel inactivation is reduced by the presence of Ca^{2+} chelators, which thereby prolong the Ca^{2+} transient (Plant et al, 1983), suggesting that endogenous Ca^{2+} buffers may have a similar effect. In this manner, CaBP-D28k may have a role in facilitating LTP.

Kohr et al (1991) found support for this hypothesis in kindled hippocampal granule cells, known to have reduced CaBP-D28k-IR (e.g. Kohr et al, 1991; Baimbridge and Miller, 1984, but see later). Whole cell patch clamp measurements of Ca^{2+} currents in granule cells whose CaBP-D28k content has

been decreased in this manner, show that inactivation of L-type Ca^{2+} currents is significantly increased, but can be returned to control levels (i.e. levels of CaBP-D28k-IR neurones) by the addition of the rapid, high-affinity Ca^{2+} chelator, BAPTA (Kohr et al, 1991), suggesting that the presence of CaBP-D28k would prolong the Ca^{2+} transient. In addition, the duration of Ca^{2+} transients in axotomised rat sympathetic ganglion has also been found to be increased, coincident with an elevation of CaBP-D28k-IR (Sanchez-Vives et al, 1994). It is not clear, in this paradigm, which occurs first; it could be that increased neuronal Ca^{2+} permeability induced by axotomy causes increased CaBP-D28k expression.

Conversely, patch clamp measurement of Ca^{2+} currents in a pituitary tumour cell line shows that the expression of CaBP-D28k by these cells causes an increase in L and T type channel inactivation (Lledo et al, 1992). The authors postulate that CaBP-D28k may also have a "trigger" function whereby, once bound to Ca^{2+}, it interacts directly with Ca^{2+} channels to alter their activity. The reasons for the contrasting findings are not clear, but may reflect the difference between neuronal and non-neuronal phenotypes.

Thus, it would seem that CaBP-D28k serves both to buffer the fast component of the Ca^{2+} influx, which may have a neuroprotective outcome in pathological conditions, and thereafter to prolong the channel open time, which might even exacerbate Ca^{2+} related damage. In fact, it may be that the primary function of CaBP-D28k is to shape the wave form of synaptic Ca^{2+} transients in a physiologically meaningful manner (Airaksinen et al, 1997a), and hence it is possible that the total build up of free $[Ca^{2+}]_i$ during Ca^{2+} influx may be comparable to that in neurones lacking CaBP-D28k.

Further quantification of Ca^{2+} changes in the presence and absence of Ca^{2+} binding proteins is required before conclusions can be drawn about their potential to protect or heighten vulnerability to excessive levels of $[Ca^{2+}]_i$. Indeed according to the findings reviewed above, the decrease in peak amplitude of the fast component of the Ca^{2+} transient is 75% in the presence of CaBP-D28k. With a little more information it should be possible to calculate if there is an overall change in total Ca^{2+} entry. It should also be noted that all of these studies examined levels of $[Ca^{2+}]_i$ *within normal physiological ranges.* The effects of Ca^{2+} binding protein activity may be quite different under conditions of excessively high $[Ca^{2+}]_i$. Furthermore, this evidence is derived from non-motoneuronal cell types. It is not necessarily the case that the activity of CaBP-D28ks will have the identical physiological outcome for different types of neurone.

Other arguments for Ca^{2+} binding protein mediated neuroprotection

Other evidence for neuroprotective Ca^{2+} buffering by CaBP-D28k and PV has been inferred from three main types of finding. Firstly, and somewhat paradoxically, those studies localising the proteins to populations of cells that are vulnerable to a range of acute and degenerative pathological states related to (or in some cases, theoretically related to) Ca^{2+} influx. These may be interpreted as supporting either a protective or exacerbating role for Ca^{2+} binding proteins in Ca^{2+}-related damage, but findings of decreased expression after injury may support the latter conclusion. Next are those studies demonstrating Ca^{2+}-binding protein localisation in neuronal populations that are resistant to a range of acute and degenerative pathological states related to (or in some cases, theoretically related to) Ca^{2+} influx. The post-injury elevations of Ca^{2+} binding protein expression within resistant cell groups found by some researchers support the conclusions of neuroprotection derived from these studies. Finally, further

arguments for a neuroprotective role of Ca^{2+}-binding proteins are derived from those studies investigating the *in vitro* effects of CaBP-D28k expression on neuronal resistance to Ca^{2+} toxicity. These three sources of evidence will be explored below.

Localisation of proteins to vulnerable populations of cells

Data on the correlation of Ca^{2+} binding protein localisation with disease or injury vulnerability are abundant in the literature (for a review see Heizmann and Braun, 1992) with many studies leading to the conclusion that Ca^{2+} binding protein status alone is not sufficient to predict patterns of neuronal vulnerability.

A substantial body of work localises Ca^{2+} binding proteins to vulnerable neuronal groups. For example, in his extensive study of the distribution of PV-IR and CaBP-D28k-IR in the rat CNS, Celio (1990) noted that CaBP-D28k-IR seemed localised to populations that are known to be lost in Parkinson's disease (PD), Huntington's disease (HD), and in Alzheimer's disease (AD). This supported his earlier hypothesis (Celio, 1986), that Ca^{2+} binding proteins are preferentially located in neurones that are more prone to 'intolerable' levels of $[Ca^{2+}]_i$.

In further support of this it was found that, in ageing, expression of CaBP-D28k (Iacopino and Christakos, 1990, Kishimoto et al, 1998), but not PV (Kishimoto et al, 1998), is significantly decreased. Brains from patients with HD, AD, and PD also show significant decreases of CaBP-D28k and PV from levels in age matched controls in affected areas (Iacopino and Christakos, 1990). In addition, loss of PV-IR neurones in the hippocampus has been reported in temporal lobe epilepsy (TLE) (Guentchev et al, 1997).

These findings give rise to a scenario of age-related decreases of protection against Ca^{2+} within neurones that are unusually susceptible to large Ca^{2+} influxes. This would both explain the susceptibility of neurones containing Ca^{2+} binding protein, whilst supporting a neuroprotective role for those proteins. However, it is not possible to conclude from these findings that the decrease in Ca^{2+} binding protein causes the susceptibility. An equally reasonable interpretation could be that Ca^{2+} binding proteins cause vulnerability - perhaps by decreasing Ca^{2+}-dependent Ca^{2+} channel inactivation - and the loss of expression in affected neurones may represent a defence against increasing levels of total $[Ca^{2+}]_i$.

The hypothesis of Ca^{2+} binding protein reduction as a neuronal defence might be supported by the observations that Ca^{2+} binding protein levels are sometimes decreased when neurones are challenged with high levels of Ca^{2+}. After repeated sub-convulsive stimulation of hippocampal neurones (kindling), pyramidal cells of CA1 are lost, with sparing of the granule cells. Using radioimmunoassay (RIA) to measure levels of protein, as well as immunocytochemistry, Baimbridge and Miller have shown that CaBP-D28k levels are significantly and permanently decreased in the granule cells from the earliest stages of kindling (Baimbridge and Miller, 1984; Miller and Baimbridge, 1983; also Kohr et al, 1991), although others have found no change in mRNA levels up to 24 hours after kindling (Sonnenberg et al, 1991). Reduced immunoreactivity for CaBP-D28k and PV has also been documented after ischaemia in the vulnerable CA1 pyramidal cells (Johansen et al, 1990) although the decrease in PV-IR was transient and occurred between the third and tenth day after ischaemic challenge.

Other explanations put forward to account for these findings include the effect of increased Ca^{2+}-binding on CaBP-D28k immunoreactivity. In the present

study the addition of Ca^{2+} or the Ca^{2+} chelator EGTA during incubation with the primary antibody did not affect immunostaining. It is nevertheless possible that the aldehyde fixation of Ca^{2+}-bound protein results in an irreversible inhibition of antibody binding, which remains unaffected by the alteration of Ca^{2+} levels after fixation.

Localisation of proteins to resistant populations of cells

A closer examination of the relationship of Ca^{2+}-binding protein expression and disease or injury susceptibility suggests that in fact these proteins may be markers of protected sub-populations within vulnerable areas such as the hippocampus. Sloviter (1989) reported that although the hippocampus contains CaBP-D28k and PV, and is susceptible to epileptic and ischaemic damage, there is an inverse correlation between the staining intensity of each sub-region and the vulnerability of that region, with CA2 being the least vulnerable region (Guentchev et al, 1997) and most highly immunoreactive for CaBP-D28k and PV (Sloviter, 1989). Rami et al (1998) also found very high staining in CA1-2, but failed to differentiate between them. CA1 is more vulnerable to these insults and closer inspection of this sub-region suggests that it contains fewer CaBP-D28k-IR and PV-IR neurones and those that do have immunoreactivity are only weakly stained (Sloviter, 1989). Outside the hippocampus proper, the entorhinal cortex is composed of glutamatergic neurones, of which 60% are CaBP-D28k-IR, and non-glutamatergic neurones, of which none are CaBP-D28k-IR (Peterson et al, 1996). After axotomy, only glutamatergic neurones lacking CaBP-D28k-IR were lost, with sparing of CaBP-D28k-IR neurones and non-glutamatergic neurones, suggesting that lack of CaBP-D28k may only be required to protect a sub-population of more vulnerable neurones as suggested by Celio (1990).

The pars compacta of the substantia nigra (SN_c) is another case in point. A closer inspection of cellular vulnerability in PD demonstrates the selective sparing of CaBP-D28k-IR neurones within the vulnerable SN_c (Yamada et al, 1990), which is well mimicked by the MPTP model (Ng et al, 1996) and echoed in the selective resistance of these neurones to axotomy induced degeneration (Alexi and Hefti, 1996). The use of extremely dilute primary antibody (1:100 000) in the latter study also facilitated detection of a 228% increase in CaBP-D28k-IR, suggesting that, in this model, CaBP-D28k may be up-regulated as a defence against the effects of MPTP (Ng et al, 1996). Similarly, in motoneurones, upregulation of CaBP-D28k mRNA was detected 8 days after hypoglossal axotomy (Dassesse et al, 1998). However, there is no increase in SNc neuronal loss after MPTP treatment in CaBP-D28k-deficient mice, suggesting that, in the MPTP model, CaBP-D28k upregulation may not be a critical event (Airaksinen et al, 1997b). Since the toxin primarily targets the mitochondrion (Cleeter et al, 1992; Bates et al, 1994), and the Ca^{2+} insult may therefore be secondary, the finding of non-protection of CaBP-D28k within the context of MPTP toxicity is not totally at odds with the broader hypothesis of neuroprotection against insults that are primarily Ca^{2+} -mediated.

Findings relating to HD, where excitotoxic modelling provides a more direct link to Ca^{2+}-mediated neuronal damage, show a fairly consistent pattern of sparing. In striatum and neocortex, CaBP-D28k-IR and PV-IR neurones were found to persist in the face of substantial cell loss in the HD lesion (Storey et al, 1992; Huang et al, 1995). Modelling of this lesion with excitotoxins leads to selective sparing of PV-IR neurones in the cortex (NMDA lesion: Storey et al, 1992) and of PV-IR and CaBP-D28k-IR neurones the striatum (QUIN lesion: Figueredo-Cardenas et al, 1998; Huang et al, 1995). Reports of increased immunostaining for CaBP-D28k-IR both in HD and the QUIN model were, however, poorly

quantified and unconvincing (Huang et al, 1995). Interestingly, Figueredo-Cardenas et al also observed increasing selectivity of the lesion at greater distances from the injection site. Thus, Ca^{2+} binding proteins are probably more effective in a neuroprotective role within certain tolerances.

The in vitro effects of CaBP-D28k expression on neuronal resistance to Ca^{2+} toxicity

The final group of findings supporting an argument for Ca^{2+}-binding protein dependent neuroprotection relates to the effects of altering neuronal levels of Ca^{2+} -binding protein. For example, the level of CaBP-D28k-IR in CA1-2 of the hippocampus can be increased by chronic pre-treatment with corticosterone. Subsequent to corticosterone treatment, ischaemic cell death within these regions was significantly reduced, whilst neuronal loss in the non-calbindinergic but relatively resistant CA3-4 neurones was unaltered (Rami et al, 1998). In vitro motoneurones transfected with an ALS mutant form of SOD-1 (G93A, N139k, or G41R) undergo cell death that is largely blocked by Ca^{2+} channel blockers and antagonists of the permeable form of AMPA receptor. In this model, complete neuroprotection was achieved when the motoneurones were made to co-express CaBP-D28k (Roy et al, 1998). In addition, the *in vitro* cell death seen after treatment with ALS IgG is also blocked by retroviral infection of the motoneurone hybrid cells with CaBP-D28k cDNA (Ho et al, 1998).

Conclusions and speculations

The role of Ca^{2+}-binding buffer proteins in conditions of excessive Ca^{2+} influx is not clear cut. A greater understanding of the absolute changes in $[Ca^{2+}]_i$ in the presence of these proteins is required to enable a more sound hypothesis to be reached. However, it is not unreasonable to suggest that whether a Ca^{2+} -buffering protein is neuroprotective or not depends on the context (injury type,

neurone type etc) and the actual levels of the protein expressed. That is to say that for different neurones and different injuries there may be optimal levels of Ca^{2+}-binding protein. To illustrate, the effects of CaBP-D28k on the wave form of Ca^{2+} transients may have implications for the contexts in which it may or may not confer neuroprotection. In acute ischaemic or epileptic type insults of fast neurones, any reduction in Ca^{2+} channel inactivation brought about by the normal levels of endogenous Ca^{2+} buffering activity might increase the excitability of the cell and hence exacerbate the damage. Thus, the decreases of CaBP-D28k seen in kindling and after ischaemia may well be a protective alteration (Baimbridge and Miller, 1984; Kohr et al, 1991) and yet the higher levels of CaBP-D28k induced by chronic corticosterone treatment may be neuroprotective by simply enabling the neurone to cope with the increased Ca^{2+} (Rami et al, 1998). On the other hand, it may be that slow, chronic lesions, of the kind that develop in neurodegenerative conditions, are not exacerbated by the altered inactivation of the Ca^{2+} transients, but instead the 75% reduction in amplitude (Airaksinen et al, 1997a) may become the critical factor for these cells.

Why ON and VL should differ from the rest of the cord in this respect is also unclear. The maintenance of tonic contraction of the sphincter muscles innervated by ON means that these motoneurones are likely to have different synaptology, connectivity, and physiology from other motoneuronal groups. Recent findings in cortical control of primate hand muscles suggests that tonic contractions are associated with synchronous firing patterns (Baker et al, 1997). It is possible that ON maintains sphincteric contraction by a similar mechanism, potentially mediated by and thus accounting for the unusually dense and localised bundling of its dendrites, approximately 44% of which form dendro-dendritic connections (Ramirez-Leon and Ullfhake, 1993). Indeed, CaBP-D28k-

expression has been related to physiological neuronal characteristics such as dendritic Ca^{2+} currents (in Baimbridge et al, 1992). It may be that this form of firing activity requires a better Ca^{2+} buffering mechanism than is required by the average motoneuronal physiology. Further physiological studies would be required to confirm this hypothesis.

3.3.3ii The Ca^{2+} -binding "trigger" proteins: CM and CaN

CM

CM-IR in the present study was found throughout the spinal cord, in a variety of neuronal types and the dorsal horn fibres. Characteristically, neuronal immunostaining was found in the cytoplasm and nucleus, but not the nucleolus, with nuclear staining often being the most intense. Nuclear staining is consistent with the observations of Vendrell et al (1991) and Sola et al (1999) who found high levels of CM in the nuclei of neurones from rat and mouse brain. Here CM may interact with gene transcription (in Sola et al, 1999) and may also contribute to alterations in actin-myosin motility, as suggested by Vendrell et al (1991).

CM is an ubiquitous protein which interacts with a vast range of proteins, particularly those involved in phosphorylation (e.g. the CaM-kinases) and dephosphorylation (e.g. calcineurin). Through its effects on these proteins, CM is integrally involved in transducing the Ca^{2+} signal, the generation of LTP (e.g. Silva et al, 1992a; Silva et al, 1992b), stabilising the cytoskeleton, and controlling gene transcription via its interactions with a wide range of other proteins (see Klee et al, 1980; and Sola et al, 1999 for a review). It is not surprising, therefore, that CM was localised within a variety of different subtypes of neurone in this study. Nevertheless, interneurones were significantly different from motoneurones in terms of their distribution across

stain levels. The motoneuronal frequency distribution was significantly 'flatter' suggesting a greater variability in levels of gene product, whilst interneurones generally contained a fairly consistent amount of antigen within a narrower range. It is possible that the higher degree of motoneuronal variability might be related to the differing physiological characteristics of motoneurones belonging to different types of motor unit. Overall, however, the difference was subtle and this is reflected in the statistically non-significant level of the difference between means.

There are no reports in the literature concerning the possibility of segmental variations in the localisation of CM in the spinal cord. Segmental variability in the current study only showed subtle variation, with ON showing no differences from motoneurones from other segments, but VL and VM having the highest MBLs. The mean bin location for VL was found to be significantly higher than that of the cervical motoneurones, which appeared to be clustered towards the palest end of the range. It is quite possible that this result reflects sampling bias, since measurements of CM-IR in cervical motoneurones were not derived from the same animals as measurements for VL. Thoracic CM-IR was restricted to a much narrower band of staining levels than the distributions from any other segments. Given that thoracic motoneurones were measured in the same animals as motoneurones from all other segments, this result is more likely to represent a genuine biological difference.

The homogeneity of CM levels in thoracic motoneurones could well be a reflection of the different type of physiological activity involved in respiratory motor control, which is geared towards tonic activity (Iscoe, 1998). For example, it may be that the muscle groups involved in respiratory motor control are composed of relatively homogeneous populations of motor units in comparison

to limb motoneurones, which may require a wider range of physiological subtypes to co-ordinate the diversity of speeds and forces of contraction required for limb muscle function. At the levels of the thoracic cord examined in this study, motoneurones present innervate a mixture of intercostal (Coffey, 1972 ; Tani et al, 1994) and abdominal (Tani et al, 1994; also see Iscoe, 1998) musculature. Abdominal muscles (external oblique, internal oblique, rectus abdominus, and transversus abdominus) in man are mostly composed of slowly contracting fibres, with a relatively small component of fast twitch muscle fibres, and are supplied by nerves with a narrow range of peak firing frequencies (in Iscoe, 1998). Thus it appears that the more limited range of physiological properties expressed by the thoracic motoneurones measured correlates with a narrower range in levels of CM in this population.

CaN

Using the CaN-Aα antibody in rat, Strack and coworkers (1996) have demonstrated strong IR of α-motoneurones and of a dense meshwork of labelled fibres around motor nuclei, which they deemed to be motoneurone dendrites. In the present work, punctate and fibrous structures strongly reactive for CaN-A were observed in and around all motor nuclei, which are similarly likely to represent dendritic processes. The only major departure between the present findings and those of Strack, is that in the rat the antibody only stained around 25% of the motoneuron pool, whilst in the present cat study unstained motoneurones were rarely observed in the spinal cord. Indeed, levels of CaN-IR were found to be very high in cat motoneurones and immunoreactivity for CaN was also present to a lesser extent in ventral horn interneurones. These levels of staining were consistent throughout the spinal cord, with no segmental variations.

In the human spinal cord Goto et al (1990) described immunocytochemical staining of ventral horn cells, dorsal horn cells, and the neurones of Clarke's column. In the absence of any information about the specificity of their antibody, or the location and size of the stained ventral horn neurones, it is difficult to make any comparisons between the current findings in cat spinal cord and those using human tissue.

In the present work, CaN-A immunostaining was characterisitically dispersed throughout the cytoplasm, sometimes with foci of higher intensity staining close to neuronal or nuclear membranes, but nuclear staining per se was never observed.

The localisation of CaN in neuronal processes, as well as in perikaryal cytosol, and in close association with membranes is concordant with its known structure and activities. In structural terms, CaN is myristoylated and thus has a tendency to be membrane bound (in Morioka et al, 1999). Functionally, CaN binds Ca^{2+} in its EF-hand portion, as well as Ca^{2+}-CM, which activates its serine-threonine phosphatase activity. CaN is then responsible for dephosphorylation of an array of proteins involved in the regulation of intracellular Ca^{2+} stores, synaptic transmission, ultrastructural stabilisation, NO generation, and apoptotic and delayed ischaemic neuronal cell death (Dawson et al, 1993; Zhu and Yakel, 1997; Wang et al, 1999; Morioka et al, 1999). Ultrastructurally, CaN has been found to localise to dendrites, post-synaptic densities, microtubules, around mitochondria and generally to be dispersed within the cytoplasm (Goto et al, 1986).

3.3.3.iii Proteins involved in free radical homeostasis: nNOS and SOD

nNOS

nNOS is one of four identified forms of nitric oxide synthase, and the protein is known to contain a nicotinamide adenine dinucleotide phosphate (NADPH) binding site reflecting its requirement for NADPH in addition to Ca^{2+}-CM and CaN. A series of publications document the presence of nNOS in neurones with NADPH-d activity (Dawson et al, 1991; Bredt et al, 1991) leading to the conclusion that the two are synonymous, and that indeed nNOS is responsible for the diaphorase activity of these neurones. By and large, this tenet has become the received wisdom for many working with an interest in these substances, with NADPH-d histochemistry being used as a means of identifying nNOS-containing cells (e.g. Gu et al, 1997; Kanda, 1996; Kristensson et al, 1994; Wu et al, 1994a & b; Wu et al, 1995).

The validity of this assumption of synonymity is not beyond question, it would seem. A number of papers suggest that nNOS-IR is only found in a small subset of neurones possessing NADPH-d activity (Yu, 1994; Vizzard et al, 1994; Zhou et al, 1998). Closer investigations of double labelled sections in cat spinal cord reveal cells reactive for either nNOS or NADPH-d processing, but not both (Pullen and Humphreys, 1995). More recently it has been demonstrated that NADPH-d histochemistry is dependent on Ca^{2+}-CM (Morris et al, 1997), suggesting that as well as detecting nNOS negative neurones, this technique is not sensitive to *inactive* nNOS. Thus the failure to detect NADPH-d activity in neurones does not necessarily mean that those neurones do not contain the nNOS protein. Finally, the demonstration that the reactions required for the production of NO from nNOS can also occur independently of NADPH (Witteveen et al, 1998) dispels the notion that NADPH-d activity is essential for NO generation. For these reasons, the current study has evaluated the

localisation of nNOS by the use of nNOS immunocytochemistry rather than NADPH-d histochemistry.

Because of the tendency to equate nNOS and NADPH-d, much of the work describing nNOS distributions in the nervous system actually documents NADPH-d activity and hence the literature on the distribution of nNOS in the spinal cord must be interpreted with caution. NADPH-d activity has been documented in motoneurones only after injury (Gu et al, 1997; Wu et al, 1994a and b; Wu et al, 1993; Yu, 1994), in the wobbler mouse (Clowry and McHanwell, 1996), or in aging (Kanda, 1996).

Antibodies to nNOS in the hands of some researchers also fail to detect the presence of the protein in rat, mouse, cat and squirrel monkey motoneurones, in agreement with the general findings on the distribution of NADPH-d in normal spinal cord (Dun et al, 1993; Saito et al, 1994). In contrast, using immunocytochemistry, Terenghi and coworkers report a distribution very similar to that observed here, with a strong presence of nNOS-IR in some ventral horn motoneurones of both man and rat (Terenghi et al, 1993). Generally, however, the focus of the majority of papers on spinal cord nNOS localisation focus on sensory and autonomic systems.

In the current work, extensive characterisation of nNOS localisation revealed numerous nNOS-IR motoneurones, which were commonly more highly stained than ventral horn interneurones. The sacral cord showed a far greater proportion of high nNOS-IR motoneurones than any other segment. This is in agreement with previous observations from our laboratory when comparison was made of thoracic and sacral segments using nNOS immunocytochemistry (Pullen et al, 1997), although using the NADPH-d reaction, others have not

observed positive staining in the lumbosacral ventral horn (Zhou and Ling, 1997). Immunoadsorption experiments in the former work also showed that the antibody used (which was the same as the antibody used for the current work) is specific for nNOS and shows no cross-reactivity for iNOS or eNOS, and furthermore that antibodies to iNOS and eNOS do not give rise to motoneuronal immunostaining.

Relaxation of the external urethral sphincter, the striated muscle innervated by ON, has been shown to be mediated by NO (von Heyden et al, 1995; Parlani et al, 1993), presumably released from the NOS containing fibres found within the muscle (Radziszewski et al, 1996) originating in the pudendal nerve (Parlani et al, 1993). Since the pudendal nerve is somatic and contains fibres originating from the motoneurones of ON, it is likely that the nNOS-IR seen in ON is related to its presence in the pudendal nerve and the use of NO as a co-transmitter. It is possible, for example, that at high rates of firing contraction is enhanced by ACh release, whilst during decreased firing, under inhibitory signals from the pontine micturition centre, relaxation is enhanced via NO release. Similar phenomena have been described elsewhere in the nervous system (Kupfermann, 1991), but further work is required to evaluate whether sacral somatic motoneurones do indeed co-release ACh and NO.

SOD-1

Many authors have noted the relatively high levels of SOD1-IR or mRNA present in spinal motoneurones of rodent (Tsuda et al, 1994; Moreno et al, 1997; Rothstein et al, 1999) and human (Pardo et al, 1995; Bergeron et al, 1996; Shaw et al, 1997; Rothstein et al, 1999) that were observed here in the cat. In the present study immunostaining was weak in comparison with other antigens and experimental variability leaves a question mark over the robustness of this

result. Nevertheless, levels of SOD-1-IR were higher in cat motoneurones than any other spinal cord cell type.

The preferential localisation of SOD-1 in motoneurones has been interpreted as a predisposal to ALS neuronal vulnerability, however segmental comparisons have not been made previously. In view of the higher levels of SOD-1-IR in ON than motoneurones from other segments, paired with Bergeron's finding of high levels in human oculomotor motoneurones (Bergeron et al, 1996), it is unlikely that expression of SOD-1 is sufficient alone to determine vulnerability. In addition, levels of SOD-1 have been shown to be the highest in Purkinje cells of the rat cerebellum (Tsuda et al, 1994). Nevertheless, higher levels in motoneurones than other spinal cord cell types may be a predisposing factor with other protective factors influencing the fate of motoneurones of ON and the oculomotor group.

CHAPTER 4

AXOTOMY RESULTS

4.1 Neuronal Sizes

In spite of the absence of significant changes in the mean motoneuronal diameter for any sacral motoneuronal type after axotomy of the pudendal nerve, there was an increase in the percentage of motoneurones in ipsilateral ON with a mean diameter larger than 50µm at both one and two weeks after surgery, and a decrease in the percentage of motoneurones with a mean diameter less than 25µm (Figs 4.1-1 and 4.1-2). In absolute terms, from a control mean diameter of 32µm, by the second week ON motoneurones had a mean diameter of 35µm bilaterally, indicating that some swelling had taken place.

Figure 4.1-1. % of motoneurones with mean diameters greater than 50 microns in ON after pudendal axotomy.

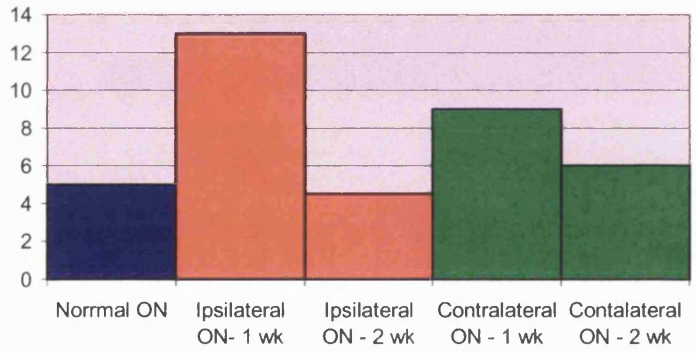

Figure 4.1-2. % of motoneurones with mean diameters less than 25 microns in ON after pudendal axotomy.

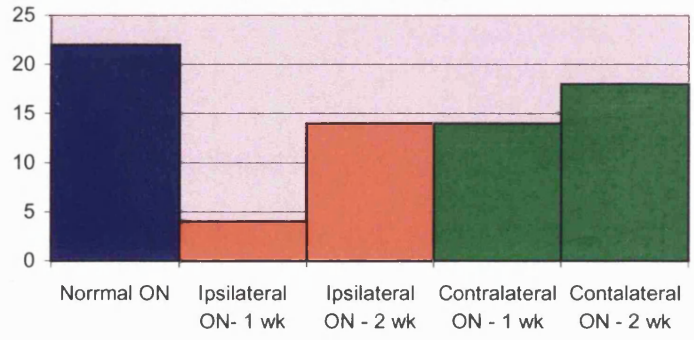

Two weeks after axotomy of the nerve innervating the sartorius, a significant bilateral increase in the mean motoneuronal diameter of sartorius motoneurones from 39µm to 48µm was observed (t-test $p<.0001$). This increase is reflected in the large alteration in the percentage of sartorius motoneurones with a mean diameter larger than 55µm, and a decrease in the percentage of sartorius motoneurones with a mean diameter smaller than 25µm (Figs 4.1-3 and 4.1-4). There was a modest increase in the percentage of iliacus motoneurones with large mean diameters, but the mean difference from normality was not significant.

Figure 4.1-3.
% of motoneurones in L4-5 larger than 55 microns in mean diameter after axotomy to n. sartorius.

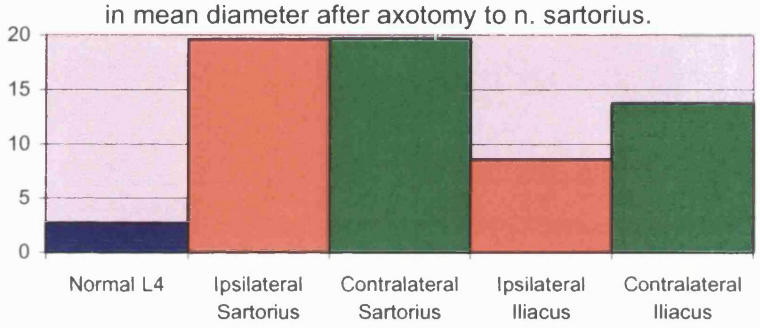

Figure 4.1-4. % of motoneurones in L4--5 smaller than 35 microns in mean diameter after axotomy to n. sartorius.

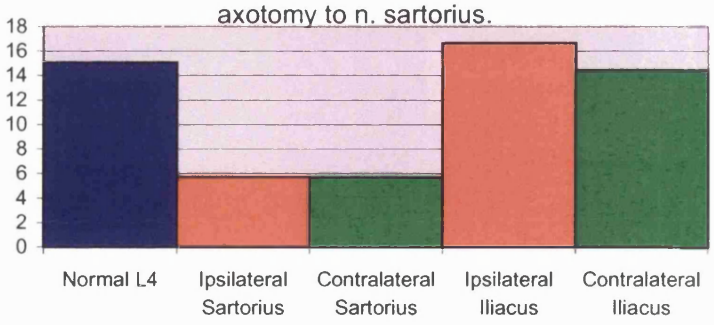

It would thus appear that following pudendal axotomy there is a small degree of acute motoneuronal swelling at one week after the lesion which is more prominent ipsilaterally. Meanwhile, two weeks after sartorius axotomy there is a large bilateral increase in motoneuronal mean diameter for sartorius motoneurones.

4.2 Post-Axotomy Antigenicity

Bin locations were calculated as previously described (see Chapters 2 and 3). Despite the visual impression of little alteration in levels of immunostaining in axotomised motoneurones, quantitative analyses revealed some interesting differences from normality. Of the six proteins examined, four showed significant alterations in MBL after axotomy. Each of these will be reported in turn below.

4.2.1 nNOS and SOD

No significant changes were found in SOD-IR. The results for nNOS only will be presented below.

4.2.1.i. Pudendal Nerve Axotomy

Qualitatively, alterations in nNOS were not consistently apparent. However, at one week after pudendal axotomy (N=3), ON MBL for nNOS was marginally

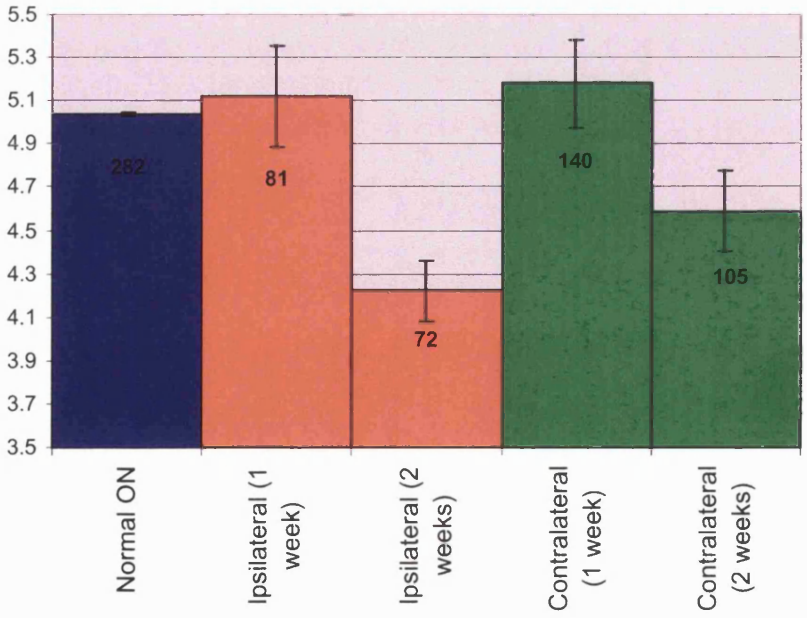

Figure 4.2.1-1. Graph to show MBL of nNOS immunostaining for the motoneurones of ON in normality and after injury to the pudendal nerve. N for each mean value is shown at the top of each bar. Blue bar = normal MBL, red bars = ipsilateral MBLs, green bars = contralateral MBLs. Error bar = S.E.M.

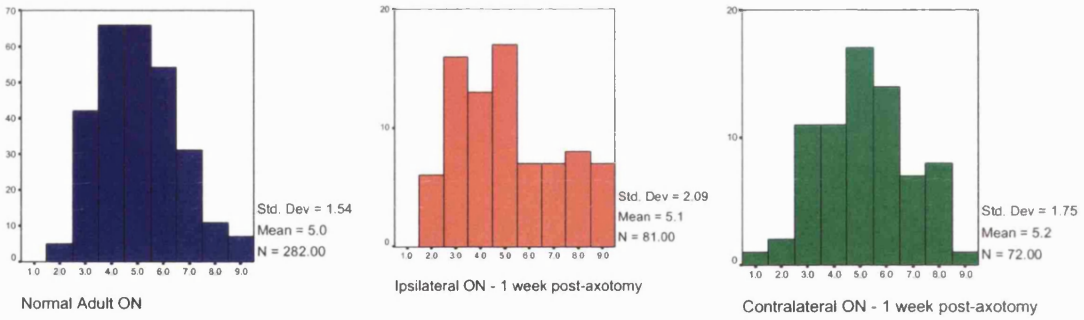

Figure 4.2.1-2. Histograms to show the distribution of nNOS bin locations in ON in normality and 1 week after pudendal axotomy. Blue bars - normal ON, red bars - ipsilateral ON, green bars - contralateral ON

increased on both sides of the spinal cord, at 5.12 ipsilaterally and 5.18 contralaterally, compared with a normal MBL of 5.04. According to the results of the Dunnett's T3, this difference was not significant. The S.E.M. had also dramatically increased (see Fig. 4.2.1-1), possibly reflecting an increased range of staining due to selectively increased expression in some motoneurones or possibly reflecting the smaller sample examined (N(normal ON motoneurones) = 282; N(1 week axotomised ON motoneurones) = 81). At this stage, ON still had a significantly higher MBL than the motoneurone groups in cervical, thoracic and lumbar segments.

To establish the significance of the altered distribution, comparisons of bin location distributions of the motoneurones of ON before axotomy and 1 week after axotomy of the pudendal nerve were made using the 2 sample Kolmogorov-Smirnov Z-test. In spite of an apparently flatter spread of the data for axotomised ON at one week, with a seemingly higher proportion of cells in the 9th data bin (Fig. 4.2.1-2), the distribution was not significantly different from the normal distribution (K-S Z = .96, p = .31 (ipsilateral), K-S Z = .46, p = .98 (contralateral)).

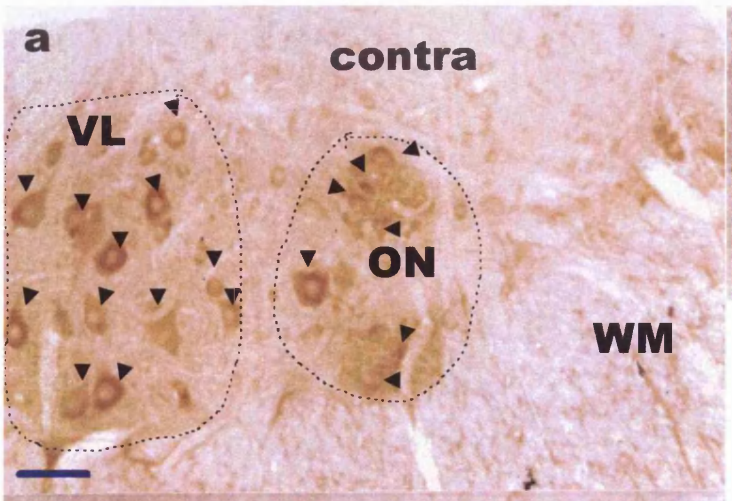

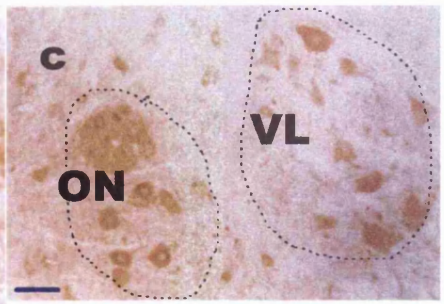

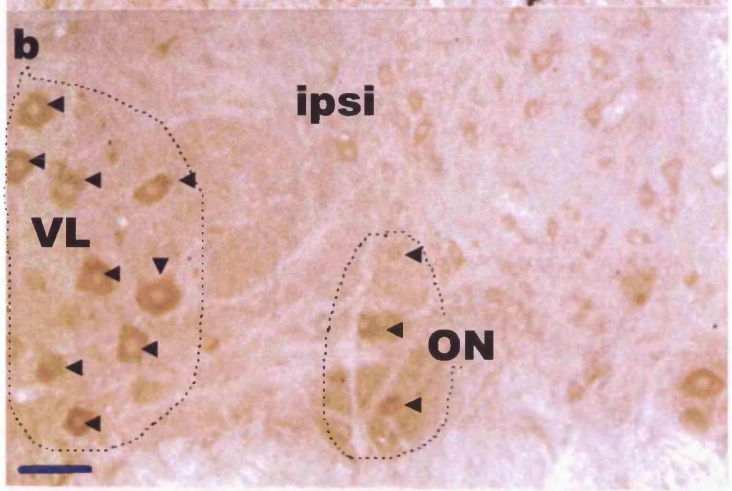

Figure 4.2.1-3. Contralateral (a,d) and ipsilateral (b,e) sacral cord two weeks after pudendal axotomy. Motoneurones (arrowheads) have normal levels of nNOS-IR contralateral to the lesion, but there is a visible decrease on the ipsilateral side. Normal sacral levels of nNOS-IR are shown in (c) for comparison.

WM - white matter; bars = 100μm.

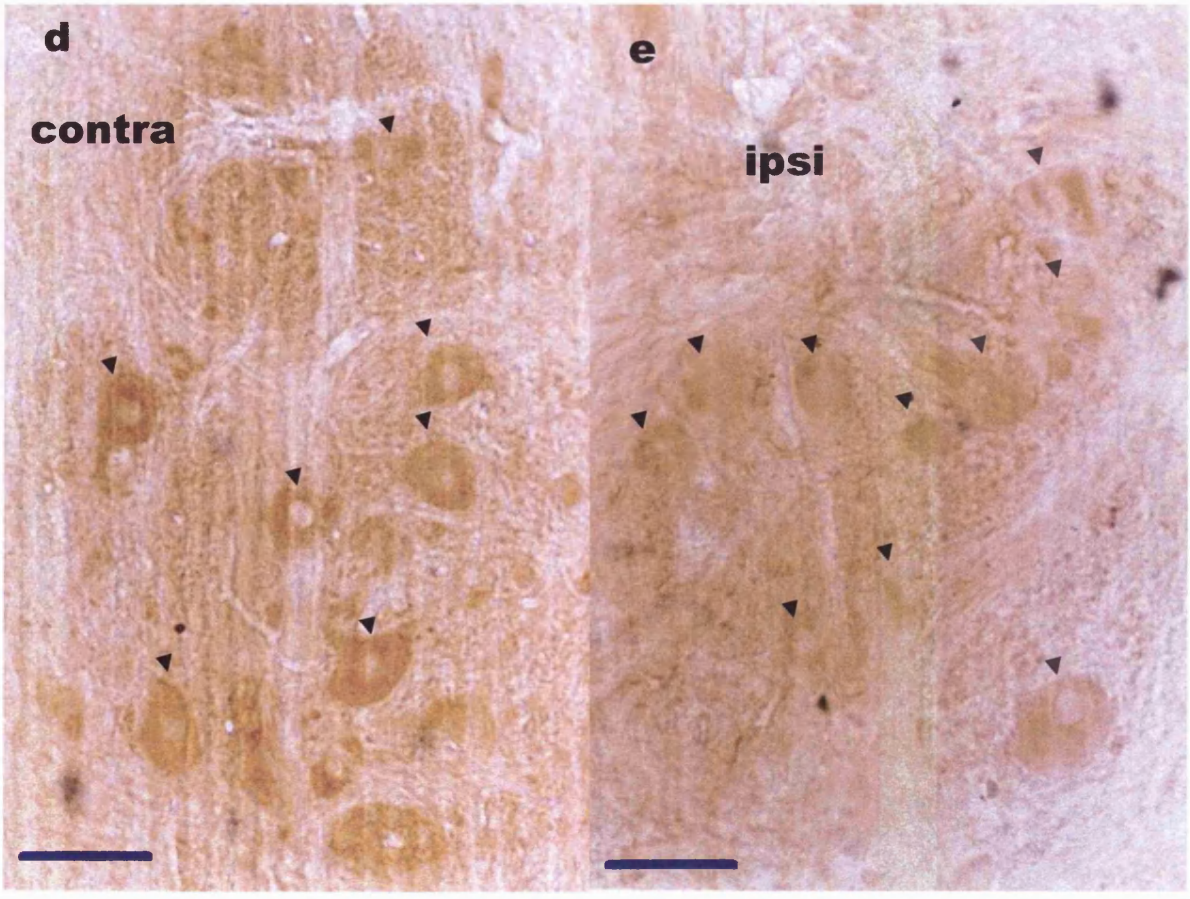

By the second week of recovery, however, a sharp decline in motoneuronal MBL was observed in ON, on both sides of the cord (N=3). This decline was subtle but consistent (Fig. 4.2.1-3). This effect was most pronounced ipsilaterally, where MBL declined to 4.23 compared to a contralateral MBL of 4.59, and a normal MBL of 5.04. Dunnett's T3 showed this reduction in MBL to be significant only on the ipsilateral side ($p = .001$), although according to the Kolmogorov-Smirnov Z test, both distributions were significantly more positively skewed (i.e. ordinate amplitudes greater towards 0)(K-S $Z = 2.19$, $p < .001$ (ipsilateral) K-S $Z = 1.7$, $p = .006$ (ipsilateral) (see Fig. 4.2.1-4). Whilst the MBL for ON was still significantly higher than most non-sacral motoneurone groups, by the second week there was no difference between ON on either side of the cord and the MBL for lumbar motoneurones. Furthermore, two weeks after axotomy of the sartorius nerve, the mean motoneuronal MBL for the motoneurones supplying m.sartorius (5.17) was significantly higher than the MBL for axotomised ON after an equivalent post-operative period (Dunnett's T3, $p < .001$).

Whilst no alterations were seen in MBL for the VM group, alterations in MBL of the VL group occurred earlier and more dramatically than those in ON (see Fig. 4.2.1-5). By the first week after pudendal axotomy, VL MBL for nNOS had decreased from 5.22 to 3.91 on the ipsilateral side and 4.53 on the contralateral side. One week later, MBL had further decreased ipsilaterally to 3.6 and contralaterally to 4.33. At both time points, the Dunnett's T3 showed a significant difference between either side and the normal VL group. Furthermore, by the first week, VL MBL was no longer significantly higher than that of lumbar motoneurones, and by two weeks it was also no longer significantly higher than the cervical motoneurones. At both time periods for the ipsilateral VL and at two weeks for the contralateral VL group, the MBL was significantly lower than the MBL of axotomised motoneurones formerly innervating m. sartorius. The distribution of VL motoneurones across the nine

Figure 4.2.1-4 Histograms to show the distribution of nNOS bin locations in ON in normality and 2 weeks after pudendal axotomy. Blue bars - normal ON, red bars - ipsilateral ON, green bars - contralateral ON

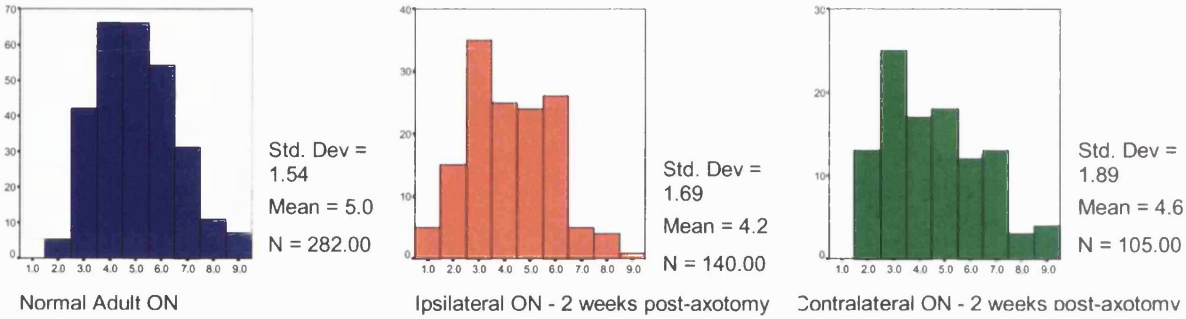

bin locations also significantly differed from the normal to the axotomised animal at both post-operative time points and on both sides of the cord (K-S Z-test, $p<.001$). Distributions are shown in Fig. 4.2.1-6.

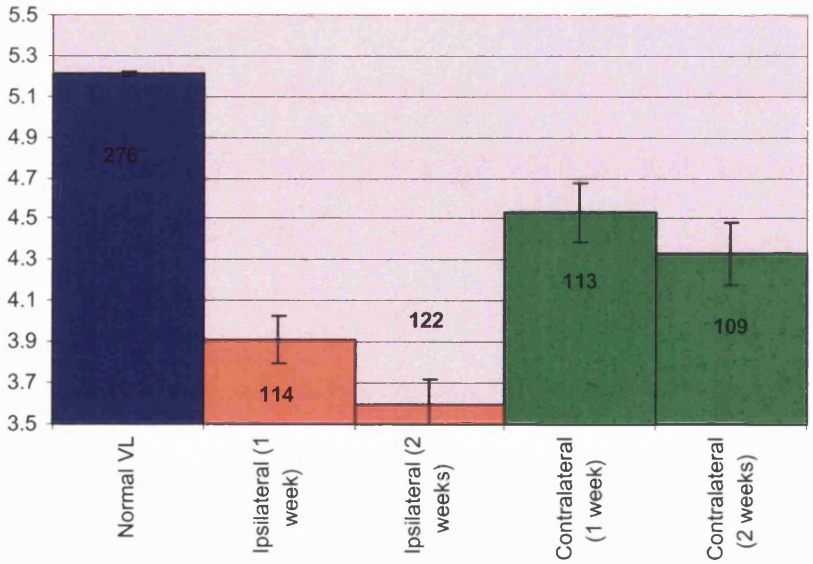

Figure 4.2.1-5. Graph to show MBL of nNOS immunostaining for the motoneurones of the VL group in normality and after injury to the pudendal nerve. N for each mean value is shown at the top of each bar. Blue bar = normal MBL, red bars = ipsilateral MBLs, green bars = contralateral MBLs. Error bar represents S.E.M.

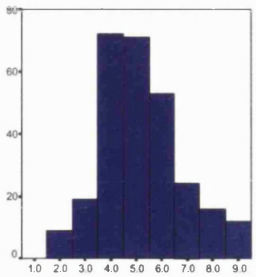

Normal Adult VL

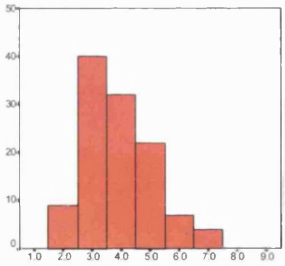

Ipsilateral VL - 1 week post-axotomy

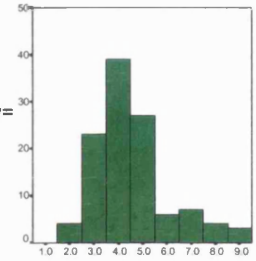

Contralateral VL - 1 week post-axotom

Figure 4.2.1-6. Histograms to show the distribution of nNOS bin locations in VL in normality and after pudendal axotomy. Blue bars - normal VL, red bars - ipsilateral VL, green bars - contralateral VL.

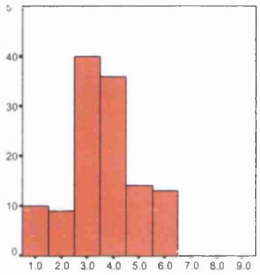

Ilpsilateral VL - 2 weeks post-axotomy

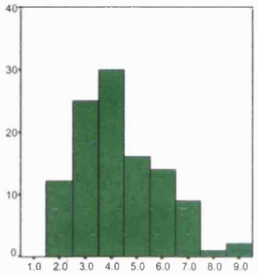

Contralateral VL - 2 weeks post-axotomy

4.2.1.ii. *N. Sartorius* Axotomy

Tissue from three animals was examined 2 weeks after axotomy of n.sartorius. Both ipsilateral and contralateral motoneurones showed large elevations in MBL for nNOS in the motor group giving rise to the *n.sartorius* (MBL = 5.18 ipsilaterally and 5.16 contralaterally), in comparison with normal motoneurones of the fourth lumbar segment (MBL = 3.95) (see Fig. 4.2.1-7). These elevations were significant according to Dunnett's T3 (p. <.001). The MBL of the sartorius motor group 2 weeks after *n.sartorius* axotomy was also significantly higher than the MBL of ON and VL 2 weeks after pudendal axotomy (p < .001). This is a reversal of the usual relationship between these cell groups, where normal sacral motoneurones have a significantly higher MBL than lumbar (see Chapter 3).

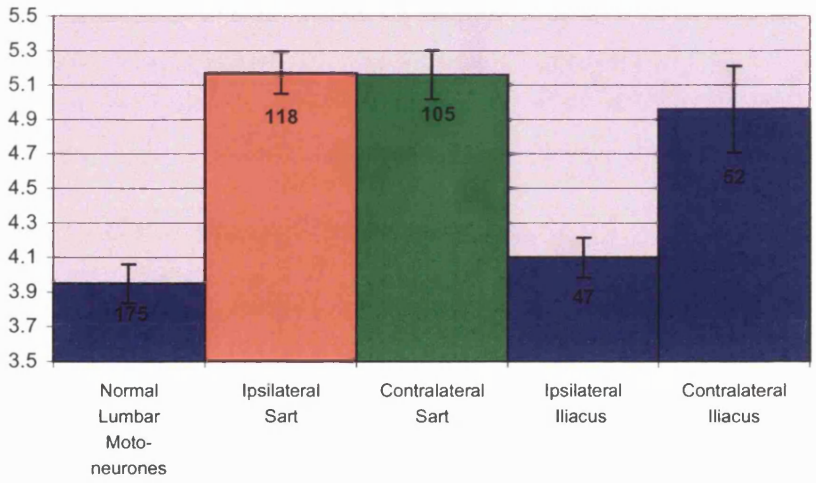

Figure 4.2.1-7. Graph to show MBL of nNOS-IR for the motoneurones of the fourth lumbar segment in normality and after injury to the sartorius nerve. N for each mean value is shown at the top of each bar. Blue bars = normal/unoperated MBLs, red bars = ipsilateral MBLs, green bars = contralateral MBLs. Error bar represents S.E.M.

Meanwhile, as an internal control, the MBL was also calculated for an anatomically discrete motor group originating from the same segment, conforming in position to the motoneurone group which innervates *m. iliacus.* Unlike the adjacent axotomised motoneurones innervating *m. sartorius,* the *iliacus* MBL was not significantly higher than the MBL of normal lumbar

motoneurones either ipsilateral (MBL = 4.1) or contralateral to the lesion (MBL = 4.95), confirming a selective response in the axotomised sartorius neurones. Variability in staining on the contralateral side was high, however, and thus the contralateral iliacus motoneurones were also not different from axotomised sartorius motoneurones on that side of the cord. Lumbar distributions of motoneurones across bin locations can be seen graphically in figure 4.2.1-8 and

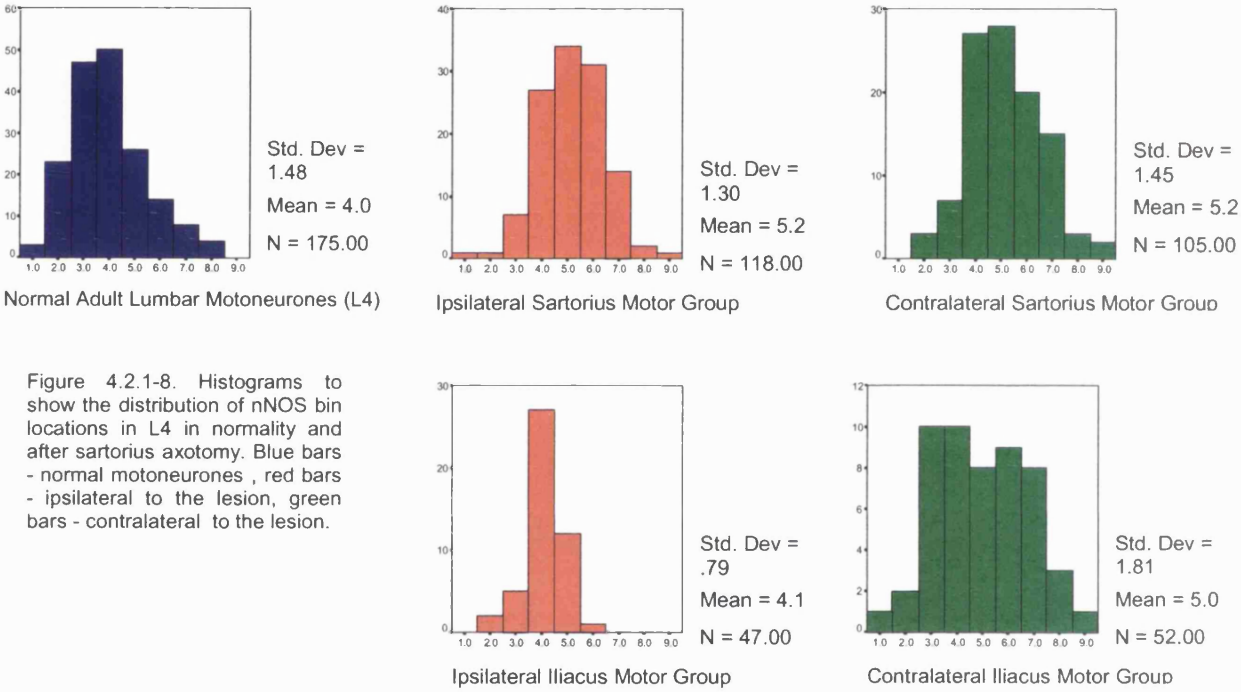

Figure 4.2.1-8. Histograms to show the distribution of nNOS bin locations in L4 in normality and after sartorius axotomy. Blue bars - normal motoneurones , red bars - ipsilateral to the lesion, green bars - contralateral to the lesion.

post-axotomy alterations are shown photographically in figure 4.2.1-9.

4.2.1.iii. Discussion

In the adult rat, axotomies of cervical nerves at distances of 8mm from the spinal cord are not associated with alterations in nNOS/NADPH-d whilst ventral root avulsion is (Wu et al, 1994a; Wu et al, 1994b; Wu, 1996; Gu et al, 1997). This has led to the concept that nNOS upregulation after axotomy is dependent on the proximity of the injury to the cell body, with more distal lesions unlikely to evoke a response. Meanwhile, motoneuronal elevations of nNOS/NADPH-d

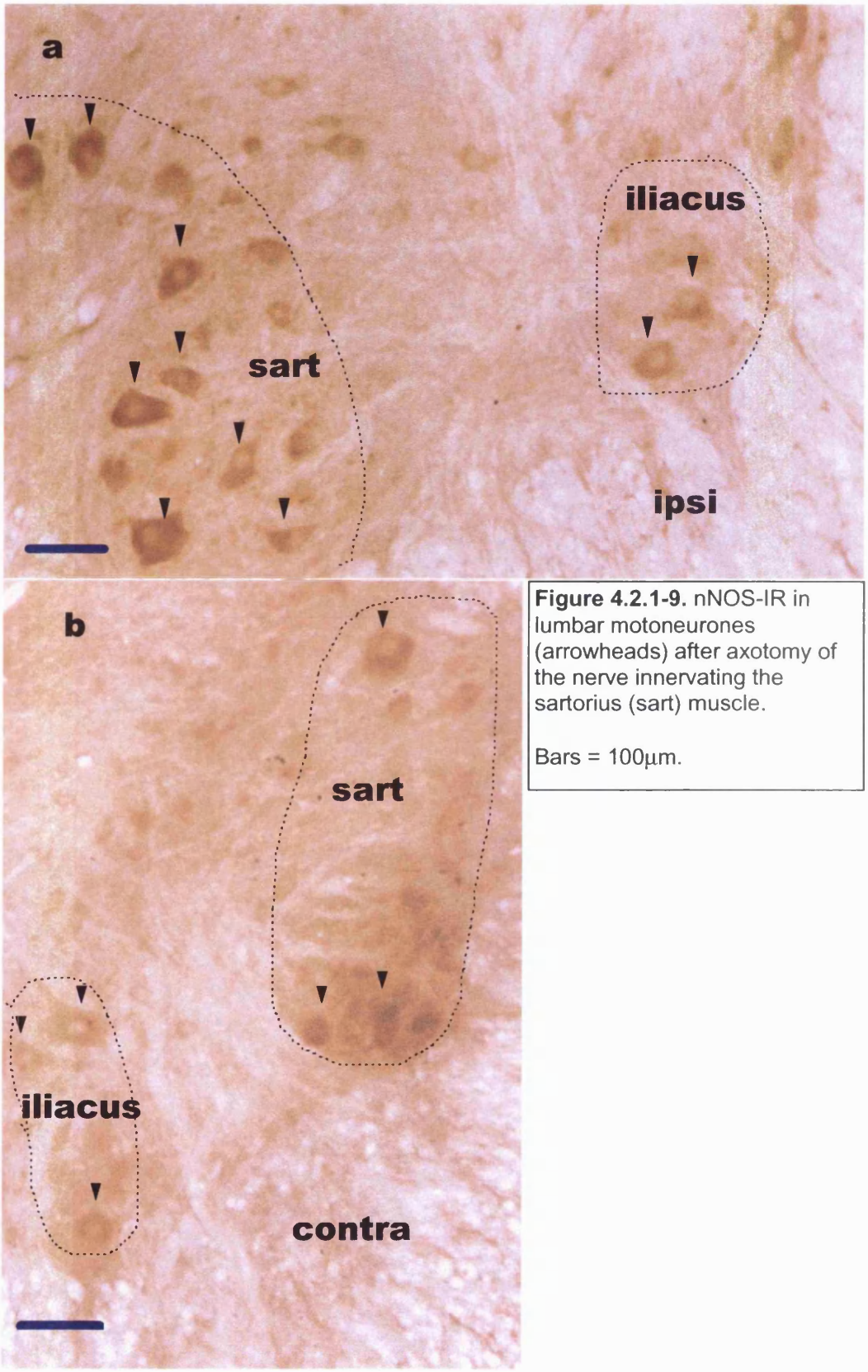

Figure 4.2.1-9. nNOS-IR in lumbar motoneurones (arrowheads) after axotomy of the nerve innervating the sartorius (sart) muscle.

Bars = 100μm.

are seen after axotomies at greater distances (~11-14mm) from the cell body in adult rat brainstem motor nuclei (Yu, 1994; Yu, 1997; Kristensson et al, 1994) suggesting the possibility of segmental variability in sensitivity of nNOS regulation to axotomy. Transections in the present study were carried out at distances of ~100mm from the cord, and did evoke alterations in nNOS-ir possibly reflecting segmental and species differences, but also reflecting the sensitivity of our antibody which detects motoneuronal nNOS-ir in normality that is not detected by other laboratories.

The extent and duration of nNOS elevation has been found to correlate with the likelihood of subsequent neuronal cell death (Kristensson et al, 1994; Gu et al, 1997). For example there is a decline in NADPH-d levels by the second week after hypoglossal axotomy, motoneurones of which show lesser neuronal loss than other groups with protracted NADPH-d elevation (Kristensson et al, 1994). Two weeks after pudendal axotomy in the present study, decreases in nNOS were found, when persistent elevation was observed at the same time point after sartorius axotomy. The sacral decrease coincides with the time point at which elevated NADPH-d declines in axotomised hypoglossal motoneurones (Kristensson et al, 1994). Since this group of motoneurones are more resistant to the injury than other brainstem neurones, which display continuing elevations of nNOS up to at least 4 weeks after surgery, the mechanism underlying the delayed down-regulation of nNOS at this time point may be important in understanding differential susceptibilities to degenerative changes.

The reasons for suppression of the hypoglossal nNOS response are not clear, however, the decrease in pudendal nNOS-ir may be related to afferent signals conveying information about altered bladder function. An acute elevation of nNOS/NADPH-d in lumbosacral motoneurones has been previously noted up to the 2nd day after urethral obstruction in the guinea pig (Zhou and Ling, 1997).

Afferent signals in response to bladder distension may be partially responsible for this increase, via both autonomic connections and descending signals from the pontine micturition centre, in an attempt to overcome outlet resistance by increasing the relaxing NO signal to the sphincter. If somatic regulation of nNOS is sensitive to afferent signals relating to chronic alterations in bladder function, it is equally likely that nNOS might be down-regulated in response to signals conveying a decrease in contractility of the external sphincter, such as is likely to occur after the loss of 50% of sphincter innervation caused by unilateral axotomy. Further investigation is required to understand more fully the regulation of nNOS in pudendal motoneurones in relation to bladder function.

Another feature of post-axotomy changes in nNOS-ir is the striking bilaterality of the response in the sartorius motor group, contrasting the unilateral decrease in axotomised ON. Bilateral elevations in NADPH-d have also been seen in lumbar motoneurones after knee joint immobilisation in guinea pigs (He et al, 1997). The unilaterality of sacral response contrasted with the bilaterality of lumbar motoneuronal alterations will be seen to be a recurring segmental difference in axotomy responses and will therefore be discussed in greater depth in Chapter 5.

4.2.2 CaN-A and CM

CaN-A

4.2.2.i. Pudendal Nerve Axotomy

A large decrease from normal CaN-IR was observed in axotomised sacral motoneurones ipsilateral to the lesion (Fig. 4.2.2-1, overleaf). In confirmation of the qualitative observations, MBL for CaN-A was significantly decreased in ON on the side of the lesion one week after pudendal nerve axotomy (MBL = 3.2), and had begun to return to normal by the second week of recovery (MBL = 4.2, vs. normal MBL of 4.7)(See Fig. 4.2.2-2). These differences were only significant at one week in terms of both means (Dunnett's T3, $p < 001$) and distributions (K-S $Z = 2.95$, $p<.001$), although a one-tailed t-test showed a marginal difference between ipsilateral (axotomised) and normal ON at the second week ($t=1.866$, $p <.05$). At one week after injury, ipsilateral ON was also significantly lower in MBL than all other motoneurones measured (Dunnett's T3, all $p < .001$) with the exception of normal VL, but including injured lumbar motoneurones significantly different from $Z = 1.772$, $p = .004$).

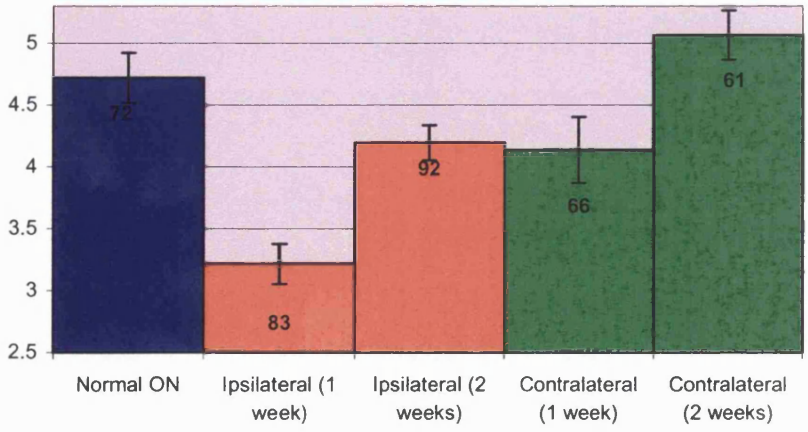

Figure 4.2.2-2. Graph to show MBL of CaN-IR for the motoneurones of ON in normality and after injury to the pudendal nerve. N for each mean value is shown at the top of each bar. Blue bar = normal MBL, red bars = ipsilateral MBLs, green bars = contralateral MBLs. Error bars represent S.E.M.

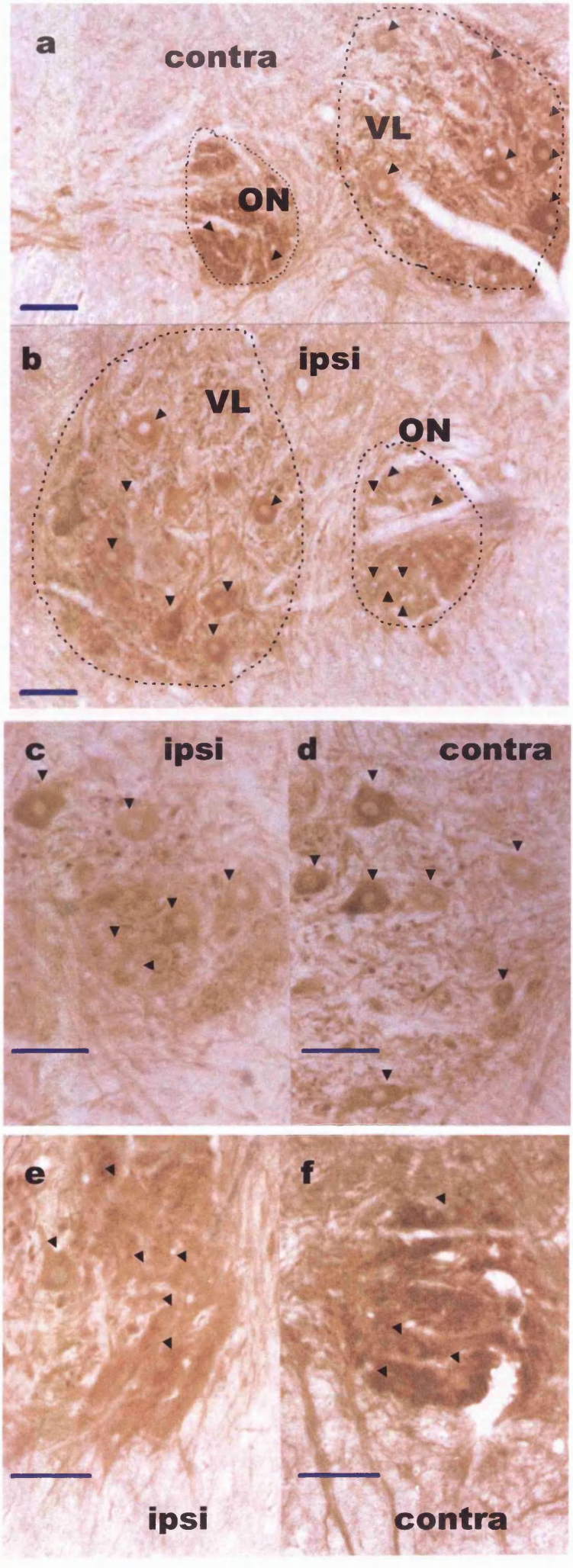

Figure 4.2.2-1. Reduced CaN-IR in sacral motoneurones (arrowheads) after pudendal axotomy. The ipsilateral motoneurones are distinctly less IR at one week (e) and two weeks (b,c), than the contralateral motoneurones (one week - (f); two weeks - (a,d)). To facilitate visualisation, outlines have been given to motoneurones that are difficult to distinguish from the background, which is raised due to the localisation of the antigen within the surrounding fibres.

Bars = 100μm.

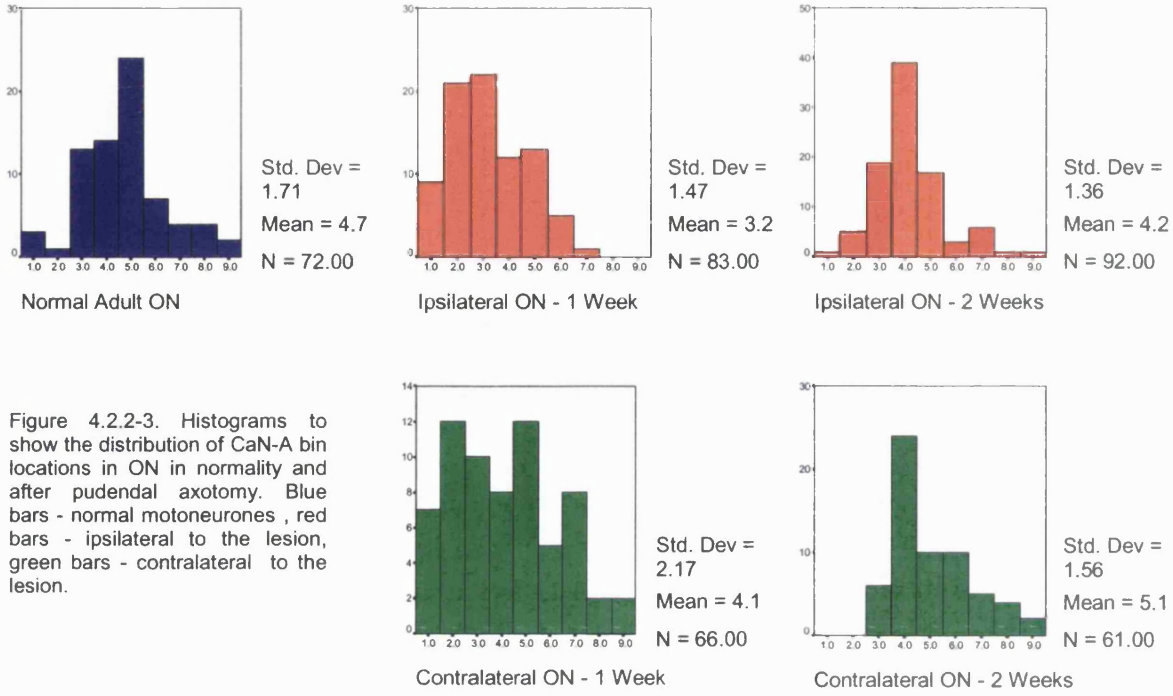

Figure 4.2.2-3. Histograms to show the distribution of CaN-A bin locations in ON in normality and after pudendal axotomy. Blue bars - normal motoneurones , red bars - ipsilateral to the lesion, green bars - contralateral to the lesion.

Distributions for normal and injured ON across the nine data bins are shown in figure 4.2.2-3.

The VL group was no different from the normal VL one week after pudendal axotomy in terms of MBL on either side of the cord, but by the second week the MBL was significantly higher bilaterally than at either one week or in normality (Dunnett's T3, p = .003 ipsilaterally, p = .05 contralaterally). Contralaterally, the VL MBL was higher than that in the ipsilateral ON at both 1 and 2 weeks, and the ipsilateral VL MBL was higher than the ipsilateral MBL for ON two weeks post-operatively (Dunnett's T3, P <.001). The time-dependent changes in the MBL are compared in Fig. 4.2.2-4. and distributions are shown in Fig. 4.2.2-5.

Figure 4.2.2-4. Graph to show MBL of CaN-IR for the motoneurones of VL in normality and after injury to the pudendal nerve. N for each mean value is shown at the top of each bar. Blue bar = normal MBL, red bars = ipsilateral MBLs, green bars = contralateral MBLs. Error bars represent S.E.M.

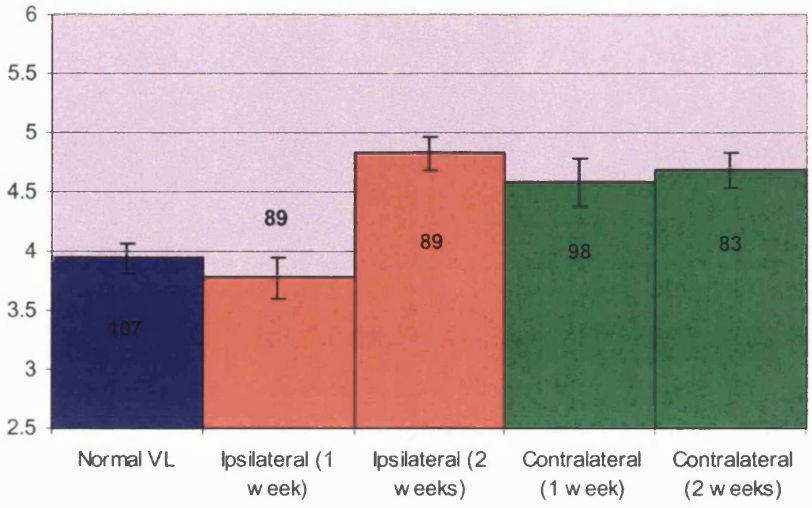

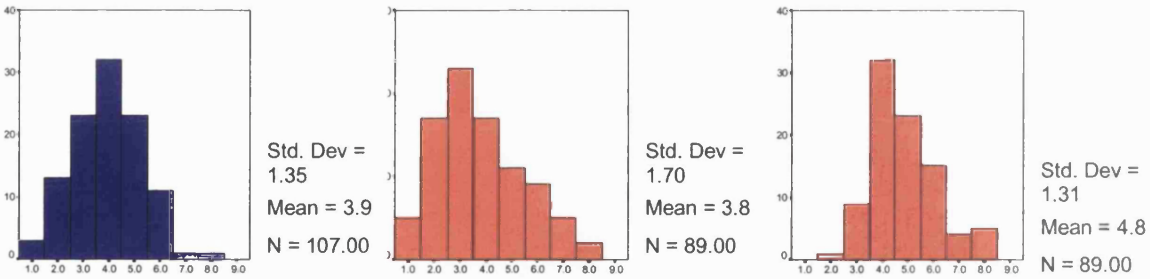

Figure 4.2.2-5. Histograms to show the distribution of CaN-A bin locations in VL in normality and after pudendal axotomy. Blue bars - normal motoneurones , red bars - ipsilateral to the lesion, green bars - contralateral to the lesion.

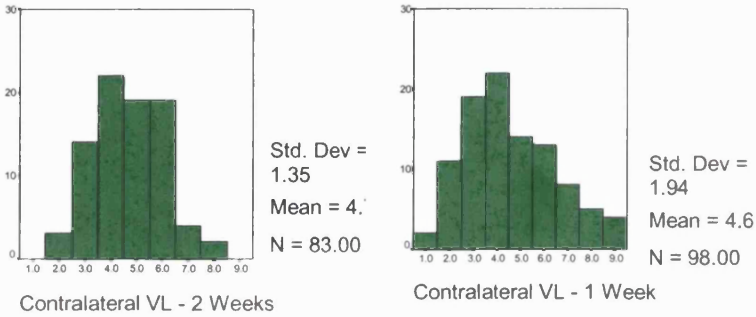

4.2.2.ii. *N. Sartorius* Axotomy

Post-axotomy changes in the lumbar cord were more subtle than those seen in the sacral cord after pudendal nerve axotomy(Fig. 4.2.2-6). Nevertheless, 2 weeks after axotomy, the MBL for the sartorius motor group was lower than for either normal lumbar motoneurones (MBL = 4.87) or the neighbouring neurones of the iliacus motor group (MBL = 5.5 bilaterally). This difference was

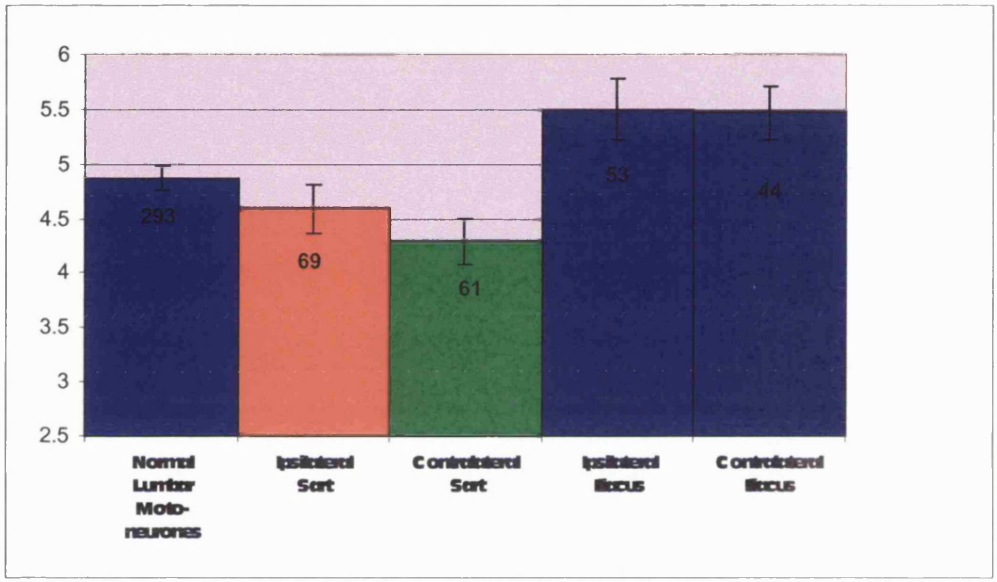

Figure 4.2.2-7. Graph to show MBL for the L4 motoneurones in normality and after injury to the sartorius nerve.The N for each mean value is shown at the top of each bar. Blue bar = normal MBL, red bars = ipsilateral MBLs, green bars = contralateral MBLs. Error bars represent S.E.M. Sart. = sartorius.

most pronounced on the side of the cord contralateral to the lesioned nerve (contralateral sartorius MBL = 4.29, ipsilateral MBL = 4.59) (see Fig. 4.2.2-7). The only significant difference detected by the Dunnett's T3 was between the contralateral sartorius motor group and other ipsilateral lumbar motoneurones from a slightly more rostral portion of L4 than the iliacus and sartorius nuclei, which had a higher MBL of 5.5. The Kolmogorov-Smirnov Z-test also showed the axotomised sartorius group to be no differently distributed than normal lumbar motoneurones, although the ipsilateral sartorius motor group results were significantly more positively skewed in distribution than neighbouring

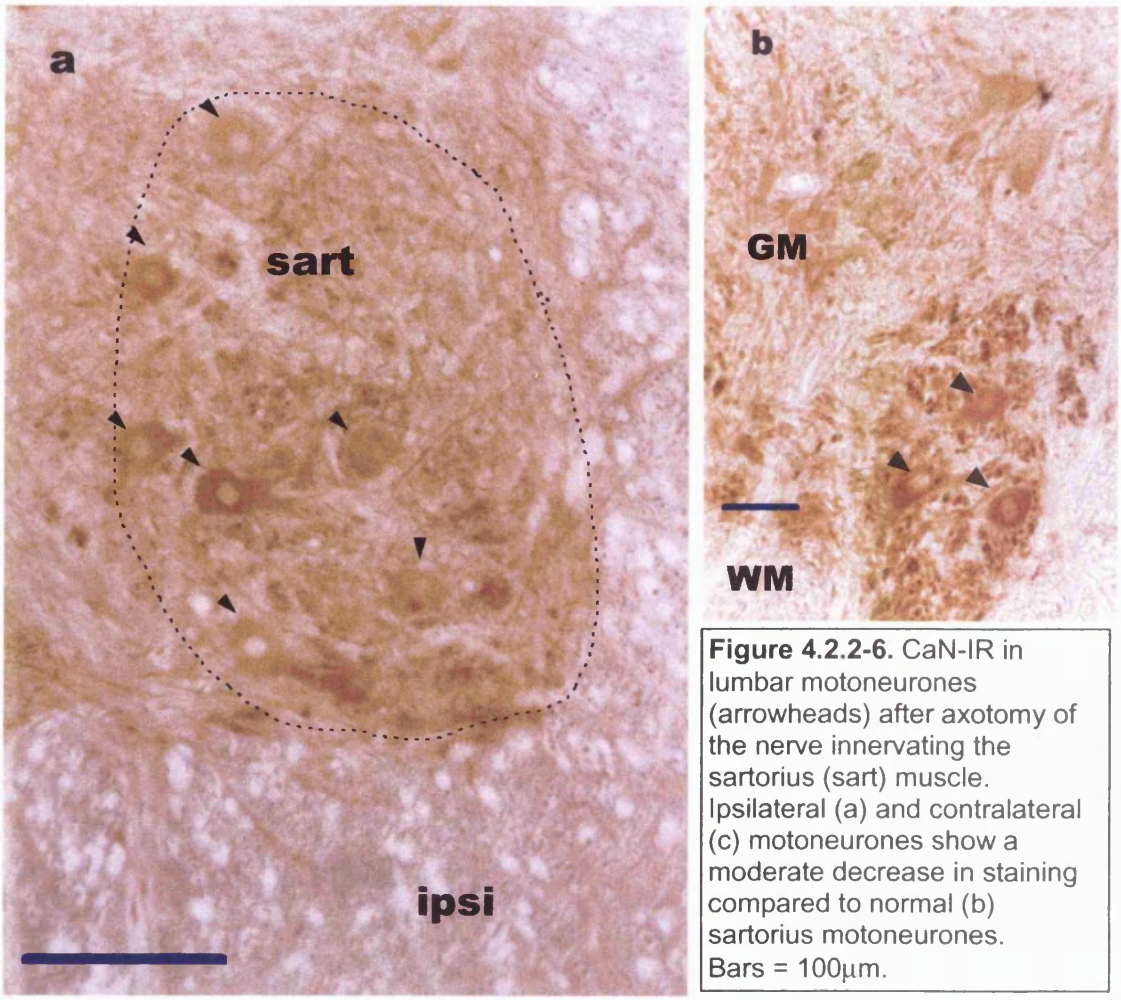

Figure 4.2.2-6. CaN-IR in lumbar motoneurones (arrowheads) after axotomy of the nerve innervating the sartorius (sart) muscle. Ipsilateral (a) and contralateral (c) motoneurones show a moderate decrease in staining compared to normal (b) sartorius motoneurones. Bars = 100μm.

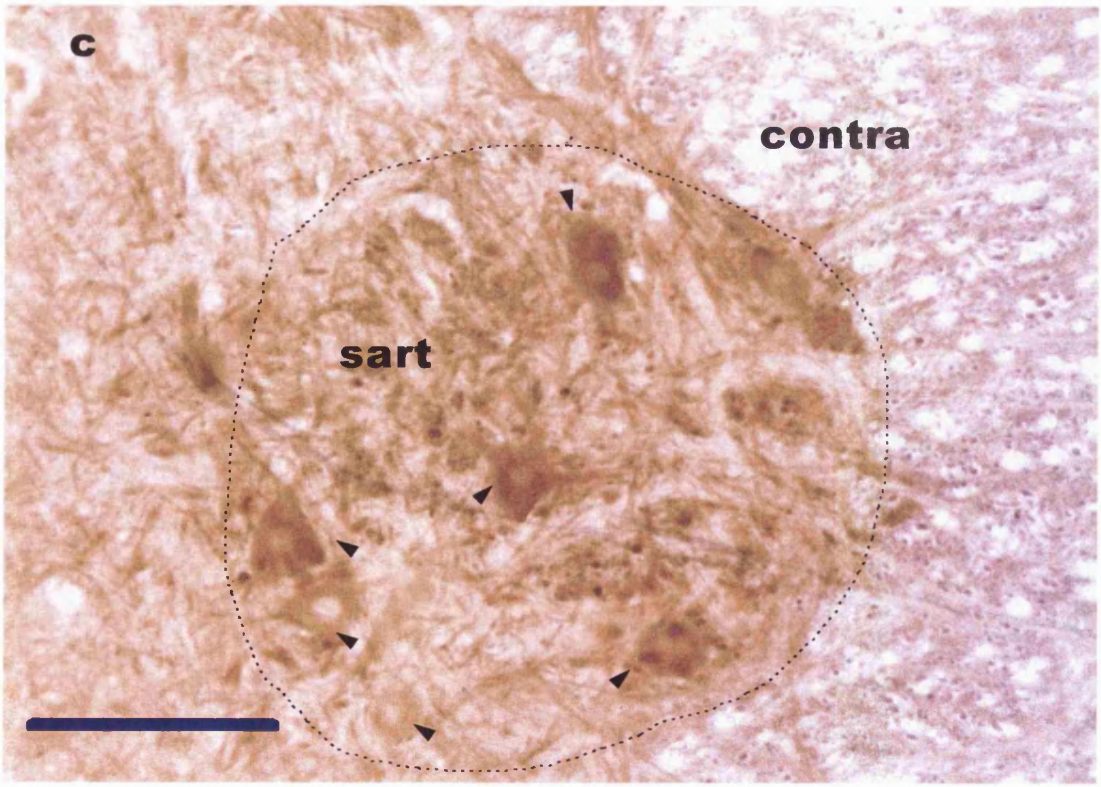

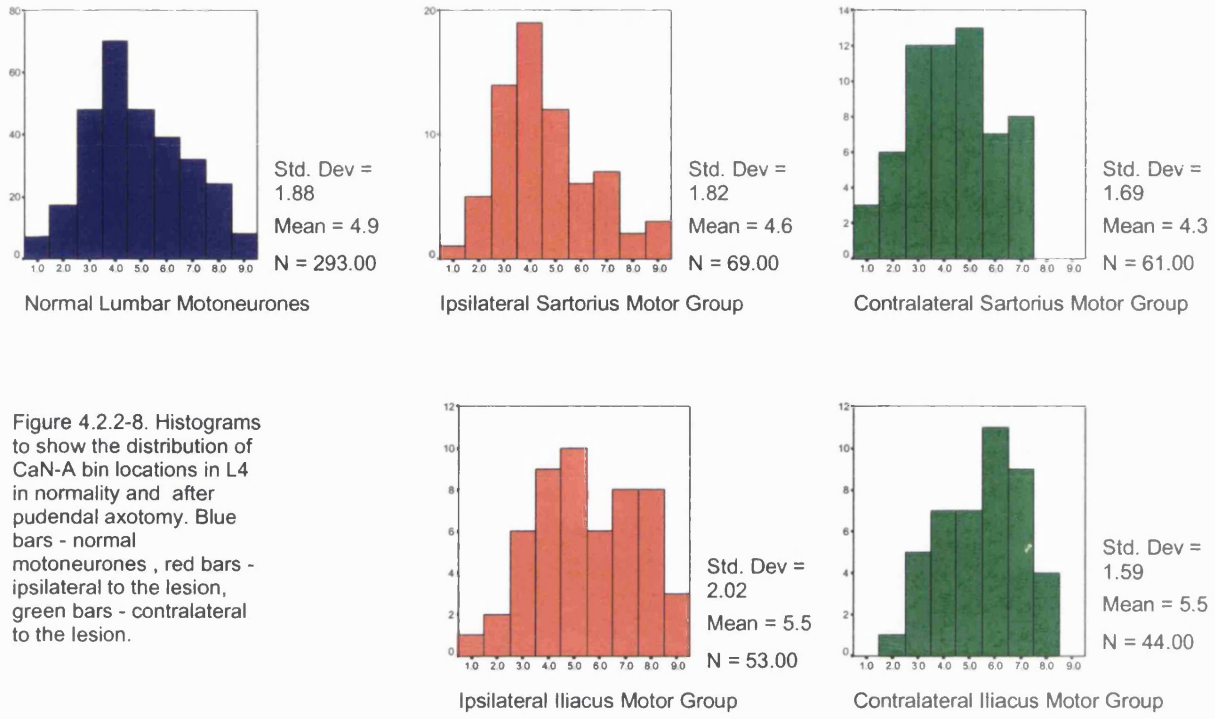

Figure 4.2.2-8. Histograms to show the distribution of CaN-A bin locations in L4 in normality and after pudendal axotomy. Blue bars - normal motoneurones , red bars - ipsilateral to the lesion, green bars - contralateral to the lesion.

iliacus motoneurones on the same side of the cord (K-s Z = 1.794, p = .003)(for distributions see Fig. 4.2.2-8).

Since post-hoc tests are more conservative than standard statistical tests to account for the effects of making multiple and random comparisons, and since in this case the result under examination was a specific alteration in a predictable group of cells, two-tailed t-tests were also used to test specific pairs. The results of the t-tests showed the axotomised sartorius motor group to have a significantly lower MBL on both sides of the cord than normal lumbar motoneurones (ipsilateral p =.01, contralateral p = .018).

4.2.2.iii. Discussion

To date, there are no reports in the literature concerning changes in CaN after axotomy. The present findings are therefore original and indicate that pudendal axotomy induces a decrease in CaN-IR within the first week. By the second week, levels have begun to return to normal. Two weeks after section of *n. sartorius*, a bilateral decrease in CaN-IR levels is apparent, although the

difference from normal levels is not as great as in ON two weeks after the pudendal axotomy. This observed decrease could result from: increased Ca^{2+} binding, increased breakdown/decreased utilisation, or active suppression.

Increased Ca^{2+}-binding might produce a decrease in antigenicity because, when CaN's Ca^{2+}-binding sites are fully occupied, CaN undergoes a conformational change which allows access of substrates to its active, catalytic domain (see Morioka et al, 1999). It is not clear whether this structural change interferes with antibody binding; however, in preliminary tests in this study added Ca^{2+} caused a modest decrease in CaN-IR. Since this was in fixed tissue, where conformational changes in proteins are restricted because of aldehyde cross-linking, it is possible that in unfixed tissue Ca^{2+} could cause a more marked inhibition of CaN antigenicity. Thus CaN-IR may be decreased as a result of the post-axotomy increases in $[Ca^{2+}]_i$, causing greater levels of activity.

Increased breakdown or decreased expression of CaN may occur if the protein is not being utilised. CM was also shown to be decreased within the same time frame, and since CaN requires CM for full activity, this could contribute to such an effect. Given the likelihood of high levels of Ca^{2+} influx after axotomy, this is a less probable explanation of the decreased antigenicity. It is also less likely that suppressed CM expression would be a primary event than a reaction to changes in expression of other target proteins such as CaN, given the range of important pathways in which CM is involved (summarised later). Also, decreases in CaN-IR observed after ischaemic insult, a form of damage which is also associated with increased $[Ca^{2+}]_i$, were not accompanied by increases in CaN breakdown products(Morioka et al, 1999).

Finally, an active suppression of CaN might occur. This scenario is most likely if decreasing CaN activity is of neuroprotective benefit. In fact, CaN activity is a double-edged sword, alleviating $[Ca^{2+}]_i$ (e.g. Zhu and Yakel, 1997) whilst mediating excitotoxicity by promoting NO formation from nNOS (Dawson et al, 1993; Sharkey and Butcher, 1994) and potentially activating apoptotis (Wang et al, 1999). Which of these pathways is favoured may depend on the availability of substrates and the level of CaN activation.

Sartorius versus pudendal results

Two main differences were found between the outcome of pudendal axotomy and section of *n. sartorius*. Firstly, the decrease in CaN-IR in ON was greater than in motoneurones innervating sartorius. Secondly, the response in ON was unilateral but in the sartorius motor pool the response to axotomy was bilateral. Possible reasons for this first difference are considered below. Since segmental differences in the laterality of axotomy induced changes are common to several antigens please see Chapter 5 for a discussion.

The differential degree of alteration between the two motor groups may be artefactual. Since the sartorius motoneurones were not examined after the first week post-axotomy, it is possible that there may have been a similar magnitude of decrease in CaN-IR at this time point in both motor groups. The "faster" return to normal in sartorius is likely to reflect the inclusion of uninjured motoneurones since the lateral motor group of the fourth lumbar segment is not a pure group (Vanderhorst and Holstege, 1997). Nevertheless, given the dramatic difference between ON and sartorius in post-axotomy changes of nNOS-IR (see above), and given the involvement of CaN in nNOS activation, it is not unlikely that CaN levels would be different between the two types of

axotomised motoneurone, although clearly it is not possible to deduce which alteration would be primary.

CM

4.2.2.iv. Pudendal Nerve Axotomy

Owing to the very low levels of immunostaining in some experiments, rendering them unmeasurable, quantitative data were only acquired from 2 of the pudendal axotomies, one at each time point. As such, the Ns are very low for each of the cell types examined and findings should be treated with caution. Nevertheless, the Dunnett's T3 and the Tamhane's T2 highlighted a significant reduction in MBL (MBL = 1) for ipsilateral ON by the second post-operative week ($p<.001$) in comparison to normal ON (MBL = 3.48). At this stage ON was also significantly lower than all non-sacral motoneurone types measured ($p. <.001$). However, it was no different from the contralateral ON (MBL = 3.3). Whilst at one week no differences in bin location distributions were present, by 2 weeks the ipsilateral bin location distribution for ON was also found to differ significantly from the distribution for normal ON (K-S Z = 2.274, $p <.001$)(See Fig 4.2.2-9 for MBL comparisons and Fig. 4.2.2-10 for distributions across bin locations).

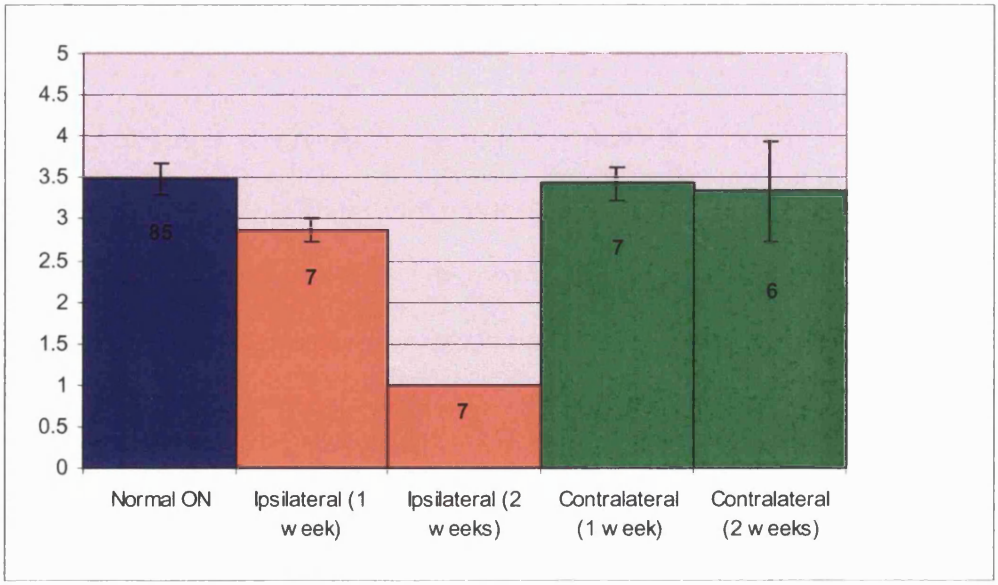

Figure 4.2.2-9. Graph to show MBL of CM-IR for the motoneurones of ON in normality and after injury to the pudendal nerve. N for each mean value is shown at the top of each bar. Blue bar = normal MBL, red bars = ipsilateral MBLs, green bars = contralateral MBLs. Error bars represent S.E.M.s.

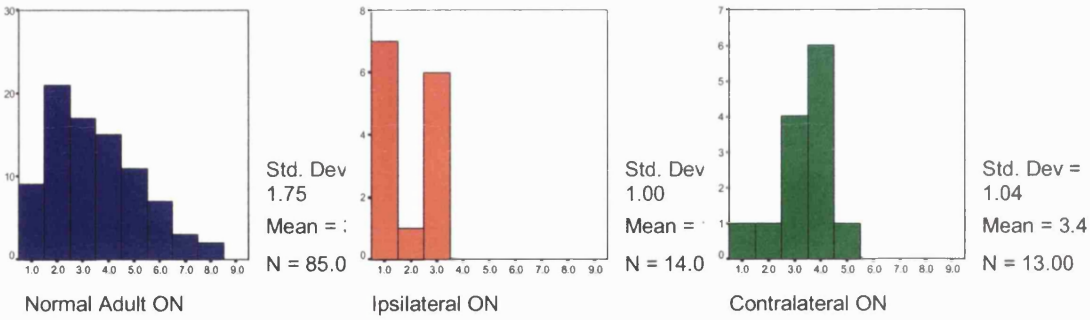

Figure 4.2.2-10. Histograms to show the distribution of CM bin locations in ON in normality and after pudendal axotomy. Post-axotomy results represent a summary of data at both post-axotomy time points, which have been combined due to the lower N. Blue bars - normal ON, red bars - ipsilateral ON, green bars - contralateral ON.

Since the number of animals was low, this result was examined further using a number of techniques to investigate the robustness of the finding. Levene's test for homogeneity of variance showed the variance of the axotomy and normal data to be unequal and a corrected t-test was therefore applied. This showed significant reductions in MBL at both one and two weeks on the ipsilateral side only (one week: $t = 2.632$, $p = .012$; two weeks: $t = 13$, $p < .001$). In addition, at both one and two weeks the ipsilateral MBL was significantly lower than the contralateral MBL (one week: $t = 2.3$, $p = .042$; two weeks: $t = 3.8$, $p = .013$).

With such small samples of neurones, it is possible that the result may reflect sampling bias - that is to say that more motoneurones were measured from pale sections on the ipsilateral side, and the majority of the contralateral motoneurones were measured in more darkly stained sections. To control for this possibility, averages of grayscales (as % GMBG) were made for each side of each section and compared in a paired t-test, thus removing the effect of section variance on the outcome. Since the MBL of the VL group was also reduced ipsilaterally by the axotomy and the number of sections for ON only was too low for the statistical procedure, the paired t-test was performed on the combined data for ON and VL and showed a significant side-to-side difference ($p = .03$).

The robustness of this result is reflected in the fact that in no section was the mean % GMBG for the contralateral side either equal to or less than the mean % GMBG for the ipsilateral side. A similar side to side comparison was made for all control data and no significant differences were found. Photographic examples of the alterations in CM-IR can be seen in Figure 4.2.2-11.

As mentioned earlier, the ipsilateral MBL for VL (one week: MBL = 2.8, 2 weeks: MBL = 1) also showed a reduction from normality (MBL = 4.48) after pudendal axotomy (see Fig. 4.2.2-12). This reduction was significant at both time points in terms of MBL (Dunnett's T3 and Tamhane's T2, one week: p = .002, two weeks, p<.001) and distribution profile (one week: K-S Z = 1.76, p =.004; two weeks, K-S Z = 2.157, p <.001)(see Fig. 4.2.2-13). The distribution profiles across the nine bin locations were also significantly different from ipsilateral to contralateral VL by the second week after axotomy (K-S Z = 1.79, p = .003), and showed a tendency toward significance at the first week (K-S Z = 1.32, p = .06).

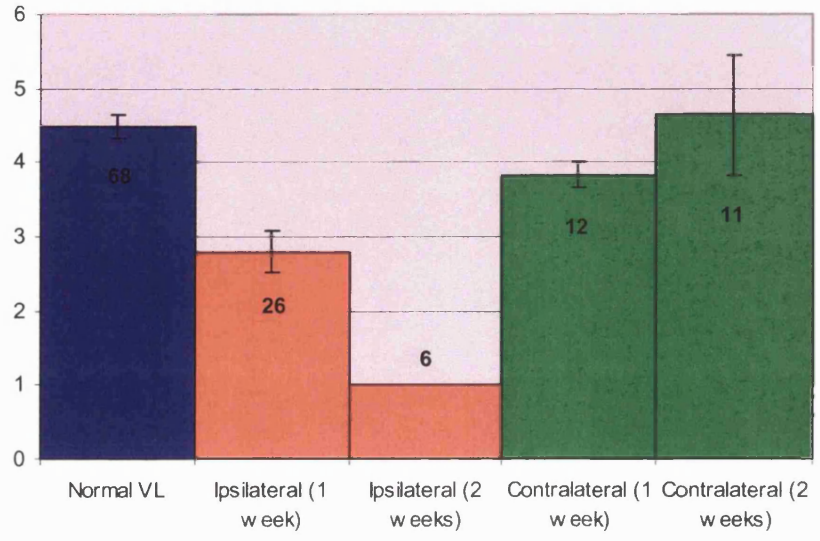

Figure 4.2.2-12. Graph to show MBL of CM-IR for the motoneurones of VL in normality and after injury to the pudendal nerve. N for each mean value is shown at the top of each bar. Blue bar = normal MBL, red bars = ipsilateral MBLs, green bars = contralateral MBLs. Error bars represent S.E.M.s

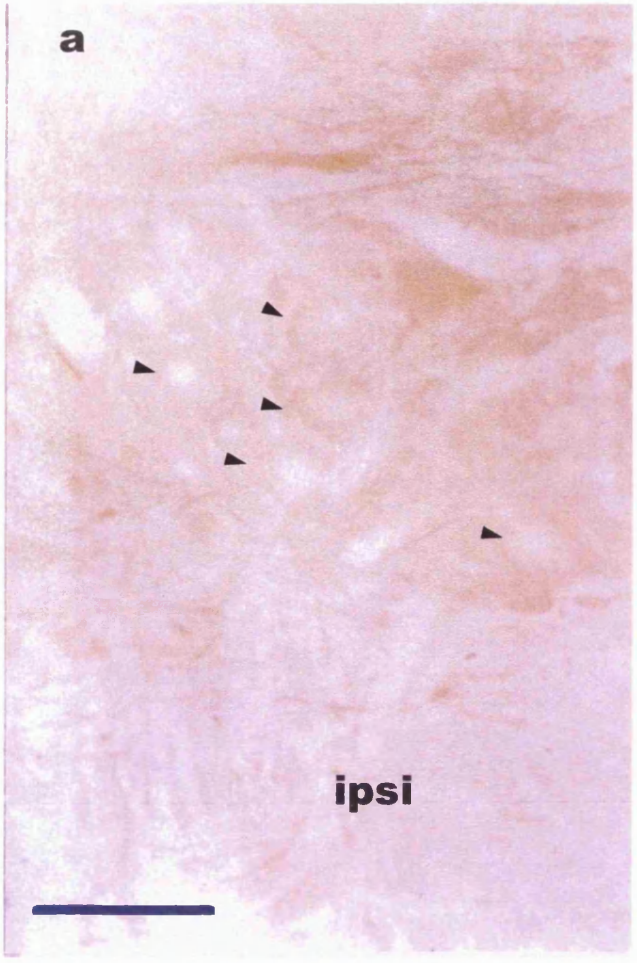

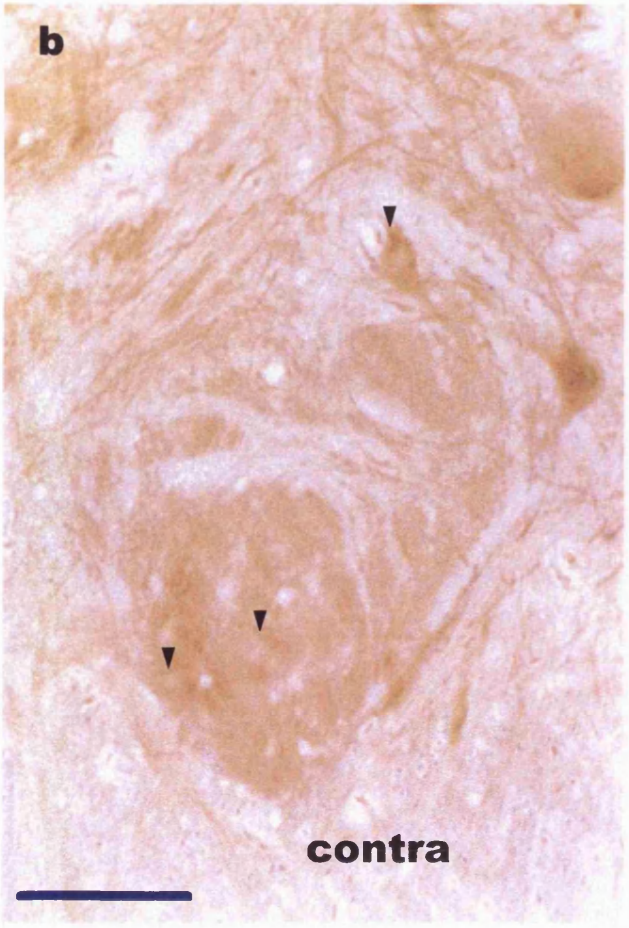

Figure 4.2.2-11. Ipsilateral (a) and contralateral (b) ON two weeks after pudendal axotomy. Motoneurones are indicated by arrowheads.

Bars = 100µm.

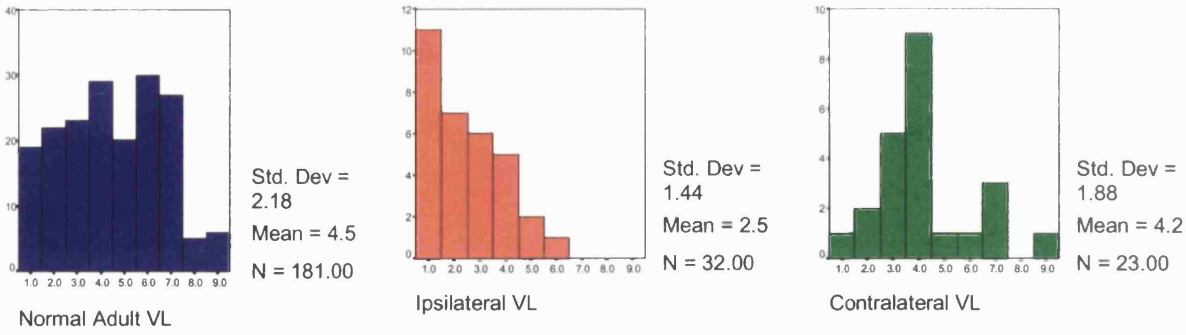

Figure 4.2.2-13. Histograms to show the distribution of CM bin locations in VL in normality and after pudendal axotomy. Post-axotomy results represent a summary of data at both post-axotomy time points, which have been combined due to the lower N. Blue bars - normal VL, red bars - ipsilateral VL, green bars - contralateral VL.

4.2.2.v. *N. Sartorius* Axotomy

Post-hoc analyses did not reveal any significant differences between axotomised sartorius motoneurones and any other motoneuronal group, even though the MBL for both sides (ipsilateral MBL = 3.7, contralateral MBL = 3.48) was lower than the normal L4 MBL (4.16) and the iliacus group on either side (ipsilateral MBL = 4.17, contralateral MBL = 4.3)(See Fig. 4.2.2-14). Differences in distribution were only detected between the contralateral sartorius motor group and normal lumbar motoneurones (K-S Z = 1.76, p = .004)(See Fig. 4.2.2-15 for distributions). As before two-tailed t-tests were used to examine specific

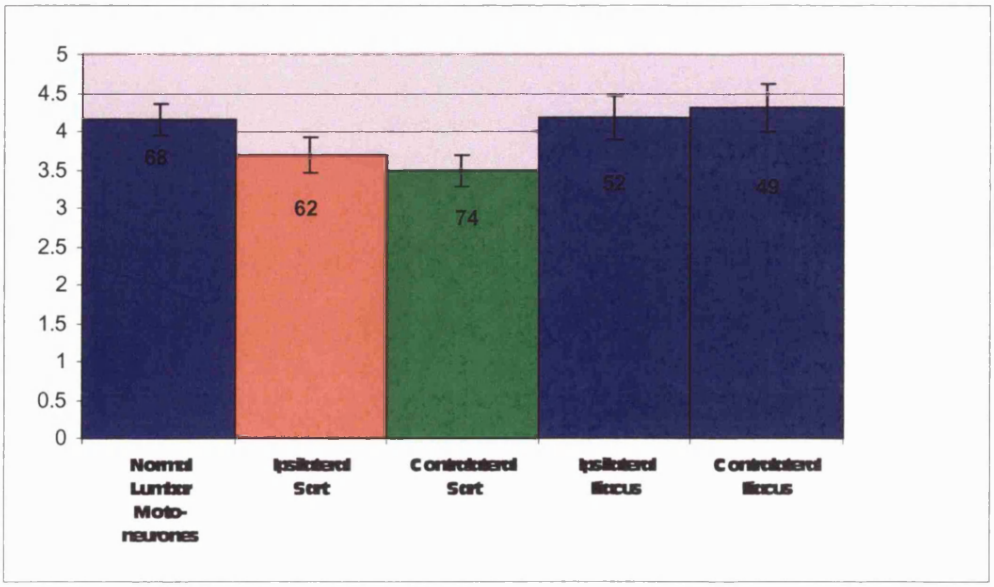

Figure 4.2.2-14. Graph to show MBL of CM-IR for the L4 motoneurones in normality and after injury to the sartorius nerve.The N for each mean value is shown at the top of each bar. Blue bar = normal MBL, red bars = ipsilateral MBLs, green bars = contralateral MBLs. Error bars represent S. E. M.s.

alterations, and these showed significant reductions only in contralateral sartorius MBL as compared with the MBL of normal lumbar motoneurones (t = 2.25, p = .025) and the MBL of contralateral iliacus motoneurones (t = 2.2, p = .027). Post-axotomy antigenicity in L4 is shown in Figure 4.2.2-16.

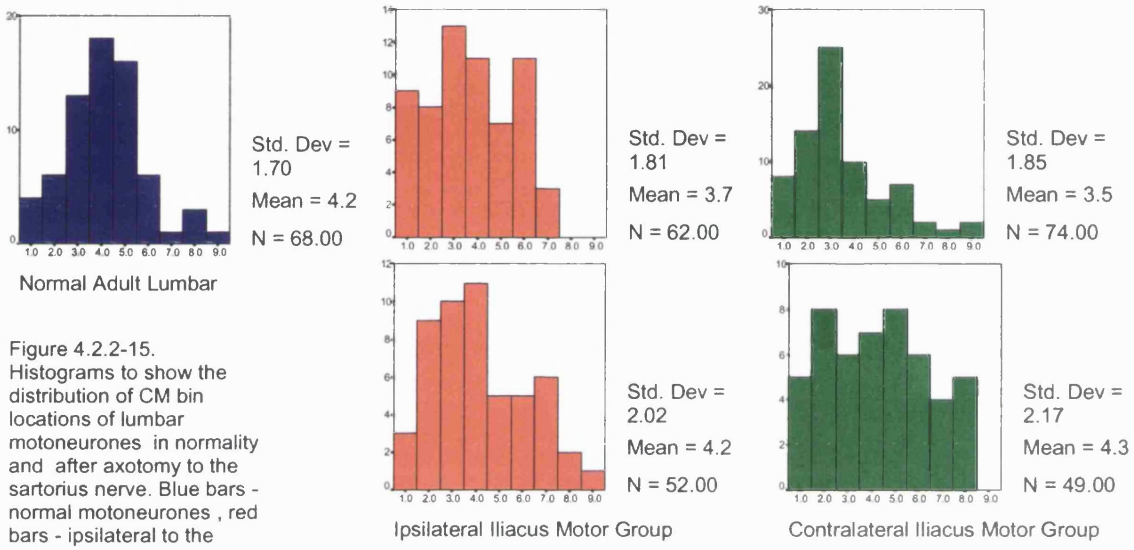

Figure 4.2.2-15. Histograms to show the distribution of CM bin locations of lumbar motoneurones in normality and after axotomy to the sartorius nerve. Blue bars - normal motoneurones , red bars - ipsilateral to the lesion, green bars - contralateral to the lesion.

4.2.2.vi. Discussion

Two weeks after axotomy of the pudendal nerve, decreases were seen in the levels of CM-IR in injured motoneurones and in the nearby neurones of VL which were confirmed by quantitation. These changes were not apparent 1 week after axotomy. However, four of the sacral axotomies showed low levels of staining that precluded the possibility of reliable quantitation. No decreases in CM-IR were seen contralaterally or in VM on either side of the cord. The motoneurones innervating the sartorius only showed a very slight bilateral decrease in CM-IR after axotomy. Statistically this decrease was only significantly different from control lumbar motoneurones or nearby iliacus motoneurones in the contralateral group.

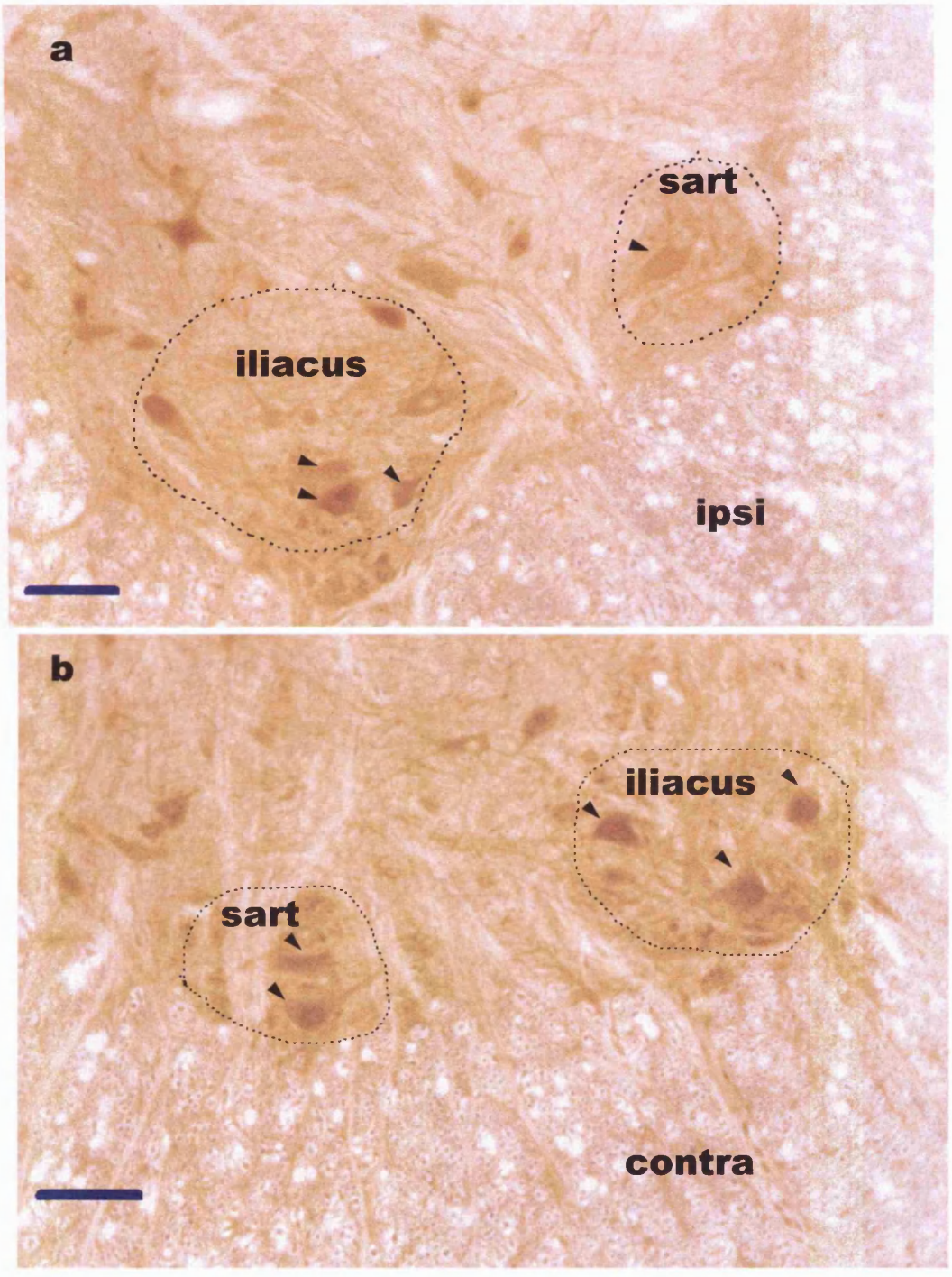

Figure 4.2.2-16. CM-IR in lumbar motoneurones (arrowheads) after axotomy of the nerve to the sartorius (sart) muscle. There appears to be some reduction in immunostaining bilaterally in comparison to the unlesioned motoneurones supplying the iliacus muscle.

Bars = 100μm.

The reasons for the paucity of immunostaining in four of the sacral axotomy experiments are not clear. The antibody was found to be somewhat capricious, in spite of maintaining high standards of consistency in the washing and incubation of the tissue, which may account for some of the variability. In addition, the decrease of immunoreactivity resulting from the injury might also have exacerbated the problem. The reasons for the inclusion of other ventral horn cell types in this response are not clear, but could relate to transneuronal effects of axotomy. Thus the decrease of total ventral horn immunoreactivity in those experiments may have been - at least in part - a genuine reflection of the injury-induced changes in CM-IR.

In spite of a low residual sample size, however, the findings of CM-IR decreases were particularly robust and were examined using a variety of statistical procedures, the results of which were all highly significant. and are in agreement with the only other published account of post-axotomy motoneuronal immunoreactivity for CM.

A decrease in CM-IR, but not mRNA, has been reported in axotomised rat hypoglossal motoneurones between the 2nd and 21st day after nerve transection (Dassesse et al, 1998), suggesting a decrease in stored gene product. These authors postulate a post-transcriptional factor such as Ca^{2+} dependent ubiquitination and degradation to account for the apparent decrease in CM-IR.

The reduction in levels of immunoreactivity in the absence of changes in mRNA levels may alternatively be explained by two hypothetical mechanisms of decreasing antibody access: increased substrate binding or conformational changes. Firstly, in the presence of axotomy-induced increases in $[Ca^{2+}]_i$, the association of CM with its target proteins may be elevated. Secondly, axotomy-

induced elevations or de novo expression of proteins that are involved in the regenerative changes resulting from axotomy may lead to a shift of CM binding tendencies in favour of these novel or up-regulated substrates, altering its conformation. For example, GAP-43, which has been described as a "calmodulin sponge" (Skene, 1990), is bilaterally elevated in the motoneuronal cell bodies and fibres after axotomy (Booth and Brown, 1993; Piehl et al, 1993). Increased or altered substrate binding by CM could then interfere with the ability of the antibody to detect the antigen due to conformational changes or masking of the antibody binding site.

An additional interpretation of these data may be that CM transcription after axotomy is actively suppressed to reduce the activity of degeneration promoting pathways, although given the breadth of neuronal functions that CM supports, it seems more likely that the CM substrates involved in neurotoxic events, such as CaN and nNOS, would be preferred targets for active and selective suppression. Indeed it may be the case that a primary decrease in levels of CaN and nNOS seen after axotomy (see above) causes a decrease in the utilisation of CM. CM's other major target protein is CaM kinase, and CaM kinase II has also been found to be decreased after axotomy (Lund and McQuarrie, 1997). Due to decreased utilisation, the surplus CM might then be rapidly eliminated from the cell. In such circumstances, the observed decrease in CM would be a secondary outcome of a decrease of another protein which is of greater relevance to the injury response process.

Such a hypothesis would concur with the findings of the present study. Significant decreases of nNOS-IR and CaN-IR were observed in axotomised pudendal motoneurones. The selective reduction of these two proteins in ON, both of which are normal targets of CM activity, might contribute to the

decrease in the CM-IR of ON as described above. Meanwhile, by the second week after section of *n. sartorius,* CaN-IR was only slightly decreased and nNOS-IR was elevated. In this case the binding of CM to its target proteins may remain unchanged, and would not be expected to affect levels of stored gene product in the same way. This hypothesis might thus account for the differences between the two segments in injury response.

4.2.3 CaBP- D28k and PV

No changes were seen in motoneuronal PV-IR after axotomy. The results for CaBP-D28K-IR are presented below.

4.2.3.i. Pudendal nerve axotomy

The post-axotomy reductions in levels of CaBP-D28K-IR in ON and VL were clear - particularly affecting the fibres running through ON - and highly significant (Fig. 4.2.3-1). An interesting feature of the pudendal axotomy response was the observation of the occasional swollen motoneurone with an eccentric nucleus which had a higher level of immunostaining than surrounding motoneurones (Fig. 4.2.3-2).

One week after pudendal axotomy the reduction is bilateral, the MBL for VL reducing from 5 to 1.88 and that of ON from 4.22 to 2.9. By the second post-operative week the contralateral MBLs for both VL and ON have returned to normal levels.. A reduction of the MBL for VM is also evident at week one, suggesting a more widespread response for CaBP-D28K than other antigens. In addition, even though the MBL for VL is significantly reduced from normal on both sides of the cord at the first week, the contralateral side (MBL = 2.2) also has a significantly higher MBL than the ipsilateral side (MBL = 1.88, Dunnett's T3 sig. p. = .044) showing that the effect is still more pronounced ipsilaterally. Table 4.2.3-1 below summarises the confidence intervals for each post-axotomy reduction, Figure 4.2.3-3 gives the MBLs, and Figures 4.2.3-4 - 4.2.3-6, the distributions.

4.2.3.ii. *N. Sartorius* Axotomy

After axotomy of *n. sartorius,* the MBL of both ipsilateral (1.46) and contralateral (1.47) sartorius motoneurones was significantly lower than that of

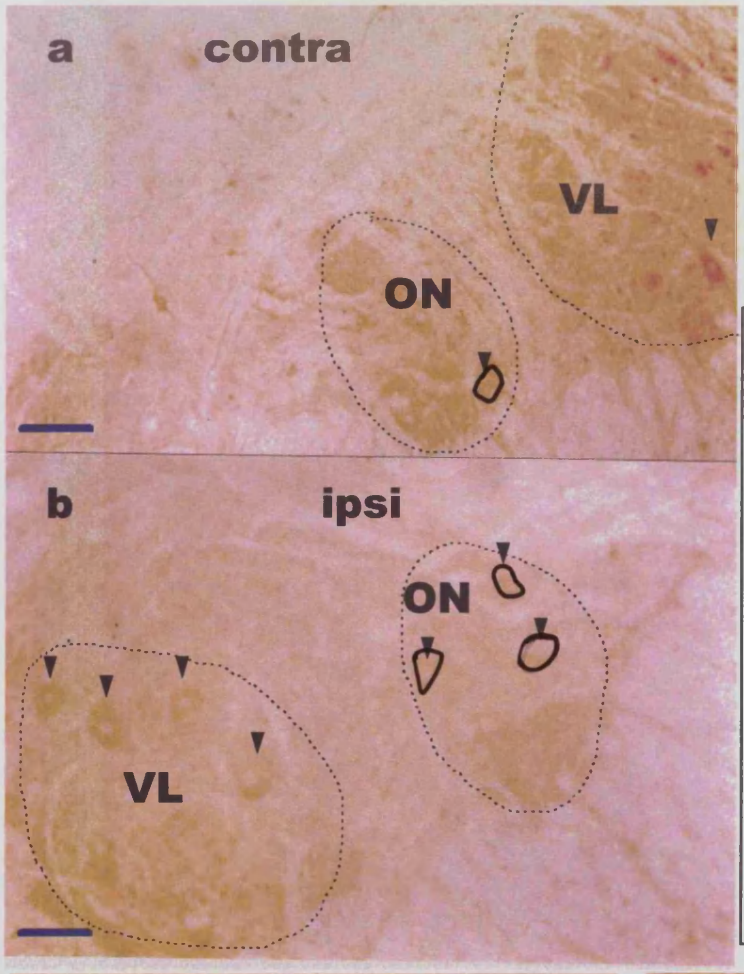

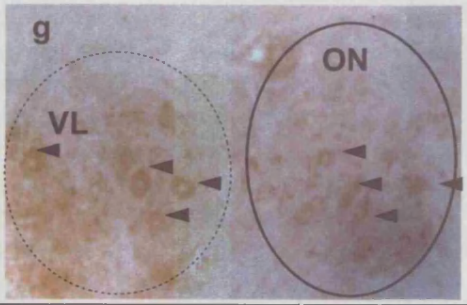

Figure 4.2.3-1. After pudendal axotomy an ipsilateral decrease in CaBP-IR is evident both in motoneurones and fibres of ON (b,c). At one week (c) the alteration is more pronounced wiith a total loss of IR in the fibres of ipsilateral ON. Contralaterally (e) motoneuronal cell bodies are showing levels of immunostaining no higher than the surrounding fibres, unlike the normal (g) pattern of CaBP-IR. By the second week (a) the contralateral ON shows CaBP-IR similar to normal ON (g), whilst a reduction is still apparent ipsilaterally (b). Oblique lighting has been introduced in (d) and (f) to aid identification of cell bodies in (c) and (e). Bars = 100μm.

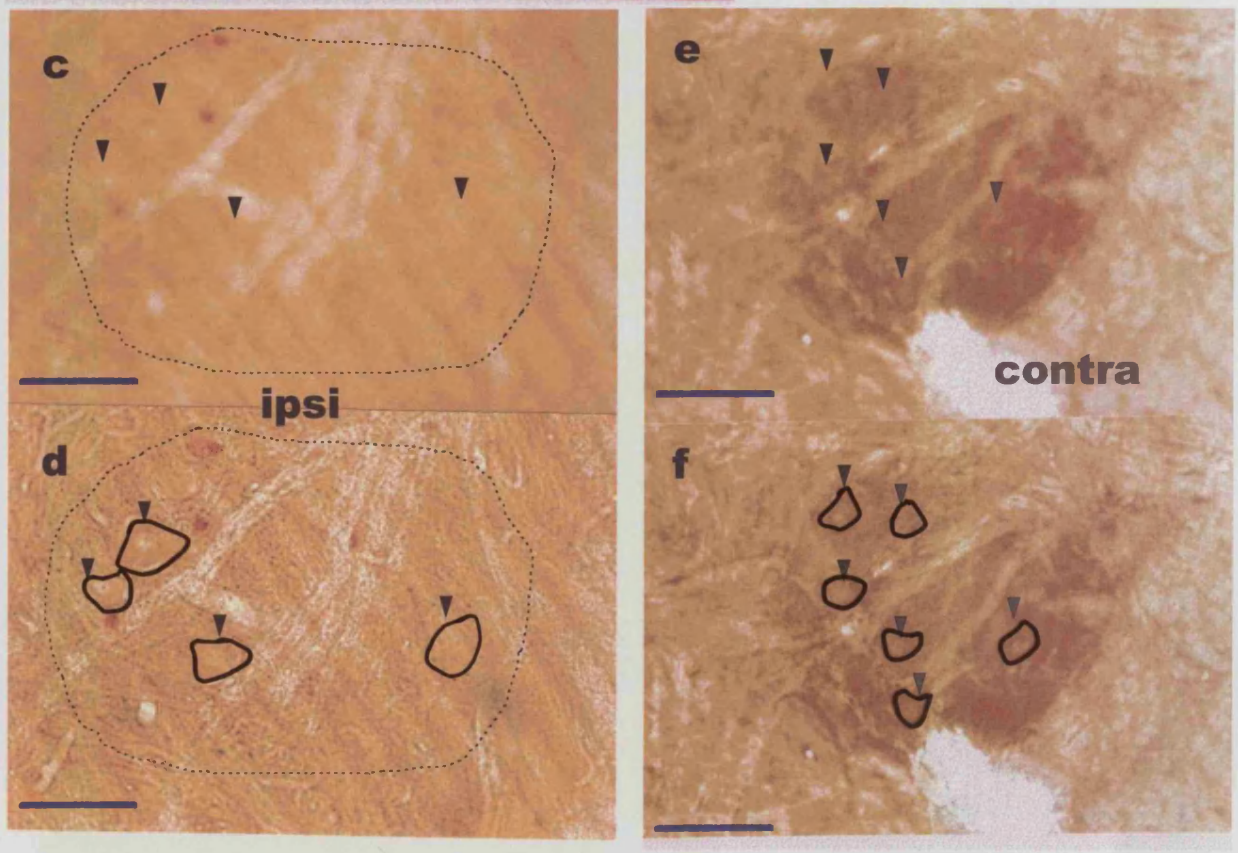

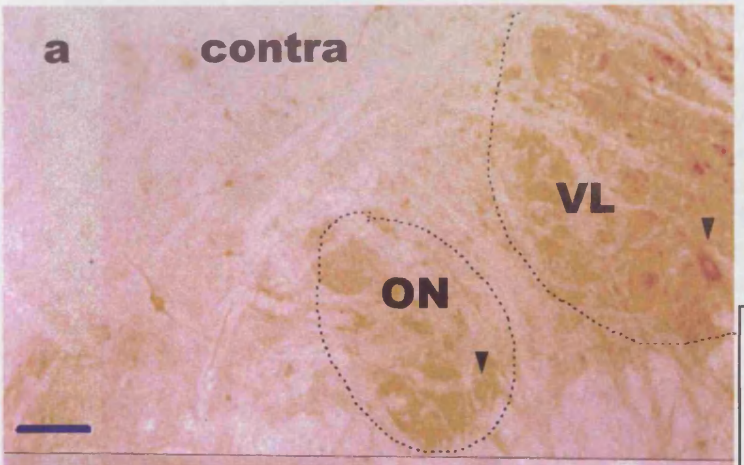

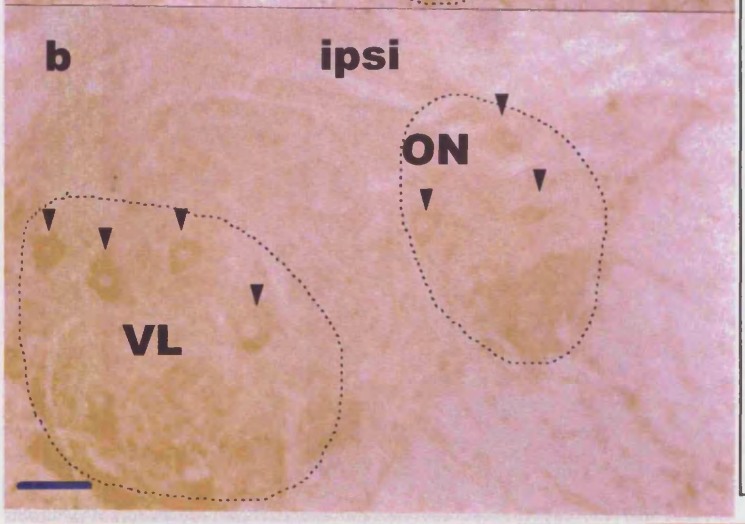

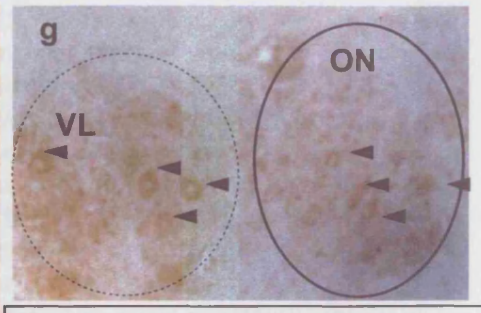

Figure 4.2.3-1. After pudendal axotomy an ipsilateral decrease in CaBP-IR is evident both in motoneurones and fibres of ON (b,c). At one week (c) the alteration is more pronounced wiith a total loss of IR in the fibres of ipsilateral ON. Contralaterally (e) motoneuronal cell bodies are showing levels of immunostaining no higher than the surrounding fibres, unlike the normal (g) pattern of CaBP-IR. By the second week (a) the contralateral ON shows CaBP-IR similar to normal ON (g), whilst a reduction is still apparent ipsilaterally (b). Oblique lighting has been introduced in (d) and (f) to aid identification of cell bodies in (c) and (e). Bars = 100μm.

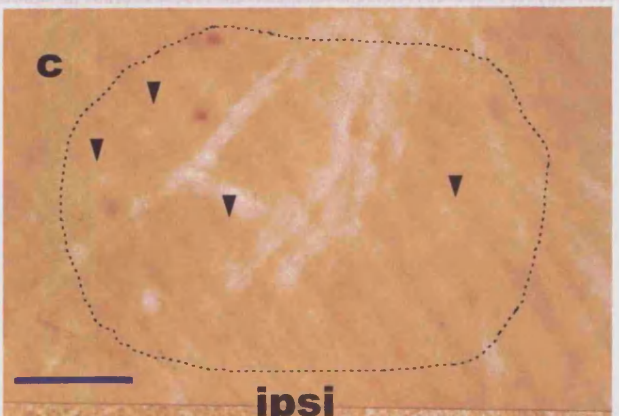

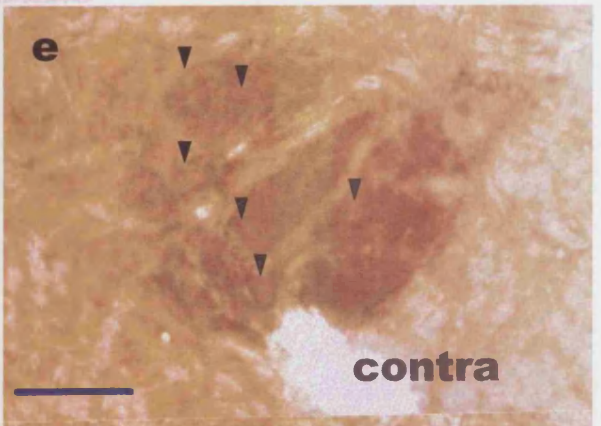

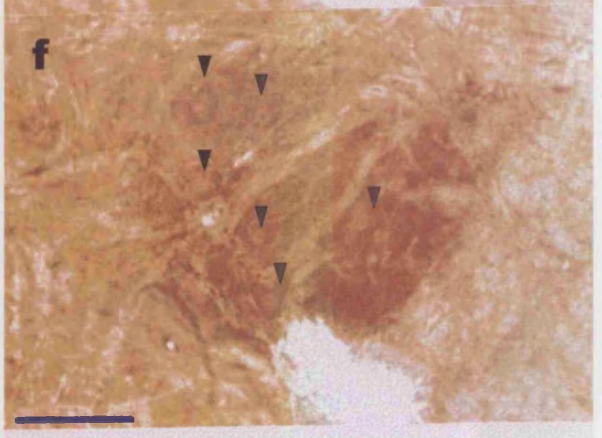

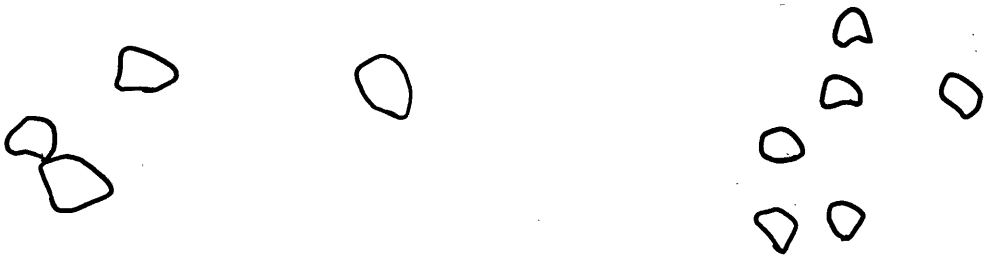

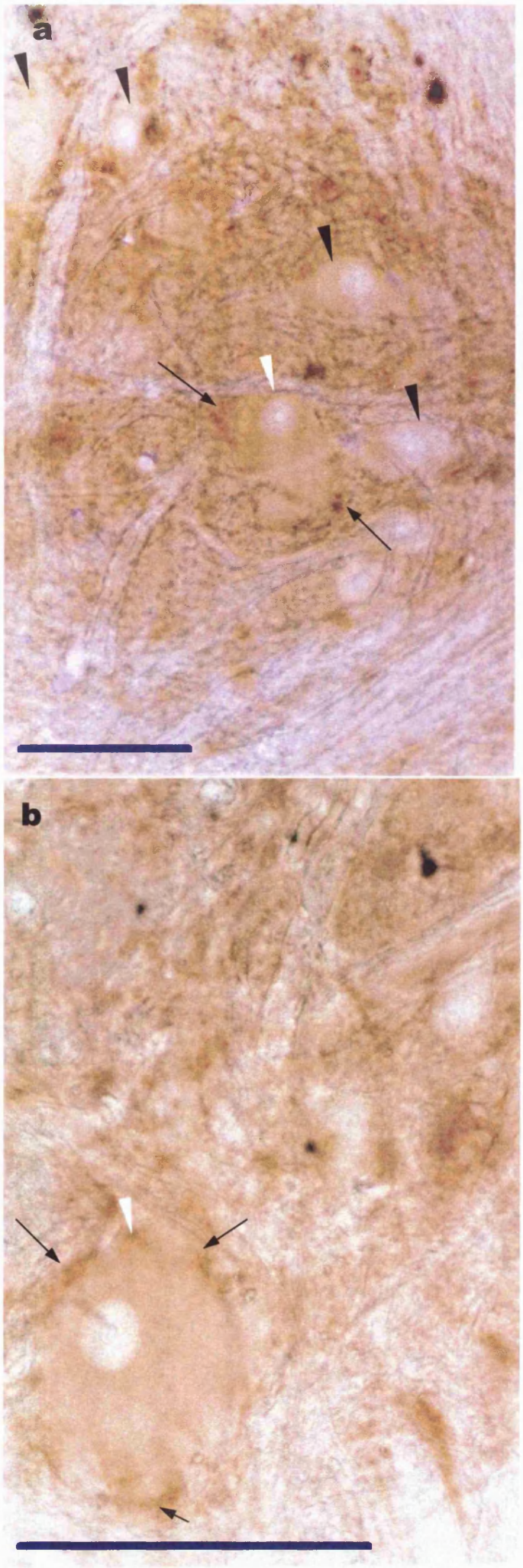

Figure 4.2.3-2. (a) and (b). Chromatolytic CaBPD28K-IR motoneurones (white arrowheads) in ipsilateral ON 2 weeks after pudendal section. Cel bodies are swollen, with eccentric nuclei and are surrounded by IR structures (arrows). Unstained motoneurones (heavy arrowheads in (a)) are smaller, and have more central nuclei.

Bars = 100μm.

normal lumbar motoneurones (2.89), whilst the MBLs for iliacus motoneurones on either side of the cord were unchanged from normal (ipsilateral MBL =2 and contralateral MBL = 1.85). There were, however, no significant differences between motoneuronal MBL of iliacus and sartorius. For illustrations see Figure 4.2.3-7.

Table 4.2.3-1. **To show significance levels of the Dunnett's T3 for the difference between the MBL of each celi type and its normal equivalent after axotomy of a nerve originating from the same spinai segment. All significant differences are decreases in the post-axotomy condition. NS = not signficant.**

Week	Side	VL	ON	VM	Sart.	iliacus
1	Ipsi	.000	.000	.000	-	-
1	Contra	.000	.000	.000	-	-
2	Ipsi	.033	.037	NS	.000	NS
2	Contra	NS	NS	NS	.000	NS

A less common feature of the regulation of CaBP-D28K in either lumbar or sacral segments after axotomy was the selective immunoreactivity of neuronal nuclei in some sections, where the neuronal cell bodies themselves were devoid of staining (Fig. 4.2.3-8).

Fig. 4.2.3-3. To show the MBLs of ON, VL, and lumbar motoneurones in normality and after pudendal or sartorius nerve axotomy. N for each mean value is shown at the top of each bar. Blue bar = normal MBL, red bars = ipsilateral MBLs, green bars = contralateral MBLs. Error bars represent S.E.M.s.

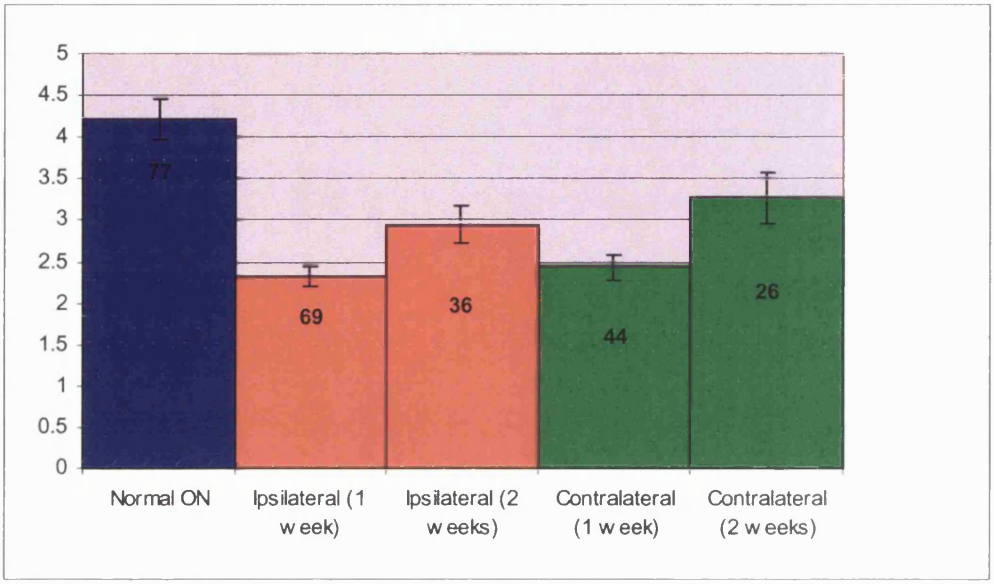

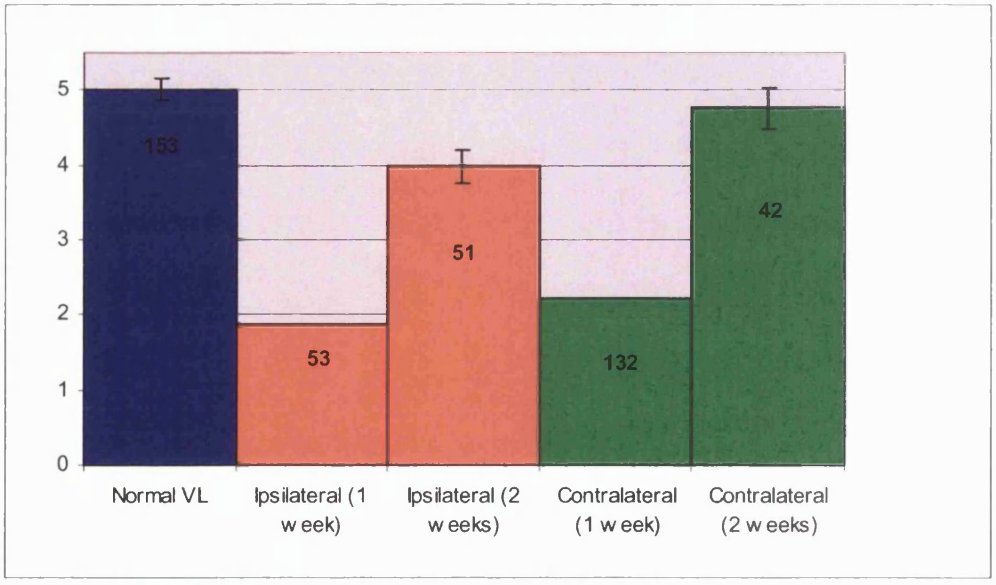

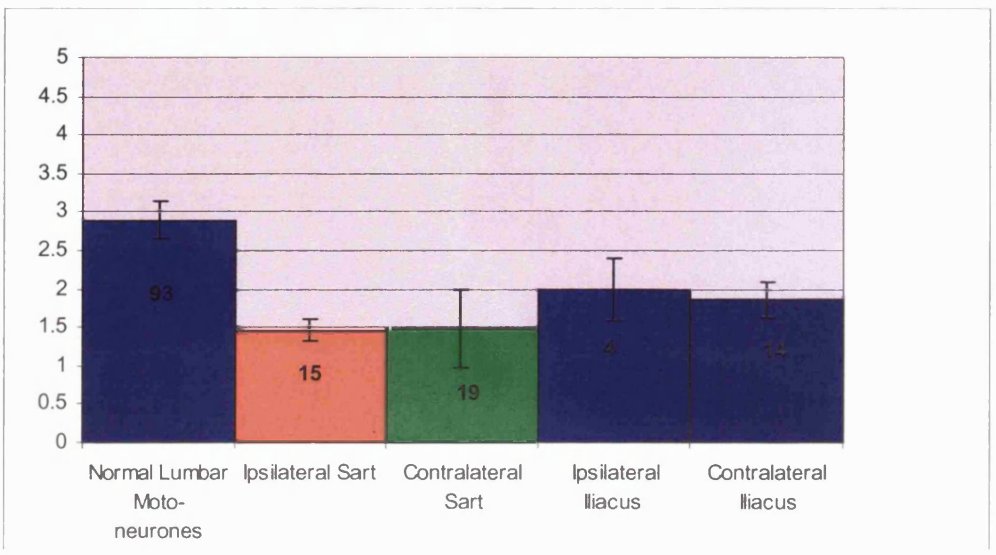

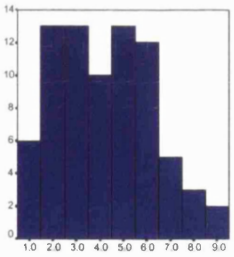

Std. Dev = 2.05
Mean = 4.2
N = 77.00

Normal Adult ON

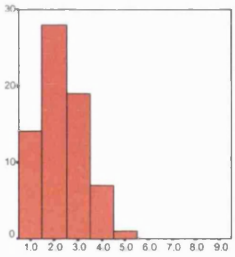

Std. Dev = .96
Mean = 2.3
N = 69.00

Ipsilateral ON - 1 Week

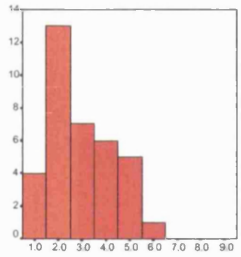

Std. Dev = 1.35
Mean = 2.9
N = 36.00

Ipsilateral ON - 2 Weeks

Figure 4.2.3-4. Histograms to show the distribution of CaBP-D28k-IR bin locations in ON in normality and after pudendal axotomy. Blue bars - normal motoneurones , red bars - ipsilateral to the lesion, green bars - contralateral to the lesion.

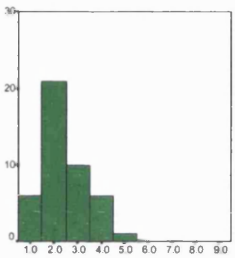

Std. Dev = .97
Mean = 2.4
N = 44.00

Contralateral ON - 1 Week

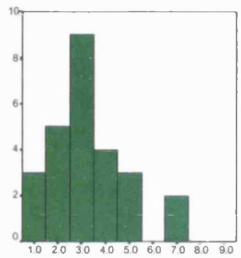

Std. Dev = 1.59
Mean = 3.3
N = 26.00

Contralateral ON - 2 Weeks

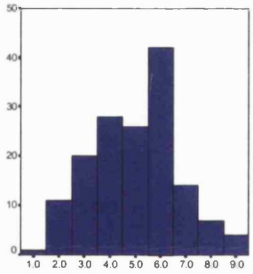

Std. Dev = 1.72
Mean = 5.0
N = 153.00

Normal Adult VL

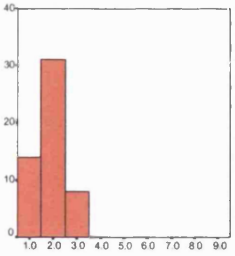

Std. Dev = .64
Mean = 1.9
N = 53.00

Ipsilateral VL - 1 Week

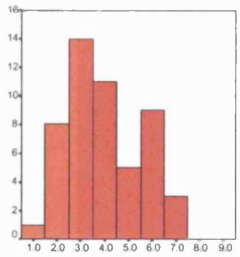

Std. Dev = 1.57
Mean = 4.0
N = 51.00

Ipsilateral VL - 2 Weeks

Figure 4.2.3-5. Histograms to show the distribution of CaBP-D28k bin locations in VL in normality and after pudendal axotomy. Blue bars - normal motoneurones , red bars - ipsilateral to the lesion, green bars - contralateral to the lesion.

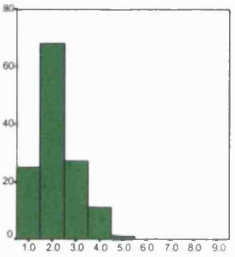

Std. Dev = .87
Mean = 2.2
N = 132.00

Contralateral VL - 1 Week

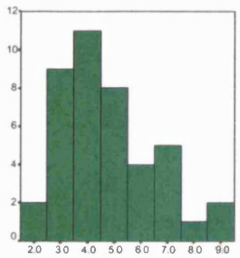

Std. Dev = 1.76
Mean = 4.8
N = 42.00

Contralateral VL - 2 Weeks

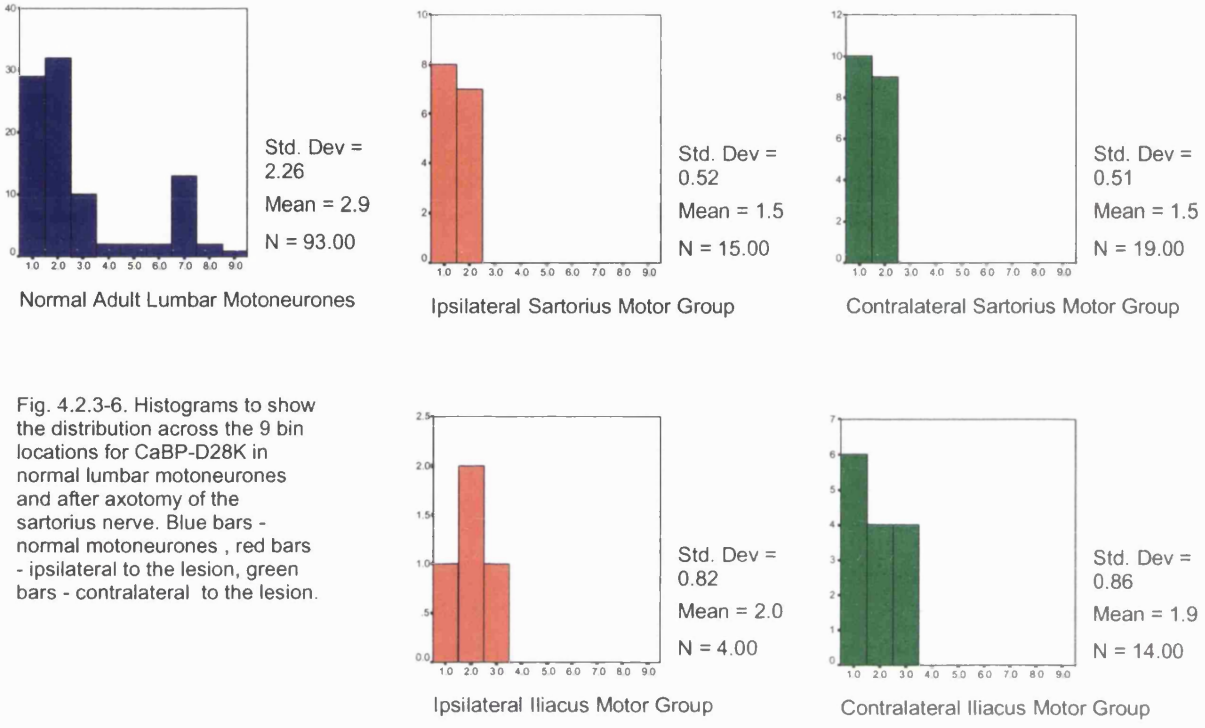

Fig. 4.2.3-6. Histograms to show the distribution across the 9 bin locations for CaBP-D28K in normal lumbar motoneurones and after axotomy of the sartorius nerve. Blue bars - normal motoneurones , red bars - ipsilateral to the lesion, green bars - contralateral to the lesion.

4.2.3.iii. Discussion

In spite of the possible importance of Ca^{2+}-binding proteins in vulnerability and protection, and the involvement of Ca^{2+} influx in the neuronal response to axotomy, there is a dearth of publications documenting the direct effects of axotomy on the levels of Ca^{2+}-binding proteins, particularly in motoneurones. Findings include decreases of CaBP-D28k-IR in the axotomised laryngeal motoneurones of *Xenopus laevis* , which are vulnerable to cell death after axotomy (Perez and Kelley, 1997), and in the inferior olive of the adult rat (Buffo et al, 1998) the neurones of which have a high regenerative capacity. In contrast, a 200% increase in CaBP-D28k mRNA on post-operative day 7 and the de novo appearance of CaBP-D28k-IR on post-operative day 14 has been reported in axotomised motoneurones of the rat hypoglossal nucleus, which are highly vulnerable to death after axotomy (Dassesse et al, 1998), de novo

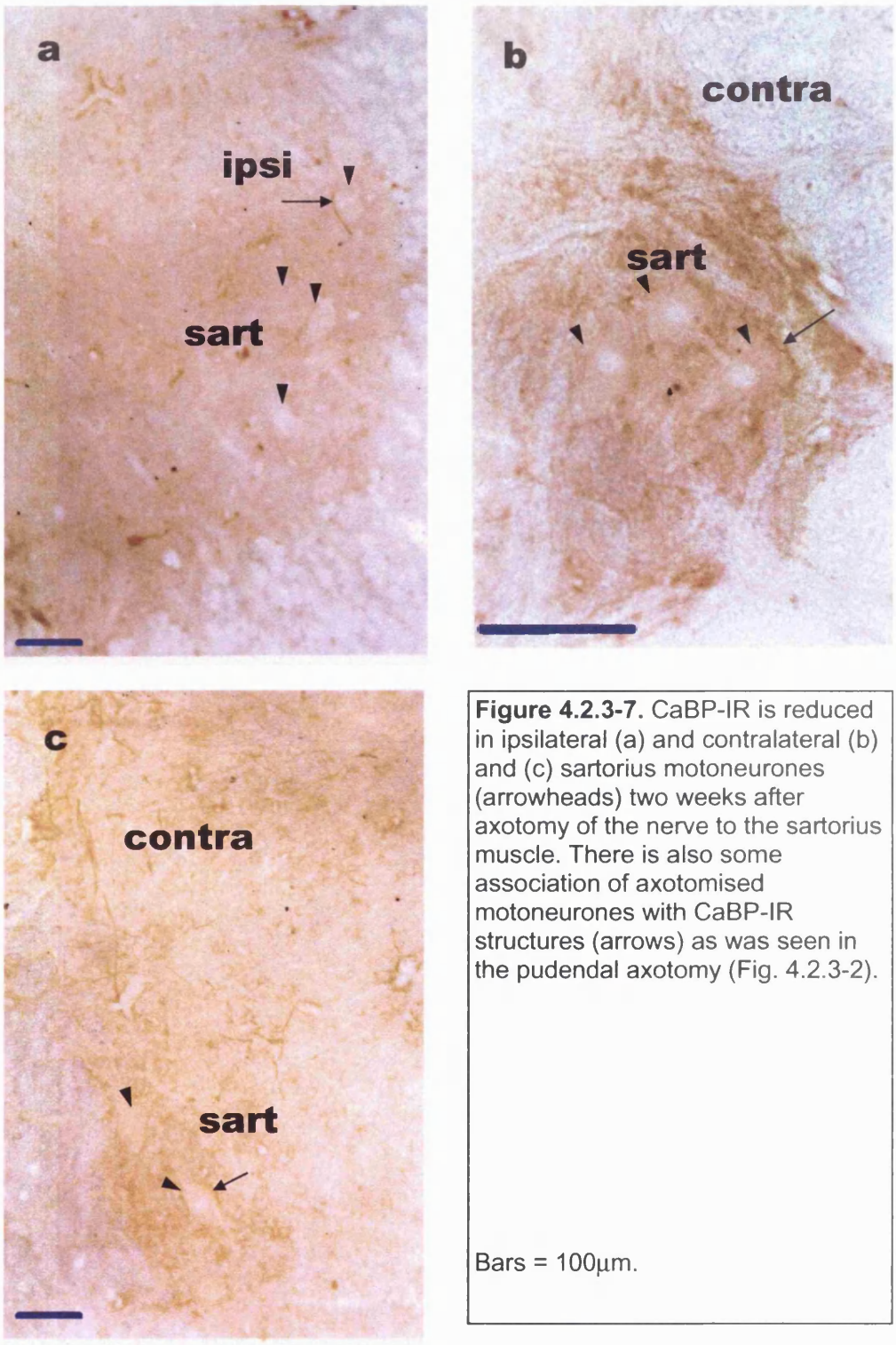

Figure 4.2.3-7. CaBP-IR is reduced in ipsilateral (a) and contralateral (b) and (c) sartorius motoneurones (arrowheads) two weeks after axotomy of the nerve to the sartorius muscle. There is also some association of axotomised motoneurones with CaBP-IR structures (arrows) as was seen in the pudendal axotomy (Fig. 4.2.3-2).

Bars = 100μm.

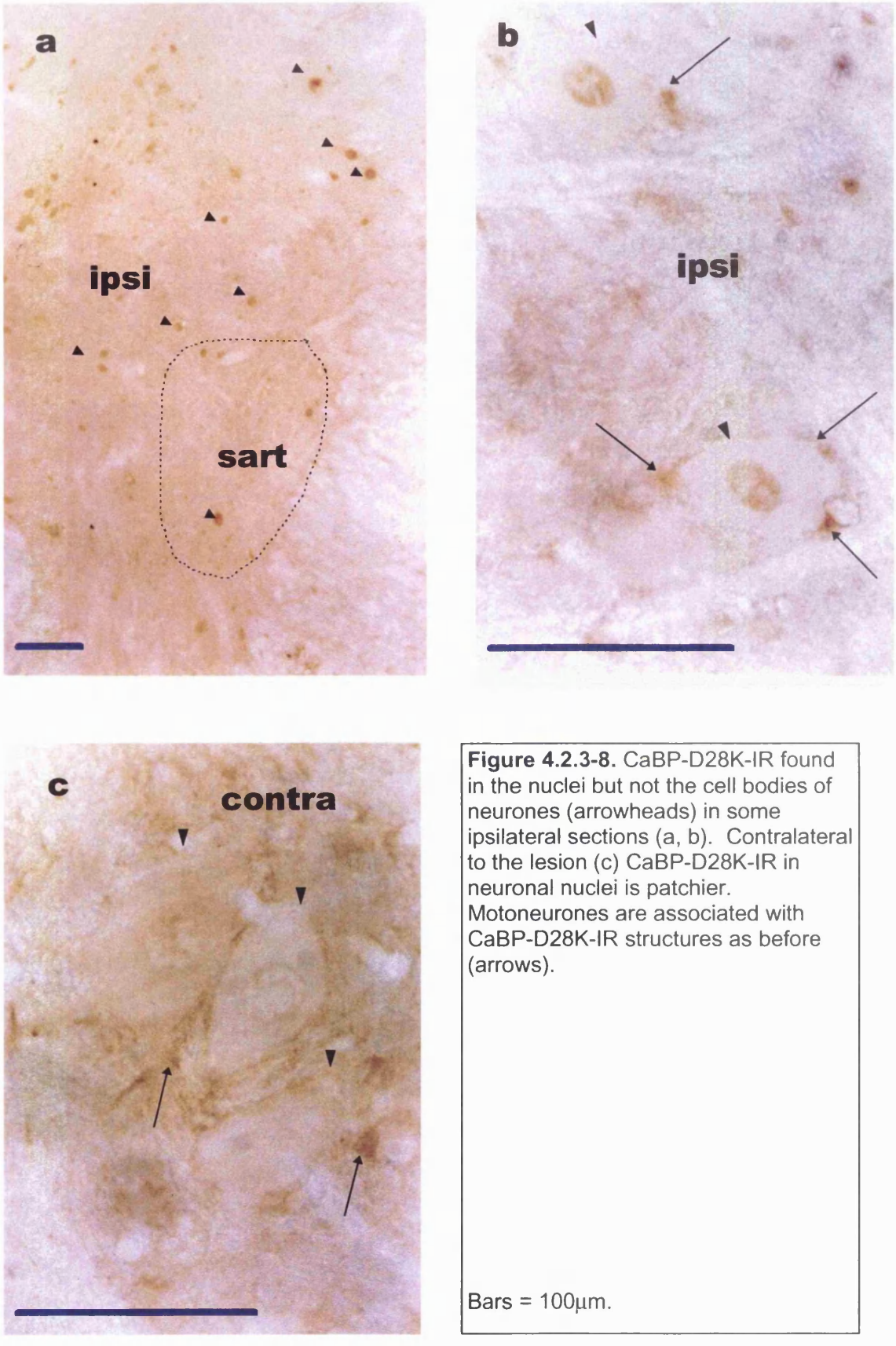

Figure 4.2.3-8. CaBP-D28K-IR found in the nuclei but not the cell bodies of neurones (arrowheads) in some ipsilateral sections (a, b). Contralateral to the lesion (c) CaBP-D28K-IR in neuronal nuclei is patchier. Motoneurones are associated with CaBP-D28K-IR structures as before (arrows).

Bars = 100μm.

expression of CaBP-D28k in 28 times the number of control neurones in 7-10 day axotomised neurones of the sympathetic ganglion (Sanchez-Vives et al, 1994), and de novo CaBP-D28k-IR in the cervical motoneurones of developing and adult rats (Fallah and Clowry, 1999). In the latter study, with increasing age, fewer motoneurones became CaBP-D28k-IR after axotomy and there was also greater capacity for motoneuronal survival. It is possible that the elevation of CaBP-D28k in these more vulnerable motoneurones may reflect the severity of the injury for those cells.

In the present study, a statistically significant decrease was observed in CaBP-D28k-IR but not in PV-IR in both axotomised sartorius motoneurones and axotomised pudendal motoneurones, and no segmental differences were noted in the axotomy responses of the two motoneurone groups. The reason for the selective increase of nuclear CaBP-D28k-IR seen in the neurones of some axotomised animals is not clear, and may reflect a generalised response to altered Ca^{2+} homeostasis.

Target deprivation has been shown to prevent CaBP-D28k expression *in vitro* in the DRG of the developing chick (Barakat and Droz, 1989). However, it was possible to induce CaBP-D28k expression by addition of muscle extract to the medium. It is, therefore, tempting to speculate that loss of a muscle-derived factor may be responsible for the decrease in CaBP-D28k-IR. In the present study, however, two weeks after injury, a few motoneurones of ON showed higher levels of antigenicity, and showed signs of chromatolysis. In this sense, the current findings are supportive of a dual regulation of CaBP-D28k whereby it is decreased in neurones destined to survive the insult and increased in those whose viability is threatened by the insult.

CHAPTER 5

DISCUSSION

5.1 The quantification of immunocytochemistry

There is a paucity of data on the normal spinal cord distribution of the proteins examined in this study, particularly in cat. Before reviewing the distributions observed in the present study, it is pertinent to consider differences between this and earlier studies in the methods used to evaluate these distributions.

Usually data on the immunocytochemical localisation of proteins in the CNS is primarily qualitative, with authors relaying the visual impression of the levels of staining in the immunostained tissue. Semi-quantitative analyses are sometimes employed, and this either involves categorising neurones as having high or low staining levels, or assigning a level of stain to a neurone on the basis of visual appearance on a three or four point scale. These data may then be analysed quantitatively with standard statistical procedures.

This system is problematic, however, because perceptual features of the human visual system which actively alter the cortical representation of actual objects, such as colour constancy (which allows different wavelengths to be perceived as the same colour under certain conditions), can reduce the ability of the observer to detect subtle differences. Conversely, similarly stained neurones may be perceived to be different in the degree of staining due to fluctuations in local background staining levels, which could artefactually exaggerate or diminish the appearance of neuronal staining, due to the context dependence of colour perception. This problem is exacerbated by fluctuations of staining due to variations in section thickness.

This problem is particularly pertinent when evaluating staining levels of motoneurones within ON since the dendrites of these neurones form a dense dendritic bundle, which runs transversely through the nucleus. This means that when ON motoneurones are immunoreactive for a given antigen, the immediate local background is often also immunoreactive. Thus the immediate surrounding of the average ON motoneurone is often much darker than that of the average motoneurone from another segment, making subjective qualitative comparisons less reliable.

A more quantitative technique which is also commonly used - that is, comparisons of grayscale levels expressed as % of background (e.g. Rami et al, 1998) - is also not an optimal solution. From experiment to experiment, staining levels can vary for any number of reasons. For example, the potency of DAB is degraded over time leading to a degree of variability in the chromogenic reaction. Sharp contrasts in the time taken for tissue to reach optimal staining levels have been noted in our laboratory between batches of DAB from the same supplier. The quality of perfusion and further exposure of the tissue to the fixative or buffer rinses are other examples of the many factors affecting antigenicity between experiments.

Whilst efforts are always made to minimise this variability within the laboratory, the present study has in addition utilised a novel mathematical approach to reduce the influence of this variability on the result. Raw grayscale data was transformed to a single scale, similar to that employed in the qualitative techniques described above, but with two important differences. Firstly, the scale is spread over nine points or bin locations, rather than 2 - 4, increasing the sensitivity of the index to subtle shifts. Secondly, the assignment of data to the bin locations is made on the basis of purely quantitative data - the measured

levels of grayscale as a percentage of tissue background - removing the influence of human perception on the result. However, the assignment of a given neurone to a bin location is relative to the entire staining range for the experiment, including all neuronal types measured. This removes the influence of absolute values on the result, and with it the influence of experiment to experiment variability in absolute staining levels.

Clearly, the resulting data cannot be interpreted as representing actual protein content, since the relationship of immunocytochemical staining to actual protein content is not a straightforward one. It is, however, reasonable to assume that more strongly labelled neurones contain more protein (for a discussion see Polak and Van Noorden, 1997). By setting upper and lower limits of the data range by the darkest (/highest protein content) and palest (/lowest protein content) cells from the whole ventral horn region, it is easy to locate neuronal groups that consistently fall the same distance from either end of that range. In this way it is also easy to pinpoint relative shifts after injury. It is not so easy, however, to detect alterations in cell groups that fall at the outer limits. If changes occur in these groups, the effect would be to widen or narrow the data bin widths for the whole experiment, causing a change in the spread of the data, but not necessarily in mean values. For this reason it is important to examine distributions as well as mean changes. Within these interpretative limits however, the technique employed here represents a reasonable solution to the thorny problem of quantifying immunocytochemistry.

5.2 Overview and conclusions

This project has sought to answer three questions. Specifically, the central focus in these lines of enquiry was on differences between ON, which benefits from a prolonged resistance to the pathology of ALS, and other, more vulnerable, motoneuronal groups. Since these questions also focus on post-injury alterations, it was necessary to use non-human animals so that the nerve injury could be produced experimentally by defined procedures.

To explore these issues, six proteins were chosen which are of relevance to current theories of cell death in ALS: calcium-binding "buffer" proteins CaBP-D28K, PV; calcium-binding "trigger" proteins CM and CaN-B; and SOD and nNOS, which are involved in free radical homeostasis. The research presented here has addressed these questions as follows:

5.2.1 Do differences exist between motoneuronal groups in terms of the distribution of proteins involved in cytotoxic or protective pathways, and might these be predictive of differences in response to injury or neuropathology?

The findings presented here strongly suggest that motoneurone groups are not identical in their relative levels of protein content. Higher levels of CaBP-D28k-ir, nNOS-ir, and SOD-1-ir, were found in the sacral somatic motoneurones than in motoneurones of cervical, thoracic, and lumbar spinal segments.

Higher levels of sacral motoneuronal CaBP-D28k, as also observed by Alexianu et al (1994), might be predictive of greater resistance in ON to pathological conditions relating to abnormally high $[Ca^{2+}]_i$, due to the greater resultant Ca^{2+}

buffering capacity, alongside other properties of this nucleus. It was suggested earlier that the different type of physiological activity involved in the maintenance of sphincter tone may underlie the enrichment of CaBP-D28k in these neurones, with the transverse dendritic bundle representing a useful anatomical substrate for the generation of synchronous firing patterns. Since the evidence suggests that CaBP-D28k has a role in shaping the form of synaptic Ca^{2+} transients, it would be of interest to investigate the possibilities that a/ ON's firing behaviour is largely synchronous and b/ the presence of CaBP-D28k facilitates synchronous firing, which might usefully be assessed in CaBP-D28k null mutant mice.

The enrichment of nNOS in ON echoes earlier findings from this laboratory (Pullen et al, 1997), and it is likely that this is related to the use of NO as a co-transmitter in the pudendal nerve (Parlani et al, 1993). It has been suggested that neurones that constitutively express and utilise nNOS may have superior endogenous protection against NO-mediated neurotoxicity (Dawson et al, 1991; Dawson et al, 1993; Yu, 1994). Indeed, neurones expressing nNOS are spared from the lesion of Huntington's Chorea (in Kowall, 1987) and from certain types of excitotoxic (Ferrante et al, 1993) and bioenergetic lesions (Beal et al, 1993; Brouillet et al, 1993). Thus, higher levels of endogenous expression of this protein in ON in normality may provide some benefit during the early stages of deterioration in ALS.

Finally, SOD-ir was shown to be slightly higher in ON, and has previously been found to be high in the other motoneurone group resistant to ALS, the oculomotor nucleus (Bergeron et al, 1996). Since an abnormality in this protein's activity is implicated in the pathogenesis of a percentage of ALS cases, it

is not clear how an enrichment in SOD-1 might benefit these two groups of motoneurones.

Nevertheless, these findings underscore the fact that these sphincteric motoneurones, which appear to share the common properties of somatic motoneurones, may - on balance - have internal milieus that are significantly different from other motoneurones, causing them to respond differently in pathological states.

Why ON and VL should be similar in their patterns and levels of immunoreactivity for these proteins is not clear. An extensive search of the literature unearthed very few studies of the anatomy and physiology of VL. Although rat VL has been found to contain anal and vesicular sphincteric motoneurones (Katagiri et al, 1986), the motoneurones of VL in cat have only been reported to innervate the intrinsic muscles of the foot (Egger et al, 1980; Vanderhorst and Holstege, 1997). More information is needed on the connections of this sacral VL group before any firm conclusions can be drawn.

5.2.2 Are there differences in the pre- and post-injury profiles of motoneuronal groups in terms of proteins involved in cytotoxic or protective pathways?

The overall changes seen in antigenicity after axotomy are summarised in Table 5.2.2-1 below.

Elevations in nNOS/NADPH-d, seen here after the sectioning of hindlimb nerves, are commonly seen in axotomised motoneurones (Yu, 1994; Yu, 1997; Kristensson et al, 1994; Wu et al, 1994a Wu et al, 1994b; Wu et al, 1996; Wu, 1996; Hu et al, 1996; Novikov et al, 1995). The reasons for increased

expression/activity of this protein are not clear. Although associated with cell death after prolonged expression in severely injured neurones (Kristensson et al, 1994; Wu et al, 1994a Wu et al, 1994b; Wu et al, 1996; Wu, 1996; Hu et al, 1996; Novikov et al, 1995), it is thought that the initial increase in nNOS/NADPH-d is elicited by the loss of certain neurotrophic factors (Novikov et al, 1995) and may be of some neuroprotective benefit perhaps by positive effects on factors supporting regeneration such as increasing local blood flow (Yu, 1997).

In rat, elevations in CaBP-D28k-ir have been observed in axotomised neurones likely to die after the insult (Dassesse et al, 1998; Fallah and Clowry, 1999), and decreases in CaBP-D28k-ir observed in surviving neurones (Buffo et al, 1998). It is reasonable to postulate that this relationship reflects the severity of the injury, with dying neurones becoming increasingly Ca^{2+} permeable due to the failure of energy-dependent mechanisms and therefore upregulating CaBP-D28k. Less seriously injured neurones which have lost contact with their target will undergo presynaptic reorganisation. It is possible that in these circumstances CaBP-D28k is down-regulated in response to alterations in the physiological activity of the neurone.

Table 5.2.2-1. Alterations in protein immunoreactivity after unilateral nerve section.

CaBP-D28k	PV	CM	CaN-A	nNOS	SOD-1
↓	no change	↓	↓	↑	no change

The post-axotomy decrease seen in CM-ir here is similar to that observed by Dassesse et al (1998), who nevertheless found no concomitant alteration of CM

mRNA levels after axotomy. It seems probable that increased degradation of CM may be secondary to the decreased presence and activity of some of CM's target proteins, such as that of CaN-A. For the first time it has been shown here that motoneurones, which usually have high levels of CaN, exhibit a dramatic reduction in CaN-A levels after axotomy. This may well be a neuroprotective response, given CaN's involvement in NO generation (Sharkey and Butcher, 1994) and apoptosis (Wang et al, 1999).

5.2.3 Are there differences between motoneuronal groups in post-injury alterations of protein immunoreactivity?

Two potentially important differences were observed between the axotomy response of ON and that of the motoneurones innervating the sartorius muscle. Firstly, the alterations in CaBP-D28k, CM, CaN, and nNOS in axotomised sacral motoneurones appeared to occur unilaterally, whilst sartorius motoneurones showed similar alterations on the lesioned and uninjured sides of the spinal cord. Secondly, nNOS was found to be elevated in axotomised lumbar motoneurones and greatly diminished in axotomised sacral motoneurones. Both of these phenomena are discussed below.

Bilateral vs. Unilateral responses

The bilaterality of post-axotomy changes in sartorius, but not ON, is unlikely to be an artefact since the lumbar alteration was specific to the lateral motor group. The adjacent medial group innervating *m. iliacus*, which was measured in the same sections as the sartorius motoneurones, was statistically no different from normal lumbar motoneurones.[1]

[1] Due to the lack of control measurements specifically for sartorius motoneurones as a group, the possibility persists that normal sartorius motoneurones may have antigenicity profiles for the proteins deemed to have "altered" after injury herein that differ from other lumbar motoneurones. Nevertheless, the recent observations of bilateral post-axotomy changes in other motoneuronal groups suggest a genuine biological explanation to be plausible - this evidence is discussed overleaf.

Contralateral responses to injury, whilst counter-intuitive, are becoming widely documented. Unilateral nerve section has been shown to cause bilateral alterations in levels of a number of antigens (Booth and Brown, 1993; Piehl et al, 1993; Rydh-Rinder et al, 1996; Jung et al, 1997). Furthermore, recent work in the neonatal rat suggests that the apoptotic motoneuronal and interneuronal death that follows nerve crush at this age occurs bilaterally (Lawson and Lowrie, 1998), indicating that contralateral antigenic alterations may belie challenges to contralateral neuronal viability.

Bilateral alterations after axotomy may result from a combination of three factors. To begin with, the glial response may not be restricted to one side, and may cause inflammatory alterations across the segment. If this were the case here, however, the iliacus motor group (which flanks the sartorius motor group) ought to be affected. Furthermore, bilateral glial activation does not occur after axotomy of the rat hypoglossal nerve (Barron et al, 1990). A second contributory factor may be compensatory muscular activity on the contralateral side which could induce changes in motoneuronal protein expression. Under such circumstances, one might also expect compensatory activity in other ipsilateral hindlimb musculature. To assess this possibility, the immunoreactivity of motoneurones innervating muscles which are most likely to be involved in compensation needs investigation in further experiments. Finally, there may be a trans-neuronal effect of the degenerative changes. Hindlimb motoneurones are known to have contralateral connections (Rotto-Percelay et al, 1992) and reciprocal crossed inhibition has been observed in these and other motoneuronal groups (Jankowska et al, 1978; Duysens and Loeb, 1980; Harrison and Zytnicki, 1984). Thus alterations in connectivity after axotomy may extend trans-neuronally to contralateral cell groups and induce fluctuations in protein expression in these motoneurones. Evidence in favour of bilateral synaptic

changes after axotomy also comes from work demonstrating elevations of GAP-43 on both sides of the cord after unilateral nerve section (Booth and Brown, 1993; Piehl et al, 1993) or botulinum intoxication (Jung et al, 1997).

Synaptic remodelling might also engender alterations in receptor expression. The relative balance of receptor types after injury will affect the Ca^{2+}-permeability of these neurones. Preliminary findings suggest that after axotomy, motoneurones have a higher proportion of Ca^{2+} permeable AMPA receptors (Kennis and Holstege, 1997). It would be of interest to examine further the laterality of changes in the relative density of different receptor subtypes in axotomised pudendal and lumbar motoneurones.

By contrast, bilateral changes in CaN-IR, nNOS-ir, CaBP-D28k, or CM-ir were not seen in the sacral cord after pudendal axotomy. Work from this laboratory has previously shown that ipsilateral axotomised pudendal motoneurones undergo a loss of 40% of afferent synaptic contacts and elevations in levels of GAP 43-ir (Pullen et al, 1997) indicating a high level of synaptic remodelling in ON after axotomy. However, pudendal motoneurones do not display crossed inhibition (Jankowska et al, 1978) and are therefore likely to have a smaller degree of commissural connectivity. Experiments using a trans-neuronally transported label such as wheat germ agglutinin-horseradish peroxidase or pseudorabies virus would be useful to assess the hypothesis that injury responses in the sacral cord are more confined in laterality due to limited bilateral connections in comparison with other somatic motoneurone groups. In combination with other factors, the more restricted injury response in ON may be an important property involved in prolonging the survival of its motoneurones in the face of progressive diseases such as ALS.

Elevation or suppression of nNOS?

The other factor that differed between the two motoneuronal groups was the post-axotomy regulation of nNOS. Observations of axotomy-induced increases in nNOS are plentiful in the literature, with prolonged nNOS expression being found in neurones more likely to die after the injury (see Chapter 4, Section 4.3.1.iii).

The down-regulation of nNOS in the axotomised pudendal motoneurones may well be a response to an injury induced partial loss of sphincter tone. As NO is thought to be used by the motoneurones of ON as a co-transmitter which is involved in generating sphincter relaxation, and mechanical urethral obstruction induces increased nNOS expression as an attempt to decrease sphincter tone (Zhou and Ling, 1997), it is plausible that the converse is true - i.e. decreased sphincter tone leads to a suppression of nNOS expression.

A greater understanding of the role of NO in pudendal nerve activity is vital. Given the association of nNOS with excitotoxicity, free radical generation, and neuronal death, the differential regulation of nNOS by the motoneurones of ON may be another important component of its ability to survive in the face of relentless degeneration in diseases such as ALS.

Conclusion

In this thesis, an extensive evaluation of relative levels of immunoreactivity for proteins in different motoneuronal groups has been carried out, using an exhaustive quantitative approach. Particular attention has been given to ON which enjoys relative resistance to degenerative motor diseases such as ALS. The results suggest that in addition to its unique interaction with the autonomic nervous system, which provides a rich peptidergic input to this nucleus (Gibson

et al, 1988), ON may benefit from greater Ca^{2+}-buffering capacity than other somatic motoneurone groups, high endogenous nNOS-ir which may be correlated with autoprotection against NO-mediated toxicity, a lesser bilateral component in its injury response than other somatic motoneurones, and a tendency to show reduced nNOS levels after nerve injury. A greater understanding of these and other features of this interesting nucleus will add to a growing body of knowledge about the anatomical, physiological and biochemical factors underlying the mysterious patterns of selective vulnerability and protection that characterise a range of neurodegenerative conditions. Ultimately, insight into these factors should shed light on both mechanisms of pathogenesis and possible avenues for therapeutic approaches.

REFERENCES

Airaksinen, M.S.; Eilers, J.; Garaschuk, O.; Thoenen, H.; Konnerth, A. and Meyer, M. Ataxia and altered dendritic calcium signalling in mice carrying a targeted mull mutation of the calbindin D28k gene. *PNAS USA, 1997a.* 94: 1488-93.

Airaksinen, M.S.; Thoenen, H. and Meyer, M. Vulnerability of midbrain dopaminergic neurones in calbindin-D28k-deficient mice: lack of evidence for a neuroprotective role of endogenous calbindin in MPTP-treated and Weaver mice *Eur. J. Neurosci. 1997b.* 9: 120-7.

Albin, R. and Greenamyre, J.T. Alternative excitotoxic hypotheses. *Neurol. 1992.* 42: 733-8.

Alexi, T. and Hefti, F. Neurotrophin-4/5 selectively protects nigral calbindin-containing neurons in rats with medial forebrain bundle transections. *Neurosci. 1996.* 72(4): 911-21.

Alexianu, M. E.; Bao-Kuang Ho; Habib Mohamed, H; La Bella, V; Smith, R. G.; and Appel, S. H. The role of calcium-binding proteins in selective motoneurone vulnerability in amyotrophic lateral sclerosis. *Ann. Neurol. 1994.* 36: 846-58.

Appel, S.H.; Engelhardt, J.I.; Garcia, J.; and Stefani, E. Immunoglobulins from animal models of motor neuron disease in human ALS passively transfer physiological abnormalities of the neuromuscular junction. *PNAS USA, 1991.* 88: 647-51.

Armand, J. The origin, course and terminations of corticospinal fibres in various mammals. In Descending Pathways to the Spinal Cord (eds. H.G.J.M. Kuypers and G.F. Martin). *Prog. Br. Res. 1982.* 57: 330-60

Baimbridge, K.G., Celio, M. R. and Rogers, J. H. Calcium-binding proteins in the nervous system. *TINS 1992.* 15 (8): 303-8.

Baimbridge, K.G. and Miller, J.J. Hippocampal calcium-binding protein during commissural kindling-induced epileptogenesis: progressive decline and effects of anticonvulsants. *Br. Res. 1984.* 324: 85-90.

Baker, S.N.; Kilner, J.M.; Pinches, E.M.; and Lemon, R.N. The role of synchrony and oscillations in the motor output. *Exp. Br. Res. 1999.* 128: 109-17.

Barakat, I. and Droz, B. Calbindin-immunoreactive sensory neurones in dissociated dorsal root ganglion cell cultures of chick embryo: role of culture conditions. *Br. Res. Dev. Br. Res. 1989.* 50(2): 205-16.

Barron, K.D.; Marciano, F.F.; Amonson, R. and Mankes, R. Perineuronal glial responses after axotomy of central and peripheral axons. A comparison. *Br. Res. 1990.* 523: 219-29.

Bates, T.E.; Heales, S.J.R.; Davies, S.E.C.; Boakye, P.; and Clarke, J.B. Effects of 1-methyl-4-phenylpyridinium on isolated rat brain mitochondria: evidence for a primary involvement of energy depletion. *J. Neurochem. 1994.* 63: 640-8.

Beal, M.F.; Brouillet, E.; Jenkins, B.G; Ferrante, R.J.; Kowall, N.W.; Miller, J.M.; Storey, E.; Srivastava, R.; Rosen, B.R.; and Hyman, B.T. Neurochemical and histologic characterisation of striatal excitotoxic lesions produced by the mitochondrial toxin, 3-nitropropionic acid. *J. Neurosci. 1993b.* 13(10): 4181-92.

Beal, M.F.; Brouillet, E.; Jenkins, B.G.; Henshaw, R.; Rosen, B.r.; and Hyman, B.T. Age-dependent striatal excitotoxic lesions produced by the endogenous mitochondrial inhibitor malonate. *J. Neurochem. 1993a.* 61: 1147-50.

Beal, M. F.; Ferrante, R. J.; Browne, S. E.; Matthews, R. T.; Kowall, N. W.; and Brown Jnr, R. H. Increased 3-nitrotyrosine in both sporadic and familial amyotrophic lateral sclerosis. *Ann. Neurol. 1997.* 42: 646-54

Beckman, J. S.; Chen, J.; Crow, J. P. and Zu Ye, Y. Reactions of nitric oxide, superoxide and peroxynitrite with superoxide dismutase in neurodegeneration. *Prog. Br. Res. 1994.* 103: (Chapter 31) 371-80.

Beckman J.S. and Koppenol W.H. Nitric oxide and peroxynitrite: the good, the bad, and the ugly. *Am. J. Physiol. 1996.* 271 (Cell Physiology 40): C1424 - C1437.

Bell, C. Idea of a New Anatomy of the Brain. Birmingham, Classics of Neurology and Neurosurgery Library. *1987.* (Reprint of 1811 pamphlet.)

Bergeron, C.; Muntasser, S.; Somerville, M.J.; Weyer, L.; and Percy, M.E. Copper/zinc superoxide dismutase mRNA levels are increased in sporadic amyotrophic lateral sclerosis motoneurones. *Br. Res. 1994.* 659(1-2): 272-6.

Bergeron, C.; Petrunka, C.; and Weyer, L. Copper/zinc superoxide dismutase expression in the human central nervous system. Correlation with selective neuronal vulnerability. *Am. J. Pathol. 1996.* 148(1): 273-9.

Blaauwgeers, H.G.; Vianney de Jong, J.M.; Verspaget, H.W. van den Berg, F.M.; and Troost, D. Enhanced superoxide dismutase-2 immunoreactivity of astrocytes and occasional neurones in amyotrophic lateral sclerosis. *J. Neurol. Sci. 1996.* 140(1-2): 21-9.

Booth, C.M.; and Brown, M.C. Expression of GAP-43 mRNA in mouse spinal cord following unilateral peripheral nerve damage: is there a contralateral effect? *Eur. J. Neurosci. 1993.* 5: 1663-76.

Borchelt, D.r; Li, M.K.; Slunt, H.S.; Guranieri, M.; Xu, Z-S.; Wong, P.C.; Brown, R.H.; Prie, D.L.; Sisodia, S.S.; and Cleveland, D.W. Superoxide dismutase 1 with mutations linked to familial amyotrophic lateral sclerosis possesses significant activity. *PNAS USA 1994.* 91: 8292-6.

Bowling, A.C.; Schulz, J.B.; Brown, R.H.Jr; and Beal, M.F. Superoxide dismutase activity, oxidative damage, and mitochondrial energy metabolism in familial and sporadic amyotrophic lateral sclerosis. *J. Neurochem. 1993.* 61(6): 2322-5.

Bras, H., Callavari, P. and Jankowska, E. Demonstration of initial axon collaterals of cells of origin of the ventral spinocerebellar tract in the cat. *J. Comp. Neurol. 1988.* 273: 584-92.

Bredt, D.S.; Glatt, C.E.; Huang, P.M.; Fotuhi, M.; Dawson, T.M.; and Snyder, S.H. Nitric oxide synthase protein and mRNA are discretely localised in neuronal populations of the mammalian CNS together with NADPH-diaphorase. *Neuron 1991.* 7: 615-24.

Brouillet, E.; Jenkins, B.G.; Hyman, B.T.; Ferrante, R.J.; Kowall, N.W.; Srivastava, R.; Roy, D.S.; Rosen, B.R.; and Beal, M.F. Age-dependent vulnerability of the striatum to the mitochondrial toxin 3-nitropropionic acid. *J. Neurochem. 1993.* 60: 356-9.

Brujin, L. I.; Beal, M. F.; Becher, M. W.; Schulz, J. B.; Wong, P. C.; Price, D. L.; and Cleveland, D. W. Elevated free nitrotyrosine levels, but not protein-bound nitrotyrosine or hydroxyl radicals, throughout amyotrophic lateral sclerosis (ALS)-like disease implicate tyrosine nitration as an aberrant *in vivo* property of one familial ALS-linked superoxide dismutase 1 mutant. *PNAS USA 1997.* 94: 7606-11.

Brujin, L.; Houseweart, M. K.; Kato, S.; Anderson, K. L.; Anderson, S. D.; Ohama, E.; Reaume, A. G.; Scott, R. W.; and Cleveland, D. W. Aggregation and motor neuron toxicity of an ALS-linked SOD1 mutant independent from wild-type SOD1. *Science 1998.* 281: 1851- 53.

Buffo, A.; Fronte, M.; Oestreicher, A.B.; and Rossi, F. Degenerative phenomena and reactive modifications of the adult rat inferior olivary neurones following axotomy and disconnection from their targets. *Neurosci. 1998.* 85: 587-604.

Campa, J. F. and Engel, W. K. Histochemistry of motor neurones and interneurones in the cat lumbar spinal cord. *Neurology 1970*. 20: 559-68.

Casanovas, A.; Ribera, J.; Hukkanen, M.; Riveros-Moreno, V.; and Esquerda, J.E. Prevention by lamotrigine, MK801, and N omega-nitro-L-arginine methyl ester of motoneurone cell death after neonatal axotomy. *Neurosci. 1996.* 71(2): 313-25.

Celio, M. R. Calbindin D-28k and parvalbumin in the rat nervous system. *Neuroscience 1990.* 35: 375-475.

Celio, M.R. Calcium-binding proteins and neurodegeneration. *J. R. Soc. Med. 1986.* 79: 753.

Chinnery, R.M.; Shaw, P.J.; Ince, P.G.; and Johnson, M. Autoradiographic distribution of binding sites of the non-NMDA receptor antagonist [^{3}H] CNQX in human motor cortex, brainstem, and spinal cord. *Br. Res. 1993.* 630: 75-81.

Choi, D.W. Ca^{2+}: still centre-stage in hypoxic-ischaemic neuronal death. *TINS 1995.* 18(2): 58-60.

Chou, S. M.; Wang, H.S.; and Komai, K. Colocalisation of NOS and SOD1 in neurofilament accumulation within motor neurones of amyotrophic lateral sclerosis: an immunohistochemical study. *J. Chem. Neuroanat. 1996.* 10(3-4): 249-58.

Cleeter, M.W.J.; Cooper, J.M.; and Schapira, A.H.V. Irreversible inhibition of mitochondrial complex I by 1-methyl-4-phenylpyridinium: evidence for free radical involvement. *J. Neurochem. 1992.* 58: 786-9.

Clowry, G.J. and McHanwell, S. Expression of nitric oxide synthase by motoneurones in the spinal cord of the mutant mouse wobbler. *Neurosci. Letts. 1996.* 215: 177-80.

Coffey, G.L. The distribution of respiratory motoneurones in the thoracic spinal cord of the cat. PhD Thesis: University of London, *1972.*

Coggeshall, R.E. Law of separation of function of the spinal roots. *Physiol. Rev. 1980.* 60: 716-55.

Conradi, S. Ultrastructure and distribution of neuronal and glial elements on the motoneurone surface in the lumbosacral spinal cord of the adult cat. *Acta Physiol. Scand. (1969).* (Suppl.) 332: 5-48.

Cooper, S. and Sherrington, C. S. Gower's tract and spinal border cells. *Brain 1940.* 63 (2): 123 - 134.

Couratier, P.; Hugon, J.; Sindou, P.; Vallat, J.M.; and Dumas, M. Cell culture evidence for neuronal degeneration in amyotrophic lateral sclerosis being linked to glutamate AMPA/kainate receptors. *Lancet 1993.* 341: 265-8.

Croall, D. E. and Demartino, G. N. Calcium-activated neutral protease (calpain) system: structure, function, and regulation. *Physiol. Rev. 1991.* 71(3): 813-47.

Crow, J. P.; Sampson, J. B.; Zhuang, Y.; Thompson, J. A. and Beckman, J. S. Decreased zinc affinity of amyotrophic lateral sclerosis-associated superoxide dismutase mutants leads to enhanced catalysis of tyrosine nitration by peroxynitrite. *J. Neurochem. 1997a.* 69: 1936-44.

Crow, J. P.; Ye, Y. Z.; Strong, M.; Kirk, M.; Barnes, S. and Beckman, J. S. Superoxide dismutase catalyses nitration of tyrosines by peroxynitrite in the rod and head domains of neurofilament-L. *J. Neurochem. 1997b.* 69: 1945-53

Culcasi, M., Lafon-Cazal, M., Pietri, S., and Bockaert, J. Glutamate receptors induce a burst of superoxide via activation of nitric oxide synthase in arginine-depleted neurones. *J. Biol. Chem. 1994.* 269(17): 12589-93.

Dassesse, D.; Cuvelier, L.; Krebs, C.; Streppel, M.; Guntinas-Lichius, O.; Neiss, W.F.; and Pochet, R. Differential expression of calbindin and calmodulin in motoneurones after hypoglossal axotomy. *Br. Res. 1998.* 786: 181-8.

Davies,S.W. and Roberts, P.J. Models of Huntington's disease. *Science 1988.* 241: 474-5.

Dawson, T.M.; Bredt, D.S.; Fotuhi, M.; Hwang, P.M.; and Snyder, S.H. Nitric oxide synthase and neuronal NADPH diaphorase are identical in brain and peripheral tissues. *PNAS USA 1991.* 88: 7797-801.

Dawson, V.L.; Kizushi, V.M.; Huang, P.L.; Snyder, S.H.; and Dawson, T.M. Resistance to neurotoxicity in cortical cultures from neuronal nitric oxide synthaes-deficient mice. *J. Neurosci. 1996.*16(8): 2479-87.

Dawson, T.M.; Sainer, J. P.; Dawson, V.L.; Dinerman, J.L.; Uhl, G.R.; and Snyder, S.H. Immunosuppressant FK506 enhances phosphorylation of nitric oxide synthase and protects against glutamate neurotoxicity. *PNAS USA 1993.* 90: 9808-12.

Delbono, O.; Garcia, J.; Appel, S.H.; and Stefani, E. Calcium current and charge movement of mammalian muscle: action of amyotrophic lateral sclerosis immunoglobulins. *J. Physiol. (Lond). 1991.* 444: 723-44.

Dhib-Jalbut, S. and Liwnicz, B.H. Immunocytochemical binding of serum IgG from a patient with oat cell tumour and paraneoplastic motoneurone disease to normal human cerebral cortex and molecular layer of the cerebellum. *Acta Neuropathol. (Berl) 1986*: 69: 96-102

Drachman, D.B.; Chaudhry, V.; Cornblath, D. et al Trial of immunosuppression in amyotrophic lateral sclerosis using total lymphoid irradiation. *Ann. Neurol. 1994.* 35: 142-50.

Drachman, D.B.; Fishman, P.S.; Rothstein, J.D.; Motomura, M.; Lsng, B.; Vincent, A.; and Mellits, E.D. Amyotrophic lateral sclerosis - an autoimmune disease? IN: *Pathogenesis and therapy of amyotrohic lateral sclerosis.* G. Serratrice and T. Munsat, eds. *Adv. Neurol. 1995*: 68: 59-65.

Dun, N.J.; Dun, S.L.; Wu, S.Y.; Forstermann, U.; Schmidt, H.H.H.W.; and Tseng, L.F. Nitric oxide synthase immunoreactivity in the rat, mouse, cat, and squirrel monkey spinal cord. *Neurosci. 1993.* 54(4): 845-57.

Duncan, M.W. Role of the cycad neurotoxin BMAA in the amyotrophic lateral sclerosis-parkinsonism-dementia complex of the Western Pacific. IN Advances in Neurology 56: Amyotrophic Lateral Sclerosis and Other Motor Neuron Diseases. Rowland, L. P. (Ed.). Raven Press. *1991.* Chapter 25, pp301-10.

Duysens, J. and Loeb, G.E. Modulation of ipsi- and contralateral reflex responses in unrestrained walking cats. *J. Neurophysiol. 1980.* 44(5): 1024-37.

Dykens, J.A. Isolated cerebral and cerebellar mitochondria produce free radicals when exposed to elevated Ca^{2+} and Na^{+}: implications for neurodegneration. *J. Neurochem. 1994.* 63: 584-91.

Egger, M.D.; Freeman, N.C.; and Proshansky, E. Morphology of spinal motoneurones mediating a cutaneous spinal reflex in the cat. *J. Physiol. (Lond). 1980.* 306: 349-63.

Eichler, M.E.; Dubinsky, J.M.; Tong, J.; and Rich, K.M. The ability of diphenylpiperazines to prevent neuronal death in dorsal root ganglion neurones *in vitro* after nerve growth factor deprivation and *in vivo* after axotomy. *J. Neurochem. 1994.* 62(6): 2148-57.

Engelhardt, J.I. and Appel, S.H. IgG reactivity in the spinal cord and motor cortex in amyotrophic lateral sclerosis *Arch. Neurol. 1974.* 30: 332-3.

Engelhardt, J.I.; Appel, S.H.; Killian, J.M. Experimental autoimmune motoneurone disease *Ann. Neurol. 1989.* 26: 368-76.

Engelhardt, J.I.; Siklos, L.; Komuves, L.; Glenn Smith, R.; and Appel, S.H. Antibodies to calcium channels from ALS patients passively transferred to mice selectively increase intracelluolar calcium and induce ultrastructural changes in motoneurones. *Synapse 1995*: 20: 185-99.

Fallah, Z. and Clowry, G.J. The effect of a peripheral nerve lesion on calbindin-D-28k immunoreactivity in the cervical ventral horn of developing and adult rats. *Exp. Neurol. 1999.* 156(1): 111-20.

Farinelli, S. E., Park, D. S. & Greene, L. A. Nitric oxide delays the death of trophic factor-deprived PC12 cells and sympathetic neurons by a cGMP-mediated mechanism. *J. Neurosci. 1996.* 16(7): 2325-2334.

Ferrante, R. J.; Browne, S. E.; Shinobu, L. A.; Bowling, A. C.; Baik, M. J.; MacGarvey, U.; Kowall, N. W.; Brown, R. H. Jr; and Beal, M. F. Evidence of increased oxidative damage in both sporadic and familial amyotrophic lateral sclerosis. *J. Neurochem. 1997a.* 69: 2064-74.

Ferrante, R.J.; Kowall, N.W.; Cipolloni, P.B.; Storey, E. and Beal, M.F. Excitotoxin lesions in primates as a model for Huntington's disease: histopathologic and neurochemical characterisation. *Exp. Neurol. 1993.* 119: 46-71.

Ferrante, R. J.; Shinobu, L. A.; Schulz, J. B.; Matthews, R. T.; Thomas, C. E.; Kowall, N. W.; Gurney, M. E. and Beal, M. F. Increased 3-nitrotyrosine and oxidative damage in mice with a human copper/zinc superoxide dismutase mutation. *Ann. Neurol. 1997b.* 42: 326-34.

Figueredo-Cardenas, G.; Harris, C.L; Anderson, K.D.; and Reiner, A. Relative resistance of striatal neurones containing calbindin or parvalbumin to quinolinic acid-mediated excitotoxicity compared to other striatal neurones types *Exp. Neurol. 1998.* 149: 356-72.

Fitzmaurice, P. S.; Shaw, I. C.; and Mitchell, J.D. Alteration of superoxide dismutase activity in the anterior horn in motoneurone disease patients. *J. Neurol. Sci.1995.* 129 (Suppl): 96-98.

Forloni, G.L.; Angeretti, N.; Rizzi, M.; and Vezzani, A. Chronic infusion of quinolinic acid in rat striatum: effects on discrete neuronal populations. *J. Neurol. Sci. 1992.* 108: 129-36.

Fyffe, R.E.W. Evidence for separate morphological classes of Renshaw cells in the cat's spinal cord. *Br. Res. 1990.* 536: 301-4.

Fyffe, R.E.W. Spatial distributiopn of recurrent inhibitory synapses on spinal motoneurones in the cat. *J. Neurophysiol. 1991.* 65 (5): 1134-1149.

Garruto, R.M.; Yanagihara, R.; and Gajdusek, D.C. Disappearance of high incidence amyotrophic lateral sclerosis and parkinsonism-dementia on Guam. *Neurol. 1985.* 35: 193-8.

Garthwaite, J. Glutamate, nitric oxide, and cell-cell signalling in the nervous system. *TINS 1991.* 14(2): 60-7.

Geiger, J. R. P.; Meicher, T.; Koh, D-S.; Sakmann, B.; Seeburg, P. H. and Jonas, P. Relative abundance of subunit mRNAs determines gating and Ca^{2+} permeability of AMPA receptors in principle neurones and interneurones in rat CNS. *Neuron 1995.* 15: 193-204

George, E.B.; Glass, J. D.; and Griffin, J.W. Axotomy-induced axonal degeneration is mediated by calcium influx through ion-specific channels. *J. Neurosci. 1995.* 5(10): 6445-52.

Gibson, S.J.; Polak, J.M.; Katagiri, T.; Su, H.; Weller, R.O.; Brownell, D.B.; Holland, S.; Hughes, J.T.; Kikuyama, S.; Ball, J.; Bloom, S.R.; Steiner, T.J.; de Bellereoche, J.; and Rose, F.C. A comparison of the distributions of 8 peptides in spinal cord from normal controls and cases of motor neurone disease with special reference to Onuf's nucleus. *Br. Res. 1988.* 474: 255-78.

Gitler, D. and Spira, M.E. Real time imaging of calcium-induced localised proteolytic activity after axotomy and its relation to growth cone formation. *Neuron 1998.* 20(6): 1123-35.

Gordon, D. C.; Loeb, G. E., and Richmond, F. J. R. Distribution of motoneurones supplying cat sartorius and tensor fasciae latae, demonstrated by retrograde multi-labelling methods. J. Comp. Neurol. 1991. 304: 357-72.

Gordon, D.C.; Loeb, G.E.; and Richmond, F.J. Distribution of motoneurones supplying cat sartorius and tensor fasciae latae, demonstrated by retrograde multiple-labelling methods. *J. Comp. Neurol. 1991.* 304(3): 357-72.

Goto, S., Hirano,A. & Pearson, J. Calcineurin and synaptophysin in the human spinal cord of normal individuals and patients with familial dysautonomia. *Acta Neuropathol. (Berl) 1990.* 79(6): 647-52.

Goto, S.; Matsukado, Y.; Mihara, Y.; Inoue, N.; and Miyamoto, E. The distribution of calcineurin in rat brain by light and electron microscopic immunohistochemistry and enzyme-immunoassay. *Br. Res. 1986.* 397: 161-72.

Granit, R. The Basis of Motor Control. Academic Press *1970.*

Grant, G.; Wiksten, B.; Berkley, K. J. and Aldskogus, H. The location of cerebellar-projecting neurones within the lumbosacral spinal cord in the cat. An anatomical study with HRP and retrograde chromatolysis. *J. Comp. Neurol. 1982.* 204: 336-48.

Gu, Y.; Spasic, Z.; and Wu, W. The effects of remaining axons on motoneurone survival and NOS expression following axotomy in the adult rat. *Dev. Neurosci. 1997.* 19: 255-259.

Guentchev, M.; Hainfellner, J-A.; Trabattoni, G.R.; and Budka, H. Distribution of parvalbumin immunoreactive neurones in brain correlates with hippocampal and temporal cortical pathology in Creutzfeld-Jakob disease. *J. Neuropathol. Exp. Neurol. 1997.* 50(10): 1119-24.

Gurney, M. E.; Cutting, F. B.; Zhai, P.; Doble, A.; Taylor, C. P.; Andrus, P. K.; & Hall, E. D. Benefit of Vitamin E, riluzole, and gabapentin in a transgenic model of familial amyotrophic lateral sclerosis. *Ann. Neurol. 1996.* 39: 147-57

Gurney, M.E.; Pe, H.; Chiu, A.Y.; Dal Canto, M.C.; Polchow, C.Y.; Alexander, D.D. et al. Motor neurone degeneration in mice that express a human Cu/Zn superoxide dismutase mutation. *Science 1994.* .264: 1772-5.

Harrison, P.J.; and Zytnicki, D. Crossed actions of group I muscle afferents in the cat. *J. Physiol.1984.* 356: 263-73.

Heizmann, C.W. and Braun, K. Changes in Ca^{2+}-binding proteins in human neurodegenerative disorders. *TINS 1992.* 15(7): 259-64.

Hirano, A. Cytopathology of amyotrophic lateral sclerosis. IN Advances in Neurology 56: Amyotrophic Lateral Sclerosis and Other Motor Neurone Diseases. Rowland, L. P. (Ed.). Raven Press. 1991 Chapter 23 pp271-86

Ho, B.K.; Alexianu, M.E.; Colom, L.V.; Mohamed, A.H.; Serrano, F.; and Appel, S.H. Expression of calbindin-D28k in motoneurone hybrid cells after retroviral infection with calbindin-D28k cDNA prevents amyotrophic lateral sclerosis IgG-mediated cytotoxicity. *PNAS USA. 1996.* 93(13): 6796-801.

Hoover, J. E. and Durkovicz, R. G. Morphological relationships among extensor digitorum longus, tibialis anterior, and semitendinosus motor nuclei of the cat: an investigation employing the retrograde transport of multiple fluorescent tracers. *J. Comp. Neurol. 1991.* 303: 255-66.

Horwich, M.S.; ENgel, W.K.; and Chauvin, P.B. Amyotrophic lateral sclerosis sera applied to cultured motor neurones. *Arch. Neurol. 1974*: 30: 332-4

Hu, W.H., Le e, F.C., Wan, X.S., Chen, Y.T., & Jen, M.F. Dynorphin neurotoxicity induced nitric oxide synthase expression in ventral horn cells of rat spinal cord. *Neurosci. Lett. 1996.* 203 (1): 13-6.

Huang,Q.;Zhou,D.;Sapp, E.; Aizawa, H.; Ge, P.; Bird, E.D.; Vonsattel, J-P.; and DiFiglia,M. Quinolinic acid-induced increases in calbindin D28k immunoreactivity in rat striatal neurones *in vivo* and *in vitro* mimic the pattern seen in Huntington's disease. *Neuroscience, 1995.* 65: 397-407.

Hugon, J.; Vallat, J. M.; Spencer, P. S.; Leboutet, M. J. and Barthe, D. Kainic acid induced early and delayed degenerative neuronal changes in rat spinal cord. *Neurosci. Letts. 1989.* 104: 258-62.

Hyrc, K.; Handran, S. D.; Rothman, S. M. and Goldberg, M. P. Ionised intracellular calcium concentration predicts excitotoxic neuronal death: observations with low-affinity fluorescent calcium indicators. *J. Neurosci. 1997.* 17 (17): 6669-77.

Iacopino, A. M. and Cristakos, S. Specific reduction of calcium-binding protein (28-kilodalton calbindin-D) gene expression in aging and neurodegenerative diseases. *PNAS USA 1990.* 87: 4078-82.

Illert, M., Lundberg, A. and Tanaka, R. Integration in descending motor pathways controlling the forelimb in the cat. 1. Pyramidal effects on motoneurones. *Exp. Br. Res. 1976.* 26: 509-19.

Illert, M., Lundberg, A. and Tanaka, R. Integration in descending motor pathways controlling the forelimb in the cat. 2. Convergence on neurones mediating disynaptic cortico-motoneuronal excitation. *Exp. Br. Res. 1976.* 26: 521-40.

Ince, P.; Stout, N.; Shaw, P.; Slade, J.; Hunziker, W.; Heizmann, C. W.; And Baimbridge, K. G. Parvalbumin and calbindin D-28k in the human motor system and in motor neuron disease. *Neuropathol. Appl. Neurobiol. 1993.* 19: 291-9.

Ince, P.G.; Shaw, P.J.; Candy, J.M.; Mantle, D.; Tandon, L.; Ehmann, W.D.; and Markesbery, W.R. Iron, selenium, and glutathione peroxidase activity are elevated in sporadic motor neurone disease. *Neurosci. Lett. 1994.* 182(1): 87-90.

Iscoe, S. Control of abdominal muscles. *Prog. Neurobiol. 1998.* 56(4): 433-506

Jankowska, E. Identification of interneurones interposed in different spinal reflex pathways. Golgi Centennial Symposium Proc. *1975.* Santini, M. (Ed.). Raven Press. New York.

Jankowska, E. and Lindstrom, S. Morphological identification of Renshaw cells. *Acta Physiol. Scand. 1971.* 81(3): 428-30.

Jankowska, E. and Lindstrom, S. Morphology of interneurones mediating Ia reciprocal inhibition of motoneurones in the spinal cord of the cat. *J. Physiol. 1972.* 226: 805—23.

Jankowska, E.; Padel, Y.; and Zarzecki, P. Crossed disynaptic inhibition of sacral motoneurones. J. Physiol. 1978. 285: 425-44.

Jassar, B.S.; Pennefather, P.S.; and Smith, P.A. Changes in sodium and calcium channel activity following axotomy of B-cells in bullfrog sympathetic ganglion. *J. Physiol. (Lond) 1993.* 472: 203-31.

Johansen, F.F.; Tonder, N.; Zimmer, J.; Baimbridge, K.G.; and Diemer, N.H. Short-term changes of parvalbumin and calbindin immunoreactivity in the rat hippocampus following cerebral ischaemia. *Neurosci. Letts. 1990.* 210: 171-4.

Johnson, I. P. A quantitative ultrastructural comparison of alpha and gamma motoneurones in the thoracic region of the spinal cord of the adult cat. *J. Anat. 1986.* 147: 55-72.

Jung, H.H.; Lauterburg, Th.; and Burgunder, J.-M. Expression of neurotransmitter genes in rat spinal motoneurones after chemodenervation with botulinum toxin. *Neurosci. 1997.* 78(2): 469-79.

Junttila, T.; Kostinaho, H.; Rechardt, L.; Hidaka, H.; Okazaki, K.; Pelto-Huikko, M. Localisation of neurocalcin-like immunoreactivity in rat cranial motoneurones and spinal cord interneruones. *Neurosci. Letts. 1995.* 183(1-2): 100-3.

Kanda, K. Expression of neuronal nitric oxide synthase in spinal motoneurones in aged rats. *Neurosci. Letts. 1996.* 219: 41-44.

Katagiri, T.; Gibson, S.J.; Su, H.C.; and Polak, J.M. Composition and central projections of the pudendal nerve in the rat investigated by combined peptide

immunocytochemistry and retrograde fluorescent labelling. *Br. Res. 1986.* 372(2): 313-22.

Kennis, J. H. H. and Holstege, J. C. A differential and time-dependent decrease in AMPA-type glutamate receptor subunits in spinal motoneurones after sciatic nerve injury. *Exp. Neurol. 1997.* 147 (1): 18-27.

Kishimoto, J.; Tsuchiya, T.; Cox, H.; Emson, P.C.; and Nakayama, Y. Age-related changes of calbindin-D28k, calretinin, and parvalbumin mRNAs in the hamster brain. *Neurobiol. Aging 1998.* 19(1): 77-82.

Kohr, G.; Lambert, C.E.; and Mody, I. Calbindin-D28k (CaBP) levels and calcium currents in acutely dissociated epileptic neurones. *Exp. Br. Res. 1991.* 85(3): 543-51.

Kowall, N.W.; Ferrante, R.J.; and Martin, J.B. Patterns of cell loss in Huntington's disease. *TINS 1987.* 10: 24-9.

Kristensson, K. Retrograde axonal transport of horseradish peroxidase. Uptake at mouse neuromuscular junctions following systemic injection. *Acta Neuropathol. (Berl). 1977.* 38(2): 143-7.

Kristensson, K. and Olsson, Y. Uptake and retrograde axonal transport of peroxidase in hypoglossal neurones. *Acta Neuropath. (Berl). 1971.* 19: 1-9.

Kristensson, K., Aldskogius, M. Peng, Z-C, Olsson, T., Aldskogius, H, & Bentivoglio, M. Co-induction of neuronal interferon gamma and nitric oxide synthase in rat motor neurons after axotomy: a role in nerve repair or death? *J. Neurocytol. 1994.* 23: 453-9.

Kruman, I.I.; Pederson, W.A.; Springer, J.E.; and Mattson, M.P. ALS-linked Cu/Zn-SOD mutation increases vulnerability of motoneurones to excitotoxicity by a mechanism involving increased oxidative stress and perturbed calcium homeostasis. *Exp. Neurol. 1999.* 160: 28-39.

Kruman, I.I. and Mattson, M.P. Pivotal role of mitochondrial calcium uptake in neural cell apoptosis and necrosis. *J. Neurochem. 1999.* 72(2): 529-40.

Kupfermann, I. Functional studies of cotransmission. *Physiol. Rev. 1991.* 71(3): 683-732.

Lagerback, P-A. and Kellerth, J-O. Light microscopic observations on cat Renshaw cells after intracellular staining with horseradish peroxidase. II. The cell bodies and dendrites. *J. Comp. Neurol. 1985.* 240: 368-376.

Lagerback, P-A. and Ronnevi, L-O. An ultrastructural study of serially sectioned Renshaw cells I. Architecture of the cell body, axon hillock, initial axon segment and proximal dendrites. *Br. Res. 1982.* 235: 1-15.

Laiwand, R.; Werman, R.; and Yarom, Y. Electrophysiology of degenerating neurones in the vagal motor nucleus of the guinea pig following axotomy. *J. Physiol. (Lond) 1988.* 404: 749-66.

Lavine, L.; Steele, J. C.; Wolfe, N.; Calne, D. B.; O'Brien, P. C.; Williams, D. B.; Kurland, L. T. and Schoenberg, B. S. Amyotrophic lateral sclerosis/parkinsonism dementia complex in southern Guam: is it disappearing? IN Advances in Neurology 56: Amyotrophic Lateral Sclerosis and Other Motor Neuron Diseases. Rowland, L. P. (Ed.). Raven Press. *1991.* Chapter 23 pp271-86.

Lawson, S.J. and Lowrie, M.B. The role of apoptosis and excitotoxicity in the death of spinal motoneurones and interneurones after neonatal nerve injury. *Neurosci. 1998.* 87: 337-48.

Leist, M; Volbracht, C; Fava, E; & Nicotera, P. 1-methyl-4-phenylpyridinium induces autocrine excitotoxicity, protease activation, and neuronal apoptosis. *Mol. Pharm. 1998.* 54(5): 789-801.

Li, M.; Sczcepanik, A. M.; Brooks, K.M. and Wilmot, C. A. Nitric oxide and free radicals mediate NMDA-induced neurodegeneration. *Soc. Neurosci. Abtrs. 1992.*18: 645 (276.8).

Lipski, J. and Martin-Body, R. L. Morphological properties of respiratory intercostal motoneurones in cats as revealed by intracellular injection of horseradish peroxidase. *J. Comp. Neurol. 1987.* 260: 423-434.

Lipton, S. A. and Rosenberg, P.A. Excitatory amino acids as a final common pathway for neurologic disorders. N.E.J.M. 1994. 330(9): 613-22.

Lledo, PM.; Somasundaram, B.; Morton, A.J.; Emson, P.C.; and Mason, W.T. Stable transfection of calbindin-D28k into the GH3 cell line alters calcium currents and intracellular calcium homeostasis. *Neuron 1992.* 9: 943-54.

Llinas, R.; Sugimori, M.; Cherskey, B.D.; Glenn Smith, R.; Delbono, O.; Stefani, E.; and Appel, S.H. IgG from amyotrophic lateral sclerosis patients increases current through P-type Ca^{2+} channels in mammalian cerebellar Purkinje cells and in isolated channel protein in lipid bilayer. *PNAS USA 1993:* 90: 11743-7.

LoPachin, R.M. and Lehning, E.J. Mechanism of calcium entry during axon injury and degeneration. *Toxicol. Appl. Pharmacol. 1997.* 143(2): 233-44.

Lowrie, M. B.; Krishnan, S.; and Vrbova, G. Recovery of slow and fast muscles following nerve injury during early post-natal development in the rat. *J. Physiol. 1982.* 331: 51-66.

Lowrie, M.B.; Krishnan, S.; and Vrbova, G. Permanent changes in muscle and motoneurones induced by nerve injury during a criticlal period of development of the rat. *Dev. Br. Res. 1987.* 31: 91-101.

Lund, L.M. and McQuarrie, I.G. Calcium/calmodulin-dependent protein kinase II expression in motoneurones: effect of axotomy. *J. Neurobiol. 1997.* 33(6): 796-810.

Matthews, P.B.C. Muscle spindles and their motor control. *Physiol. Rev. 1964.* 44: 219-88.

McLaughlin, B.J. The fine structure of neurons and synapses in the motor nuclei of the cat spinal cord. *J. Comp. Neurol.1972a.* 144: 429-460.

McLaughlin, B.J. Dorsal root projections to the motor nuclei in the cat spinal cord. *J. Comp. Neurol. (1972)b.* 144: 461-474.

McLaughlin, B.J. Propriospinal and supraspinal projections to the motor nuclei in the cat spinal cord. *J. Comp. Neurol.(1972)c.* 144: 474-500.

McNamara, J.O. and Friedovich, I. Did radicals strike Lou Gehrig? *Nature 1993.* 362: 20-1.

Meldrum, B. S. Neuroprotection by NMDA and non-NMDA glutamate antagonists. In Direct and allosteric control of glutamate receptors. CRC Press. (Eds. I. J. Reynolds and P. Skolnick). *1994.*

Miller, J.J. and Baimbridge, K.G. Biochemical and immunohistochemical correlates of kindling-induced epilepsy: role of calcium binding protein. *Br. Res. 1983.* 278(1-2): 322-6.

Molinari, S.; Battini, R.; Ferrari, S.; Pozi, L.; Killcross, A.S.; Robbins, T.W.; Jouvenceau, A.; Billard, J.M.; Dutar, P.; Lamour, Y.; Baker, W.A.; Con, H.; and Emson, P.C. Deficits in memory and hippocampal long term potentiation in mice with reduced calbindin D28k expression. *PNAS USA, 1996.* 93: 8028-33.

Moreno, S.; Nardacci, R.; and Ceru, M.P. Regional and ultrastructural immunolocalisation of copper-zinc superoxide dismutase in rat central nervous system. *J. Histochem. Cytochem. 1997.* 45: 1611-22.

Morioka, M.; Hamada, J.-I.; Ushio, Y.; and Miyamoto, E. Potential role of calcineurin for brain ischaemia and traumatic injury. *Prog. Neurobiol. 1999.* 58: 1-30.

Morris, B.J.; Simpson, C.S.; Mudell, S.; Maceachern, K.; Johnston, H.M.; and Nolan, A.M. Dynamic changes in NADPH-diaphorase staining reflects activity of nitric oxide synthase: evidence for a dopaminergic regulation of striatal nitric oxide release. *Neuropharm. 1997.* 36(11-12): 1589-99.

Morrison, B. M.; Gordon, J. W.; Ripps, M.E. and Morrison, J.H. Quantitative immunocytochemical analysis of the spinal cord in G86R superoxide dismutase transgenic mice: neurochemical correlates of selective vulnerability. *J. Comp. Neurol. 1996.* 373: 619-31.

Ng, M.C.; Iacopino, A.M.; Quintero, E.M.; Marches, F.; Sonsalla, P.K.; Liang, C.L.; Speciale, S.G.; and German, D.C. The neurotoxin MPTP increases calbindin-D28k levels in mouse midbrain dopaminergic neurones. *Br. Res. Mol. Br. Res. 1996.* 36: 329-36

Novikov, L.; Novikova, L.; and Kellerth, J.-O. Brain-derived neurotrophic factor promotes survival and blocks nitric oxide synthase expression in adult rat spinal motoneurones after ventral root avulsion. *Neurosci. Letts. 1995.* 200: 45-8.

Nyberg-Hansen, R. and Brodal, A. Sites of termination of corticospinal fibres in the cat. An experimental study with silver impregnation methods. *J. Comp. Neurol. 1963.* 120: 369 -91.

Olsson, Y. Vascular permeability in the peripheral nervous system. *IN Peripheral Neuropathy.* P.J. Dyck., P.K. Thomas, and H. Lambert (Eds.). Philadelphia: W.B. Saunders and Co. *1975.* pp190-200.

Oscarsson, O. Functional organisation of the spino- and cuneocerebellar tracts. *Physiol. Rev. 1965.* 45: 495-522.

Pardo, C. A., Xu, Z., Borchelt, D. R., Price, D. L., Sisodia, S. S., And Cleveland, D. W. Superoxide dismutase is an abundant component in cell bodies, dendrites, and axons of motor neurons and in a subset of other neurones. *PNAS USA 1995.* 92: 954-58.

Parlani, M.; Conte, B.; and Manzini, S. Nonadrenergic, noncholinergic inhibitory control of the rat external urethral sphincter: involvement of nitric oxide. *J. Pharmacol. Exp. Ther. 1993.* 265(2): 713-9.

Peng, T-I.; Jou, M-J.; Sheu, S-S. and Greenamyre, T. J. Visualisation of NMDA receptor-induced mitochondrial calcium accumulation in striatal neurones. *Exp. Neurol. 1998.* 149 (1): 1-12.

Perez, J. and Kelley, D.B. Androgen mitigates axotomy-induced decreases in calbindin expression in motor neurones. *J. Neurosci. 1997.* 17: 7396-403.

Perry, T.L.; Krieger, C.; Hansen, S.; and Eisen, A. Amyotrophic lateral sclerosis: amino acid levels in plasma and cerebrospinal fluid. *Ann. Neurol. 1990.* 28: 12-17.

Peterson, D. A.; Lucidi-Phillipi, C.A.; Murphy, D.P.; Ray, J.; and Gage, F.H. Fibroblaast Growth Factor-2 protects entorhinal layer II glutamatergic neurones from axotomy-induced death *J. Neurosci, 1996.* 16(3): 886-898.

Piehl, F.; Arvidsson, U.; Johnson, H.; Cullheim, S.; Dagerlind, A.; Ulfhake, B.; Cao, Y.; Elde, R.; Pettersson, R.F.; Terenius, L.; and Hokfelt, T. GAP-43, aFGF, CCK and α- and β-CGRP in rat spinal motoneurones subjected to axotomy and/or dorsal root severance. *Eur. J. Neurosci. 1993.* 5: 1321-33.

Plaitakis, A. Glutamate disfunction and selective motoneurone degeneration in amyotrophic lateral sclerosis: a hypothesis. *Ann. Neurol. 1990.* 28: 3-8.

Plaitakis, A. Altered glutamatergic mechanisms and selective motoneurone degeneration in amyotrophic lateral sclerosis: possible role of glycine. In *Advances in Neurology 56*; Amyotrophic lateral sclerosis and other motoneurone diseases. (Ed. L.P. Rowland) *1991.* Pp. 319-26

Plant,. T.D.; Standen, N.B.; and Ward, T.A. The effects of injection of calcium ions and calcium chelators on calcium channel inactivation in Helix neurones. *J. Physiol. (Lond). 1983.* 334: 189-212.

Polak, J.M. and Van Noorden, S. Introduction to immunocytochemistry. BIOS Scientific Publishers. Springer-Verlag Inc. NY. *2nd Edition. 1997.*

Przedborski, S.; Donaldson, D.; Jakowec, M.; Kish, S. J.; Guttman, M.; Rosoklija, G. & Hays, A. P. Brain superoxide dismutase, catalase, and glutathione peroxidase activities in amyotrophic lateral sclerosis. *Ann Neurol. 1996.* 39: 158-65.

Pullen, A.H. Quantitative synaptology of feline motoneurones to external anal sphincter muscle. *J. Comp. Neurol. 1988.* 269: 414-24.

Pullen, A.H. and Humphreys, P. Diversity in localisation of nitric oxide synthase antigen and NADPH-diaphorase histochemical staining in sacral somatic motoneurones of the cat. *Neurosci. Letts. 1995.* 196: 33-6.

Pullen, A.H. and Martin, J.E. Ultrastructural abnormalities with inclusions in Onuf's nucleus in motoneurone disease (amyotrophic lateral sclerosis). *Neuropathol. Appl. Neurobiol. 1995.* 21(4): 327-40.

Pullen, A.H., Humphreys, P.; and Baxter, R.G. Comparative analysis of nitric oxide synthase immunoreactivity in the sacral spinal cord of the cat, macaque and human. *J. Anat. 1997.* 191: 161-75.

Puttfarcken, P.S.; Getz, R.L.; and Coyle, J.T. Kainic acid induced lipid peroxidation: protection with lipophilic antioxidants in cerebellar granule cell cultures. Soc. Neurosci. Abstr. 1992. 18: 645 (276.3).

Radziszewski, P.; Ekblad, E.; Sundler, F.; and Mattiasson, A. Distribution of neuropeptide-, tyrosine hydroxylase-, and nitric oxide sythase containing nerve fibres in the external urethral sphincter of the rat. *Scand. J. Urol. Nephrol. Suppl. 1996.* 179: 81-5.

Rami, A.; Rabie, A., and Winckler, J. Synergy between chromic corticosterone treatment and cerebral ischaemia in producing damage in noncalbindinergic neurones. *Exp. Neurol. 1998.* 149: 439-46.

Ramirez-Leon, V. and Ulfhake, B. GABA-like immunoreactive innervation and dendro-dendritic contacts in the ventrolateral dendritic bundle in the cat S1 spinal cord segment: an electron microscopic study. *Exp. Br. Res. 1993.* 97(1): 1-12.

Regan, R.F. The vulnerability of spinal cord neurones to excitotoxic injury: comparison with cortical neurones. *Neurosci. Letts. 1996.* 213: 9-12.

Reiner, A., Medina, L., Figueredo-Cardenas, G., and Anfinson, S. Brainstem motoneuron pools that are selectively resistant in amyotrophic lateral sclerosis are preferentially enriched in parvalbumin: evidence from monkey brainstem for a calcium-mediated mechanism in sporadic ALS. *Exp. Neurol. 1995.* 239-50.

Ren, K. and Ruda, M.A. A comparative study of the calcium-binding proteins calbindin-D28K, calretinin, calmodulin, and parvalbumin in the rat spinal cord. *Br. Res. Rev. 1994.* 19: 163-79.

Renshaw, B. Influence of discharge of motoneurones upon excitation of neighbouring motoneurones. *J Neurophysiol. 1941.* 4: 167-183.

Renshaw, B. Central effects of centripetal impulses in axons of spinal ventral roots. *J. Neurophysiol. 1946.* 9: 191-204.

Rexed, B. The cytoarchitectonic organisation of the spinal cord in the cat. *J. Comp. Neurol. 1952.* 96: 415-95.

Ritz, L. A., Bailey, M., Murray, C. R. and Sparkes, M. L. Organisational and morphological features of cat sacrocaudal motoneurones. *J. Comp. Neurol. 1992.* 318: 209-221.

Romanes, G.J. The motor cell columns of the lumbosacral spinal cord of the cat. *J. Comp. Neurol. 1951.* 94: 313-63.

Rosen, D.R.; Siddique, T.; Patterson, D.; Figlowicz, D.A.; Sapp, P.; Hentati, A. et al. Mutations in Cu/Zn superoxide dismutase gene are associated with familial amyotrophic lateral sclerosis. *Nature 1993.* 362: 59-62.

Ross, S.M.; Seelig, M.; and Spencer, P.S. Specific antagonism of "uncommon" amino acids assayed in organotypic mouse cortical cultures. *Br. Res. 1987.* 425: 120-7.

Rossi, F.; Borsello, T.; and Strata, P. Exposure to kainic acid mimics the effects of axotomy in cerebellar Purkinje cells of the adult rat. *Eur. J. Neurosci. 1994.* 6(3): 292-402.

Rothman, S.M. and Olney, J.W. Excitotoxicity and the NMDA receptor - still lethal after 8 years. *TINS 1995.*18(2): 57-8.

Rothstein, J. D.; Dykes-Hoberg, M.; Corson, L.B.; Becker, M.; Cleveland, D.W.; Price, D.L.; Culotta, V.C.; and Wong, P.C. The copper chaperone CCS is abundant in neurones and astrocytes in human and rodent brain. *J. Neurochem. 1999.* 72(1) 422-9.

Rothstein, J.D.; Jin, L.; Dykes-Hoberg, M.; and Kuncl, R.W. Chronic inhibition of glutamate uptake produces a model of slow neurotoxicity. *PNAS USA 1993.* 90: 6591-5.

Rothstein, J. D.; Martin, L.J.; and Kuncl, R.W. Decreased glutamate transport by the brain and spinal cord in amyotrophic lateral sclerosis. *NEJM 1992.* 326 (22): 1464-8.

Rothstein, J. D.; Tsai, G.; Kuncl, R.W.; Clawson, L.; Cornblath, D.R.; Drachman, D.B.; Pestronk, A.; Stauch, B.L. and Coyle, J.T. Abnormal excitatory amino acid metabolism in amyotrophic lateral sclerosis. *Ann. Neurol. 1990.* 28: 18-25.

Rotto-Percelay, D.M.; Wheeler, J.G.; Osorio, F.A.; Platt, K.B.; and Loewy, A.D. Transneuronal labelling of spinal interneurones and sympathetic preganglionic neurons after pseudorabies virus injections in the rat gastrocnemius muscle. *Br. Res. 1992.* 574: 291-306.

Rowland, L.P. Amyotrophic lateral sclerosis with paraproteins and autoantibodies. IN Advances in Neurology 68: Pathogenesis and therapy of amyotrophic lateral sclerosis. G.T. Serratrice, and T. L. Munsat (Eds.). Lippincott-Raven Press. *1995.* Chapter 11, pp93-106.

Roy, J.; Minotti, S.; Dong, L.; Figlewicz, D. A.; and Durham, HD. Glutamate potentiates the toxicity of mutant Cu/Zn-Superoxide Dismutase in motoneurones by postsynaptic calcium-dependent mechanisms *J. Neurosci. 1998.* 18(23): 9673-84.

Russell-Mergenthal, H., McClung, R., and Goldberg, S. J. The determination of dendrite morphology on lateral rectus motoneurones in cat. *J. Comp. Neurol. 1986.* 245: 116-122.

Rydh-Rinder, M; Holmberg, K.; Elfvin, L.-G.; Wiesenfeld-Hallin, Z.; and Hokfelt, T. Effects of peripheral axotomy on neuropeptides and nitric oxide synthase in dorsasl root ganglia and spinal cord of the guinea pig: an immunohistochemical study. *Br. Res. 1996.* 707: 180-88.

Saito, S.; Kidd, G.J.; Trapp, B.D.; Dawson, T.M.; Bredt, D.S.; Wilson, D.A.; Traystman, R.J.; Snyder, S.H.; and Hanley, D.F. Rat spinal cord neurones contain nitric oxide synthase. *Neurosci. 1994.* 49(2): 447-56.

Sanchez-Vives, M.V.; Valdeolmillos, M.; Martinez, S.; and Gallego, R. Axotomy-induced changes in Ca^{2+} homeostasis in rat sympathetic ganglion cells. *Eur. J. Neuosci. 1994.* 6: 9-17.

Sato, M. Mizuno, N. and Konishi, A. Localisation of motoneurones innervating peroneal muscles: A HRP study in cat. *Br. Res.1978.* 140: 149-154.

Satoh, J.; Tabira, T.; Sano, M.; Nakayama, H.; and Tateishi, J. Parvalbumin-immunoreactive neurones in the human central nervous system are decreased in Alzheimer" disease. *Acta Neuropathol. 1991.* 81: 388-95.

Schlaepfer, W.W. Calcium-induced degeneration of axoplasm in isolated segments of rat peripheral nerve. *Br. Res. 1974.* 69(2): 203-15.

Schlaepfer, W.W. and Bunge, R.P. Effects of calcium ion concentration on the degeneration of amputated axons in tissue culture. *J. Cell. Biol. 1973.* 59(2): 456-70.

Schmidt, W.; Wolf, G.; Calka, J.; and Schmidt, H.H.H.W. Evidence for bidirectional changes in nitric oxide synthase activity in the rat striatum after excitotoxically (quinolinic acid) induced degeneration. *Neurosci. 1995.* 67 (2): 345-56.

Seagar, M.J.; Martin-Moutot, N.; Leveque, C.; Marqueze, B.; and Pouget, J. Anti-calcium channel antibodies in amyotrphic lateral sclerosis - a review of the evidence. In: *Pathogenesis and therapy of amyotrohic lateral sclerosis.* G. Serratrice and T. Munsat, eds. *Advances in Neurology, 1995*: 68: 67-72.

Sharkey, J. and Butcher, S.P. Immunophilins mediate the neuroprotective effects of FK506 in focal cerebral ischaemia. *Nature 1994.* 371(6495): 336-9.

Shaw, P.J.; Chinnery, R.M.; and Ince, P.G Non-NMDA receptors in motoneurone disease (MND): a quantitative autoradiographic study in spinal cord and motor cortex using [^{3}H]CNQX and [^{3}H] kainate. *Br. Res. 1994b.* 655: 186-94.

Shaw, P.J.; Chinnery, R.M.; Thagesen, H.; Borthwick, G.M.; and Ince, P.J. Immunocytochemical study of the distribution of the free radical scavenging enzymes Cu/Zn superoxide dismutase (SOD-1); MN superoxide dismutase (MN SOD) and catalase in the normal human spinal cord. *J. Neurol. Sci. 1997.* 147(2): 115-25.

Shaw, P.J. and Ince, P.G. A quantitative autoradiographic study of [^{3}H] kainate binding sites in the normal human spinal cord, brainstem, and motor cortex. *Br. Res. 1994.* 641: 39-45.

Shaw, P.J.; Ince, P.G.; Falkous, G. and Mantle, D. Oxidative damage to protein in sporadic motor neurone disease spinal cord. *Ann. Neurol. 1995.* 38(4): 691-5.

Shaw, P. J.; Ince, .G.; Johnson, M.; Perry, E.K.; and Candy, J.M. The quantitative autoradiographic distribution of [^{3}H] MK801 binding sites in the normal human spinal cord. *Br. Res. 1991.* 539: 164-8.

Shaw, P. J.; Ince, P.G.; Matthews, J.N.S.; Johnson, M.; and Candy, J.M. N-methyl-D-aspartate (NMDA) receptors in the spinal cord and motor cortex in motoneurone disease: a quantitative autoradiographic study using [^{3}H] MK801. *Br. Res. 1994a.* 637: 297-302.

Sherrington, C. Integrative Action of the Nervous System. Constable, London. 1906

Shibata, N.; Hirano, A.; Kobayashi, M.; Siddique, T.; Deng, H.X.; Hung, W.Y.; Kato, T. and Asayama, K. Intense superoxide dismutase-1 immunoreactivity in intracytoplasmic hylaine inclusions of familial amyotrophic lateral sclerosis with posterior column involvement. *J. Neuropath. Exp. Neurol. 1996.* 55: 481-90.

Silva, A.J.; Paylor, R.; Wehner, J.M. and Tonegawa, S. Impaired spatial learning in α-calcium-calmodulin kinase II mutant mice. *Science 1992a.* 257: 206-11.

Silva, A.J.; Stevens, C.F.; Tonegawa, S. and Wang, Y. Deficient hippocampal long term potentiation in alpha-calcium-calmodulin kinase II mutant mice. *Science 1992b.* 257(5067): 201-6.

Siman, R.; Noszek, JC; and Kegerise, C. Calpain-I activation is specifically related to excitatory amino acid induction of hippocampal damage. *J. Neurosci. 1989.* 9(5): 1579-90.

Skene, J.H. GAP-43 as a 'calmodulin sponge' and some implications for calcium signalling in axon terminals. *Neurosci. Res. Suppl. 1990.* 13: S112-25.

Sloviter, R.S. Calcium-binding protein (Calbindin-D28k) and parvalbumin immunocytochemsitry: localisation in the rat hippocampus with specific reference to the selective vulnerability of hippocampal neurones to seizure activity. *J. Comp. Neurol. 1989.* 280:183-96.

Smith, R. G. ; Alexianu, M.E.; Crawford, G.; Nyormoi, O.; Stefani, E.; and Appel, S.H. Cytotoxicity of immunoglobulins from amyotrophic lateral sclerosis patients on a hybrid motoneurone cell line. *PNAS USA 1994*: 91: 3393-7.

Smith, R. G.; Hamilton, S.; Hoffman, F.; Schneider, T.; Nastainczyk, W.; Birnbaumer, L.; Stefani, E.; Appel, S.H. Serum antibodies to L-type Ca^{2+} channels in patients with amyotrophic lateral sclerosis. *NEJM 1992:* 327: 1721-8.

Sola, C.; Barron, S.; Tusell, J.M.; and Serratosa, J. The Ca^{2+}/calmodulin signalling system in the neural response to excitability. Involvement of neuronal and glial cells. *Prog. Neurobiol. 1999.* 58(3): 207-32.

Soler, R.M.; Egea, J.; Mintenig, G.N.; Sanz-Rodriguez, C.; Iglesias, M.; and Comella, J.X. Calmodulin is involved in membrane depolarisation mediated survival of motoneurones by phosphatidylinositl-3 kinase- and MAPK-independent pathways. *J. Neurosci. 1998.* 18(4): 1230-9.

Sonnenberg, J.L.; Frantz, G.D.; Lee, S.; Heick, A.; Chu, C.; Tobin, A.J.; and Christakos, S. Calcium binding protein (calbindin-D28k) and glutamate decarboxylase gene expression after kindling induced seizures. *Br. Res. Mol. Br. Res. 1991.* 9(3): 179-90.

Spencer, P.S.; Allen, C.N.; Kisby, G.E.; Ludolph, A.C.; Ross, S.M.; and Roy, D.N. Lathyrism and Western Pacific amyotrophic lateral sclerosis: aetiology of short and

long latency motor system disorders. IN Advances in Neurology 56: Amyotrophic Lateral Sclerosis and Other Motor Neuron Diseases. Rowland, L. P. (Ed.). Raven Press. *1991.* Chapter 24 pp287-300.

Spencer, P.S.; Nunn, P.B.; Hugon, J.; Ludolph, A.C.; Ross, S.M.; Roy, D.M.; and Robertson, R.C. Guam amyotrophic lateral sclerosis-parkinsonism-dementia linked to a plant excitant neurotoxin. *Science 1987.* 237: 517-22.

Storey, E.; Kowall, N.W.; Finn, S. F.; Mazurek, M.F.; and Beal, M.F. The cortical lesion of Hunington's disease: further neurochemical characterisation, and reproduction of some of the histological and neurochemical features by *N*-methyl-$_D$-Aspartate lesions of rat cortex. *Ann. Neurol. 1992.* 32: 526-34.

Strack, S., Wadzinski, B. E., and Ebner, F.F. Localisation of the calcium/calmodulin-dependent protein phosphatase, calcineurin, in the hindbrain and spinal cord of the rat. *J. Comp. Neurol. 1996.* 375(1): 66-76.

Stretton, A.O. and Kravitz, E.A. Neuronal geometry: determination with a technique of intracellular dye injection. *Science 1968.* 162(849) 132-4.

Strong, M. J.; Sopper, M. M.; Crow, J. P.; Strong, W. L.; and Beckman, J. S. Nitration of the low molecular weight neurofilament is equivalent in sporadic amyotrophic lateral sclerosis and control cervical spinal cord. *Biochem. Biophys. Res. Comm. 1998.* 248: 157-64.

Sung, J.H. Autonomic neurones of the sacral spinal cord in amyotrophic lateral sclerosis, anterior poliomyelities, and "neuronal intranuclear hyaline inclusion disease": distribution of sacral autonomic neurones. *Acta. Neuropathol. (Berl) 1982.* 56(3): 233-7.

Sung, J.H. and Mastri, A.R. Spinal autonomic neurones in Werdnig-Hoffman disease, mannosidosis, and Hurler's syndrome: distribution of autonomic neurons in the sacral spinal cord. *J. Neuropathol. 1980.* 39(4): 441-51.

Supko, D.E.; and Johnston, M.V. Hydroxyl radical scavenger, dimethyliouria, partially attenuates NMDA receptor-mediated toxicity. *Soc. Neurosci. Abstr. 1992.* 18: 645 (276.6).

Susel, Z.; Engber, T.M.; Kuo, S.; and Chase, T.N. Prolonged infusion of quinolinic acid into rat striatum as an excitotoxic model of neurodegenerative disease. *Neurosci. Letts. 1991.* 121: 234-8.

Swash, M. and Schwartz, M.S. What do we really know about amyotrophic lateral sclerosis? *J. Neurol. Sci. 1992.* 113: 4-16.

Tang, F-R. and Sim, M-K. Expression of glutamate receptor subunits 2/3 and 4 in the hypoglossal nucleus of the rat after neurectomy. *Exp. Br. Res. 1997.* 117: 453-56.

Tani, M.; Kida, M.Y.; and Akita, K. Relationship between the arrangement of motoneurone pools in the ventral horn and ramification pattern of the spinal nerve innervating trunk muscles in the car (Felis domestica). *Exp. Neurol. 1994.* 128(2): 290-300.

Terenghi, G.; Riveros-Moreno, V.; Hudson, L.D.; Ibrahim, N.B.N.; and Polak, J.M. Immunohistochemistry of nitric oxide synthase demonstrates immunoreactive neurones in spinal cord and dorsal root ganglia of man and rat. *J. Neurol. Sci. 1993.* 118: 34-37.

Thor, K. B.; Morgan, C.; Nadelhaft, L.; Houston, M.; and deGroat, W. C. Organisation of afferent and efferent pathways in the pudendal nerve of the female cat. *J. Comp. Neurol. 1989.* 288: 263-279

Titmus, M.J. and Faber, D.S. Altered excitability of goldfish Mauthner cell following axotomy. II. Localisation and ionic basis. *J. Neurophysiol. 1986.* 55(6): 1440-54.

Touzeau, G. and Kato, A.C. ALS serum has no effect on three enzymatic activities in cultured human spinal cords. *Neurology 1986*: 36: 573-6

Troy, C. M., Derossi, D., Prochiantz, A., Greene, L. A., and Shelanski, M. L. Downregulation of Cu/Zn superoxide dismutase leads to cell death via the nitric oxide-peroxynitrite pathway. *J. Neurosci. 1996.* 16(1): 253-61.

Tsuda, T.; Munthasser, S.; Fraser, P.E.; Percy, M.E.; Rainero, I.; Vaula, G.; Pinessi, L.; Bergamini, L.; Vignocchi, G.; McLachian, D.R. et al Analysis of the functional effects of a mutation in SOD1 associated with familial amyotrophic lateral sclerosis. *Neuron. 1994.* 13(3): 727-36.

Uchino, M.; Ando, Y.; and Tanaka, Y. Decrease in Cu/Zn and Mn superoxide dismutase activities in brain and spinal cord of patients with amyotrophic lateral sclerosis. *J. Neurol. Sci. 1994.* 127 (1): 61-67.

Uchitel, O.D.; Appel, S.H.; Crawford, F.; and Sczcupak, L. Immunoglobulins from amyotrophic lateral sclerosis patients enhance spontaneous transmitter release from motor-nerve terminals. *PNAS USA 1988:* 85: 7371-4.

Uchitel, O.D.; Scornick, F.; Protti, D.A.; Fumberg, C.G.; Alvarez, V.; and Appel, S.H. Long term neuromuscular dysfunction produced by passive transfer of ALS immunoglobulins. *Neurol. 1992.* 42: 2175-80

Ulfhake, B. and Cullheim, S. A quantitative light microscopic study of the dendrites of cat spinal -motoneurones after intracellular staining with horseradish peroxidase. *J. Comp. Neurol. 1981.* 202: 585-96.

Ulfhake, B. and Kellerth, J-O. A quantitative light microscopic study of the dendrites of cat spinal α-motoneurones after intracellular staining with horseradish peroxidase. *J. Comp. Neurol. 1981.* 202: 571-583.

Ulfhake, B. and Kellerth, J-O. A quantitative morphological study of HRP-labelled cat α-motoneurones supplying different hindlimb muscles. *Br. Res. 1983.* 264: 1-19.

Vanderhorst, V.G and Holstege, G. Organisation of lumbosacral motoneuronal cell groups innervating hindlimb, pelvic floor, and axial muscles in the cat. *J. Comp. Neiurol. 1997.* 382(1): 46-76.

Vendrell, M.; Aligue, R.; Bachs, O.; and Serratosa, J. Presence of calmodulin and calmodulin-binding proteins in the nuclei of brain cells. *J. Neurochem. 1991.* 57: 622-8.

Vizzard, M.A.; Erdman, S.L.; Roppolo, J.R.; Forstermann, U.; and de Groat, W.C. Differential localisation of neuronal nitric oxide synthase immunoreactivity and NADPH-diaphorase activity in the cat spinal cord. *Cell. Tiss. Res. 1994.* 278(2): 299-309.

von Heyden, B.; Riemer, R.K.; Nunes, L.; Broack, G.B.; Lue, T.F.; and Tanagho , E.A. Response of guinea pig smooth and striated urethral spincter to cromakalim, prazosin, nifedipine, nitroprusside, and electricasl stimulation. *Neurourol. Urodyn. 1995.* 14(2): 153-68.

Wang, H.G.; Pathan, N.; Ethell, I. M.; Krajewski, S.; Yamaguchi, Y.; Shibasaki, F.; McKeon, F.; Bobo, T.; Franke, T.F.; and Reed, J.C. Ca^{2+}-induced apoptosis through calcineurin dephosphorylation of BAD. *Science 1999,* 284(5412): 339-43.

Weiss, J.H. and Choi, D.W. Slow non-NMDA receptor mediated neurotoxicity and amyotrophic lateral sclerosis. *IN Advances in Neurology 56: Amyotrophic Lateral Sclerosis and Other Motor Neuron Diseases.* Rowland, L. P. (Ed.). Raven Press. *1991.*

Williams, C.;Kozlowski, M. A.; Hinton, D. R. and Miller, C. A. Degeneration of spinocerebellar neurons in amyotrophic lateral sclerosis. *Ann. Neurol. 1990.* 27: 215-25.

Williams, T.L.; Day, N.C.; Ince, P.G.; Kamboj, R.K.; and Shaw, P.J. Calcium-permeable alpha-amino-3-hydroxy-5-methyl-4-isoxazole propionic acid receptors: a molecular determinant of selective vulnerability in amyotrophic lateral sclerosis *Ann. Neurol. 1997.* 42: 200-7.

Wink, D.A.; Hanbauer, I.; Krishna, M.C.; DeGraff, W.; Gamson, J.; and Mitchell, J.B. Nitric oxide protects against cellular damage and cytotoxicity from reactive oxygen species. *PNAS USA 1993.* 90: 9813-17.

Witteveenn, C.F.B.; Giovanelli, J.; Yim, M.B.; Gachhui, R.; Stuehr, D.J.; and Kaufman, S. Reactivity of the flavin semiquinone of nitric oxide synthase in the oxygenation of arginine to N^{G}-hydroxyarginine, the first step of nitric oxide synthesis. *Biochem. Biophys. Res. Comm. 1998.* 250: 36-42.

Wolfgram, F. and Myers, L. Amyotrophic lateral sclerosis: effect of serum on anterior horn cells in tissue culture. *Science 1973:* 179: 579-80.

Wu, W. Expression of nitric-oxide synthase (NOS) in injured CNS neurones as shown by NADPH-diaphorase histochemistry. *Exp. Neurol. 1993.* 120(2): 153-9.

Wu, W. Potential roles of gene expression change in adult rat spinal motoneurones following axonal injury: a comparison among c-jun, off-affinity nerve growth factor receptor (LNGFR), and nitric oxide synthase (NOS). *Exp. Neurol. 1996.* 141(2): 190-200.

Wu W., Han, K., Li, L., & Schinco, F.P. Implantation of PNS graft inhibits the induction of neuronal nitric oxide synthase and enhances the survival of spinal motoneurones following root avulsion. *Exp. Neurol. 1994a.* 129(2): 335-9.

Wu, W. and Li, L. Inhibition of nitric oxide synthase reduces motoneurone death due to spinal root avulsion. *Neurosci. Letts. 1993.* 153: 121-4.

Wu, Y.; Li, Y.; Liu, H.; and Wu, W. Induction of nitric oxide synthase and motoneurone death in newborn and early postnatal rats following spinal root avulsion. *Neurosci. Letts. 1995.* 194: 109-12.

Wu, W., Liuzzi, F. J., Schinco, F. P., Depto, A.S., Li, Y., Mong, J. A., Dawson, T. M., & Snyder, S. H. Neuronal nitric oxide synthase is induced in spinal neurones by traumatic injury. *Neurosci. 1994b.* 61(4): 719-26.

Yamada, T.; McGeer, P.L.; Baimbridge, K.G.; and McGeer, E.G. Relative sparing in Parkinson's disease of substantia nigra neurons containing calbindin-D28k. *Br. Res. 1990.* 526: 303-7.

Yano, DS.; Tokumitsu, H.; and Soderling, T.R. Calcium promotes cell survival through CaM-kinase activation of the protein-kinase-B pathway. *Nature 1998.* 396(6711): 584-7.

Young, A.B. What's the excitement about excitatory amino acids in amyotrophic lateral sclerosis? *Ann. Neurol. 1990.* 28(1): 9-11.

Yu, W.A. Nitric oxide synthase in motoneurones after axotomy. *J. Histochem. Cytochem. 1994.* 42(4): 451-7.

Yu, W.A. Regulation of nitric oxide synthase expression in motoneurones following nerve injury. *Dev. Neurosci. 1997.* 19: 247-254.

Zhang, J-H., Morita, Y. Hironaka, T., Emson, P. C., & Tohyama, M. Ontological study of Calbindin D-28k-like and parvalbumin-like immunoreactivities in rat spinal cord and dorsal root ganglia. *J. Comp. Neurol. 1990.* 302: 715-28.

Zhou, Y. and Ling, E.-A. Upregulation of nicotinamide adenine dinucleotide phosphate-diaphorase reactivity in the ventral horn motoneurones of lumbosacral spinal cord after urethral obstruction in the guinea pig. *Neurosci. Res. 1997.* 27: 169-74.

Zhou, Y.; Mack, P.O.; and Ling, E.A. Localisation of nicotinamde adenine dinucleotide phosphate-diaphorase reactivity and nitric oxide synthase

immunoreactivity in the lumbosacral dorsal root ganglia in guinea pigs. *J. Hirnforsch. 1998.* 39(2): 119-27.

Zhu, Y.; and Yakel, J.L. Calcineurin modulates G protein-mediated inhibition of N-type calcium channels in rat sympathetic neurones. *J. Neurophysiol. 1997.* 78: 1161-9.

Ziv, N. E. And Spira, M.E. Axotomy induces a transient and localised elevation of the free intracellular calcium concentration to the micromolar range *J. Neurophysiol. 1995.* 74 (6): 2625-37.